#204

U.S. Department
of Transportation

**Federal Railroad
Administration**

Interactions Between Magnetically Levitated Vehicles and Elevated Guideway Structures

National Maglev Initiative
Washington, D.C. 20590

DOT/FRA/NMI-92/23

July 1992
Final Report

11 - Advanced Systems

1. Report No.	2. Government Accession No.	3. Recipient's Catalog No.
DOT/FRA/NMI-92/23		

4. Title and Subtitle	5. Report Date
Interactions Between Magnetically Levitated Vehicles and Elevated Guideway Structures	July, 1992
	6. Performing Organization Code: 75738
	8. Performing Organization Report No.
7. Author(s): D.N. Wormley, R.D. Thornton, S.-H. Yu, S. Cheng	
9. Performing Organization Name and Address: Center for Transportation Studies, Massachusetts Institute of Technology, Cambridge, MA 02139	10. Work Unit No. (TRAIS)
	11. Contract or Grant No.: DTFR53-91-C-00062
	13. Type of Report and Period Covered: Final - July, 1991-August, 1992
12. Sponsoring Agency Name and Address: U.S. Department of Transportation, Federal Railroad Administration, 400 Seventh Street, SW, Room 8222, Washington, D.C. 20592	14. Sponsoring Agency Code

15. Supplementary Notes: COTR: Michael Coltman, U.S. Department of Transportation, Transportation Systems Center, Kendall Square, Cambridge, MA 02142

16. Abstract

The dynamic performance characteristics of magnetically levitated vehicles and vehicle trains relating to ride quality and magnetic gap variations have been determined using computer simulation models for one-dimensional, two-dimensional and finite length vehicles. These performance characteristics are based on vertical plane motions of vehicles with linear suspension systems which represent a number of the characteristics of both electrodynamic system (EDS) and electromagnetic system (EMS) configurations. Vehicles traversing guideways which are characterized by random roughness, by discrete guideway disturbances which occur due to the construction of elevated structures and by flexible guideway motions are considered.

The studies of vehicle performance have identified the levels of guideway disturbances and/or flexibility which can be accommodated by various suspension configurations while meeting ride quality and magnetic gap variation constraints.

17. Key Words	18. Distribution Statement
maglev, vehicle/guideway interactions, ride quality	Document is available to the U.S. public through the National Technical Information Service, Springfield, VA 22161

19. Security Classif. (of this report)	20. Security Classif. (of this page)	21. No. of Pages	22. Price
Unclassified	Unclassified	149	

Form DOT F 1700.7 (8-72) Reproduction of completed page authorized

Preface

The work in this report was sponsored by the United States Department of Transportation, Federal Railroad Administration, as a part of the National Maglev Initiative Program under Contract Number DTFR53-91-C-00062.

The results described in this report directly support the technology assessment objectives of the broad agency announcement issued under the National Maglev Initiative Program and provide data and information in the area of maglev vehicle/guideway system interactions which are expected to be useful in the development of maglev system concepts.

The authors are indebted to Mr. Michael Coltman of the John A. Volpe National Transportation Systems Center, who provided technical and administrative support of the contract.

The authors also wish to acknowledge the many fruitful technical discussions held with other BAA contractors during the period of work including Dr. Timothy Barrows, Mr. Steven Mark and Mr. Duncan McCallum of the Draper Laboratories.

TABLE OF CONTENTS

TABLE OF CONTENTS (Continued)

LIST OF ILLUSTRATIONS

LIST OF ILLUSTRATIONS (Continued)

LIST OF ILLUSTRATIONS (Continued)

LIST OF TABLES

LIST OF TABLES (Continued)

INTRODUCTION

1.1 Background

Magnetically levitated transportation systems have the potential to provide high speed (on the order 135 m/s) passenger and freight intercity transportation services utilizing vehicles which are supported and propelled by magnetic fields. Studies of these systems [1-4] have cited their potential for providing services which may utilize non fossil fuel sources of power, and of reduced maintenance costs in comparison to conventional wheel-rail systems since concentrated, high stress related forces are not generated between the vehicle and the guideway. The ultimate decision on implementation of these advanced transportation systems depends upon many factors including the potential demand for passenger and freight service and the overall costs related to both installation and operation. Since in these systems it is projected that over seventy percent of the initial system costs are related to the guideway, the potential for magnetically levitated systems to utilize guideways with relatively low installation and maintenance costs is a critical element in their potential for implementation.

While in the 1970's, many research studies of scale model magnetic suspension systems were developed in the U.S. and abroad [5-6], in the last decade research and development of full scale magnetically levitated prototype vehicles has primarily been performed in West Germany and Japan [1]. These efforts have led to the development of two basic types of high speed systems--the electromagnetic system (EMS) which has been developed extensively in Germany and the electrodynamic system (EDS) which has been developed extensively in Japan. In the typical electromagnetic system, lift is achieved using a vehicle mounted electromagnet which is attracted to a steel rail. The system employs a gap feedback sensor and active control to achieve stability [3]. In the electrodynamic system [2], a superconducting magnet configuration installed on the vehicle typically generates lift through repulsive forces as the vehicle passes over the guideway containing aluminum coils or sheets. In typical designs of these systems the electromagnetic system utilizes magnetic gaps on the order of 1.0 cm while an electrodynamic system employs magnetic gaps which may be 5 to 20 times larger than the electromagnetic system. The selection of the operating gaps for both these systems are a function of magnet technology and have direct influence on overall magnet power and efficiency. Both of these basic approaches have been proposed for implementation in a variety of specific suspension and propulsion configurations.

Engineering prototype magnetically levitated vehicle systems have been developed and tested at speeds in the 100-125 m/s range by Germany (EMS) and Japan (EDS) at test

tracks employing elevated guideway systems [2,3]. In the United States, the National Maglev Initiative (NMI) has been created to assess the role of maglev in the nation's future. The NMI office has sponsored a number of studies to define and assess maglev systems which are feasible for the United States, as well as studies focused on critical technical and economic issues [7].

In the implementation of a new transportation system, such as a magneticallly levitated system, a major part of the system installation and operating costs is related to the guideway. Because magnetically levitated systems employ noncontacting types of suspension and propulsion which result in distributed guideway forces, they have the potential, in comparison to conventional wheel rail systems, to have reduced maintenance costs and guideway construction requirements. In these systems many of the important system performance parameters including ride quality, energy consumption and noise are directly related to vehicle suspension and propulsion capabilities and to guideway structural and geometric tolerance requirements. The performance capabilities of magnetically levitated vehicle suspensions and their influence on guideway construction and maintenance practice have a direct influence on overall system cost and ultimately upon system feasibility. Thus, it is important to assess both EMS and EDS system performance with respect to guideway structural and construction requirements.

1.2 Scope and Objectives

In this study performance data are developed to identify guideway construction and maintenance tolerance and structural requirements to meet vehicle ride quality, magnetic gap variation and suspension stroke specifications for both EMS and EDS magnetic suspensions. The effort is focused on the vertical interactions which occur between vehicles and elevated guideway systems and does not specifically include issues related to vehicle lateral guidance or propulsion. The effort is based on the use of analytical, computer based models to identify guideway tolerance and structural requirements to accommodate high speed, magnetically levitated vehicles with acceptable levels of ride quality and gap variation. Specifically research tasks have been undertaken to:

(1) develop generic vehicle/guideway interaction models for both electromagnetic and electrodynamic systems interacting with flexible guideways

(2) identify limiting performance characteristics of electromagnetic and electrodynamic configurations with respect to construction-based guideway requirements

(3) develop parametric design guidelines which illustrate guideway structural and tolerance requirements for generic vehicle suspension configurations.

As part of the effort, vehicle-guideway interaction computer simulation programs have been developed which characterize vehicles or vehicle trains in terms of equivalent linear suspension elements interacting with single or multiple span guideways. Such models are useful in the early design stages of maglev systems and can effectively provide fundamental insights into overall vehicle guideway interactions. For specific vehicle design and performance evaluation, more detailed nonlinear models are appropriate.

1.3 Performance Measures

The overall performance of a magnetically levitated vehicle system in terms of passenger acceptance and utilization depends on many factors including trip cost, travel time, experience related to the cabin environment during traveling and to services provided by transit personnel. However, in terms of the direct technical issues addressed in this report, ride quality which is defined and related directly to vehicle motions, and vehicle suspension displacements--in particular variations in the magnetic gap--are considered to be primary quantitative performance measures. Studies [8-12] have shown that vehicle ride quality is related to a number of parameters including the vehicle acceleration levels. In the context of this study the vertical acceleration levels in the cabin resulting from vehicle-guideway interactions are used directly as a measure of ride quality. Specifically two quantities are utilized:

(1) the total rms acceleration existing at a point in the vehicle body during vehicle passage over a guideway section. The total rms acceleration is one component of the Peplar Ride Quality Criteria [9].

(2) the ISO ride quality criteria which is specified in terms of the rms acceleration in one third octave frequency bands over a specified range of frequencies [12].

Directly from the computation of vehicle motions and their accelerations which result from vehicle/guideway interactions, both the rms acceleration and the ISO criteria may be determined. These factors are strongly influenced by both vehicle suspension capabilities and by the levels of guideway displacements due to irregularities and deflections. Thus, to achieve an improved level of ride quality in terms of reduced vehicle acceleration levels, requires either improved suspension performance or reduced guideway construction irregularities and deflection levels resulting in either tighter tolerances on construction practices and/or reduced displacements of flexible span elements. Since both these latter factors relate directly to guideway installation and maintenance costs, a fundamental tradeoff exists for a given level of suspension performance between achievement of good ride quality and costs associated with guideway construction and maintenance.

To illustrate the suspension design requirements for high speed vehicles, a vehicle traveling at 125 m/s is considered. Table 1.1 lists for 1.0 cm amplitude sinusoidal types of disturbances, the temperal frequency and peak-to-peak accelerations corresponding to disturbance wavelengths of 5-80 m. The table shows that for this set of parameters, the equivalent accelerations corresponding to these disturbances which are imparted to the vehicle suspension elements vary from 25 g (5m wavelength) to 0.1 g (80 m wavelength). For example, to achieve a level of rms acceleration of 0.04 g which is in the acceleration range cited as desirable in ride quality studies [8-12] in a vehicle, requires a suspension which filters or reduces the acceleration levels and has transmissibilities ranging from 0.002 for the 5 m wavelength to 0.57 for the 80 m wavelength disturbance. Thus, the vehicle suspension must be designed to achieve a significant level of filtering or the guideway disturbance amplitude levels must be reduced accordingly to achieve a specified level of ride quality.

Table 1.1

Acceleration, Frequency and Suspension Transmissibility
As a Function of Wavelength
for 125 m/s Operation

Sinusoidal Disturbance Wavelength M	5	10	20	40	80
Temporal Frequency Hz	25	12.5	6.25	3.12	1.6
Acceleration for 1.0 cm Disturbance G	25	6.26	1.57	0.39	0.1
Suspension Transmiss-ibility For 0.04 G RMS Acceleration	.002	.009	.036	.14	.57

The variation in the magnetic gap is also of significant interest, with respect to both EMS and EDS systems. The electromagnetic systems generally operate at gaps on the order of 1 cm, while EDS systems generally operate with gaps on the order of 5-10 cm. A significant question with respect to these suspensions is the gap variation which may occur as a vehicle traverses a guideway. For a small gap suspension, limits on potential magnetic guideway contact are of interest. For larger gap suspensions, a significant issue

is related to the capability of the suspension to accommodate increased levels of tolerances and deflections to take advantage of the larger operating gaps. Additional factors which relate directly to required magnetic gaps to accommodate irregularities and deflections are the relationship of gap to overall suspension power and ultimately to the proximity of propulsion units to the guideway and their respective gaps.

In an overall assessment of vehicle suspensions, both ride quality and gap variation are important technical performance parameters. These parameters are studied in detail in this report and their relationship to guideway tolerances and deflections are determined for a variety of EMS and EDS suspension configurations.

2. FORMULATION OF SYSTEM MODELS

2.1 Model Objectives

Many types of specific configurations have been proposed for magnetically levitated vehicle suspension and propulsion units [1-7]. In the case of electromagnetic suspensions, most proposals for high speed vehicles have involved the use of active suspensions to stabilize the vehicle [13-14]. In vehicles employing electrodynamic systems, both suspensions interacting with sheet guideways and embedded coils have been proposed. When these types of suspensions are combined with propulsion systems, current proposals for vehicle systems include many specific vehicle suspension-propulsion configurations. In the context of this study, it is not the intent to develop comprehensive, detailed specific suspension configuration models. The objective is to capture the essential characteristics of various types of magnetic suspension configurations which fundamentally influence vehicle performance in terms of ride quality and magnetic gap variation while traversing guideways characterized in terms of roughness and flexibility. Thus, in this investigation relatively simple models are formulated to represent magnetic vehicle performance. While these models cannot characterize the detailed performance of a specific vehicle configuration, they can provide guidelines with respect to the overall suspension requirements in terms of natural frequencies and damping ratios that are required to provide good ride quality and magnetic gap variation performance for specific guideway characteristics. Thus, the types of models developed in this effort, are primarily useful in providing guidelines and overall directions for the design and development of specific suspension configurations and for identifying specific guideway requirements in terms of fundamental tolerance levels and flexibility.

2.2 Vehicle Model Formulations

The vehicle model formulated is illustrated schematically in Figure 2.1. The overall model includes a vehicle, or vehicle train, interacting in a vertical plane with an elevated, flexible, irregular guideway. In the model vehicles are represented as follows:

(1) The vehicle body is represented as a rigid body with a mass and pitch moment of inertia. The vehicle weight is carried through the suspension elements to the guideway.

(2) The vehicle is coupled to the guideway through a series of suspensions which are located on the vehicle in a symmetric manner.

(3) The suspensions which couple the vehicle to the guideway consist of linear suspension elements and interact with the guideway at a single point. The effects of

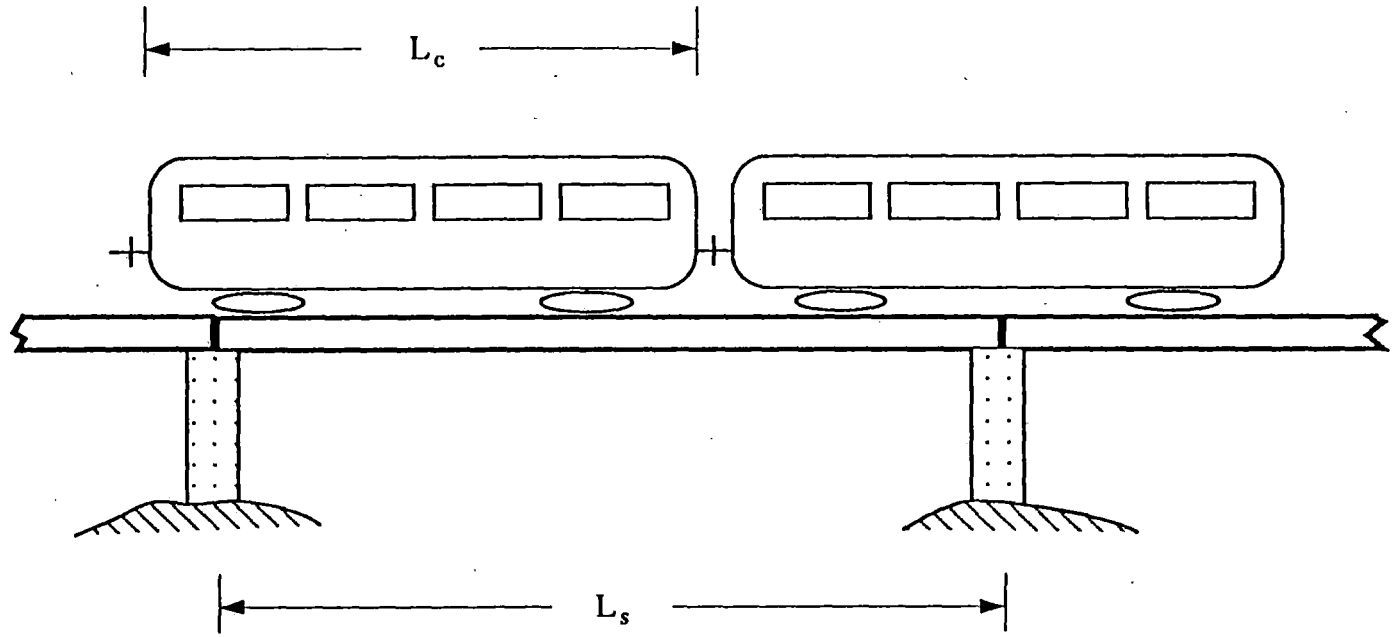

Figure 2.1 Vehicle Train Traversing Guideway Span

distributing the forces over the guideway due to finite magnet length are not included in these simple models.

(4) The guideway is represented as a surface which provides a displacement to the vehicle suspension elements that may result from guideway profile irregularities or from deflections of the guideway in response to vehicle forces.

A more detailed schematic model of a vehicle is illustrated in Figure 2.2 with suspension elements which include vehicle unsprung masses and both primary and secondary suspension elements consisting of stiffness and damping. The overall representation consists of the rigid body which can undergo heave and pitch motions coupled through suspensions to a flexible guideway surface. In the study, suspensions are represented as modular elements which are placed in a symmetric manner on the vehicle.

A limiting case of the two dimensional vehicle model is represented by a one dimensional vehicle heave model. Such models have been studied extensively in the literature and therefore are useful to consider since performance results may be compared and insights may be gained with respect to design criteria from the literature. The one dimensional models are illustrated in Figure 2.3 for four simple models. These four configurations represent limiting case representations of several generic magnetically levitated vehicle suspensions which have been proposed. The configurations illustrated have been represented with linear stiffness and damping elements and with sprung and unsprung mass elements. While the configurations portray only passive elements, they can represent passive suspensions and many of the fundamental characteristics of active suspensions. In particular they can represent active suspension functions in which forces are generated in response to measurements of either relative or absolute positions and velocities. Thus, even though the models are simple, they in many ways capture the important, fundamental characteristics of both active and passive suspensions.

Most magnetic suspensions when exercised over broad ranges of displacement and operating conditions undergo excursions which result in nonlinear relationships between forces and displacements and velocities. However, to provide an initial estimate of ride quality and magnetic gap variations, the linear suspension models are both useful and appropriate and are therefore used in this study. It is noted that in detailed suspension development, nonlinear effects must be considered and thus the results presented in this report can only be considered as estimates of performance which provide initial design guidelines.

In Figure 2.3, model I illustrates a suspension system in which only a primary suspension is employed between a vehicle body and a guideway. This case has no unsprung mass and thus is represented by a sprung mass with a stiffness and damping

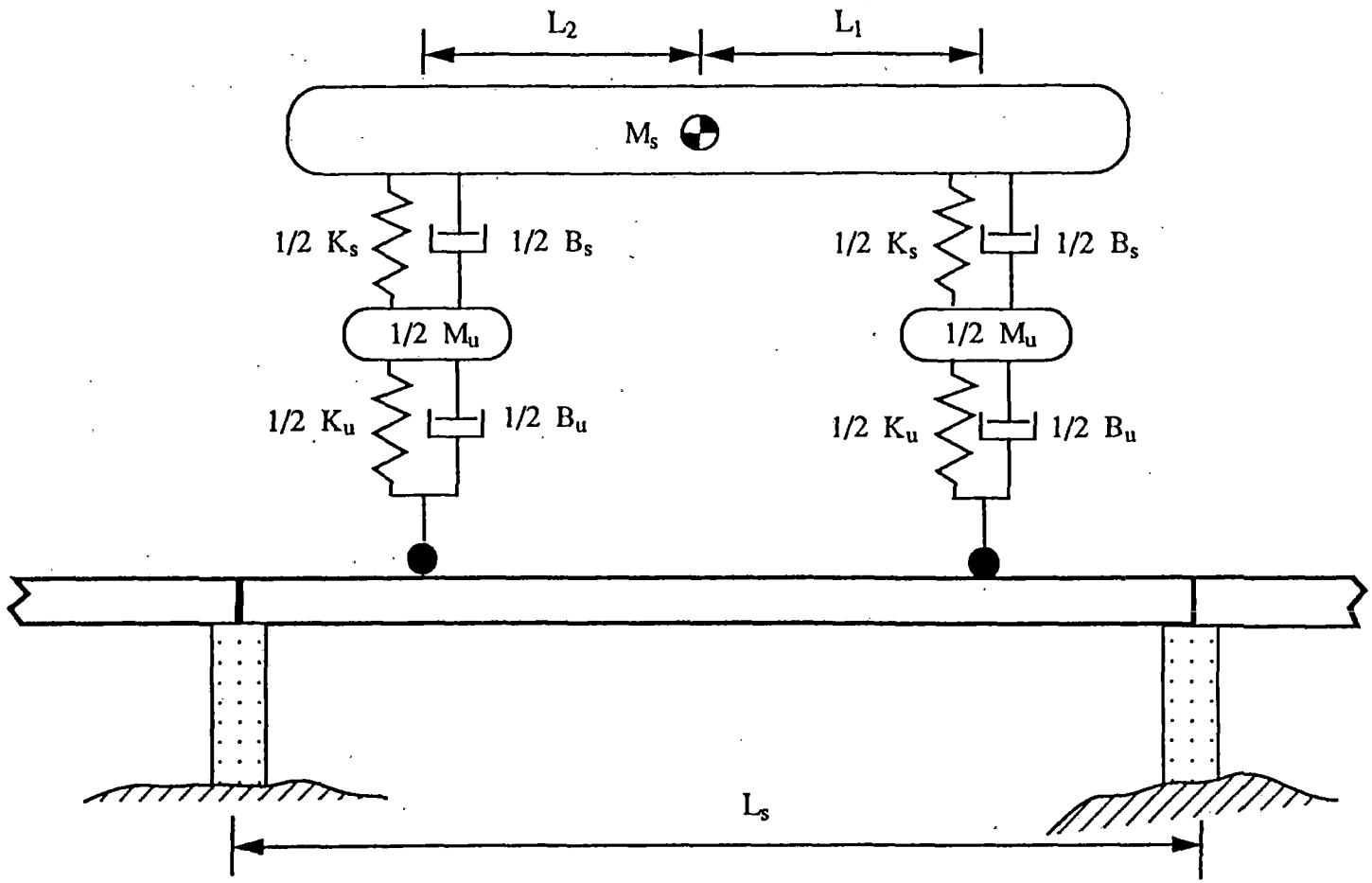

Figure 2.2 Vehicle-Guideway Interaction Model

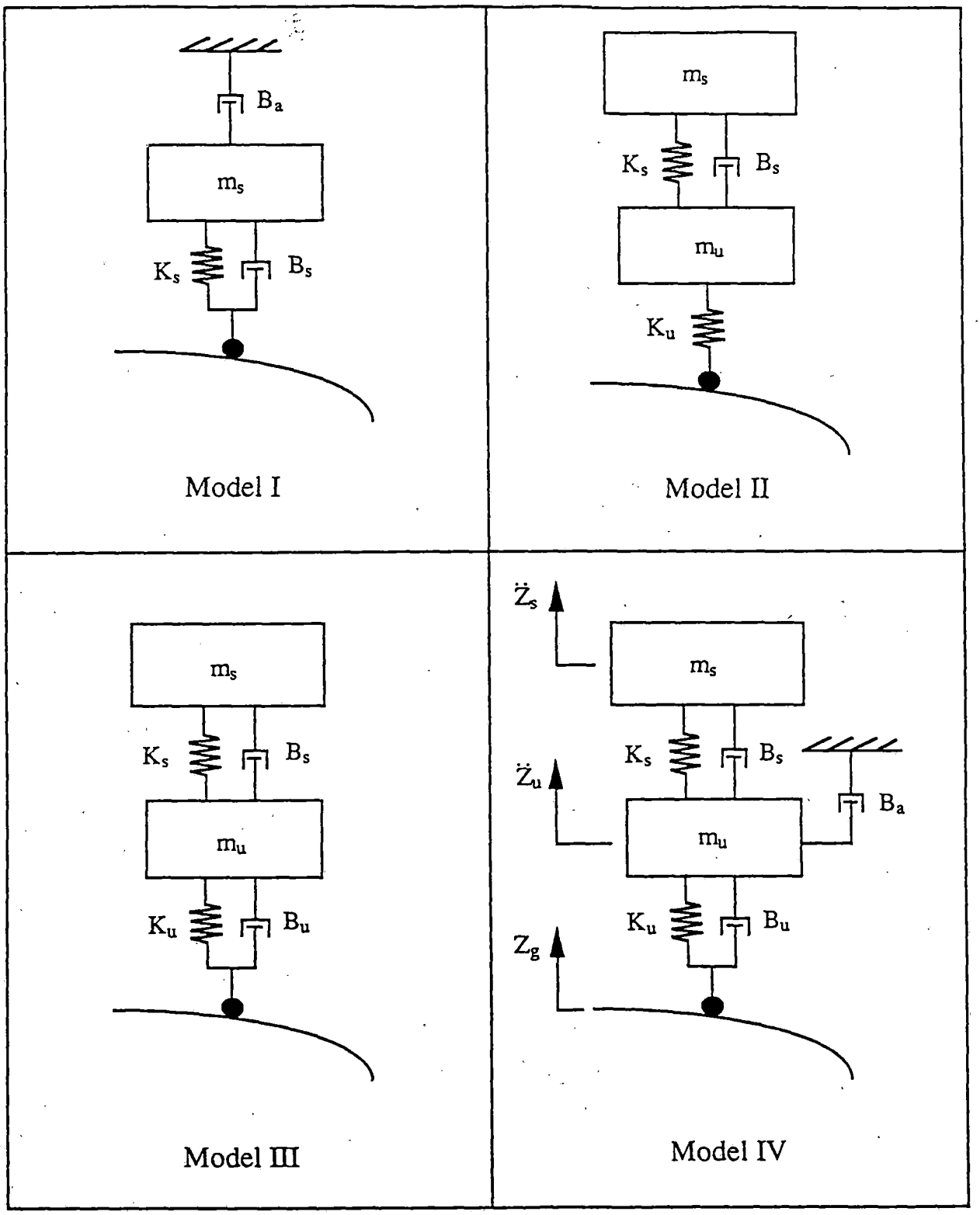

Figure 2.3 Four Suspension Model Configurations

between the mass and the guideway. Additionally Model I represents a damper to an absolute reference. The damper to the absolute reference is implemented primarily as a result of active suspension elements which may be either magnetic or aerodynamic [15]. For Model I if the damping elements between the vehicle and the guideway are set to zero and only absolute damping is provided, then the case closely approximates a suspension which has been identified as optimum in the literature for a simple heave model traversing a randomly irregular guideway [16-17]. This case is somewhat representative of one current EDS proposal [18].

Models II and III represent suspensions in which a vehicle body is connected to a magnetic module through a secondary suspension characterized by a linear stiffness and damper and the magnet module mass is coupled to a guideway through stiffness and damper elements representing the magnetic forces. These models represent a number of electrodynamic suspension configurations with Model II representing the limiting case in which essentially no magnetic damping is employed between the magnetic module and the guideway and the only damping in the system resides in the secondary suspension, while Model III includes magnetic damping between the primary suspension module and the guideway. These configurations are somewhat representative of several current EDS designs [2,19,20].

Model IV represents a suspension which has both secondary suspension stiffness and damping and primary suspension stiffness and damping and additionally absolute damping associated with the magnetic module mass motion. This case represents essential elements of an actively controlled electromagnetic suspension which may be designed to have substantial damping between the magnetic module and the guideway as well as between the magnetic module and an absolute reference because of the actively controlled elements. This model is somewhat representative of current EMS suspension designs [13,14].

The four basic suspension models have been studied in both the simple heave form illustrated in Figure 2.3 and have been incorporated in the two dimensional vehicle model illustrated in Figure 2.2. The equations of motion characterizing the models are summarized in Appendix A.

The vehicle models described above may be characterized in terms of basic suspension stiffness, damping and mass parameters which are, for convenience, expressed as natural frequencies and damping ratios. For each of the four cases the defined natural frequencies and damping ratios in terms of suspension parameters are tabulated in Table 2.1. (The defined natural frequencies and damping ratios are convenient in terms of

organizing the vehicle parameters. Only in limiting cases do they represent the frequencies of oscillation of the suspensions and the actual suspension damping.)

The natural frequencies defined in Table 2.1, include natural frequency ω_u which is based on the total vehicle mass supported by the magnetic suspension and corresponds to the undamped natural frequency of a vehicle with a rigid secondary suspension. For a number of EDS suspension designs in which a superconducting coil interacts directly with a sheet guideway, the natural frequency ω_u may be approximately related to the nominal suspension gap as [5]:

$$f_u = 1/2\pi \quad g/h_o \tag{2.1}$$

where: g = acceleration due to gravity
h_o = nominal suspension gap

Thus, for a number of EDS suspensons, the natural frequency and nominal operating gap are directly related and as the suspension natural frequency is reduced, the nominal operating gap increases. For gaps of 2.5, 5 and 10 cm, the corresponding respectively natural frequencies are 3.15, 2.23, 1.58 Hz.

The other natural frequency, f_s, is defined in terms of the sprung mass supported by the secondary suspension stiffness with the unsprung mass fixed.

In addition to the natural frequencies and damping ratios, the ratio of unsprung to sprung mass is also defined in Table 2.1. For Model I only a sprung mass is present while in Models II, III and IV both sprung and unsprung masses are present with the sprung mass representing the vehicle body and the unsprung mass representing the magnetic module. In vehicle design significant effort is often devoted to minimizing the unsprung mass because a number of studies have shown that a large unsprung mass has detrimental effects on the trade-off between ride quality and suspension gap variation. In particular, Model I represents a vehicle with no unsprung mass.

2.3 Guideway Models

The general guideway model considered in the study characterizes the guideway as an elevated, flexible structure which may contain irregularities. The structure responds to the loads imparted due to vehicle passage and provides displacements at the vehicle suspension points. A structure which contains single or multiple spans is considered.

To provide a basis for determining the influence of guideway characteristics on system performance, three specific guideway representations have been considered.

Table 2.1 Parameter Definitions For The Four Models

Parameter	Definition
Sprung Mass Natural Frequency	$f_s = \frac{1}{2\pi}\omega_s = \frac{1}{2\pi}\sqrt{\frac{K_s}{m_s}}$
Magnetic Suspension Natural Frequency	$f_u = \frac{1}{2\pi}\omega_u = \frac{1}{2\pi}\sqrt{\frac{K_u}{m_u + m_s}}$
Sprung Mass Damping Ratio	$\zeta_s = \frac{B_s}{2\sqrt{K_s m_s}}$
Unsprung Mass Damping Ratio	$\zeta_u = \frac{B_u}{2\sqrt{K_u m_u}}$
Absolute Damping Ratio	$\zeta_a = \frac{B_a}{2\sqrt{K_u m_u}}$
Mass Ratio	$\frac{m_u}{m_s + m_u} = 0.25$

A guideway which is represented as a rigid surface with randomly occurring irregularities has been considered. Measurements of many types of rigid transportation surfaces have been made and characterized in terms of the roughness amplitude power spectral density as a function of roughness wavelength [21]. For a vehicle traveling at velocity v, the amplitude power spectral density may be expressed in terms of the temperal frequency with which a vehicle traverses a guideway irregularity of specific wavelength. In this model the guideway is represented in terms of a power spectral density which is characterized for analytical purposes as:

$$\phi = Av/\omega^2 \tag{2.2}$$

where ϕ is the guideway power spectral density, A is the amplitude, ω is frequency and v is vehicle velocity.

This model provides a representation which with a selection of appropriate values of A may approximately represent surfaces with roughness characteristics ranging from welded steel rail construction to highway construction. The randomly occurring roughness model with a power spectrum given by Eq. (2.2) essentially models the guideway as having a random roughness with amplitudes which decrease as the wavelength decreases. The model does not specifically represent any of the special characteristics of elevated structures, but serves an overall representation of guideway construction which is useful in evaluating vehicle response characteristics.

A number of guideway representations have been developed to represent the special features of elevated types of structures related construction tolerances. These types of deterministic profiles are illustrated in Figure 2.4 and consist of step changes in profile due to span misalignment, elevation changes in profile due to peer misalignment and span deformation due to thermal or construction induced camber. These basic profile shapes are used to assess the influences of levels of construction related profile characteristics on vehicle performance.

A central issue in guideway design for elevated structures is the flexibility of the elevated span and the interaction resulting from a series of vehicles traversing an elevated span system [22]. Design issues relating span materials, beam cross section geometry, length, and joint continuity as well as pier stiffness have a direct bearing on vehicle performance as well as cost. A model of the guideway and vehicle has been developed in which the interaction forces between the vehicle and the guideway are computed as a continuous function of time and used to determine the guideway instantaneous response to vehicle dynamics loads and simultaneously the vehicle response to instantaneous guideway

(a) Step Discontinuities

(b) Ramp Disturbances

(c) Camber Disturbances

Figure 2.4 Guideway Perturbation Representations

deflections. The model is based on a modal representation of the guideway and has been developed specifically for single and two span continuous guideways with precamber resting on rigid piers. The guideway interacts with each vehicle suspension represented as imparting a time varying force on the guideway. The detailed description of the interaction model is given in Appendix B.

3. VEHICLE PERFORMANCE TRAVERSING A RIGID, RANDOMLY ROUGH GUIDEWAY

3.1 Scope of Study

The performance of representative models of vehicles with EDS and EMS suspensions has been computed in terms of ride quality (total rms acceleration or the ISO criteria of acceleration as a function of frequency) and magnetic gap variation (rms displacement) for operation over randomly rough guideways. The study focuses on the one dimensional heave model characterizations, while results for the two dimensional vehicle models with front and rear or multiple suspensions are described to illustrate the effects of finite length vehicles and distributed suspensions. In the study ranges of suspension and vehicle parameters have been selected from the literature [1-8] to provide realistic estimates of vehicle performance.

3.2 One Dimensional Heave Model Performance

The vehicle accelerations and magnetic gap variations have been computed for the four one dimensional vehicle models traversing a rigid guideway with a roughness equivalent to that of conventional welded steel rail, $A = 6.1 \times 10^{-8}$m [21], at a speed of 125 m/s. The results of these computations for selected values of vehicle suspension parameters are summarized in terms of rms sprung mass accelerations and rms magnetic gap variations in Table 3.1 for the four heave models.

The results for Model I in which the magnetic suspension modules are coupled directly to the vehicle body plotted in Figure 3.1 illustrate the influence of suspension natural frequency (equivalently suspension stiffness for a fixed mass) and damping on both sprung mass acceleration and gap variation. Data are presented for two types of suspension damping--damping which produces a force as a result of the relative velocity between the vehicle and guideway and damping in which the force is related to the absolute vehicle velocity. As the suspension natural frequency is decreased at a fixed damping ratio the rms acceleration levels decrease, while the rms gap variation increases. Thus, a tradeoff exists between acceleration and gap variation with respect to suspension natural frequency. For the case with an absolute damping ratio of 0.125 and zero relative damping, as the natural frequency is successively reduced from 1.5 to 1.0 to 0.5 Hz, the rms accelerations decrease respectively from 0.051 to 0.28 to 0.01 g while the rms gap variations increase respectively from 0.6 to 0.71 to 1.0 cm.

The response data show that as the relative damping ratio is increased over the range 0.125 to 0.5, vehicle accelerations increase while the gap variation decreases.

Table 3.1
Total RMS Performance of One Dimensional Vehicle Model
Traversing Irregular Guideway

Model I

				Total RMS of Sprung Mass Acceleration (g)			Total RMS of Magnetic Gap Variation (m)		
ζ_s	ζ_u	ζ_a	f_u	f_s = 0.5 Hz	f_s = 1 Hz	f_s = 1.5 Hz	f_s = 0.5 Hz	f_s = 1 Hz	f_s = 1.5 Hz
0	NA	0.125	NA	0.0098	0.0279	0.0511	0.0101	0.0071	0.0058
0	NA	0.25	NA	0.007	0.0197	0.0361	0.0077	0.0054	0.0044
0	NA	0.5	NA	0.0049	0.0139	0.0255	0.0067	0.0048	0.0039
0	NA	0.75	NA	0.004	0.0113	0.0207	0.0067	0.0049	0.0041
0	NA	1	NA	0.0035	0.0098	0.0179	0.0069	0.0052	0.0043
0.125	NA	0	NA	0.016	0.0379	0.0645	0.0098	0.0069	0.0056
0.25	NA	0	NA	0.026	0.0542	0.0844	0.0069	0.0049	0.004
0.5	NA	0	NA	0.05	0.1005	0.1514	0.0049	0.0034	0.0028

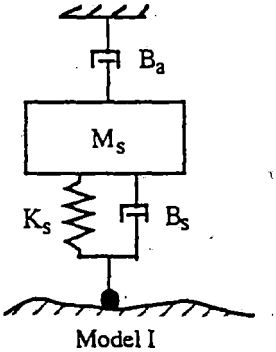

Model I

Table 3.1
Total RMS Performance of One Dimensional Vehicle Model
Traversing Irregular Guideway

Model II

				Total RMS of Sprung Mass Acceleration (g)		Total RMS of Magnetic Gap Variation (m)	
ζ_s	ζ_u	ζ_a	f_s (Hz)	f_u = 1 Hz	f_u = 5 Hz	f_u = 1 Hz	f_u = 5 Hz
0.1	0	0	0.75	0.0242	0.039	0.0057	0.005
0.25	0	0	0.75	0.0178	0.0515	0.0042	0.0032
0.75	0	0	0.75	0.0191	0.0858	0.0047	0.002
0.1	0	0	1	0.0358	0.0509	0.0077	0.0043
0.25	0	0	1	0.0255	0.0613	0.0056	0.0028
0.75	0	0	1	0.0237	0.0994	0.0056	0.0018

Model III

				Total RMS of Sprung Mass Acceleration (g)		Total RMS of Magnetic Gap Variation (m)	
ζ_s	ζ_u	ζ_a	f_s (Hz)	f_u = 1 Hz	f_u = 5 Hz	f_u = 1 Hz	f_u = 5 Hz
0.25	0.25	0	0.75	0.0153	0.0275	0.0035	0.0014
0.25	0.5	0	0.75	0.0146	0.0258	0.003	0.001
0.25	0.75	0	0.75	0.0147	0.0264	0.0026	0.0008
0.25	0.25	0	1	0.0202	0.0375	0.0043	0.0013
0.25	0.5	0	1	0.0187	0.0357	0.0036	0.001
0.25	0.75	0	1	0.0188	0.0365	0.003	0.0008

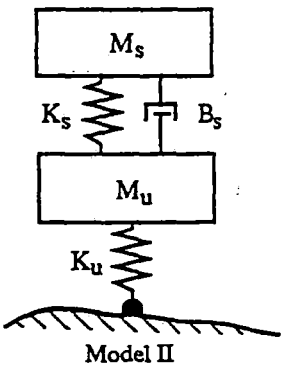

Model II

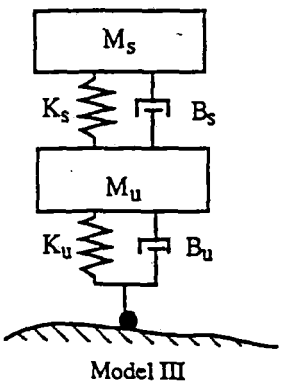

Model III

Table 3.1
Total RMS Performance of One Dimensional Vehicle Model
Traversing Irregular Guideway

Model IV

				Total RMS of Sprung Mass Acceleration (g)		Total RMS of Magnetic Gap Variation (m)	
ζ_s	ζ_u	ζ_a	f_s (Hz)	f_u = 2.5 Hz	f_u = 5 Hz	f_u = 2.5 Hz	f_u = 5 Hz
0.25	0.25	0.25	0.75	0.018	0.0222	0.0017	0.0012
0.25	0.25	0.5	0.75	0.0163	0.0198	0.0019	0.0013
0.25	0.25	0.75	0.75	0.0152	0.0183	0.0021	0.0014
0.25	0.25	0.25	1	0.0255	0.0311	0.0018	0.0012
0.25	0.25	0.5	1	0.0231	0.028	0.0019	0.0013
0.25	0.25	0.75	1	0.0213	0.026	0.0021	0.0014

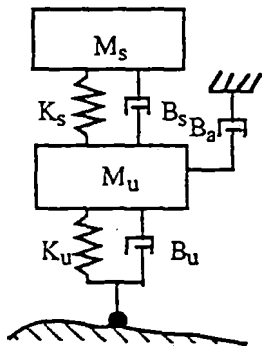

Model IV

Model I

f_s = 0.5 Hz, 1 Hz, 1.5 Hz

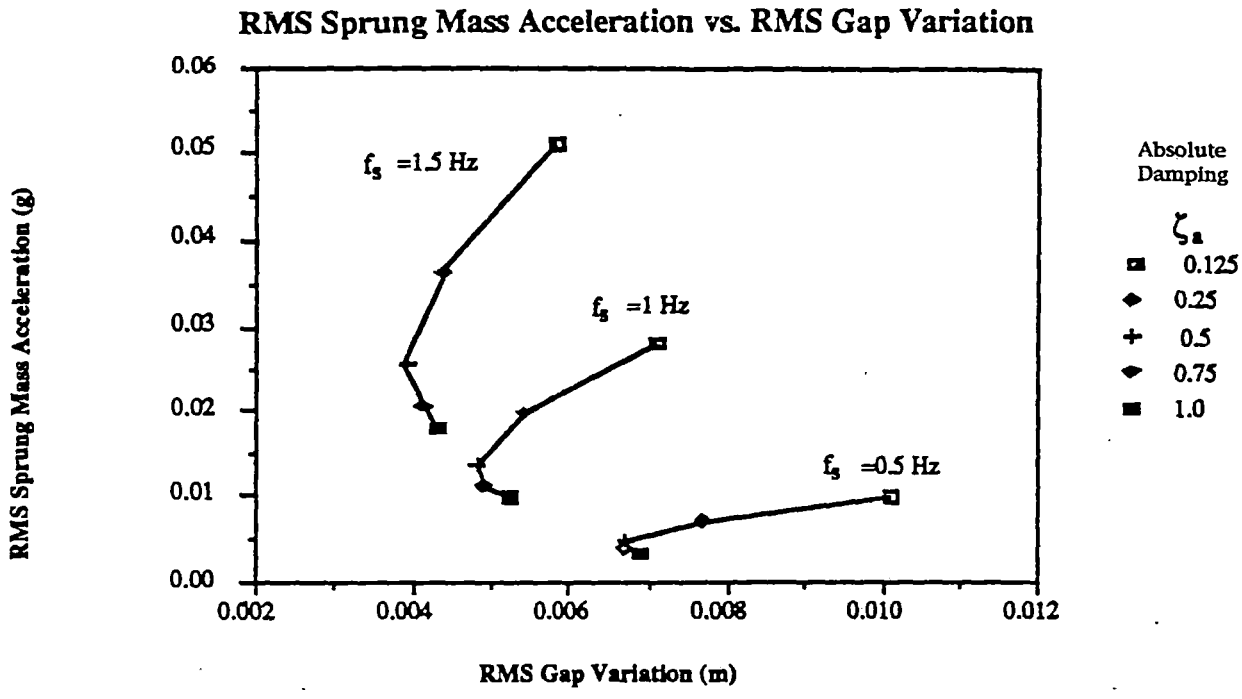

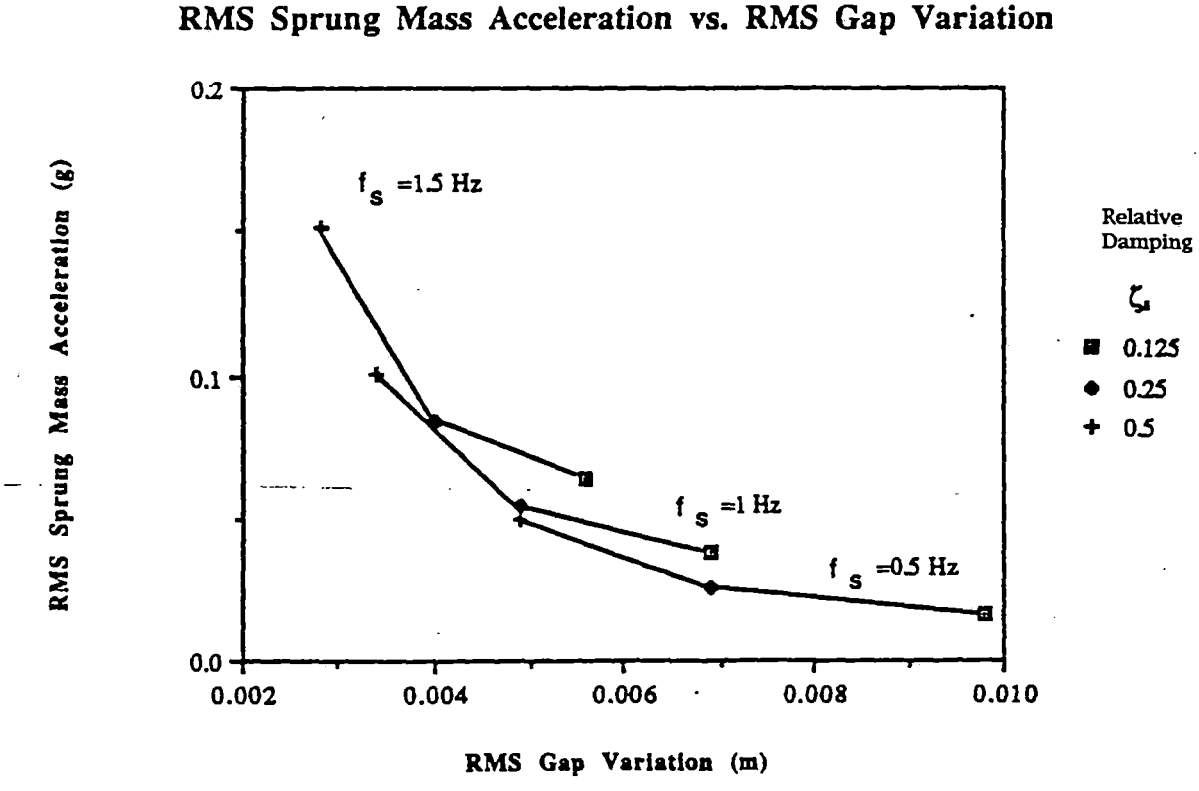

Figure 3.1 RMS Acceleration Versus Gap For Model I

However, the data which are plotted in Figure 3.1 also show that equivalent values of absolute damping produce comparable levels of gap variation with significantly lower acceleration levels. Thus, absolute damping is preferable to relative damping for this configuration. These results are consistent with suspension optimization studies, which have shown that the optimum tradeoff between rms acceleration and rms gap variation for the heave model traversing the random guideway model is obtained using absolute damping with a damping ratio of 0.707 [16-17]. While the data for the cases of absolute damping indicate damping ratios approaching 0.707 provide the optimum tradeoff betwen rms acceleration and rms gap variation, smaller values of damping are of interest since it may be difficult either aerodynamically or magnetically to practically achieve damping ratios in the 0.707 range. For a damping ratio of 0.25, with a 1.0 Hz suspension, rms acceleration levels of .02 g and a gap variation of 0.54 cm are achieved, while for a 0.125 damping ratio suspension, rms acceleration levels 0.028 g and a rms gap variation of 0.72 cm are achieved. If an rms acceleration level of 0.04 g were adopted as a design goal, the 1.0 Hz suspension with a damping ratio of 0.25 could achieve the goal operating on a guideway with roughness similar to welded steel rail. It could also meet this goal on a guideway with a roughness value of $A = 2.4 \times 10^{-7}$m which is closer in roughness to a smooth highway and thus has larger construction and maintenance tolerances. For operation on this higher level of roughness, a rms gap variation of approximately 1.0 cm is achieved. For a large gap EDS system with a nominal gap of 10 cm, the rms gap variation is 10% of the nominal gap.

If the suspension natural frequency is reduced to 0.5 Hz with a 0.25 damping ratio, the guideway roughness may be increased to $A = 2.1 \times 10^{-6}$m while providing 0.04 g rms acceleration, which is slightly rougher than a smooth highway. The corresponding rms gap variation for operation on this guideway is 4.6 cm which is 46% of a nominal 10 cm gap and is higher than normally desired in a high performance system.

The performance data for the heave suspension illustrate the tradeoffs between rms acceleration and rms magnetic gap variation as a function of suspension natural frequency and damping ratio and the relationship between improved suspension performance and increased guideway roughness tolerances.

Data for Model I with a 1.5 Hz suspension and for absolute velocity damping ratios varying from 0.125 to 1.0 are plotted in Figure 3.2 in terms of rms accelerations and gap variations in one third octive bands for operation on a guideway with roughness equivalent to welded steel rail. The data show that the one hour ISO criteria is met for the full range of damping ratios. As the damping is increased, the ISO criteria could be met with a guideway of increased roughness.

Model I

$f_s = 1.5$ Hz

$\zeta_s = 0$

RMS Sprung Mass Acceleration for the Vehicle at 125 m/s with a 1.5 Hz Primary Suspension

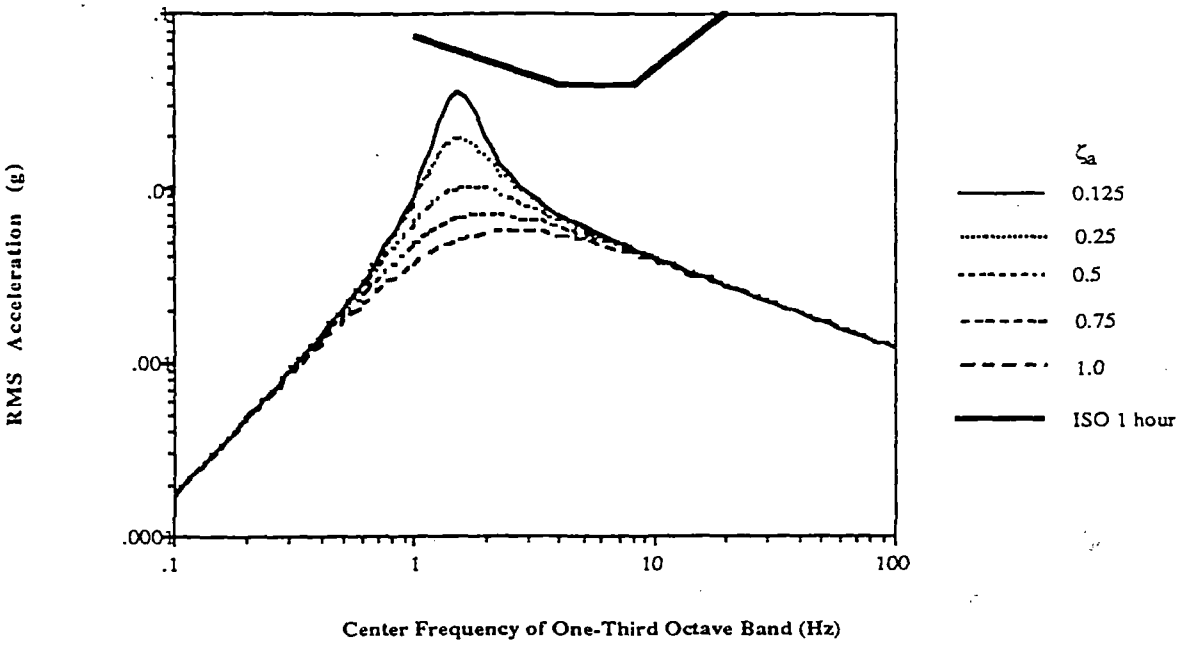

RMS Magnetic Gap Variation for the Vehicle at 125 m/s with a 1.5 Hz Primary Suspension

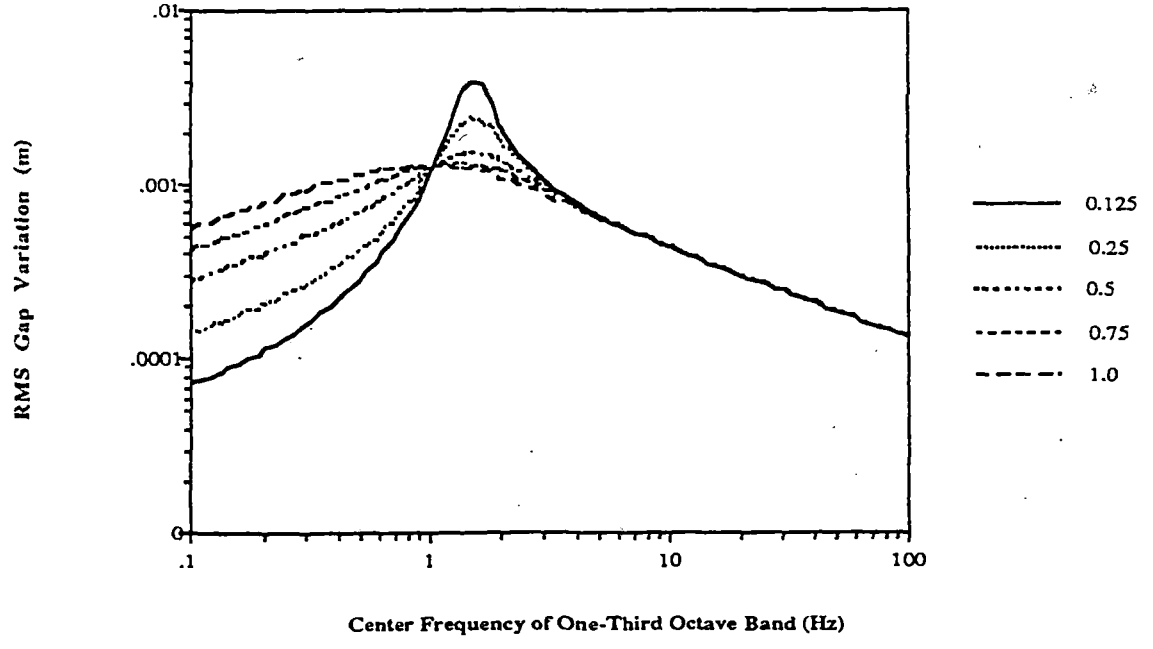

Figure 3.2 ISO Plot For Model I

Data in Table 3.1 also summarize results for vehicles represented as Models II and III with a magnetic module suspended from the vehicle with a secondary suspension, which is represented as a passive stiffness and damping. The data correspond to operation on the guideway with smoothness equivalent to welded steel rail and to a module mass that is 25% of the total vehicle mass. The data include two values of secondary suspension natural frequency, 0.75 Hz and 1.0 Hz, to represent the range of secondary passive suspension natural frequencies which are currently anticipated for magnetically levitated vehicles. Data are also included for primary suspensions with low and high stiffnesses and with and without primary suspension damping. The values of primary stiffness have been selected to represent some of the limiting characteristics which are typical of an EDS system operating on a sheet guideway (low stiffness) and an EDS null flux type of system (high stiffness) operating on a guideway with coils.

The data in Figure 3.3 for a suspension with no primary damping shows that:

(1) As a primary suspension natural frequency is reduced from 5 Hz to 1 Hz, the rms acceleration decreases while the rms magnetic gap variation increases. For example for the case of f_S = 0.75 Hz, and a damping ratio of 0.25, the rms acceleration decreases from 0.05 g to 0.02 g while the magnetic rms gap variation increases from 0.32 cm to 0.42 cm as the primary suspension frequency is decreased from 5 Hz to 1 Hz.

(2) The data show that as the sprung mass natural frequency is decreased, the rms acceleration is decreased, while the magnetic gap variation is increased, but not as significantly as with variations in primary natural frequency. For the case of a primary natural frequency of 5 Hz and a damping ratio of 0.25, the rms acceleration is reduced from 0.06 g to 0.05 g while the rms gap is increased from 0.28 cm to 0.32 cm as the secondary suspension natural frequency is decreased from 1.0 to 0.75 Hz.

(3) As the damping ratio is increased, the data for the 5 Hz primary suspension natural frequency show the rms acceleration increases and the rms gap variation decreases. For the 1 Hz primary suspension natural frequency, as the damping ratio is increased from 0.1 to 0.25 both the rms acceleration and gap variation decrease.

Overall the data indicate that levels of car body rms accelerations below 0.04 g may be obtained with rms gap variations of less than 0.6 cm with suspensions which have primary natural frequencies in the 1 Hz range and secondary suspension natural frequencies in the 0.75-1.0 Hz range. These performance levels on track which is equivalent in

Model II

f_u = 1 Hz, 5 Hz

$\zeta_a = 0, \zeta_u = 0$

RMS Sprung Mass Acceleration vs. RMS Gap Variation (f_s = 0.75 Hz)

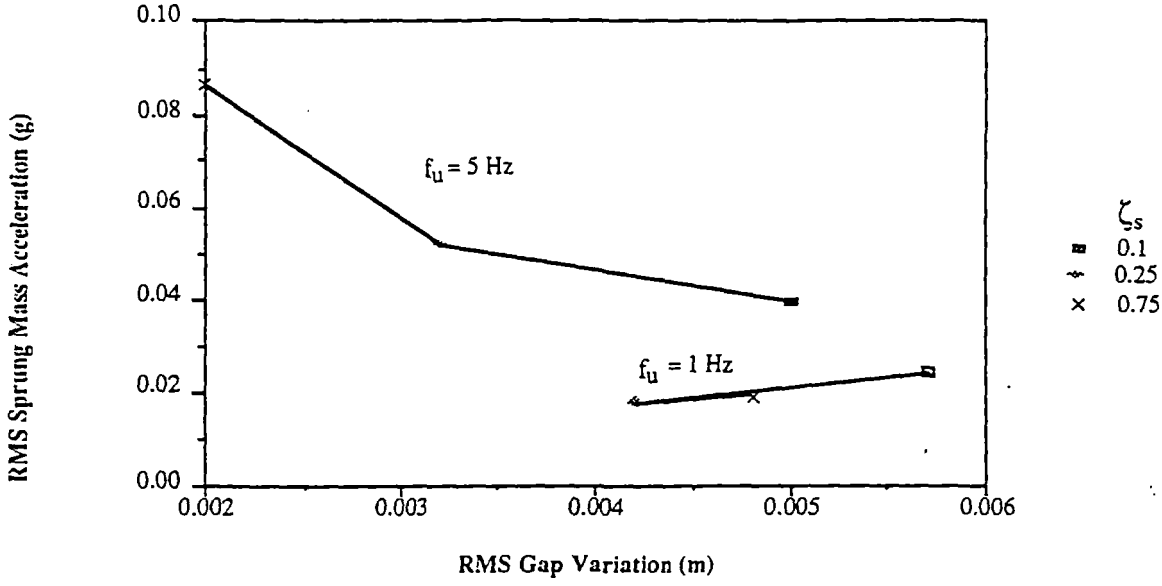

RMS Sprung Mass Acceleration vs. RMS Gap Variation (f_s = 1 Hz)

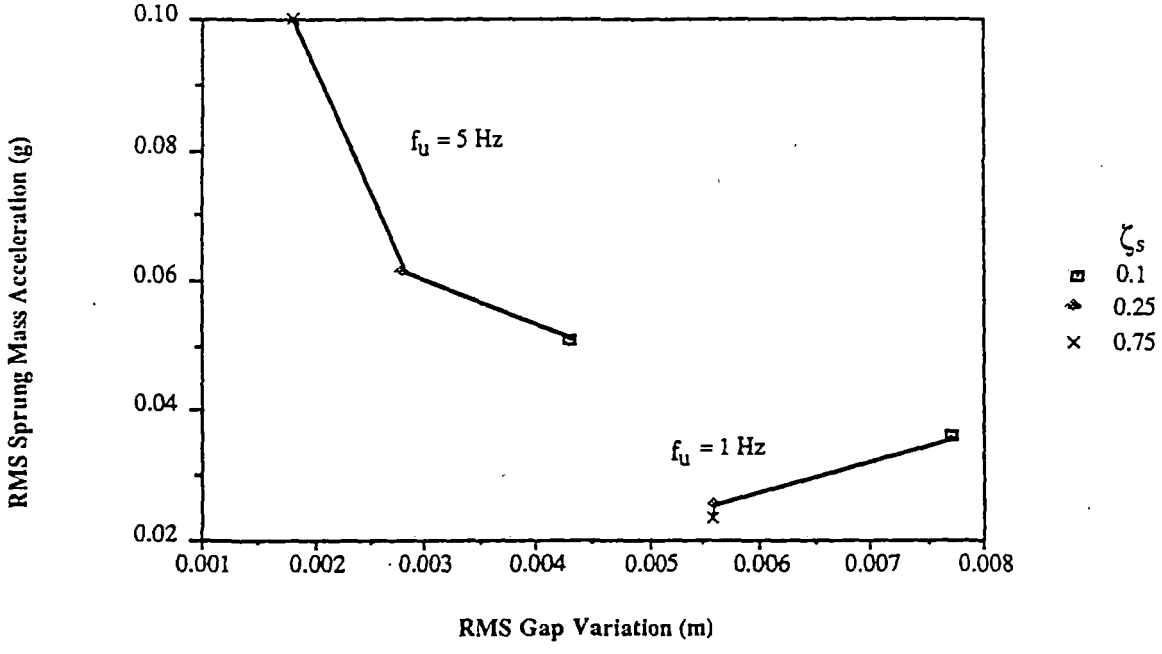

Figure 3.3 RMS Acceleration Versus Gap For Model II

smoothness to welded steel rail are achieved with no primary suspension damping and with secondary suspension damping ratios between 0.1 and 0.75. The performance is achieved with rms gap variations which are less than 0.8 cm.

The suspension performance in terms of ISO ride quality is shown in Figure 3.4 where the case for the stiff primary (5 Hz) and secondary (1 Hz) suspension is shown to meet the ISO one hour specification with damping ratios of less than 0.25 with the critical point occurring at the unsprung mass resonance condition. The data illustrate the ability of suspensions without primary damping to meet the one hour ISO ride quality criteria.

Data for Model III with primary suspension damping are summarized in Figure 3.5 which illustrate the influence of primary suspension damping for suspensions with a secondary suspension damping ratio of 0.25. These data show that the addition of primary suspension damping with damping ratios of 0.25 to 0.5 decreases both the rms acceleration level and the magnetic gap variation. As the primary suspension damping is increased for the case with a primary suspension natural frequency of 5 Hz and secondary suspension natural frequency of 1 Hz, and damping ratio of 0.25, the rms accelerations respectively are 0.06, 0.38 and 0.36 and 0.37 g while the rms magnetic gap variations respectively are 0.28, 0.13, 0.1 and 0.08 cm as values of primary damping ratio are increased from 0.0 to 0.25, to 0.5 to 0.75.

The rms acceleration versus frequency ISO plot in Figure 3.6 also shows that the addition of primary suspension damping reduces the peak rms acceleration at the unsprung mass resonant frequency. For the cases considered in Figure 3.6, the rms guideway roughness could be increased by a factor of almost 4 (the coefficient A by a factor of almost 16) and still meet the one hour ISO criteria.

Data in Table 3.1 for Model IV summarize the rms acceleration and gap variation for a suspension configuration which is similar to an EMS suspension module with an actively controlled magnetic suspension which incorporates absolute damping of the magnetic module. These data correspond to operation on a guideway with roughness equivalent to welded steel rail. The data show that as the primary suspension stiffness is increased, the rms gap variation decreases and the sprung mass acceleration increases. A summary of the data is contained in Figure 3.7. These data show as absolute damping is increased on the magnetic module from damping ratios of 0.25 to 0.75 that the rms acceleration is decreased while the magnetic gap variation is increased. For all the cases presented in the plot, the rms accelerations are less than 0.032 g and the rms magnetic gap variations are less than 0.22 cm, which corresponds to a 28% rms variation with respect to a nominal gap of 0.8 cm.

Model II

f_s = 1 Hz, f_u = 5 Hz

$\zeta_a = 0, \zeta_u = 0$

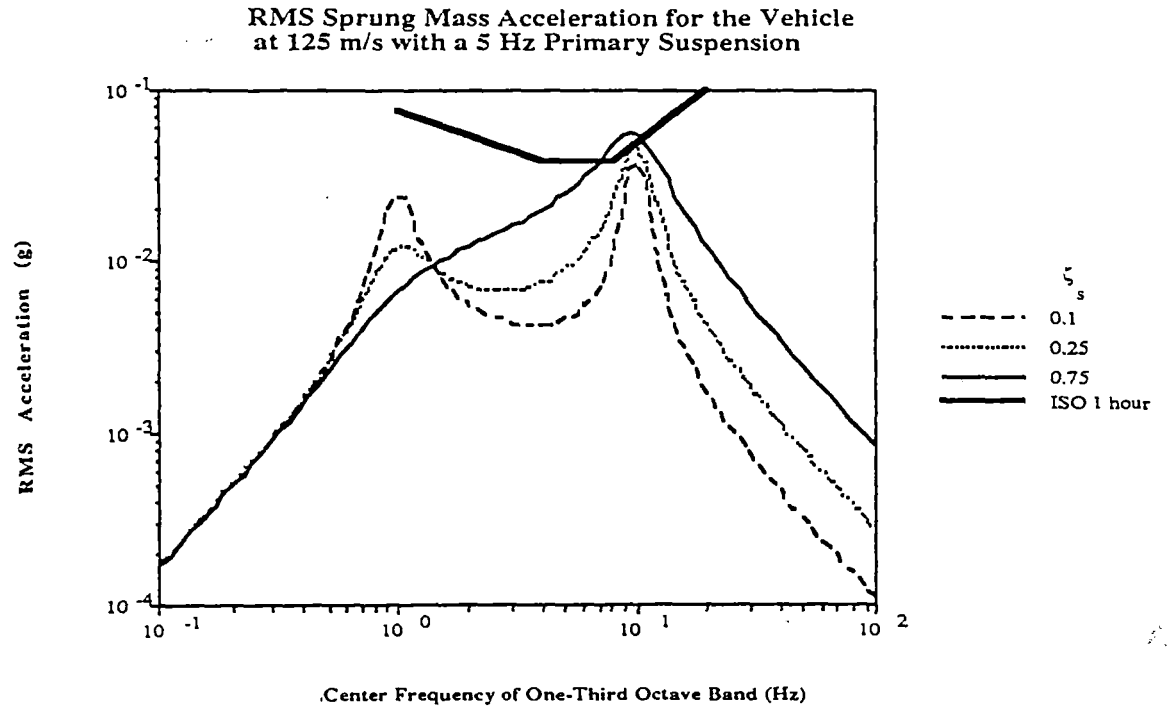

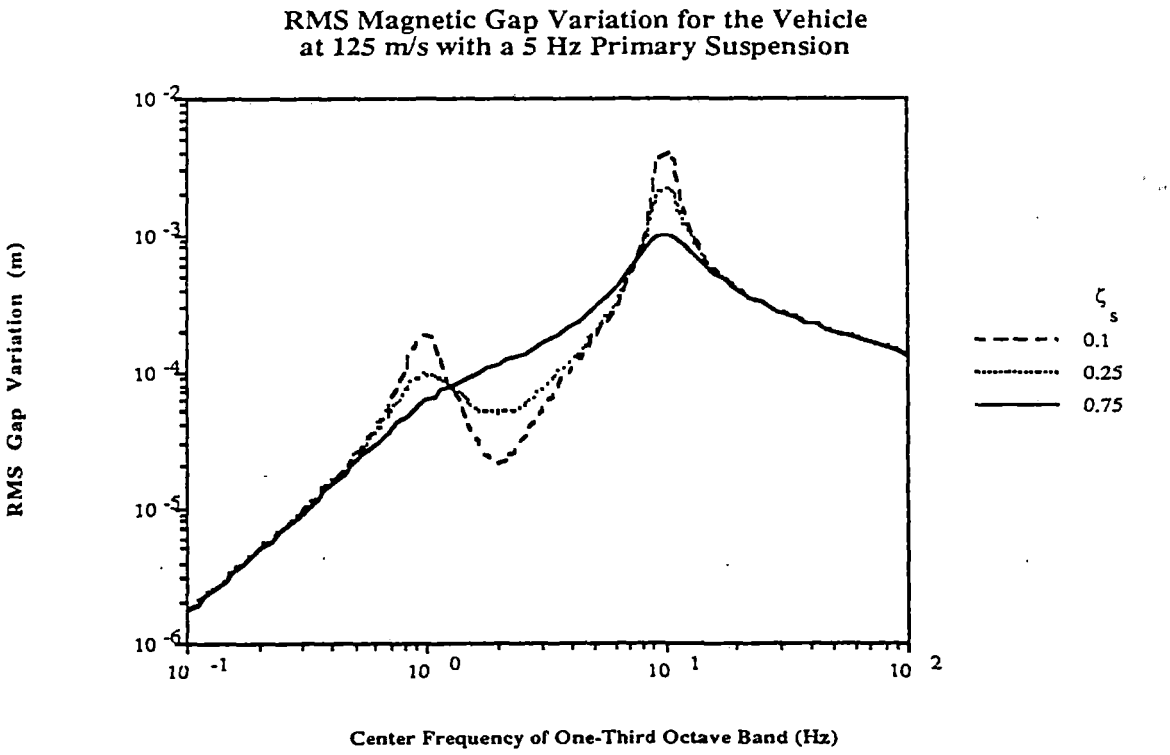

Figure 3.4 ISO Plot For Model II

Model III

f_u = 1 Hz, 5 Hz

ζ_s = 0.25, ζ_a = 0

RMS Sprung Mass Acceleration vs. RMS Gap Variation (f_s = 0.75 Hz)

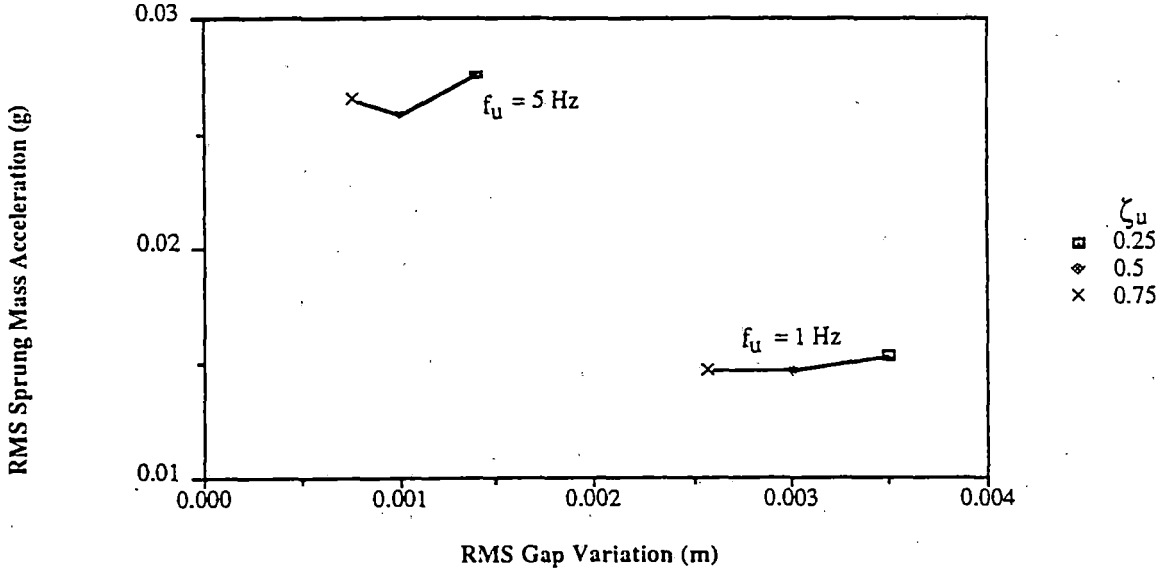

RMS Sprung Mass Acceleration vs. RMS Gap Variation (f_s = 1 Hz)

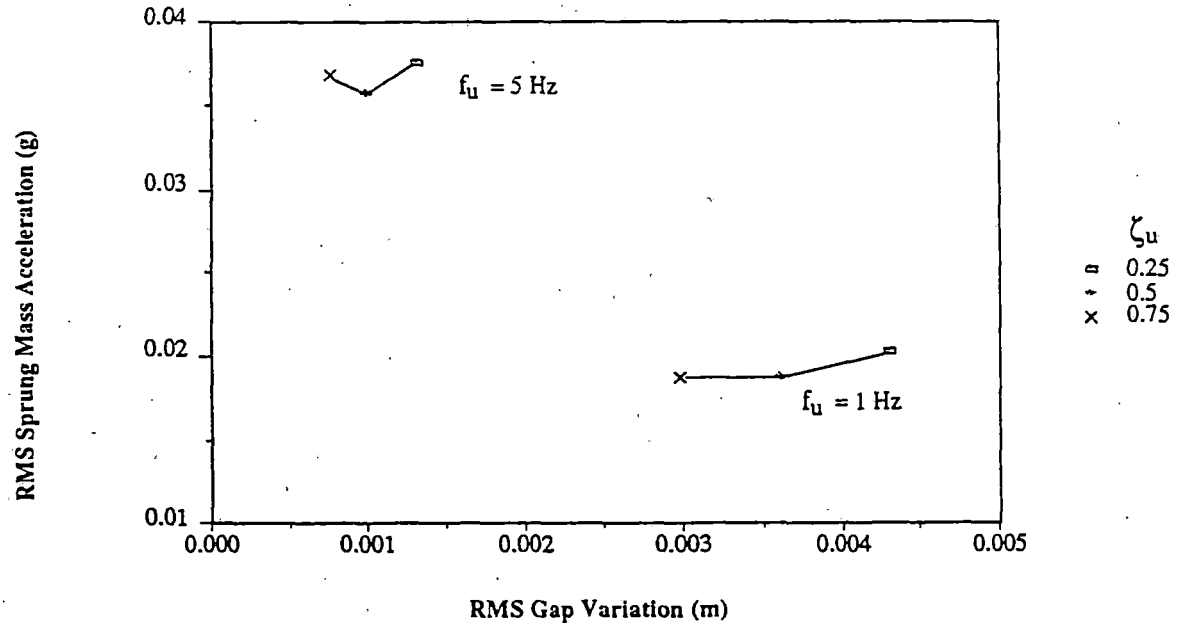

Figure 3.5 RMS Acceleration Versus Gap For Model III

Model III

$f_s = 1$ Hz, $f_u = 5$ Hz

$\zeta_s = 0.25$, $\zeta_a = 0$

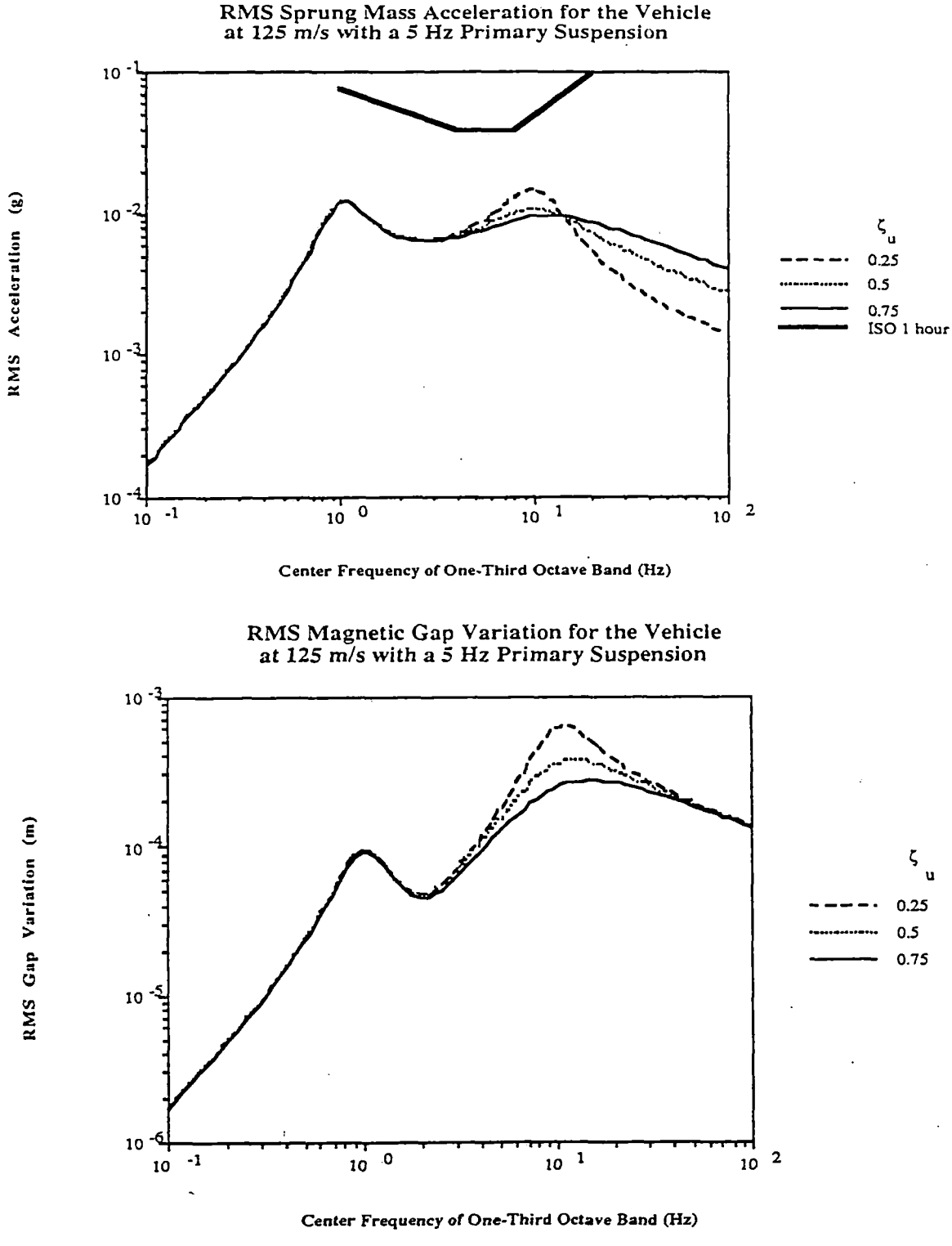

Figure 3.6 ISO Plot For Model III

Model IV

f_u = 2.5 Hz, 5 Hz

ζ_u = 0.25, ζ_s = 0.25

RMS Sprung Mass Acceleration vs. RMS Gap Variation (f_s = 0.75 Hz)

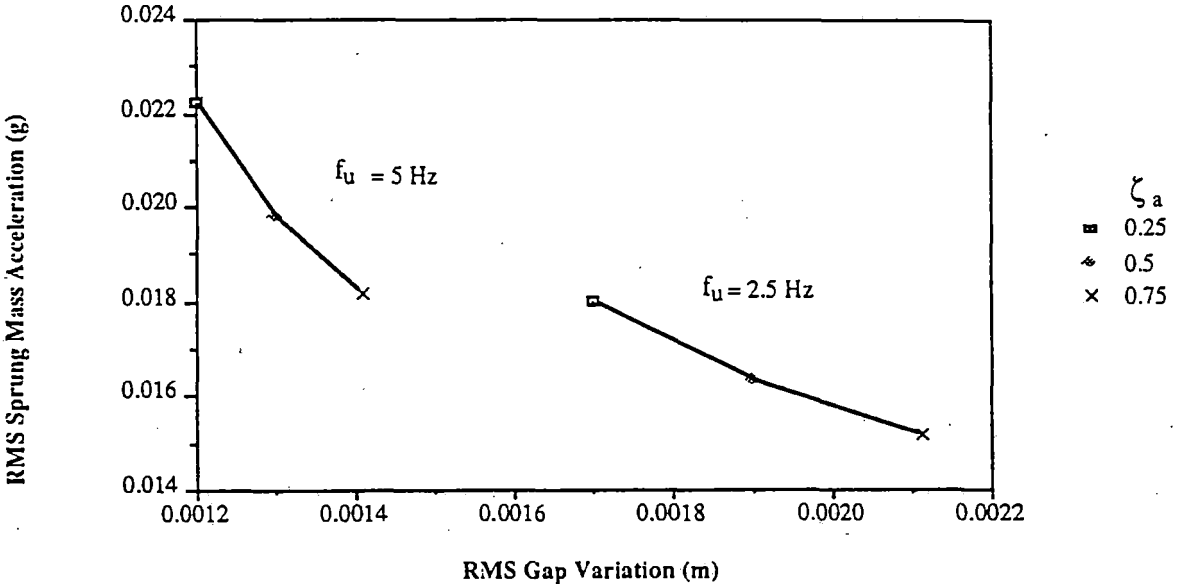

RMS Sprung Mass Acceleration vs. RMS Gap Variation (f_s = 1 Hz)

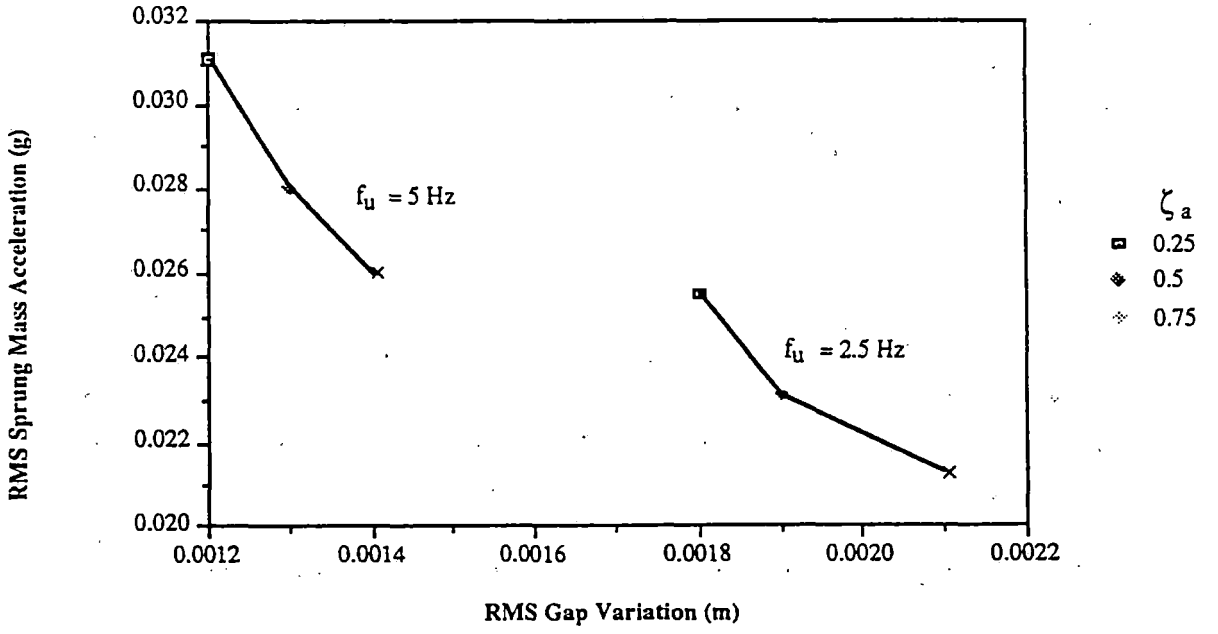

Figure 3.7 RMS Acceleration Versus Gap For Model IV

Data illustrating the performance in terms of an ISO criteria are shown in Figure 3.8 where for the cases plotted, it is noted that the rms guideway roughness could be increased by a factor of five (A by a factor of 25) and still meet the one hour ISO ride quality criteria.

For the three suspension configurations which contain an unsprung mass element, the rms accelerations and magnetic gap variations have been computed with the unsprung mass reduced to 10% of the vehicle total mass, in contrast to the cases considered above where the unsprung mass is 25% of the total mass. The data for 10% unsprung mass are summarized in Table 3.2. For suspension Model II, the reduction in unsprung mass, leads to approximately an 8-12% reduction in sprung mass rms acceleration for all the variations in suspension parameters considered. For the design cases of 1 Hz primary suspension the rms gap variation is reduced by approximately 8%, while for the 5 Hz primary suspensions, the rms gap variation is reduced by 40%. For suspension Models III and IV which have primary suspension damping, the reduction in unsprung mass, leads to no reduction or up to approximately a 10% increase in rms sprung mass acceleration. The rms gap variation for Model III with a 1 Hz primary suspension increases by up to 10%, while decreasing by approximately 30% for the 5 Hz primary suspension. For Model IV, a reduction in unsprung mass leads to approximately a 15% reduction in rms gap variation for the 2.5 Hz primary suspension design and 25-30% reduction for the 5 Hz primary suspension design. Thus, while the reduction in unsprung mass for all the configurations considered leads to changes in rms sprung mass acceleration which are within approximately 10% of the baseline, for the higher frequency primary suspensions, the rms gap variations are reduced up to 40%, while the lower frequency primary suspensions are within 15% of baseline rms gap variations.

3.3 Finite Length Vehicle Performance

The performance of a finite length vehicle shown in Figure 2.2 traversing the guideway with roughness equivalent to welded steel rail at 125 m/s has been studied. The performance data is summarized in Table 3.3 for the suspensions mounted at the front and rear of the vehicle with a suspension spacing of 20m. The four models representing EDS and EMS suspensions are considered with rms accelerations computed at the vehicle center and front and rear suspension points and rms magnetic gaps computed for the front and rear suspensions. Plots of rms acceleration versus rms magnetic gap for front and rear positions are summarized in Figures 3.9-3.16 respectively for the four suspension models. These data indicate the same relative trends with respect to the influence of suspension parameters (damping ratios and natural frequencies) on vehicle body rms acceleration and rms magnetic gap variations as occur in the one dimensional models.

Model IV

$f_s = 1$ Hz, $f_u = 5$ Hz

$\zeta_u = 0.25$, $\zeta_s = 0.25$

RMS Sprung Mass Acceleration for the Vehicle at 125 m/s with a 10 Hz Primary Suspension

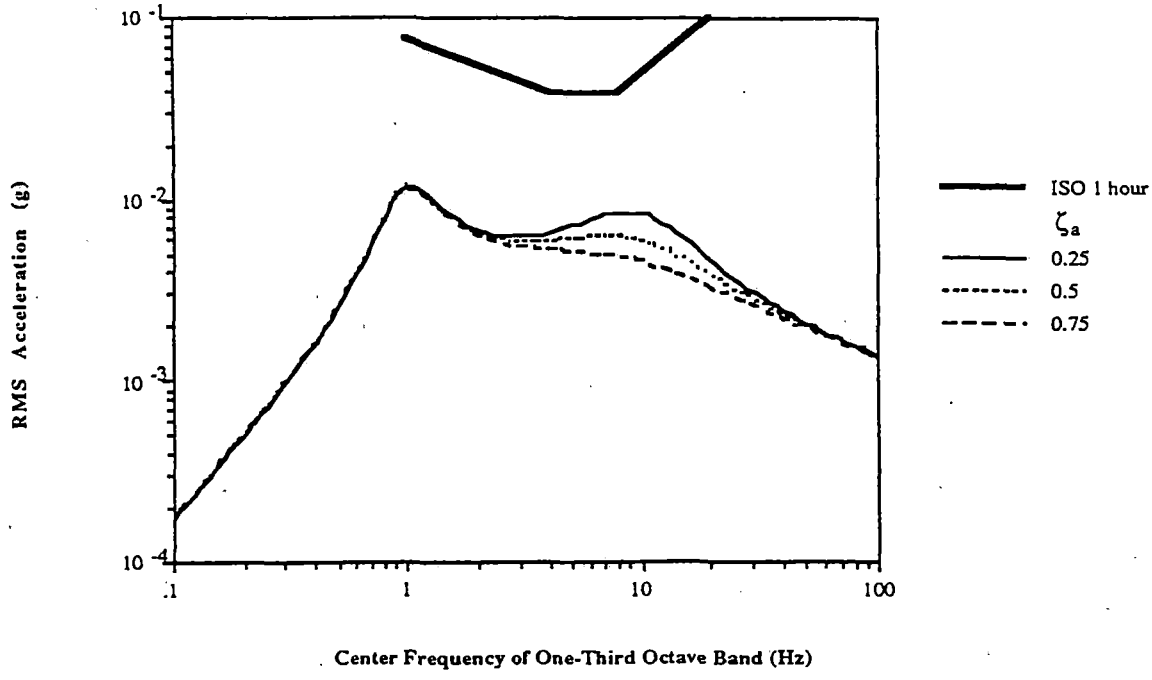

RMS Magnetic Gap Variation for the Vehicle at 125 m/s with a 10 Hz Primary Suspension

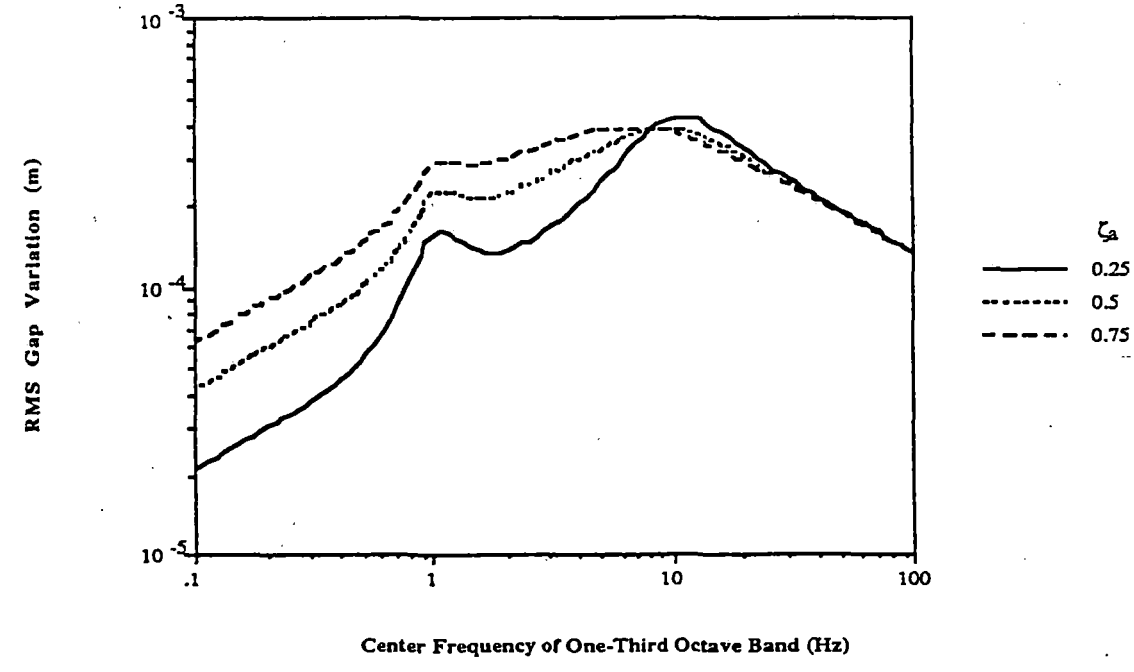

Figure 3.8 ISO Plot For Model IV

Table 3.2
Total RMS Performance of One Dimensional Vehicle Model
with Reduced Unsprung Mass Traversing Irregular Guideway

Model II

				Total RMS of Sprung Mass Acceleration (g)		Total RMS of Magnetic Gap Variation (m)	
ζ_s	ζ_u	ζ_a	f_s (Hz)	f_u = 1 Hz	f_u = 5 Hz	f_u = 1 Hz	f_u = 5 Hz
0.1	0	0	0.75	0.0221	0.0356	0.0054	0.0029
0.25	0	0	0.75	0.0162	0.0470	0.0040	0.0019
0.75	0	0	0.75	0.0174	0.0783	0.0043	0.0013

Model III

				Total RMS of Sprung Mass Acceleration (g)		Total RMS of Magnetic Gap Variation (m)	
ζ_s	ζ_u	ζ_a	f_s (Hz)	f_u = 1 Hz	f_u = 5 Hz	f_u = 1 Hz	f_u = 5 Hz
0.25	0.25	0	0.75	0.0150	0.0306	0.0035	0.0010
0.25	0.5	0	0.75	0.0148	0.0291	0.0032	0.0007
0.25	0.75	0	0.75	0.0152	0.0298	0.0029	0.0006

Model IV

				Total RMS of Sprung Mass Acceleration (g)		Total RMS of Magnetic Gap Variation (m)	
ζ_s	ζ_u	ζ_a	f_s (Hz)	f_u = 2.5 Hz	f_u = 5 Hz	f_u = 2.5 Hz	f_u = 5 Hz
0.25	0.25	0.25	0.75	0.0191	0.0249	0.0014	0.0009
0.25	0.25	0.5	0.75	0.0176	0.0221	0.0016	0.0010
0.25	0.25	0.75	0.75	0.0165	0.0203	0.0018	0.0011

Table 3.3
Total RMS Performance of Finite Length Vehicle Model
Traversing Irregular Guideway

Model I

Total RMS of Sprung Mass Acceleration (g)				f_s = 0.5 Hz			f_s = 1 Hz			f_s = 1.5 Hz		
ζ_s	ζ_u	ζ_a	f_u	Front	Center	Rear	Front	Center	Rear	Front	Center	Rear
0	NA	0.125	NA	0.0114	0.0092	0.0143	0.0393	0.0232	0.0494	0.0806	0.0354	0.0944
0	NA	0.25	NA	0.0097	0.0064	0.0104	0.0331	0.0157	0.0353	0.066	0.0242	0.067
0	NA	0.5	NA	0.0091	0.0043	0.0074	0.0314	0.0104	0.0259	0.0623	0.0167	0.0524
0	NA	0.75	NA	0.0087	0.0033	0.0064	0.0305	0.0082	0.0238	0.0614	0.0136	0.0508
0	NA	1	NA	0.0085	0.0028	0.006	0.0299	0.0069	0.0234	0.061	0.0119	0.0515
0.125	NA	0	NA	0.0284	0.0129	0.0303	0.065	0.0295	0.0734	0.1115	0.0447	0.124
0.25	NA	0	NA	0.0529	0.0188	0.0538	0.1082	0.0387	0.1118	0.1662	0.0582	0.1706
0.5	NA	0	NA	0.1038	0.0352	0.1044	0.2065	0.0703	0.2073	0.3079	0.1054	0.308
0.75	NA	0	NA	0.1543	0.0522	0.1547	0.3039	0.1039	0.3039	0.4489	0.1553	0.4483
1	NA	0	NA	0.2042	0.0692	0.2044	0.3991	0.1375	0.3987	0.5852	0.205	0.5846

Total RMS of Gap Variation (m)				f_s = 0.5 Hz			f_s = 1 Hz			f_s = 1.5 Hz		
ζ_s	ζ_u	ζ_a	f_u	Front	Center	Rear	Front	Center	Rear	Front	Center	Rear
0	NA	0.125	NA	0.0092		0.0108	0.0059		0.0077	0.0045		0.0057
0	NA	0.25	NA	0.0071		0.0082	0.0046		0.0057	0.0036		0.0043
0	NA	0.5	NA	0.0064		0.0068	0.0045		0.0045	0.0036		0.0037
0	NA	0.75	NA	0.0066		0.0067	0.0048		0.0048	0.0039		0.0039
0	NA	1	NA	0.0069		0.0069	0.0051		0.0051	0.0042		0.0042
0.125	NA	0	NA	0.0088		0.0105	0.0057		0.0074	0.0043		0.0055
0.25	NA	0	NA	0.006		0.0075	0.0038		0.0051	0.0029		0.0037
0.5	NA	0	NA	0.0042		0.0051	0.0027		0.0033	0.0021		0.0024
0.75	NA	0	NA	0.0034		0.004	0.0022		0.0025	0.0018		0.0018
1	NA	0	NA	0.0029		0.0033	0.0019		0.0021	0.0015		0.0016

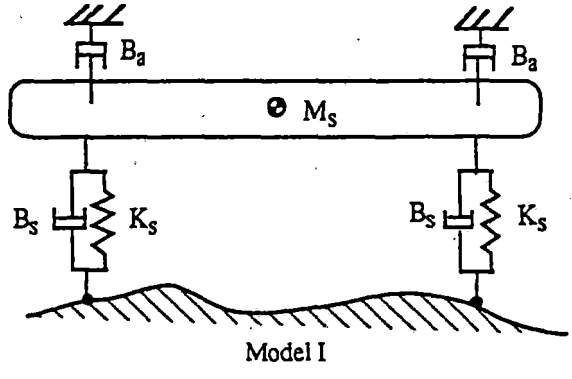

Model I

Table 3.3
Total RMS Performance of Finite Length Vehicle Model
Traversing Irregular Guideway

Model II

Total RMS of Sprung Mass Acceleration (g)				f_u = 1 Hz			f_u = 5 Hz		
ζ_s	ζ_u	ζ_a	f_s (Hz)	Front	Center	Rear	Front	Center	Rear
0.1	0	0	0.75	0.0348	0.0215	0.0403	0.0878	0.0236	0.0904
0.25	0	0	0.75	0.0271	0.0151	0.0338	0.1226	0.0283	0.1239
0.5	0	0	0.75	0.0285	0.0142	0.037	0.1636	0.042	0.1653
0.75	0	0	0.75	0.0318	0.0155	0.0423	0.1932	0.0543	0.1959
0.1	0	0	1	0.053	0.0328	0.0596	0.1083	0.0329	0.1137
0.25	0	0	1	0.0371	0.0222	0.0461	0.1407	0.0362	0.1436
0.5	0	0	1	0.0353	0.0192	0.0462	0.1848	0.0515	0.1875
0.75	0	0	1	0.0383	0..0199	0.0505	0.2169	0.0655	0.2201

Total RMS of Gap Variation (m)				f_u = 1 Hz			f_u = 5 Hz		
ζ_s	ζ_u	ζ_a	f_s (Hz)	Front	Center	Rear	Front	Center	Rear
0.1	0	0	0.75	0.0054		0.0058	0.005		0.005
0.25	0	0	0.75	0.0043		0.0048	0.0032		0.0033
0.5	0	0	0.75	0.0043		0.0055	0.0024		0.0024
0.75	0	0	0.75	0.0047		0.0065	0.0021		0.0022
0.1	0	0	1	0.0079		0.0087	0.0042		0.0043
0.25	0	0	1	0.0056		0.0067	0.0028		0.0028
0.5	0	0	1	0.0053		0.007	0.0021		0.0022
0.75	0	0	1	0.0057		0.0078	0.002		0.002

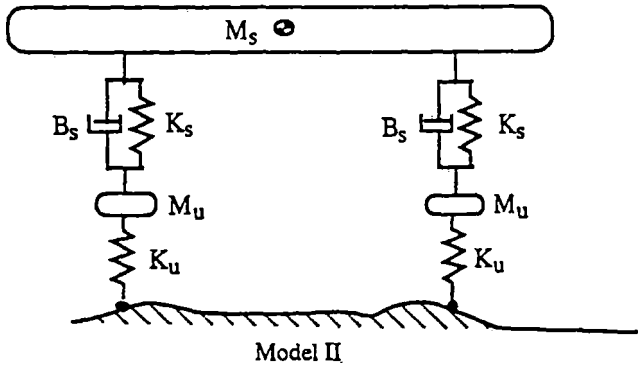

Model II

Table 3.3
Total RMS Performance of Finite Length Vehicle Model
Traversing Irregular Guideway

Model III

Total RMS of Sprung Mass Acceleration (g)				f_u = 1 Hz			f_u = 5 Hz		
ζ_s	ζ_u	ζ_a	f_s (Hz)	Front	Center	Rear	Front	Center	Rear
0.25	0.25	0	0.75	0.0208	0.0132	0.0274	0.0535	0.0201	0.0569
0.25	0.5	0	0.75	0.0207	0.0123	0.0265	0.0489	0.0194	0.0525
0.25	0.75	0	0.75	0.0223	0.0121	0.0274	0.0501	0.0198	0.0537
0.25	0.25	0	1	0.026	0.0173	0.035	0.0718	0.0271	0.0774
0.25	0.5	0	1	0.026	0.0155	0.0337	0.0666	0.0262	0.0725
0.25	0.75	0	1	0.0287	0.015	0.0353	0.0683	0.0268	0.0741

Total RMS of Gap Variation (m)				f_u = 1 Hz			f_u = 5 Hz		
ζ_s	ζ_u	ζ_a	f_s (Hz)	Front	Center	Rear	Front	Center	Rear
0.25	0.25	0	0.75	0.0033		0.0039	0.0014		0.0014
0.25	0.5	0	0.75	0.0028		0.0033	0.001		0.001
0.25	0.75	0	0.75	0.0024		0.0029	0.0008		0.0008
0.25	0.25	0	1	0.0039		0.005	0.0013		0.0013
0.25	0.5	0	1	0.0031		0.0041	0.001		0.001
0.25	0.75	0	1	0.0027		0.0034	0.0008		0.0008

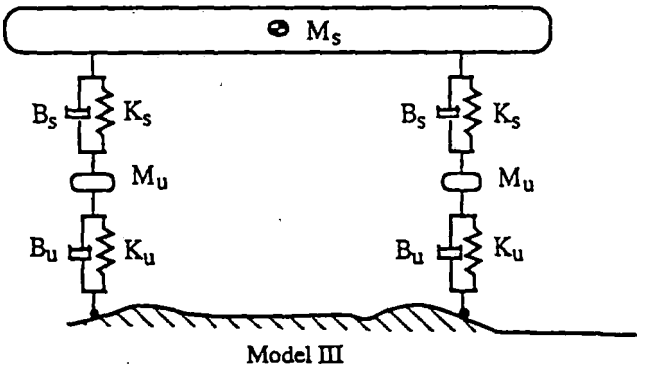

Model III

Table 3.3
Total RMS Performance of Finite Length Vehicle Model
Traversing Irregular Guideway

Model IV

Total RMS of Sprung Mass Acceleration (g)				f_u = 2.5 Hz			f_u = 5 Hz		
ζ_s	ζ_u	ζ_a	f_s (Hz)	Front	Center	Rear	Front	Center	Rear
0.25	0.25	0.25	0.75	0.0302	0.0138	0.0357	0.0407	0.0165	0.0448
0.25	0.25	0.5	0.75	0.0257	0.0127	0.0316	0.0346	0.0149	0.0393
0.25	0.25	0.75	0.75	0.0225	0.012	0.0285	0.0308	0.0139	0.0358
0.25	0.25	0.25	1	0.0422	0.0185	0.05	0.0561	0.0221	0.0618
0.25	0.25	0.5	1	0.0357	0.0169	0.0438	0.0482	0.02	0.0546
0.25	0.25	0.75	1	0.0309	0.0157	0.039	0.043	0.0186	0.0499

Total RMS of Gap Variation (m)				f_u = 2.5 Hz			f_u = 5 Hz		
ζ_s	ζ_u	ζ_a	f_s (Hz)	Front	Center	Rear	Front	Center	Rear
0.25	0.25	0.25	0.75	0.0017		0.0018	0.0012		0.0012
0.25	0.25	0.5	0.75	0.0019		0.0019	0.0013		0.0013
0.25	0.25	0.75	0.75	0.0021		0.0021	0.0014		0.0014
0.25	0.25	0.25	1	0.0017		0.0019	0.0012		0.0012
0.25	0.25	0.5	1	0.0019		0.002	0.0013		0.0013
0.25	0.25	0.75	1	0.0021		0.0022	0.0014		0.0014

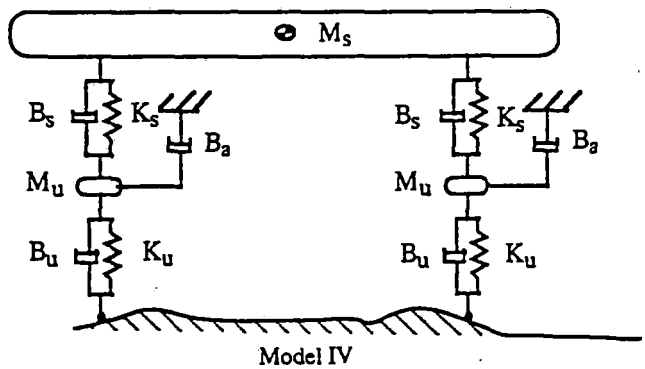

Model I

f_s = 0.5 Hz, 1 Hz, 1.5 Hz

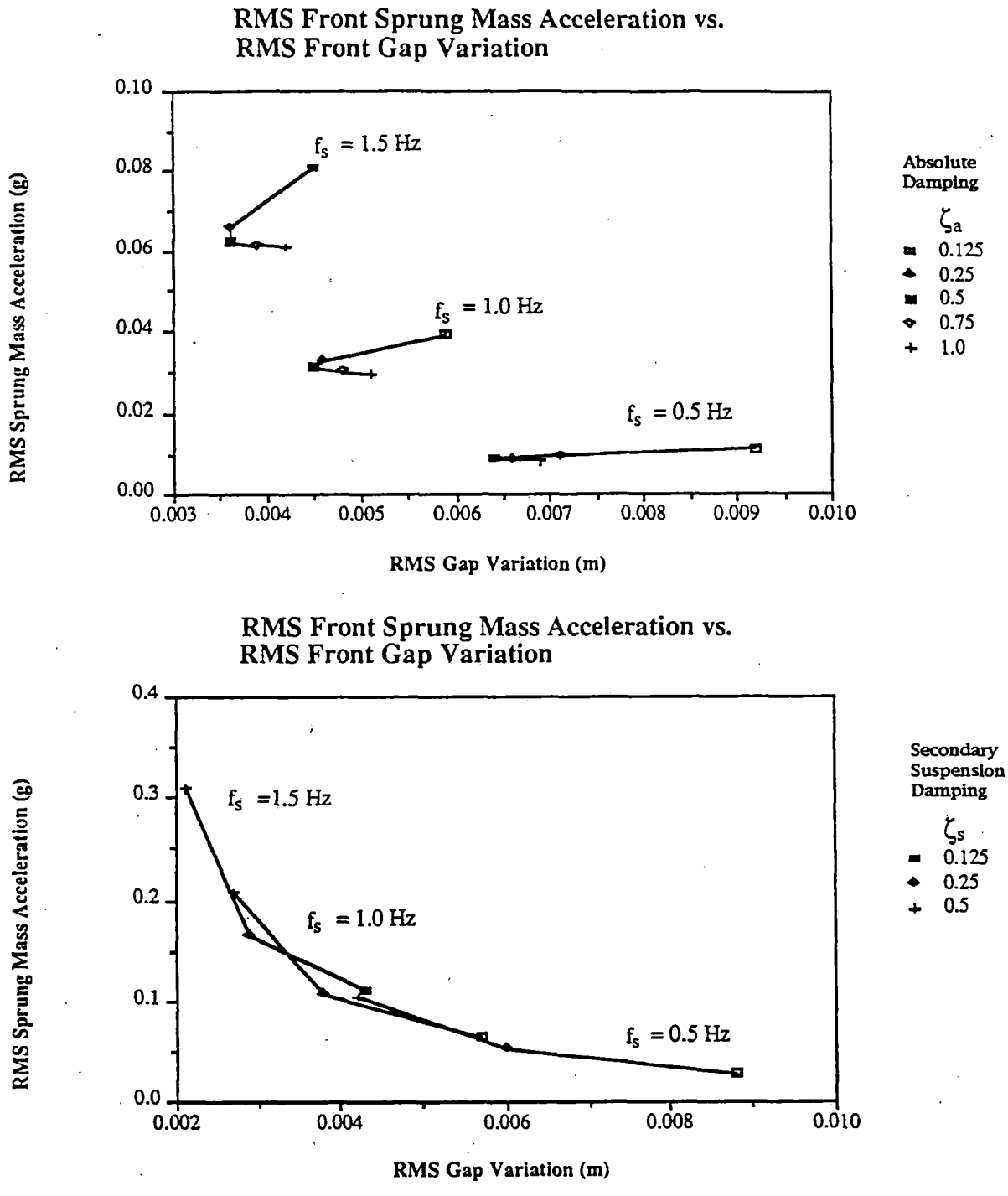

Figure 3.9(a) Front RMS Acceleration Versus Gap For Finite Length Vehicle - Model I

Model I

f_s = 0.5 Hz, 1 Hz, 1.5 Hz

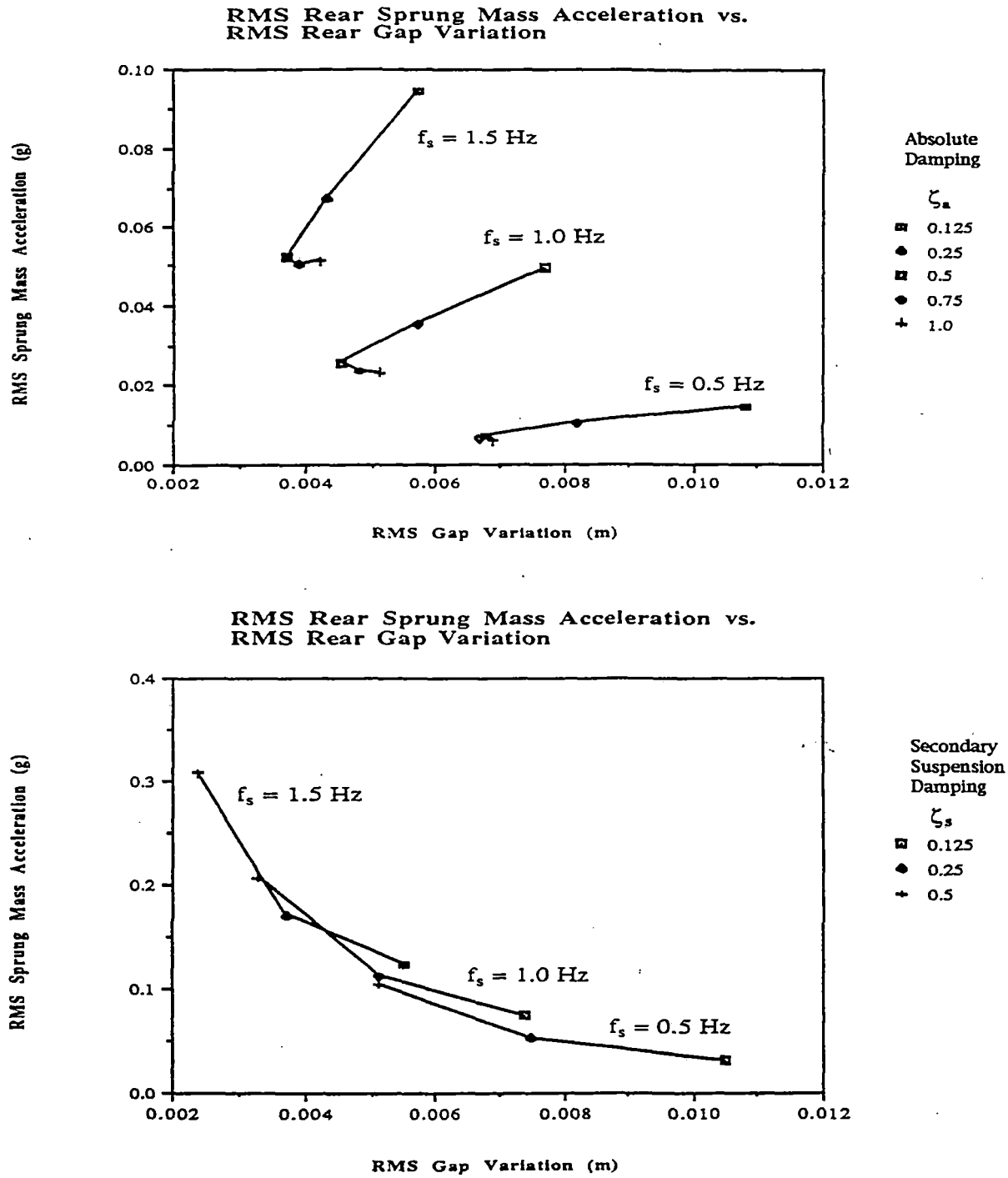

Figure 3.9(b) Rear RMS Acceleration Versus Gap For Finite Length Vehicle - Model I

Model I

f_s = 1.5 Hz

$\zeta_s = 0$

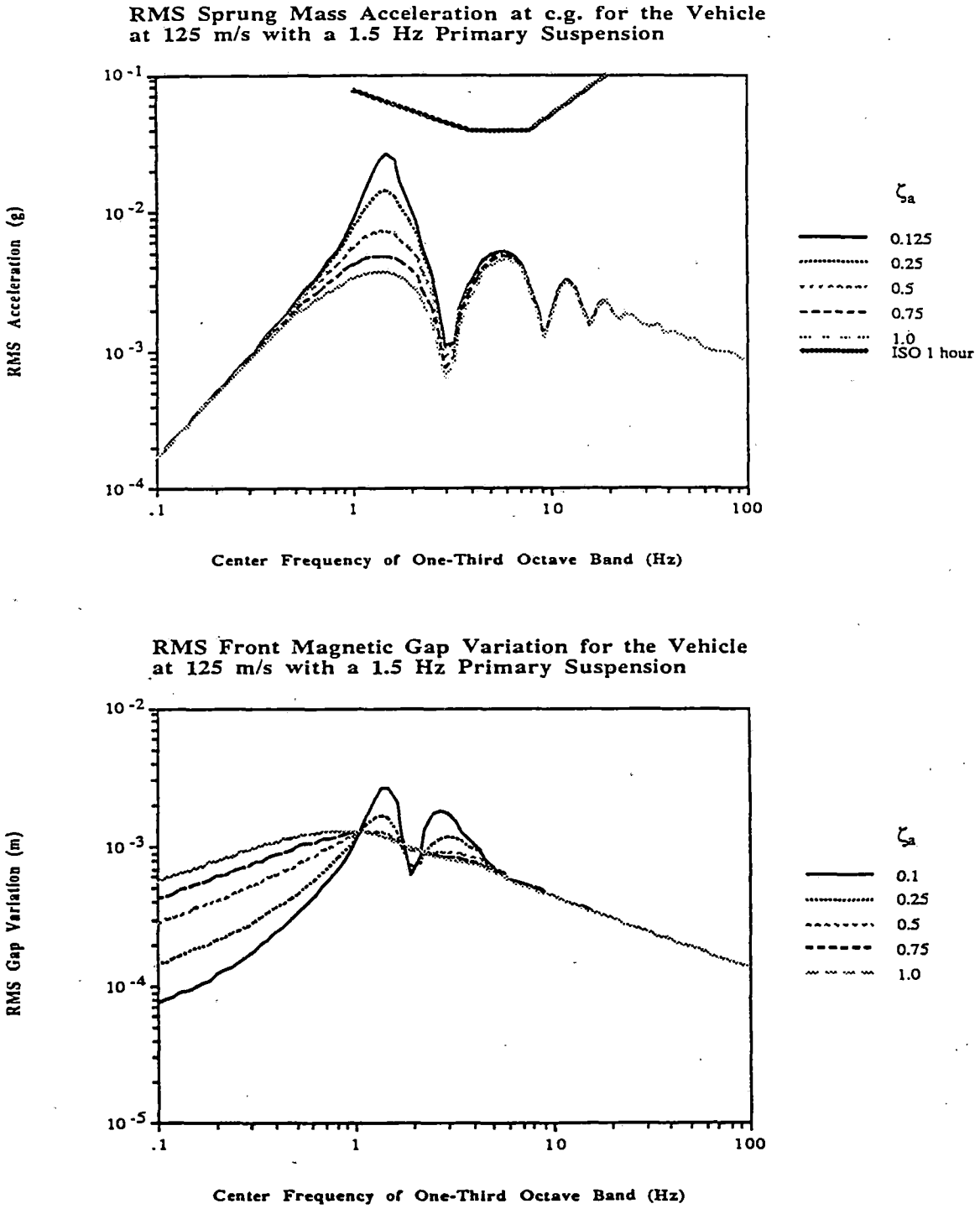

Figure 3.10 ISO Plot For Finite Length Vehicle - Model I

Model II

f_u = 1 Hz, 5 Hz

$\zeta_a = 0, \zeta_u = 0$

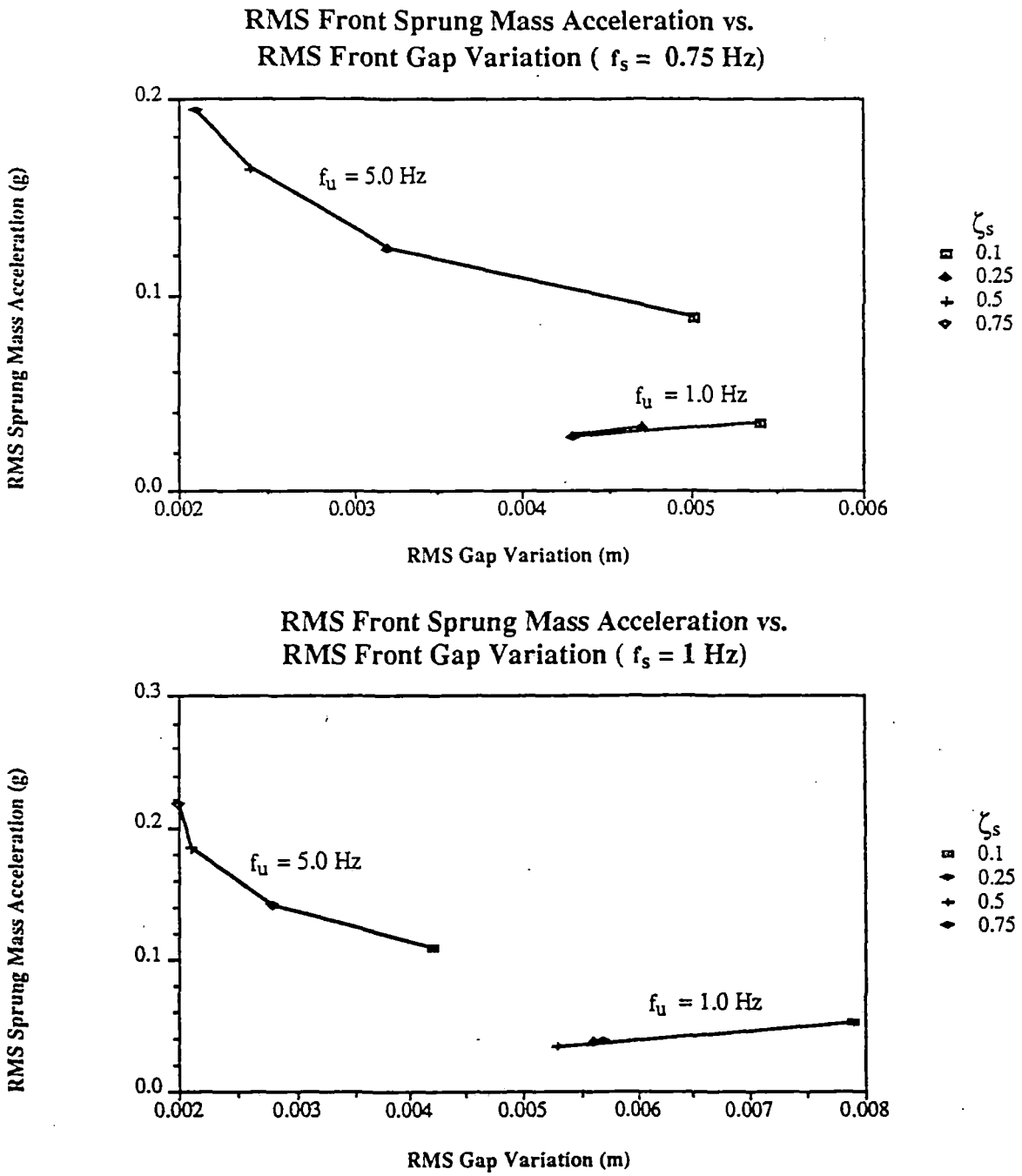

Figure 3.11(a) Front RMS Acceleration Versus Gap For Finite Length Vehicle - Model II

Model II

f_u = 1 Hz, 5 Hz

$\zeta_a = 0, \zeta_u = 0$

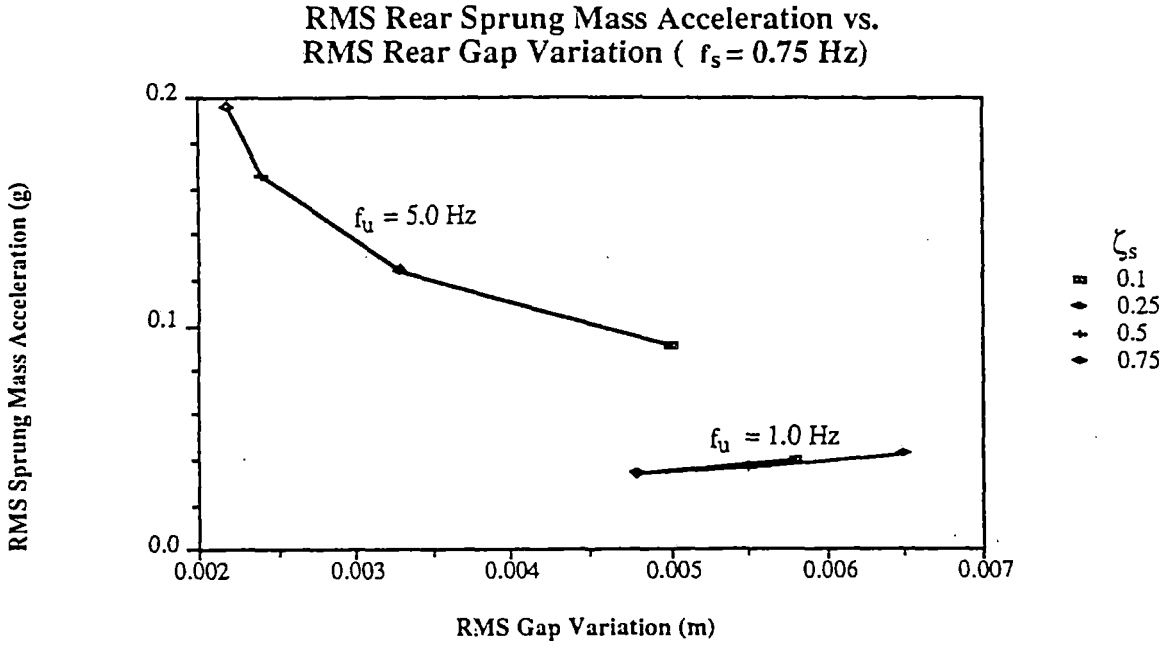

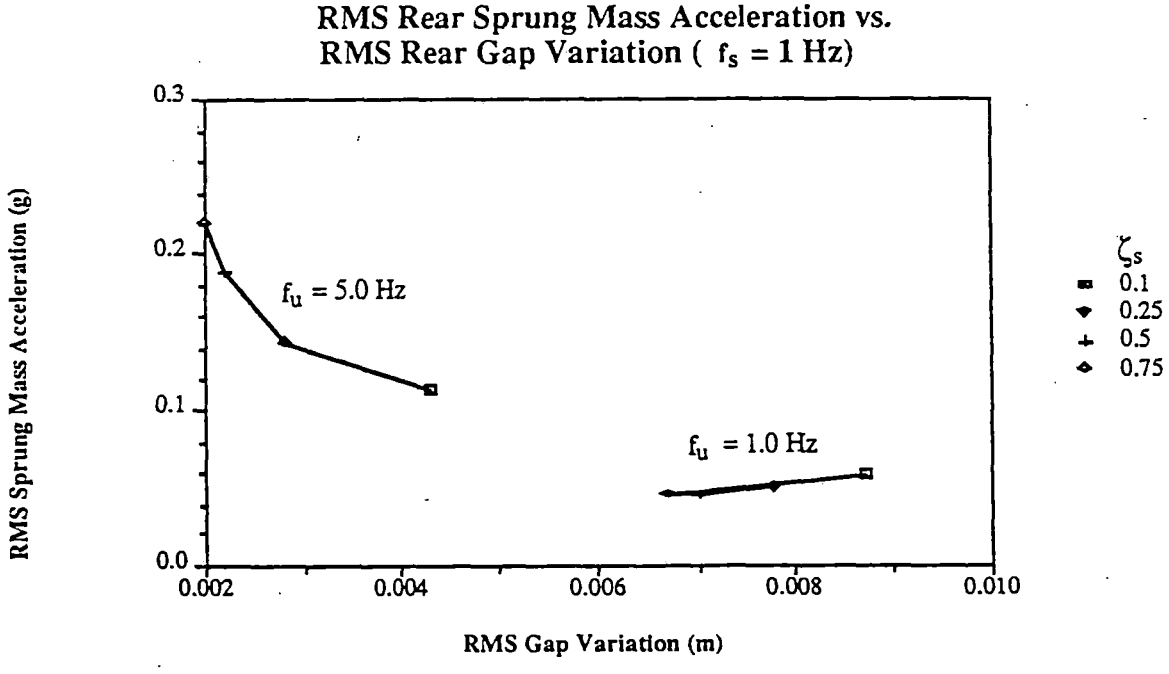

Figure 3.11(b) Rear RMS Acceleration Versus Gap For Finite Length Vehicle - Model II

Model II

$f_s = 1$ Hz, $f_u = 5$ Hz

$\zeta_a = 0$, $\zeta_u = 0$

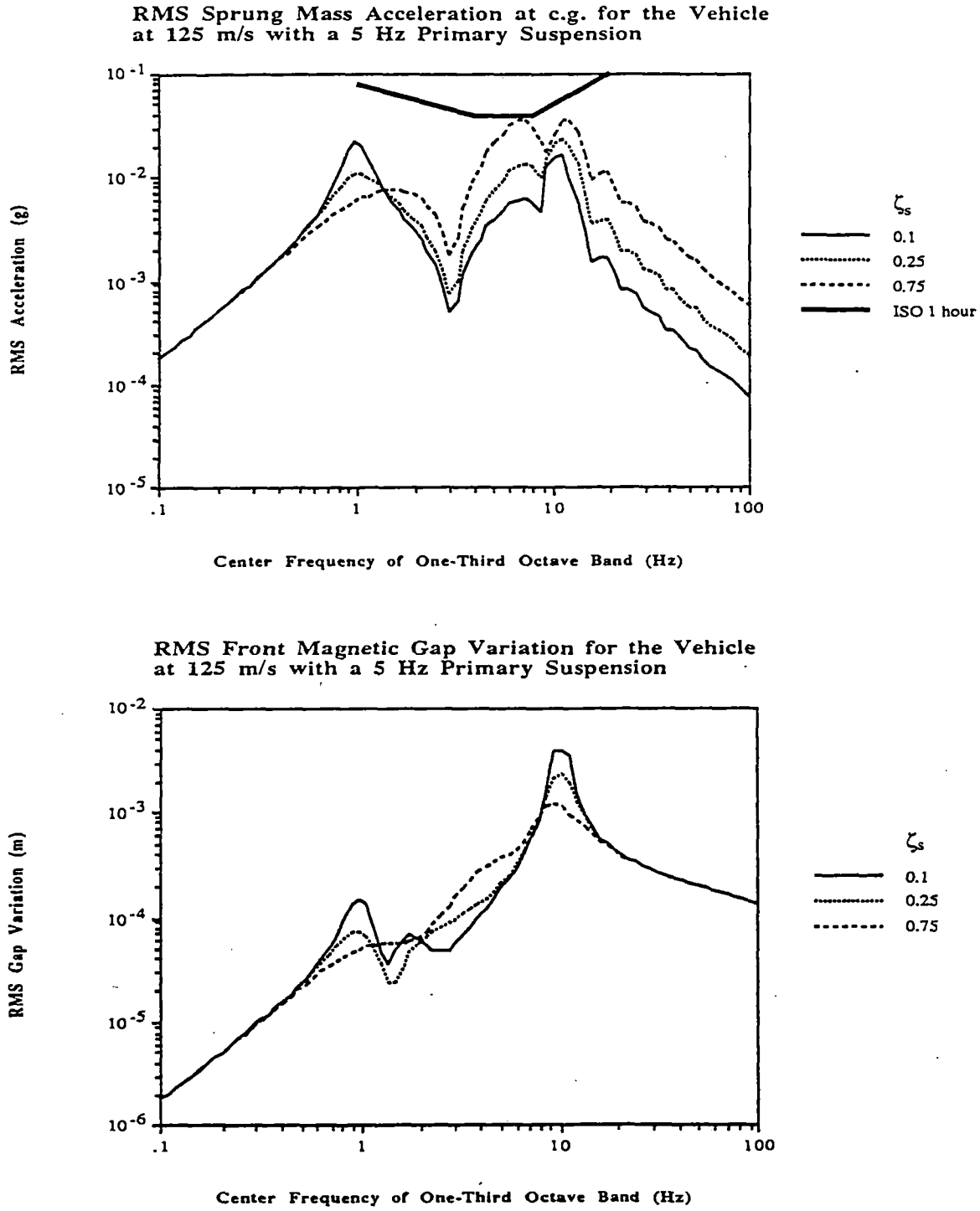

Figure 3.12 ISO Plot For Finite Length Vehicle - Model II

Model III

f_u = 1 Hz, 5 Hz

ζ_s = 0.25, ζ_a = 0

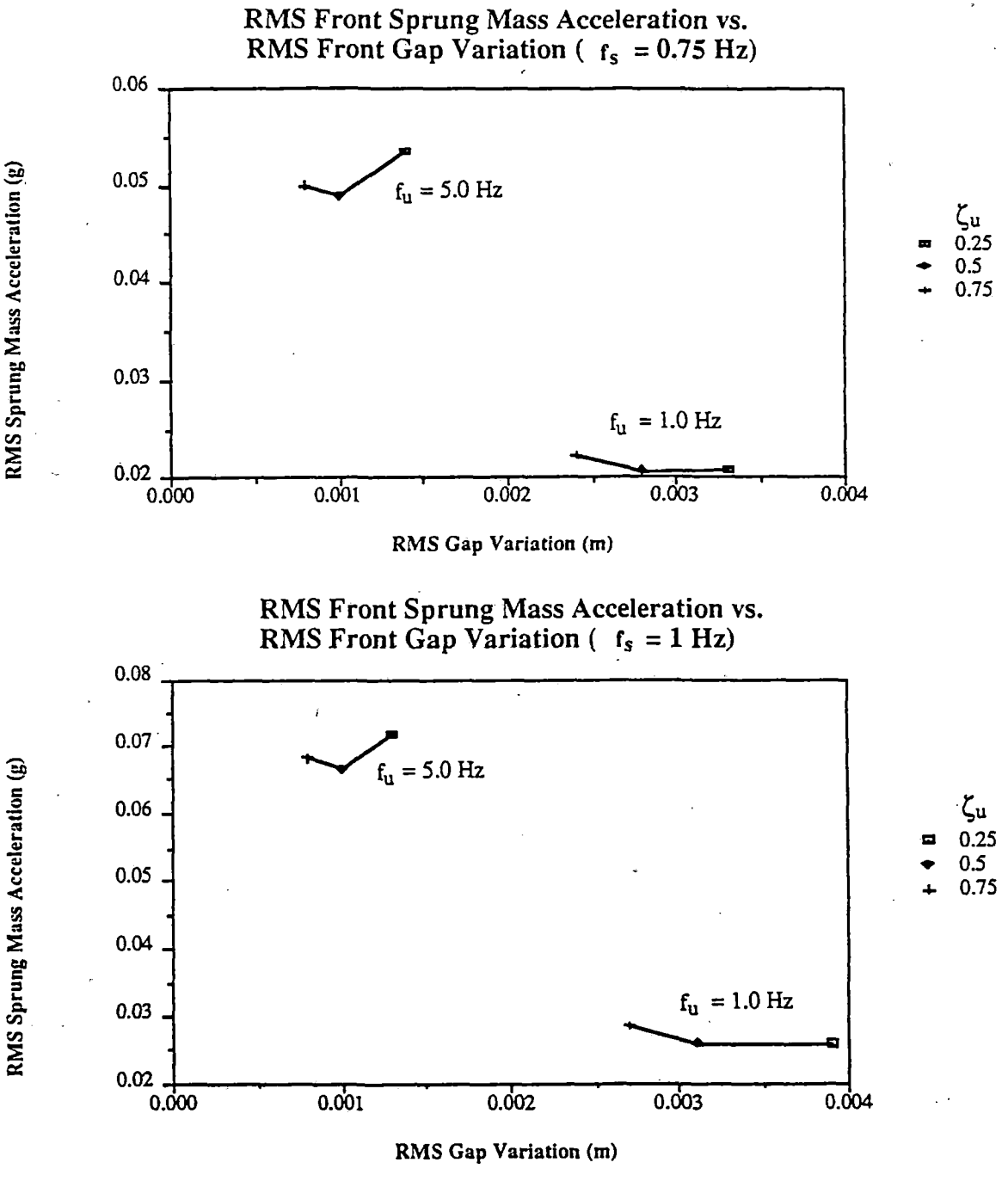

Figure 3.13(a) Front RMS Acceleration Versus Gap For Finite Length Vehicle - Model III

Model III

f_u = 1 Hz, 5 Hz

ζ_s = 0.25, ζ_a = 0

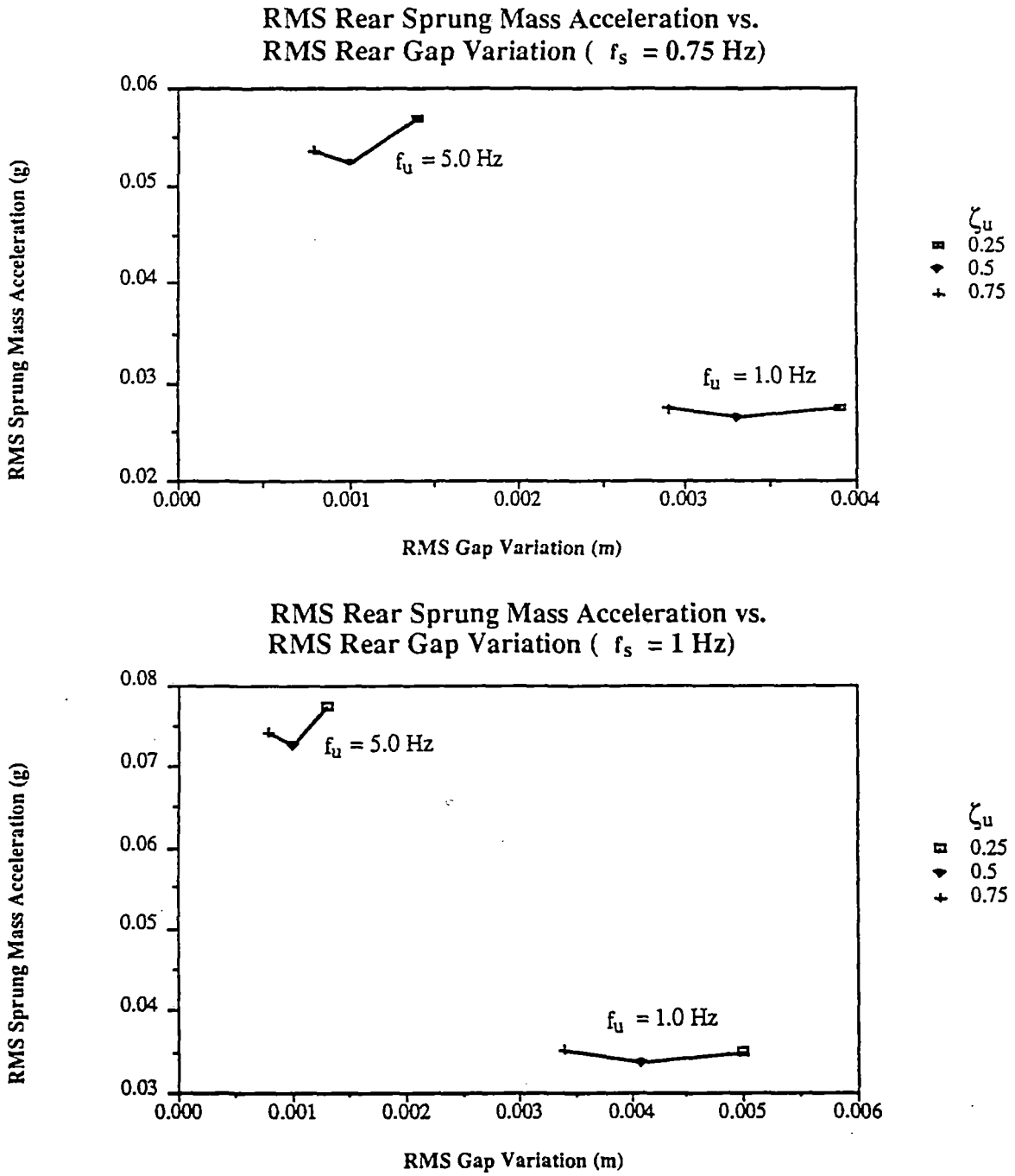

Figure 3.13(b) Rear RMS Acceleration Versus Gap For Finite Length Vehicle - Model III

Model III

$f_s = 1$ Hz, $f_u = 5$ Hz

$\zeta_s = 0.25$, $\zeta_a = 0$

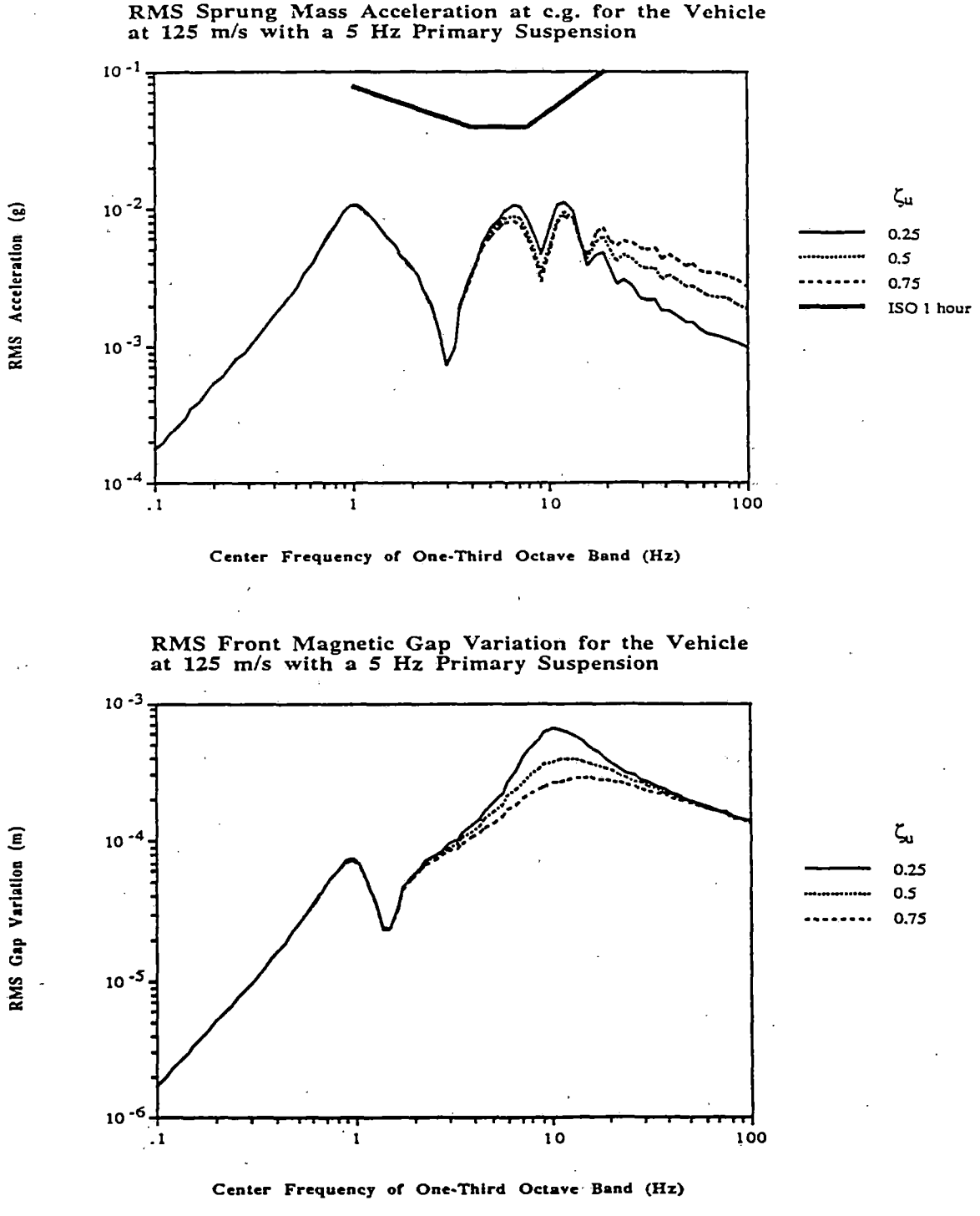

Figure 3.14 ISO Plot For Finite Length Vehicle - Model III

Model IV

f_u = 2.5 Hz, 5 Hz

ζ_u = 0.25, ζ_s = 0.25

RMS Front Sprung Mass Acceleration vs. RMS Front Gap Variation (f_s = 0.75 Hz)

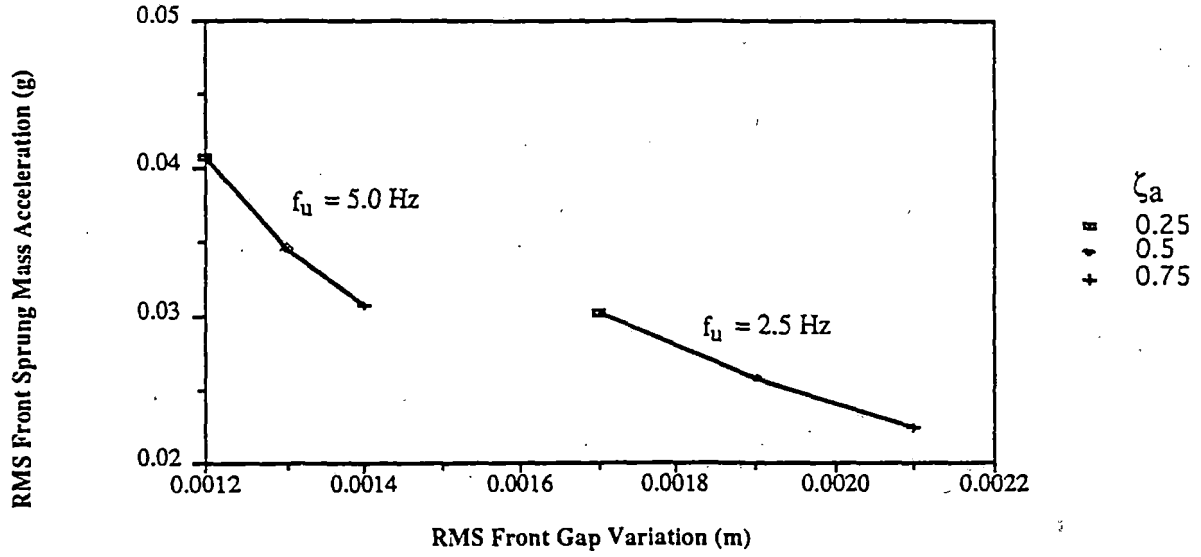

RMS Front Sprung Mass Acceleration vs. RMS Front Gap Variation (f_s = 1 Hz)

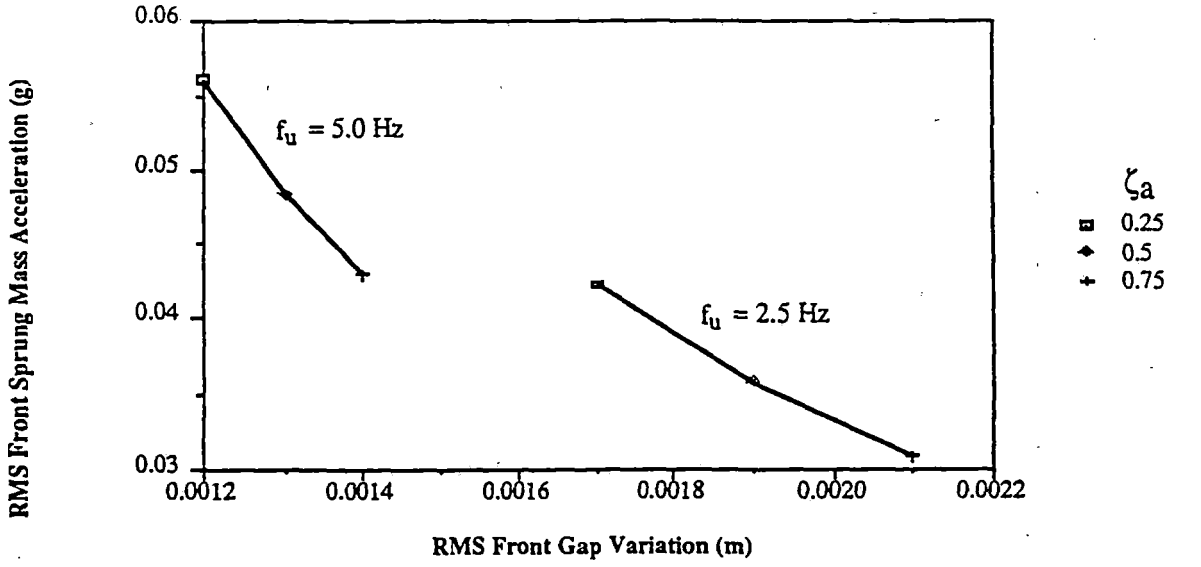

Figure 3.15(a) Front RMS Acceleration Versus Gap For Finite Length Vehicle - Model IV

Model IV

f_u = 2.5 Hz, 5 Hz

ζ_u = 0.25, ζ_s = 0.25

RMS Rear Sprung Mass Acceleration vs. RMS Rear Gap Variation (f_s = 0.75 Hz)

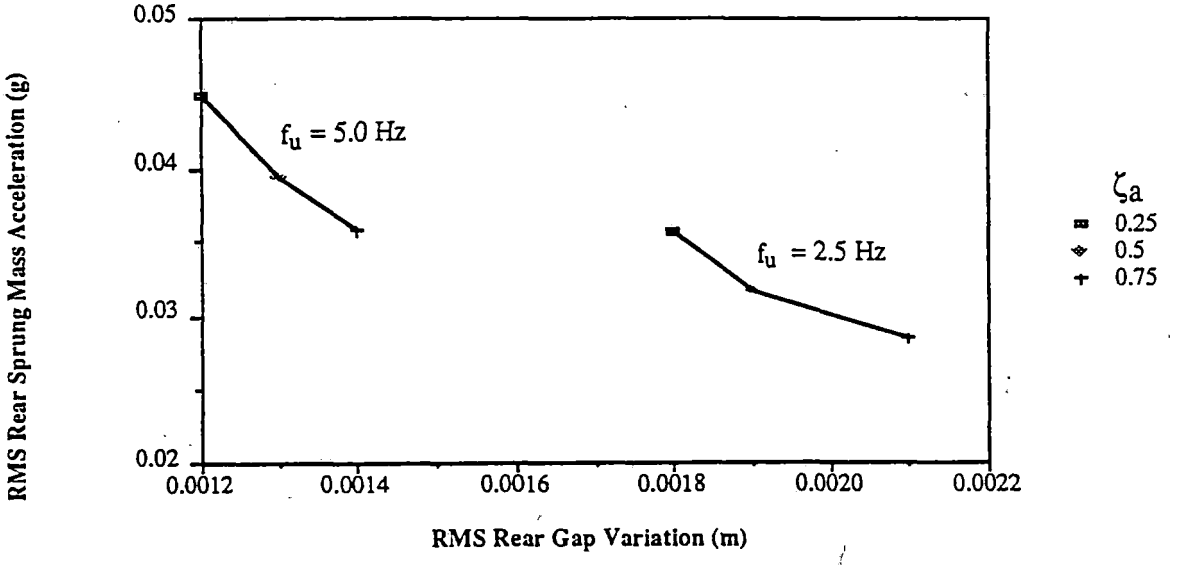

RMS Rear Sprung Mass Acceleration vs. RMS Rear Gap Variation (f_s = 1 Hz)

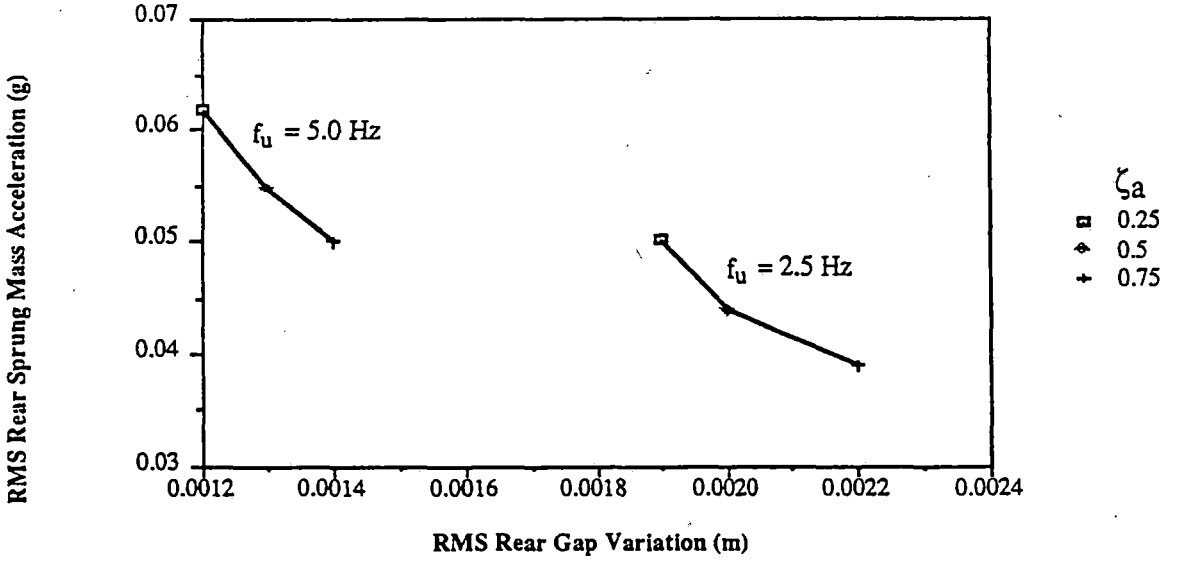

Figure 3.15(b) Rear RMS Acceleration Versus Gap For Finite Length Vehicle - Model IV

Model IV

f_s = 1 Hz, f_u = 5 Hz

ζ_u = 0.25, ζ_s = 0.25

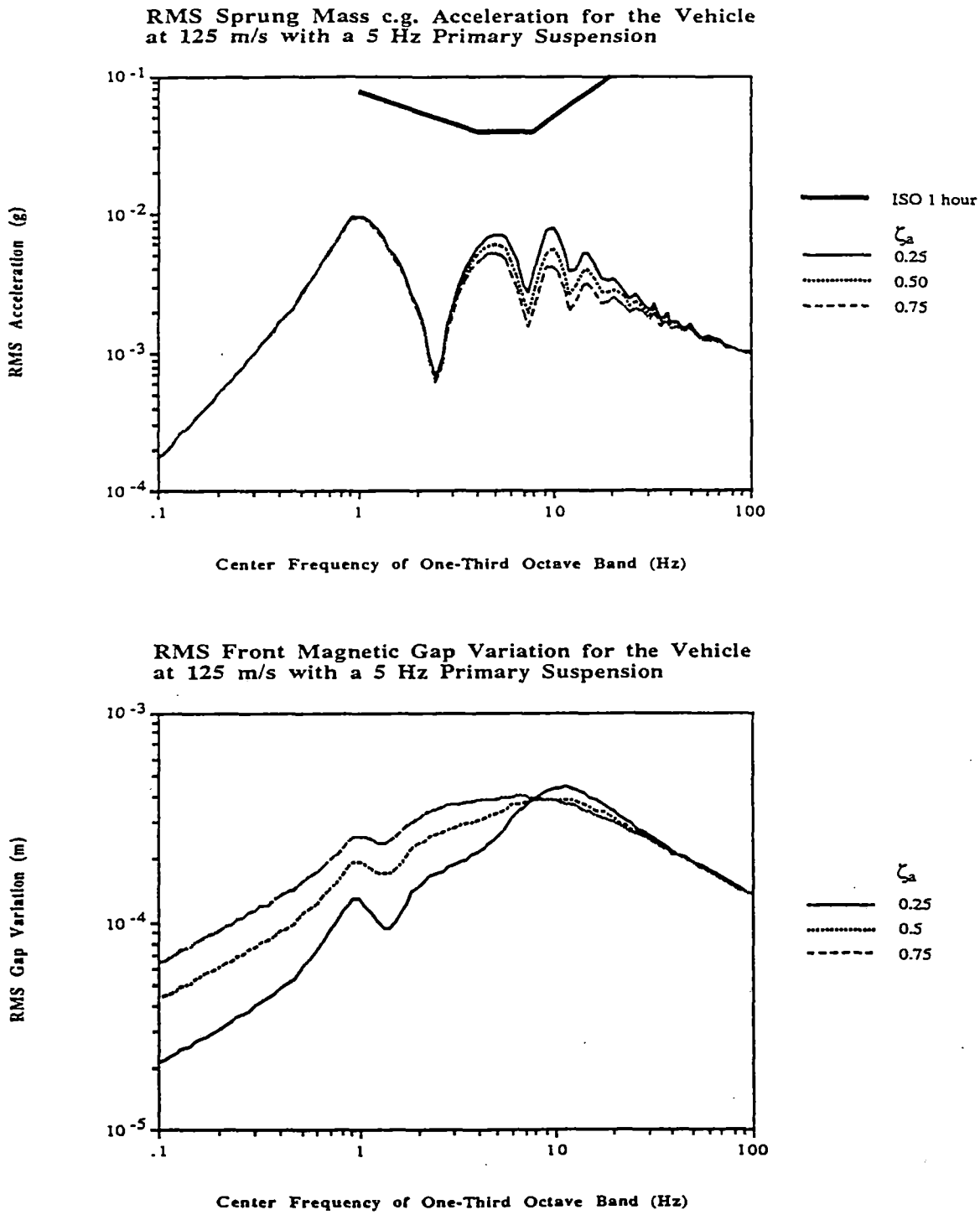

Figure 3.16 ISO Plot For Finite Length Vehicle - Model IV

Data for the finite length vehicle indicate that rms accelerations vary along the vehicle length, with accelerations at the front and rear of the vehicle significantly greater (ranging from 20% to greater than 100%) than the acceleration at the center of the vehicle. The rms front and rear accelerations are also greater than those computed with the one dimensional heave model as illustrated in the Model I suspension model with a 1.0 Hz natural frequency and a 0.25 damping ratio which has a one dimensional model acceleration of 0.02 g while the finite length vehicle has rms accelerations respectively at the front, center and rear positions of 0.033, 0.016 and 0.035 g's. While the rms acceleration at the center of the vehicle is comparable to the one dimensional model, the accelerations at the front and rear are approximately double the center acceleration. These data show that to achieve rms acceleration levels at the front and rear of the vehicle which meet, for example 0.04 g, the finite length vehicle must have a better performing suspension or travel on a smoother guideway than an equivalent one dimensional vehicle model.

The rms gap variations at the front and rear positions on the vehicle are within 25% of the values computed with the one dimensional model and, in all cases are less than 30% of the nominal operating gaps for EDS (5-10 cm) and EMS (0.8 cm) systems.

In summary, the finite length vehicle model studies indicate for the range of parameters considered that:

(1) Model I suspensions with natural frequencies of 1 Hz or less and with absolute damping ratios values of 0.25 to 1.0 yield rms vehicle accelerations of 0.04 g or less and have rms magnetic gap variations of less than 1.0 cm

(2) Model II suspensions with secondary suspension natural frequencies of 0.75 Hz and damping ratios betweeen 0.25 and 0.5 yield rms accelerations less than 0.04 g with rms magnetic gap variations less than 0.6 cm for a 1.0 Hz primary suspension frequency

(3) Model III suspensions with secondary suspension natural frequencies of 0.75-1.0 Hz and a damping ratio of 0.25, with a primary suspension natural frequency of 1.0 Hz and damping ratios between 0.25 and 0.75 yield rms accelerations of 0.04 g with maximum rms magnetic gap variations of less than 0.5 cm

(4) Model IV suspensions with a secondary suspension natural frequency of 0.75 Hz and a damping ratio of 0.25, and with a primary suspension with a relative velocity damping ratio of 0.25 and an absolute damping ratio between 0.25 and 0.75 meet a 0.04 g rms acceleration level for a 2.5 Hz primary suspension with rms magnetic gap variations of less than or equal to 0.21 cm. For an absolute damping ratio between 0.5 and 0.75, a 0.04 g rms acceleration is met with a primary suspension natural frequency of 5 Hz and an rms gap variation of less than 0.15 cm

The study of the finite length vehicle traversing a guideway equivalent to welded steel rail at 125 m/s has shown that a vehicle with front and rear suspension modular magnetic units can provide a level of rms acceleration equal to 0.04 g with any one of the four basic suspension models with the appropriate selection of system parameters. This level of ride quality is achieved with levels of rms magnetic gap variation which are less than 20% of a nominal 5 cm gap for EDS systems and less than 27% of a nominal 0.8 cm gap for EMS systems.

3.4 Multi-Suspension Vehicle Performance

A number of proposed EDS and EMS vehicle configurations employ multiple suspensions distributed along the vehicle length. To approach a representation of these systems, a finite length vehicle with five suspension modules equally spaced along the vehicle is considered. Data for each of the four suspension models implemented in the multi-suspension vehicle are summarized in Table 3.4 for selected suspension designs. These data indicate that the levels of rms acceleration and magnetic gap vary along the vehicle with the highest levels occurring near the front and rear of the vehicle. For all of the cases considered, the multiple suspension vehicle has lower rms accelerations than accelerations on a comparable two suspension vehicle with reductions ranging in most cases from 20 to 50%. The multiple suspension vehicle has gap variations in comparison to the two suspension vehicle, which are similar or in some cases increased by 25%.

A comparison of the accelerations and gaps for the Model II suspension implemented on a single module suspension, a two module suspension and a five module suspension are compared in Figure 3.17. These data show that the one dimensional model is in close agreement with the rms accelerations and magnetic gap variations occurring at the middle suspension of the five suspension vehicle; the two suspension vehicle has 30% higher rms accelerations at the rear position than the multi-suspension vehicle while having a gap which is 6% less. The data show that the use of multiple suspensions tends to reduce the maximum rms accelerations occurring on a vehicle.

Table 3.4
Total RMS Performance of Multi-Suspension Vehicle Model
Traversing Irregular Guideway

Model I

					Total RMS of Sprung Mass Acceleration (g)				
ζ_s	ζ_u	ζ_a	f_s	f_u	1st	2nd	3rd	4th	5th
0	NA	0.125	1	NA	0.0293	0.025	0.0249	0.0292	0.0364
0.125	NA	0	1	NA	0.0365	0.0285	0.0281	0.0355	0.0472
0	NA	0.125	1.5	NA	0.0576	0.0431	0.0414	0.0535	0.0729
0.125	NA	0	1.5	NA	0.0634	0.0459	0.0458	0.0631	0.0881

					Total RMS of Gap Variation (m)				
ζ_s	ζ_u	ζ_a	f_s	f_u	1st	2nd	3rd	4th	5th
0	NA	0.125	1	NA	0.0062	0.0062	0.0067	0.0075	0.0084
0.125	NA	0	1	NA	0.0059	0.006	0.0065	0.0073	0.0083
0	NA	0.125	1.5	NA	0.005	0.0047	0.0051	0.0061	0.0071
0.125	NA	0	1.5	NA	0.0048	0.0044	0.0049	0.0059	0.0071

Model II

					Total RMS of Sprung Mass Acceleration (g)				
ζ_s	ζ_u	ζ_a	f_s	f_u	1st	2nd	3rd	4th	5th
0.1	0	0	0.75	1	0.0238	0.0219	0.0227	0.026	0.031
0.1	0	0	1	1	0.0356	0.0331	0.0345	0.0396	0.0471
0.1	0	0	0.75	5	0.0299	0.0217	0.0198	0.0258	0.0359
0.1	0	0	1	5	0.0401	0.0301	0.0295	0.0387	0.0528

					Total RMS of Gap Variation (m)				
ζ_s	ζ_u	ζ_a	f_s	f_u	1st	2nd	3rd	4th	5th
0.1	0	0	0.75	1	0.0052	0.0054	0.0057	0.0059	0.0062
0.1	0	0	1	1	0.0072	0.0073	0.0077	0.0083	0.0091
0.1	0	0	0.75	5	0.005	0.0051	0.0051	0.0051	0.0051
0.1	0	0	1	5	0.0043	0.0044	0.0043	0.0043	0.0043

Table 3.4
Total RMS Performance of Multi-Suspension Vehicle Model
Traversing Irregular Guideway

Model III

					Total RMS of Sprung Mass Acceleration (g)				
ζ_s	ζ_u	ζ_a	f_s	f_u	1st	2nd	3rd	4th	5th
0.25	0.25	0	0.75	1	0.0158	0.0138	0.0139	0.0161	0.0196
0.25	0.25	0	1	1	0.0201	0.0178	0.0183	0.0215	0.0264
0.25	0.25	0	0.75	5	0.0241	0.017	0.0147	0.019	0.0271
0.25	0.25	0	1	5	0.0339	0.0238	0.021	0.0279	0.0397

					Total RMS of Gap Variation (m)				
ζ_s	ζ_u	ζ_a	f_s	f_u	1st	2nd	3rd	4th	5th
0.25	0.25	0	0.75	1	0.0033	0.0033	0.0034	0.0036	0.0038
0.25	0.25	0	1	1	0.0039	0.004	0.0042	0.0045	0.005
0.25	0.25	0	0.75	5	0.0014	0.0014	0.0014	0.0014	0.0014
0.25	0.25	0	1	5	0.0013	0.0013	0.0013	0.0013	0.0013

Model IV

					Total RMS of Sprung Mass Acceleration (g)				
ζ_s	ζ_u	ζ_a	f_s	f_u	1st	2nd	3rd	4th	5th
0.25	0.25	0.25	0.75	2.5	0.0195	0.015	0.0141	0.0173	0.023
0.25	0.25	0.25	1	2.5	0.0272	0.0209	0.02	0.0253	0.0339
0.25	0.25	0.25	0.75	5	0.0216	0.0159	0.0144	0.0181	0.0248
0.25	0.25	0.25	1	5	0.0308	0.0224	0.0205	0.0266	0.0369

					Total RMS of Gap Variation (m)				
ζ_s	ζ_u	ζ_a	f_s	f_u	1st	2nd	3rd	4th	5th
0.25	0.25	0.25	0.75	2.5	0.0017	0.0017	0.0017	0.0017	0.0018
0.25	0.25	0.25	1	2.5	0.0018	0.0017	0.0017	0.0018	0.0019
0.25	0.25	0.25	0.75	5	0.0012	0.0012	0.0012	0.0012	0.0012
0.25	0.25	0.25	1	5	0.0012	0.0012	0.0012	0.0012	0.0012

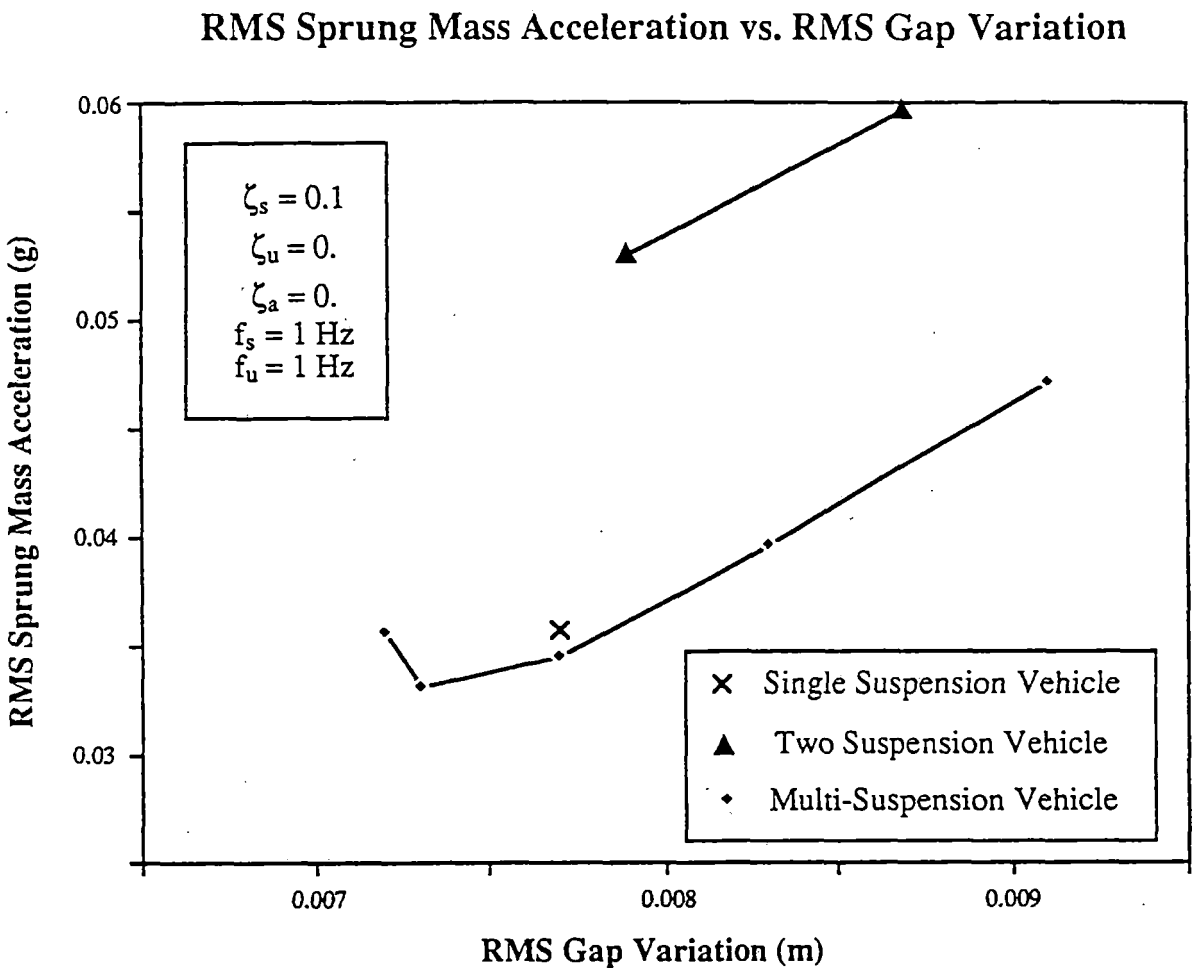

Figure 3.17 RMS Acceleration Versus Gap For Multi-Suspension, Two Suspension and Single Suspension Vehicles

4. VEHICLE PERFORMANCE TRAVERSING DISCRETE GUIDEWAY PERTURBATIONS

4.1 Discrete Guideway Perturbations

The responses of finite length vehicles to the three types of discrete perturbations illustrated in Figure 2.4 have been computed. For each of the perturbations a guideway has been constructed with the perturbations spaced uniformly occurring on a 25m periodic basis with constant perturbation amplitudes of 1.0 cm. The rms performance of the finite length vehicle models has been determined for the vehicles traversing a sufficient number of perturbations to reach a periodic response from which rms accelerations and magnetic gap variations have been computed. The four suspension configurations defined in Chapter 2 have been considered with the finite length two and multiple suspension vehicle configurations. For the two suspension case the suspensions are located 20m apart, while for the six suspension case, the suspensions are distributed uniformly across a 20 meter span.

4.2 Vehicle Response to Periodic Step Perturbations

The rms acceleration and rms gap variations for a finite length vehicle traversing step type discontinuities with two suspensions and six suspension elements are tabulated respectively in Tables 4.1 and 4.2. The step discontinuities correspond to span vertical height misalignment. For all of the vehicle configurations, the data show that the multiple suspension vehicle has reduced levels of rms acceleration in comparison to equivalent two suspension vehicle configurations. For the multiple suspension vehicle design cases considered in Table 4.2, the value of step amplitude and corresponding magnetic gap variation corresponding to a maximum level of rms acceleration of 0.04 g on the vehicle for each design are summarized in Table 4.3.

For each configuration if the rms acceleration limits were increased from 0.04g to 0.06g, for example, the amplitude of disturbance which could be tolerated would increase by 50% from the values tabulated, thus ride quality constraints have a direct influence on construction practice. The data show that Models I, II and III corresponding to possible EDS configurations, have sets of suspension parameters which can accommodate greater than 1.0 cm step amplitudes while achieving 0.04g rms accelerations with rms gap variations in the 0.5 to 0.8 cm range. Model IV, which corresponds to possible EMS designs can also provide 0.04g rms acceleration levels with 1.0 cm step amplitudes while having rms gap variations in the 0.23 to 0.32 cm range. However, EMS designs with a nominal operating gap on the order of 1 cm, could not be employed successfully on

Table 4.1
Total RMS Performance of Two Suspension Vehicle Model To Step Input
(Step Height = 0.01 m)

Model I

Total RMS of Sprung Mass Acceleration (g)				f_s = 1 Hz			f_s = 1.5 Hz		
ζ_s	ζ_u	ζ_a	f_u	Front	Center	Rear	Front	Center	Rear
0	NA	0.125	NA	0.0767	0.0097	0.0812	0.2434	0.0251	0.2805
0	NA	0.25	NA	0.0597	0.0096	0.0665	0.1183	0.0240	0.1501
0	NA	0.5	NA	0.0380	0.0093	0.0453	0.0634	0.0214	0.0836
0	NA	0.75	NA	0.0281	0.0088	0.0344	0.0478	0.0194	0.0609
0	NA	1	NA	0.0230	0.0084	0.0281	0.0403	0.0179	0.0494
0.125	NA	0	NA	0.0653	0.0091	0.0720	0.2242	0.0237	0.2604
0.25	NA	0	NA	0.0342	0.0073	0.0443	0.1029	0.0188	0.1299
0.5	NA	0	NA	0.0820	0.0025	0.0868	0.1580	0.0090	0.1751

Total RMS of Gap Variation (m)				f_s = 1 Hz			f_s = 1.5 Hz		
ζ_s	ζ_u	ζ_a	f_u	Front	Center	Rear	Front	Center	Rear
0	NA	0.125	NA	0.0074		0.0079	0.0096		0.0133
0	NA	0.25	NA	0.0064		0.0072	0.0060		0.0085
0	NA	0.5	NA	0.0055		0.0061	0.0052		0.0063
0	NA	0.75	NA	0.0053		0.0056	0.0051		0.0056
0	NA	1	NA	0.0052		0.0054	0.0051		0.0054
0.125	NA	0	NA	0.0069		0.0079	0.0085		0.0126
0.25	NA	0	NA	0.0052		0.0068	0.0040		0.0073
0.5	NA	0	NA	0.0034		0.0050	0.0027		0.0045

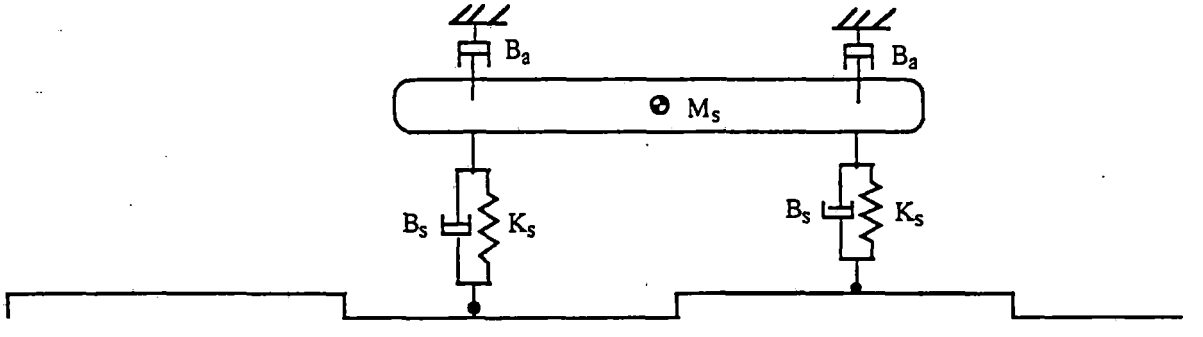

Model I

Table 4.1
Total RMS Performance of Two Suspension Vehicle Model To Step Input
(Step Height = 0.01 m)

Model II

Total RMS of Sprung Mass Acceleration (g)				f_u = 1 Hz			f_u = 5 Hz		
ζ_s	ζ_u	ζ_a	f_s (Hz)	Front	Center	Rear	Front	Center	Rear
0.1	0	0	0.75	0.0839	0.0116	0.0902	0.0556	0.0195	0.0571
0.25	0	0	0.75	0.0555	0.0078	0.0573	0.1001	0.0443	0.1062
0.5	0	0	0.75	0.0502	0.0073	0.0510	0.1697	0.0824	0.1894
0.75	0	0	0.75	0.0493	0.0075	0.0499	0.2287	0.1137	0.2664
0.1	0	0	1	0.0799	0.0125	0.0832	0.1023	0.0278	0.1065
0.25	0	0	1	0.0579	0.0084	0.0592	0.1434	0.0590	0.1562
0.5	0	0	1	0.0512	0.0077	0.0519	0.2159	0.1044	0.2490
0.75	0	0	1	0.0498	0.0079	0.0504	0.2830	0.1387	0.3408

Total RMS of Gap Variation (m)				f_u = 1 Hz			f_u = 5 Hz		
ζ_s	ζ_u	ζ_a	f_s (Hz)	Front	Center	Rear	Front	Center	Rear
0.1	0	0	0.75	0.0116		0.0117	0.0035		0.0035
0.25	0	0	0.75	0.0082		0.0073	0.0035		0.0035
0.5	0	0	0.75	0.0073		0.0068	0.0034		0.0034
0.75	0	0	0.75	0.0071		0.0067	0.0033		0.0034
0.1	0	0	1	0.0064		0.0046	0.0035		0.0035
0.25	0	0	1	0.0069		0.0061	0.0034		0.0034
0.5	0	0	1	0.0069		0.0065	0.0033		0.0034
0.75	0	0	1	0.0069		0.0066	0.0032		0.0034

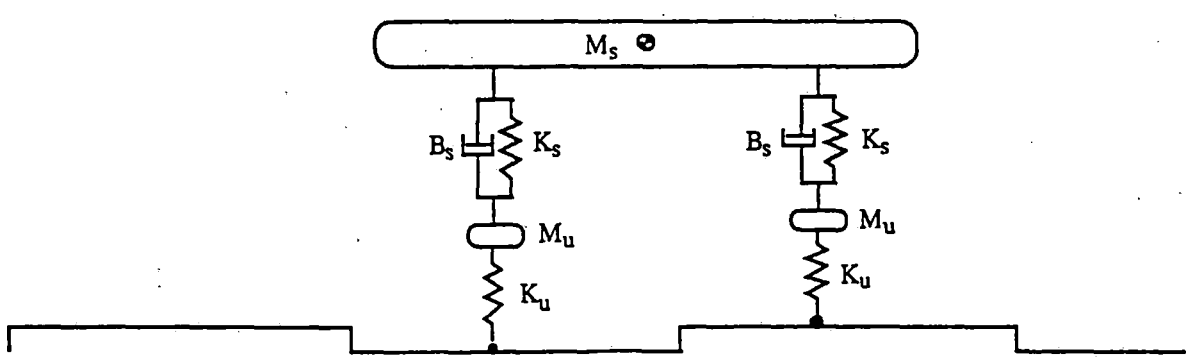

Model II

Table 4.1
Total RMS Performance of Two Suspension Vehicle Model To Step Input
(Step Height = 0.01 m)

Model III

Total RMS of Sprung Mass Acceleration (g)				f_u = 1 Hz			f_u = 5 Hz		
ζ_s	ζ_u	ζ_a	f_s (Hz)	Front	Center	Rear	Front	Center	Rear
0.25	0.25	0	0.75	0.0430	0.0061	0.0449	0.0889	0.0340	0.0940
0.25	0.5	0	0.75	0.0438	0.0075	0.0460	0.0883	0.0305	0.0925
0.25	0.75	0	0.75	0.0471	0.0094	0.0496	0.0929	0.0308	0.0966
0.25	0.25	0	1	0.0506	0.0077	0.0533	0.1286	0.0447	0.1399
0.25	0.5	0	1	0.0553	0.0099	0.0590	0.1277	0.0406	0.1378
0.25	0.75	0	1	0.0619	0.0126	0.0665	0.1331	0.0411	0.1421

Total RMS of Gap Variation (m)				f_u = 1 Hz			f_u = 5 Hz		
ζ_s	ζ_u	ζ_a	f_s (Hz)	Front	Center	Rear	Front	Center	Rear
0.25	0.25	0	0.75	0.0055		0.0051	0.0024		0.0024
0.25	0.5	0	0.75	0.0042		0.0041	0.0018		0.0018
0.25	0.75	0	0.75	0.0035		0.0034	0.0015		0.0015
0.25	0.25	0	1	0.0052		0.0049	0.0024		0.0024
0.25	0.5	0	1	0.0042		0.0041	0.0018		0.0018
0.25	0.75	0	1	0.0036		0.0035	0.0015		0.0015

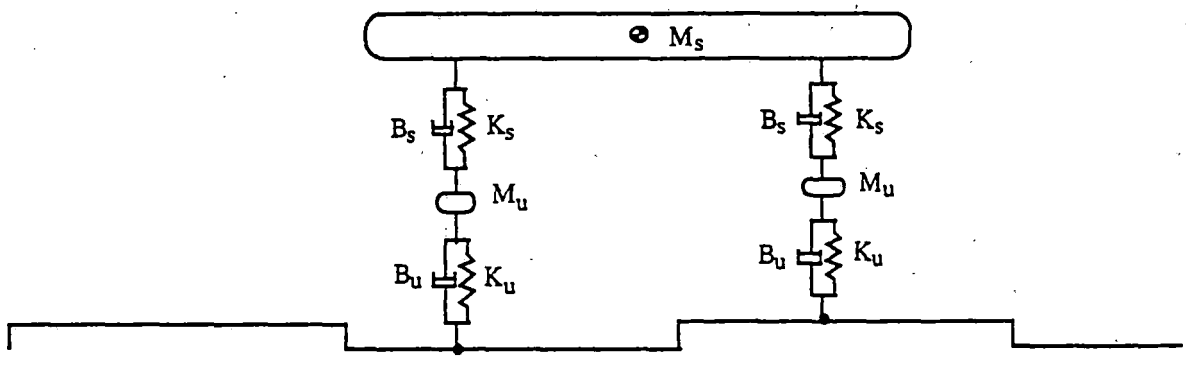

Model III

Table 4.1
Total RMS Performance of Two Suspension Vehicle Model To Step Input
(Step Height = 0.01 m)

Model IV

Total RMS of Sprung Mass Acceleration (g)				f_u = 2.5 Hz			f_u = 5 Hz		
ζ_s	ζ_u	ζ_a	f_s (Hz)	Front	Center	Rear	Front	Center	Rear
0.25	0.25	0.25	0.75	0.0647	0.0120	0.0687	0.0759	0.0236	0.0805
0.25	0.25	0.5	0.75	0.0547	0.0100	0.0582	0.0682	0.0182	0.0724
0.25	0.25	0.75	0.75	0.0468	0.0086	0.0498	0.0625	0.0150	0.0664
0.25	0.25	0.25	1	0.0970	0.0164	0.1055	0.1126	0.0315	0.1231
0.25	0.25	0.5	1	0.0816	0.0137	0.0891	0.1024	0.0246	0.1124
0.25	0.25	0.75	1	0.0698	0.0118	0.0763	0.0944	0.0205	0.1038

Total RMS of Gap Variation (m)				f_u = 2.5 Hz			f_u = 5 Hz		
ζ_s	ζ_u	ζ_a	f_s (Hz)	Front	Center	Rear	Front	Center	Rear
0.25	0.25	0.25	0.75	0.0031		0.0031	0.0022		0.0022
0.25	0.25	0.5	0.75	0.0034		0.0034	0.0023		0.0023
0.25	0.25	0.75	0.75	0.0037		0.0037	0.0026		0.0026
0.25	0.25	0.25	1	0.0033		0.0033	0.0022		0.0022
0.25	0.25	0.5	1	0.0036		0.0036	0.0023		0.0024
0.25	0.25	0.75	1	0.0038		0.0038	0.0026		0.0026

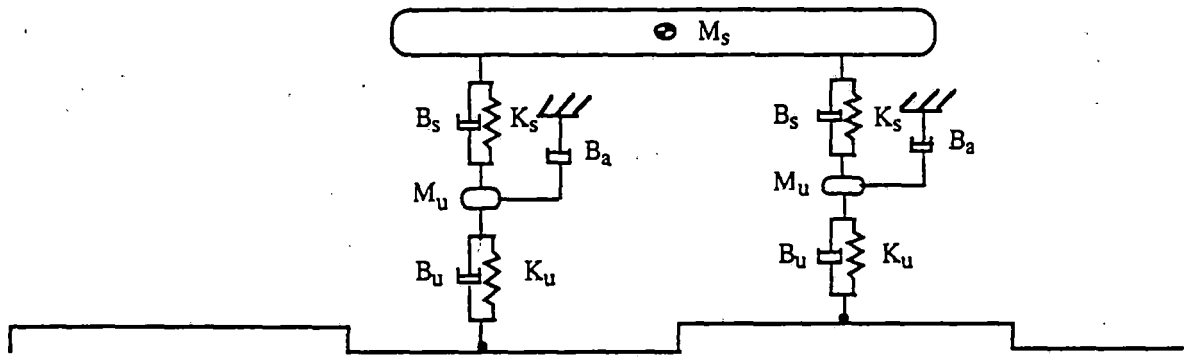

Model IV

Table 4.2
Total RMS Performance of Multi-Suspension Vehicle Model To Step Input

Model I

Design						Total RMS of Sprung Mass Acceleration (g)					
	ζ_s	ζ_u	ζ_a	f_s	f_u	1st	2nd	3rd	4th	5th	6th
a	0	NA	0.125	1	NA	0.0373	0.0246	0.0150	0.0159	0.0262	0.0390
b	0.125	NA	0	1	NA	0.0337	0.0222	0.0138	0.0152	0.0248	0.0366
c	0	NA	0.125	1.5	NA	0.1179	0.0745	0.0419	0.0501	0.0884	0.1330
d	0.125	NA	0	1.5	NA	0.1073	0.0670	0.0380	0.0486	0.0852	0.1270

Design						Total RMS of Gap Variation (m)					
	ζ_s	ζ_u	ζ_a	f_s	f_u	1st	2nd	3rd	4th	5th	6th
a	0	NA	0.125	1	NA	0.0064	0.0058	0.0055	0.0056	0.0060	0.0064
b	0.125	NA	0	1	NA	0.0064	0.0057	0.0054	0.0056	0.0060	0.0062
c	0	NA	0.125	1.5	NA	0.0093	0.0074	0.0063	0.0068	0.0083	0.0097
d	0.125	NA	0	1.5	NA	0.0092	0.0070	0.0061	0.0069	0.0083	0.0095

Model II

Design						Total RMS of Sprung Mass Acceleration (g)					
	ζ_s	ζ_u	ζ_a	f_s	f_u	1st	2nd	3rd	4th	5th	6th
a	0.25	0	0	0.75	1	0.0391	0.0265	0.0172	0.0176	0.0273	0.0401
b	0.25	0	0	0.75	5	0.0400	0.0275	0.0188	0.0197	0.0293	0.0421
c	0.25	0	0	1	1	0.0416	0.0283	0.0184	0.0187	0.0289	0.0424
d	0.25	0	0	1	5	0.0610	0.0412	0.0274	0.0296	0.0456	0.0660

Design						Total RMS of Gap Variation (m)					
	ζ_s	ζ_u	ζ_a	f_s	f_u	1st	2nd	3rd	4th	5th	6th
a	0.25	0	0	0.75	1	0.0076	0.0082	0.0084	0.0082	0.0079	0.0081
b	0.25	0	0	0.75	5	0.0034	0.0034	0.0034	0.0034	0.0034	0.0034
c	0.25	0	0	1	1	0.0058	0.0063	0.0063	0.0060	0.0059	0.0065
d	0.25	0	0	1	5	0.0034	0.0034	0.0034	0.0034	0.0034	0.0034

Table 4.2
Total RMS Performance of Multi-Suspension Vehicle Model To Step Input

Model III

Design						Total RMS of Sprung Mass Acceleration (g)					
	ζ_s	ζ_u	ζ_a	f_s	f_u	1st	2nd	3rd	4th	5th	6th
a	0.25	0.25	0	0.75	1	0.0277	0.0186	0.0119	0.0123	0.0195	0.0287
b	0.25	0.25	0	0.75	5	0.0395	0.0268	0.0178	0.0187	0.0286	0.0415
c	0.25	0.25	0	1	1	0.0335	0.0225	0.0144	0.0151	0.0237	0.0349
d	0.25	0.25	0	1	5	0.0602	0.0403	0.0262	0.0284	0.0446	0.0650

Design						Total RMS of Gap Variation (m)					
	ζ_s	ζ_u	ζ_a	f_s	f_u	1st	2nd	3rd	4th	5th	6th
a	0.25	0.25	0	0.75	1	0.0050	0.0051	0.0051	0.0050	0.0050	0.0052
b	0.25	0.25	0	0.75	5	0.0024	0.0024	0.0024	0.0024	0.0024	0.0024
c	0.25	0.25	0	1	1	0.0045	0.0045	0.0044	0.0042	0.0043	0.0047
d	0.25	0.25	0	1	5	0.0024	0.0024	0.0023	0.0023	0.0024	0.0024

Model IV

Design						Total RMS of Sprung Mass Acceleration (g)					
	ζ_s	ζ_u	ζ_a	f_s	f_u	1st	2nd	3rd	4th	5th	6th
a	0.25	0.25	0.25	0.75	2.5	0.0361	0.0240	0.0151	0.0160	0.0256	0.0379
b	0.25	0.25	0.25	0.75	5	0.0376	0.0253	0.0164	0.0173	0.0271	0.0396
c	0.25	0.25	0.25	1	2.5	0.0529	0.0349	0.0218	0.0236	0.0383	0.0566
d	0.25	0.25	0.25	1	5	0.0575	0.0382	0.0243	0.0266	0.0424	0.0623

Design						Total RMS of Gap Variation (m)					
	ζ_s	ζ_u	ζ_a	f_s	f_u	1st	2nd	3rd	4th	5th	6th
a	0.25	0.25	0.25	0.75	2.5	0.0030	0.0030	0.0030	0.0030	0.0030	0.0030
b	0.25	0.25	0.25	0.75	5	0.0022	0.0021	0.0021	0.0021	0.0021	0.0022
c	0.25	0.25	0.25	1	2.5	0.0031	0.0030	0.0029	0.0029	0.0030	0.0031
d	0.25	0.25	0.25	1	5	0.0022	0.0021	0.0021	0.0021	0.0021	0.0022

Table 4.3

Disturbance Level To Achieve a 0.04g RMS Acceleration For Step Discontinuity

DESIGN	a		b		c		d	
	Distrubance Amplitude (cm)	RMS Gap (cm)	Disturbance Amplitude (cm)	RMS Gap (cm)	Disturbance Amplitude (cm)	RMS Gap (cm)	Disturbance Amplitude (cm)	RMS Gap (cm)
I	1.0	0.64	1.1	0.70	0.34	0.30	0.31	0.30
II	1.0	0.80	0.95	0.32	0.95	0.62	0.60	0.21
III	1.39	0.72	0.96	0.23	1.15	0.53	0.62	0.15
IV	1.05	0.32	1.01	0.23	0.70	0.21	0.64	0.14

a guideway with 1 cm amplitude step disturbances, and, in fact, the disturbance levels would have to be maintained at less than 1 cm.

4.3 Vehicle Response to Periodic Variations in Slope

The responses of the four suspension configurations to periodic changes in slope, corresponding to pier misalignments, are summarized for the two suspension and multiple suspension vehicles respectively in Tables 4.4 and 4.5. Data for the multiple suspension vehicles for all configurations are less than comparable data for the two suspension vehicle. Data for the multiple suspension designs which indicate the level of slope which can be accommodated while limiting accelerations on the vehicle to 0.04g are tabulated in Table 4.6.

For Models I, II and III corresponding to possible EDS configurations, suspension design parameters exist corresponding to those in Table 4.6 for which pier misalignments on the order of 1.6 cm could be accommodated for 25m span systems while achieving a 0.04g rms acceleration level and while achieving magnetic gap variations of 0.6-0.8 cm. In a similar manner Model IV designs can accommodate approximately 1.6 cm pier misalignments while achieving 0.04g rms acceleration levels with rms gap variations ranging from approximately 0.1-0.2 cm.

4.4 Vehicle Response to Periodic Camber Disturbances

The vehicle rms acceleration and magnetic gap variation responses to periodic camber disturbances are tabulated in Tables 4.7 and 4.8 respectively for two and multiple suspension vehicles. As in the cases described above, the multiple suspension vehicle has lower values of acceleration than the vehicle with front and rear boggies. For the multiple suspension vehicle, the levels of camber which can be accommodated while achieving a 0.04g rms acceleration level are tabulated in Table 4.9.

The data in Table 4.9 indicate for Models I, II and III corresponding to EDS suspensions that amplitudes exceeding 1.0 cm of camber can be accommodated while meeting a 0.04g rms acceleration level. For some design cases the camber amplitudes are sufficiently large so that gap variations rather than acceleration would be limiting. For the Model IV designs, amplitudes in excess of 1.0 cm may also be accommodated without exceeding 0.04g; however, the rms gap variation constraints would preclude the accommodation of camber greater than 1.0 cm for design IVa if an rms gap variation of less than 0.25 cm were permitted. Thus, constraints on gap variation as well as acceleration can provide limits to allowable camber amplitudes. These limitations on camber have led to the proposal to employ two-span continuous guideways rather than simple span elevated

Table 4.4
Total RMS Performance of Two Suspension Vehicle Model To Ramp Input
(Ramp Slope = 0.001)

Model I

Total RMS of Sprung Mass Acceleration (g)				f_s = 1 Hz			f_s = 1.5 Hz		
ζ_s	ζ_u	ζ_a	f_u	Front	Center	Rear	Front	Center	Rear
0	NA	0.125	NA	0.1195	0.0109	0.1266	0.3830	0.0312	0.4424
0	NA	0.25	NA	0.0918	0.0107	0.1026	0.1799	0.0291	0.2313
0	NA	0.5	NA	0.0557	0.0100	0.0674	0.0869	0.0237	0.1201
0	NA	0.75	NA	0.0386	0.0091	0.0487	0.0592	0.0191	0.0802
0	NA	1	NA	0.0296	0.0081	0.0378	0.0456	0.0159	0.0596
0.125	NA	0	NA	0.1413	0.0145	0.1496	0.4144	0.0352	0.4786
0.25	NA	0	NA	0.1496	0.0218	0.1667	0.2378	0.0429	0.3039
0.5	NA	0	NA	0.1606	0.0381	0.1918	0.1885	0.0614	0.2513

Total RMS of Gap Variation (m)				f_s = 1 Hz			f_s = 1.5 Hz		
ζ_s	ζ_u	ζ_a	f_u	Front	Center	Rear	Front	Center	Rear
0	NA	0.125	NA	0.0113		0.0122	0.0148		0.0209
0	NA	0.25	NA	0.0097		0.0109	0.0088		0.0131
0	NA	0.5	NA	0.0081		0.0091	0.0076		0.0093
0	NA	0.75	NA	0.0077		0.0083	0.0074		0.0082
0	NA	1	NA	0.0075		0.0079	0.0074		0.0078
0.125	NA	0	NA	0.0104		0.0121	0.0131		0.0197
0.25	NA	0	NA	0.0076		0.0102	0.0055		0.0110
0.5	NA	0	NA	0.0044		0.0072	0.0028		0.0061

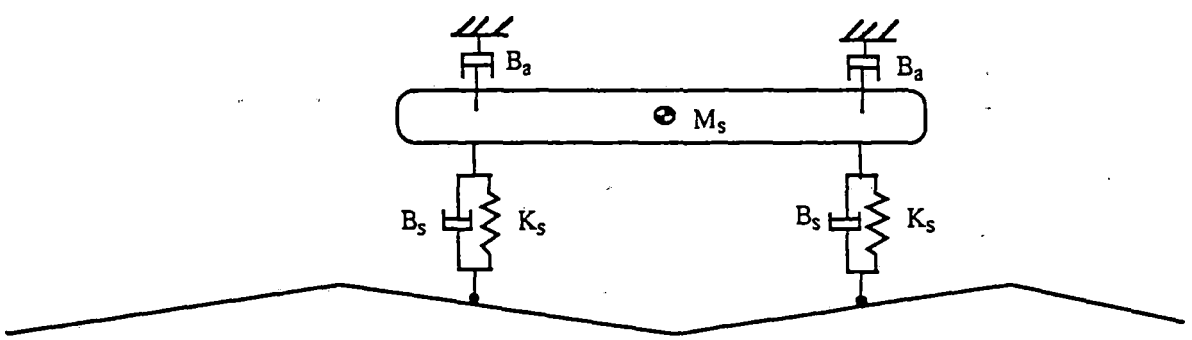

Model I

Table 4.4
Total RMS Performance of Two Suspension Vehicle Model To Ramp Input
(Ramp Slope = 0.001)

Model II

Total RMS of Sprung Mass Acceleration (g)				f_u = 1 Hz			f_u = 5 Hz		
ζ_s	ζ_u	ζ_a	f_s (Hz)	Front	Center	Rear	Front	Center	Rear
0.1	0	0	0.75	0.1335	0.0184	0.1436	0.0715	0.0109	0.0735
0.25	0	0	0.75	0.0883	0.0123	0.0911	0.1071	0.0221	0.1148
0.5	0	0	0.75	0.0796	0.0111	0.0809	0.1544	0.0408	0.1761
0.75	0	0	0.75	0.0780	0.0109	0.0788	0.1839	0.0574	0.2203
0.1	0	0	1	0.1271	0.0199	0.1324	0.1453	0.0169	0.1517
0.25	0	0	1	0.0920	0.0132	0.0941	0.1661	0.0305	0.1841
0.5	0	0	1	0.0811	0.0114	0.0821	0.1914	0.0533	0.2294
0.75	0	0	1	0.0787	0.0111	0.0793	0.2125	0.0723	0.2678

Total RMS of Gap Variation (m)				f_u = 1 Hz			f_u = 5 Hz		
ζ_s	ζ_u	ζ_a	f_s (Hz)	Front	Center	Rear	Front	Center	Rear
0.1	0	0	0.75	0.0182		0.0184	0.0013		0.0013
0.25	0	0	0.75	0.0126		0.0112	0.0014		0.0014
0.5	0	0	0.75	0.0111		0.0102	0.0015		0.0015
0.75	0	0	0.75	0.0107		0.0101	0.0015		0.0017
0.1	0	0	1	0.0096		0.0065	0.0013		0.0013
0.25	0	0	1	0.0105		0.0090	0.0014		0.0014
0.5	0	0	1	0.0105		0.0097	0.0015		0.0016
0.75	0	0	1	0.0104		0.0099	0.0015		0.0018

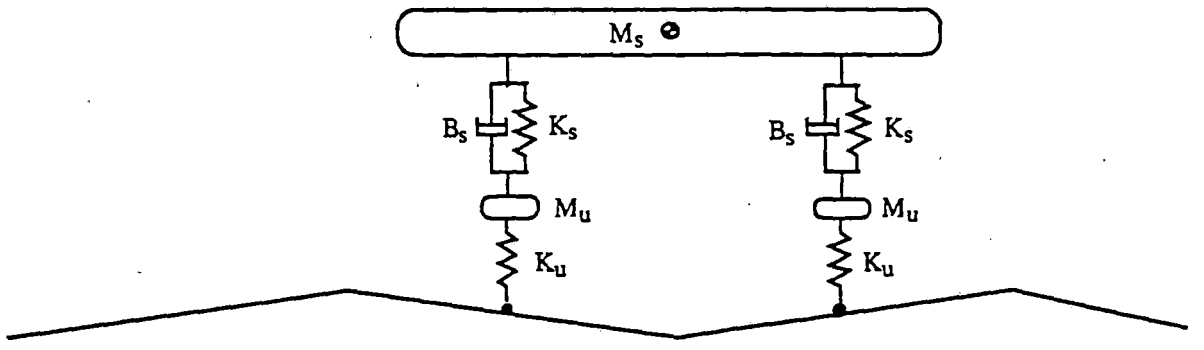

Model II

Table 4.4
Total RMS Performance of Two Suspension Vehicle Model To Ramp Input
(Ramp Slope = 0.001)

Model III

Total RMS of Sprung Mass Acceleration (g)				f_u = 1 Hz			f_u = 5 Hz		
ζ_s	ζ_u	ζ_a	f_s (Hz)	Front	Center	Rear	Front	Center	Rear
0.25	0.25	0	0.75	0.0675	0.0085	0.0705	0.1035	0.0180	0.1109
0.25	0.5	0	0.75	0.0671	0.0084	0.0706	0.1014	0.0159	0.1087
0.25	0.75	0	0.75	0.0702	0.0089	0.0742	0.1001	0.0152	0.1073
0.25	0.25	0	1	0.0792	0.0105	0.0834	0.1611	0.0251	0.1786
0.25	0.5	0	1	0.0844	0.0110	0.0902	0.1580	0.0228	0.1752
0.25	0.75	0	1	0.0921	0.0120	0.0994	0.1558	0.0219	0.1728

Total RMS of Gap Variation (m)				f_u = 1 Hz			f_u = 5 Hz		
ζ_s	ζ_u	ζ_a	f_s (Hz)	Front	Center	Rear	Front	Center	Rear
0.25	0.25	0	0.75	0.0080		0.0074	0.0010		0.0010
0.25	0.5	0	0.75	0.0058		0.0055	0.0007		0.0007
0.25	0.75	0	0.75	0.0045		0.0044	0.0006		0.0006
0.25	0.25	0	1	0.0075		0.0069	0.0010		0.0010
0.25	0.5	0	1	0.0058		0.0056	0.0008		0.0008
0.25	0.75	0	1	0.0047		0.0046	0.0007		0.0007

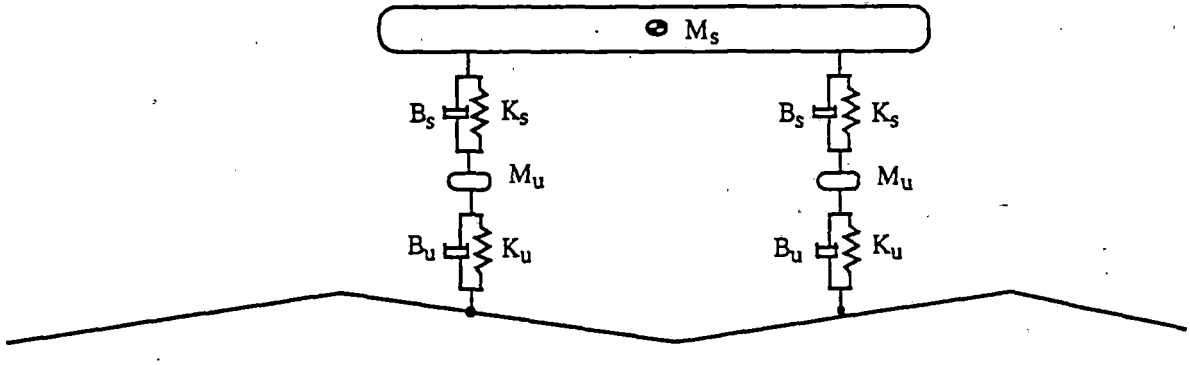

Model III

Table 4.4
Total RMS Performance of Two Suspension Vehicle Model To Ramp Input
(Ramp Slope = 0.001)

Model IV

Total RMS of Sprung Mass Acceleration (g)				f_u = 2.5 Hz			f_u = 5 Hz		
ζ_s	ζ_u	ζ_a	f_s (Hz)	Front	Center	Rear	Front	Center	Rear
0.25	0.25	0.25	0.75	0.0979	0.0115	0.1042	0.0985	0.0143	0.1056
0.25	0.25	0.5	0.75	0.0830	0.0098	0.0884	0.0935	0.0124	0.1003
0.25	0.25	0.75	0.75	0.0708	0.0083	0.0755	0.0883	0.0112	0.0947
0.25	0.25	0.25	1	0.1486	0.0166	0.1619	0.1538	0.0207	0.1706
0.25	0.25	0.5	1	0.1252	0.0142	0.1369	0.1460	0.0183	0.1620
0.25	0.25	0.75	1	0.1068	0.0122	0.1171	0.1378	0.0167	0.1529

Total RMS of Gap Variation (m)				f_u = 2.5 Hz			f_u = 5 Hz		
ζ_s	ζ_u	ζ_a	f_s (Hz)	Front	Center	Rear	Front	Center	Rear
0.25	0.25	0.25	0.75	0.0034		0.0034	0.0014		0.0014
0.25	0.25	0.5	0.75	0.0042		0.0043	0.0021		0.0021
0.25	0.25	0.75	0.75	0.0049		0.0049	0.0028		0.0028
0.25	0.25	0.25	1	0.0038		0.0040	0.0015		0.0016
0.25	0.25	0.5	1	0.0046		0.0047	0.0022		0.0023
0.25	0.25	0.75	1	0.0051		0.0052	0.0029		0.0030

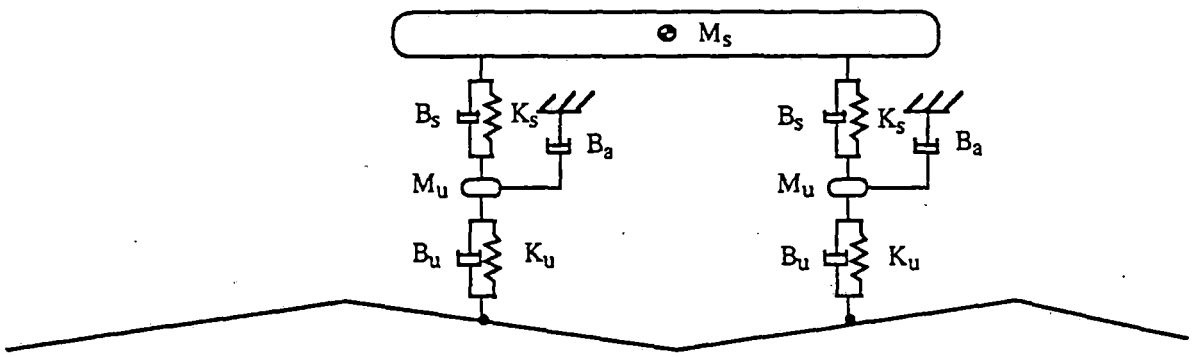

Model IV

Table 4.5
Total RMS Performance of Multi-Suspension Vehicle Model To Ramp Input

Model I

Design						Total RMS of Sprung Mass Acceleration (g)					
	ζ_s	ζ_u	ζ_a	f_s	f_u	1st	2nd	3rd	4th	5th	6th
a	0	NA	0.125	1	NA	0.0588	0.0387	0.0236	0.0250	0.0413	0.0616
b	0.125	NA	0	1	NA	0.0693	0.0456	0.0278	0.0295	0.0486	0.0726
c	0	NA	0.125	1.5	NA	0.1869	0.1179	0.0660	0.0791	0.1401	0.2109
d	0.125	NA	0	1.5	NA	0.2020	0.1275	0.0714	0.0856	0.1514	0.2279

Design						Total RMS of Gap Variation (m)					
	ζ_s	ζ_u	ζ_a	f_s	f_u	1st	2nd	3rd	4th	5th	6th
a	0	NA	0.125	1	NA	0.0095	0.0087	0.0081	0.0082	0.0089	0.0096
b	0.125	NA	0	1	NA	0.0096	0.0084	0.0079	0.0083	0.0089	0.0093
c	0	NA	0.125	1.5	NA	0.0144	0.0113	0.0095	0.0103	0.0127	0.0151
d	0.125	NA	0	1.5	NA	0.0142	0.0106	0.0091	0.0104	0.0128	0.0147

Model II

Design						Total RMS of Sprung Mass Acceleration (g)					
	ζ_s	ζ_u	ζ_a	f_s	f_u	1st	2nd	3rd	4th	5th	6th
a	0.25	0	0	0.75	1	0.0623	0.0421	0.0273	0.0280	0.0435	0.0638
b	0.25	0	0	0.75	5	0.0595	0.0396	0.0250	0.0266	0.0427	0.0629
c	0.25	0	0	1	1	0.0662	0.0450	0.0292	0.0298	0.0460	0.0674
d	0.25	0	0	1	5	0.0924	0.0608	0.0379	0.0418	0.0681	0.1006

Design						Total RMS of Gap Variation (m)					
	ζ_s	ζ_u	ζ_a	f_s	f_u	1st	2nd	3rd	4th	5th	6th
a	0.25	0	0	0.75	1	0.0116	0.0126	0.0129	0.0125	0.0121	0.0124
b	0.25	0	0	0.75	5	0.0013	0.0013	0.0013	0.0013	0.0013	0.0013
c	0.25	0	0	1	1	0.0086	0.0094	0.0093	0.0089	0.0088	0.0098
d	0.25	0	0	1	5	0.0013	0.0013	0.0013	0.0013	0.0013	0.0013

Table 4.5
Total RMS Performance of Multi-Suspension Vehicle Model To Ramp Input

Model III

Design						Total RMS of Sprung Mass Acceleration (g)					
	ζ_s	ζ_u	ζ_a	f_s	f_u	1st	2nd	3rd	4th	5th	6th
a	0.25	0.25	0	0.75	1	0.0438	0.0294	0.0187	0.0195	0.0308	0.0454
b	0.25	0.25	0	0.75	5	0.0590	0.0392	0.0246	0.0263	0.0422	0.0624
c	0.25	0.25	0	1	1	0.0529	0.0355	0.0228	0.0238	0.0375	0.0552
d	0.25	0.25	0	1	5	0.0914	0.0601	0.0374	0.0413	0.0673	0.0995

Design						Total RMS of Gap Variation (m)					
	ζ_s	ζ_u	ζ_a	f_s	f_u	1st	2nd	3rd	4th	5th	6th
a	0.25	0.25	0	0.75	1	0.0072	0.0074	0.0073	0.0071	0.0072	0.0075
b	0.25	0.25	0	0.75	5	0.0009	0.0009	0.0009	0.0009	0.0009	0.0009
c	0.25	0.25	0	1	1	0.0062	0.0063	0.0060	0.0058	0.0060	0.0067
d	0.25	0.25	0	1	5	0.0009	0.0009	0.0009	0.0009	0.0009	0.0009

Model IV

Design						Total RMS of Sprung Mass Acceleration (g)					
	ζ_s	ζ_u	ζ_a	f_s	f_u	1st	2nd	3rd	4th	5th	6th
a	0.25	0.25	0.25	0.75	2.5	0.0569	0.0378	0.0236	0.0250	0.0404	0.0598
b	0.25	0.25	0.25	0.75	5	0.0572	0.0380	0.0238	0.0254	0.0409	0.0605
c	0.25	0.25	0.25	1	2.5	0.0835	0.0550	0.0340	0.0370	0.0604	0.0895
d	0.25	0.25	0.25	1	5	0.0885	0.0582	0.0361	0.0399	0.0652	0.0963

Design						Total RMS of Gap Variation (m)					
	ζ_s	ζ_u	ζ_a	f_s	f_u	1st	2nd	3rd	4th	5th	6th
a	0.25	0.25	0.25	0.75	2.5	0.0032	0.0031	0.0031	0.0031	0.0031	0.0032
b	0.25	0.25	0.25	0.75	5	0.0014	0.0013	0.0013	0.0013	0.0013	0.0014
c	0.25	0.25	0.25	1	2.5	0.0034	0.0032	0.0031	0.0031	0.0032	0.0035
d	0.25	0.25	0.25	1	5	0.0015	0.0014	0.0014	0.0014	0.0014	0.0015

Table 4.6

Disturbance Level To Achieve a 0.04g RMS Acceleration For Slope Disturbances

DESIGN	a		b		c		d	
	Slope 10^{-3}	RMS Gap (cm)	Slope 10^{-3}	RMS Gap (cm)	Slope 10^{-3}	RMS Gap (cm)	Slope 10^{-3}	RMS Gap (cm)
I	0.67	0.60	0.55	0.50	0.19	0.28	0.17	0.25
II	0.63	0.78	0.64	0.83	0.59	0.58	0.40	0.52
III	0.88	0.66	0.64	0.65	0.72	0.48	0.40	0.36
IV	0.67	0.21	0.66	0.09	0.44	0.16	0.41	0.06

Table 4.7
Total RMS Performance of Two Suspension Vehicle Model To Camber
(Maximum Deflection = 0.01 m)

Model I

Total RMS of Sprung Mass Acceleration (g)				f_s = 1 Hz			f_s = 1.5 Hz		
ζ_s	ζ_u	ζ_a	f_u	Front	Center	Rear	Front	Center	Rear
0	NA	0.125	NA	0.0255	0.0098	0.0238	0.0660	0.0232	0.0584
0	NA	0.25	NA	0.0255	0.0097	0.0223	0.0639	0.0229	0.0506
0	NA	0.5	NA	0.0244	0.0096	0.0189	0.0552	0.0220	0.0372
0	NA	0.75	NA	0.0226	0.0093	0.0160	0.0467	0.0207	0.0295
0	NA	1	NA	0.0205	0.0090	0.0139	0.0399	0.0193	0.0251
0.125	NA	0	NA	0.0478	0.0167	0.0454	0.0936	0.0313	0.0846
0.25	NA	0	NA	0.0851	0.0289	0.0781	0.1453	0.0480	0.1238
0.5	NA	0	NA	0.1594	0.0547	0.1381	0.2417	0.0849	0.1950

Total RMS of Gap Variation (m)				f_s = 1 Hz			f_s = 1.5 Hz		
ζ_s	ζ_u	ζ_a	f_u	Front	Center	Rear	Front	Center	Rear
0	NA	0.125	NA	0.0032		0.0032	0.0036		0.0034
0	NA	0.25	NA	0.0032		0.0031	0.0036		0.0033
0	NA	0.5	NA	0.0032		0.0031	0.0035		0.0031
0	NA	0.75	NA	0.0032		0.0031	0.0034		0.0031
0	NA	1	NA	0.0032		0.0030	0.0033		0.0031
0.125	NA	0	NA	0.0033		0.0030	0.0037		0.0031
0.25	NA	0	NA	0.0034		0.0028	0.0038		0.0027
0.5	NA	0	NA	0.0034		0.0025	0.0035		0.0022

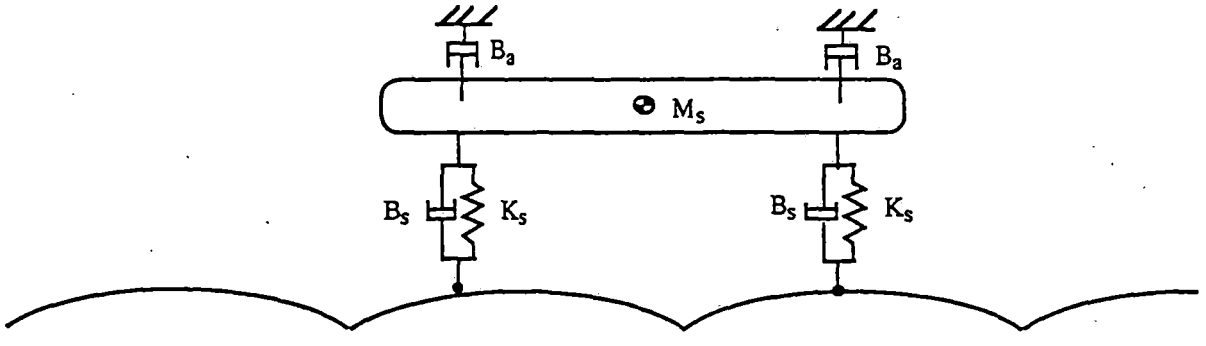

Model I

Table 4.7
Total RMS Performance of Two Suspension Vehicle Model To Camber
(Maximum Deflection = 0.01 m)

Model II

Total RMS of Sprung Mass Acceleration (g)				f_u = 1 Hz			f_u = 5 Hz		
ζ_s	ζ_u	ζ_a	f_s (Hz)	Front	Center	Rear	Front	Center	Rear
0.1	0	0	0.75	0.0044	0.0019	0.0042	0.2572	0.0319	0.2571
0.25	0	0	0.75	0.0086	0.0036	0.0077	0.2628	0.0385	0.2615
0.5	0	0	0.75	0.0133	0.0060	0.0114	0.2826	0.0560	0.2740
0.75	0	0	0.75	0.0156	0.0074	0.0134	0.3127	0.0767	0.2882
0.1	0	0	1	0.0076	0.0034	0.0070	0.2594	0.0346	0.2590
0.25	0	0	1	0.0121	0.0051	0.0103	0.2699	0.0449	0.2666
0.5	0	0	1	0.0160	0.0074	0.0135	0.3050	0.0703	0.2853
0.75	0	0	1	0.0173	0.0084	0.0150	0.3528	0.0991	0.3022

Total RMS of Gap Variation (m)				f_u = 1 Hz			f_u = 5 Hz		
ζ_s	ζ_u	ζ_a	f_s (Hz)	Front	Center	Rear	Front	Center	Rear
0.1	0	0	0.75	0.0036		0.0036	0.0144		0.0146
0.25	0	0	0.75	0.0035		0.0035	0.0062		0.0064
0.5	0	0	0.75	0.0034		0.0034	0.0035		0.0037
0.75	0	0	0.75	0.0033		0.0033	0.0028		0.0029
0.1	0	0	1	0.0036		0.0036	0.0101		0.0103
0.25	0	0	1	0.0035		0.0035	0.0046		0.0048
0.5	0	0	1	0.0033		0.0034	0.0028		0.0030
0.75	0	0	1	0.0032		0.0033	0.0026		0.0025

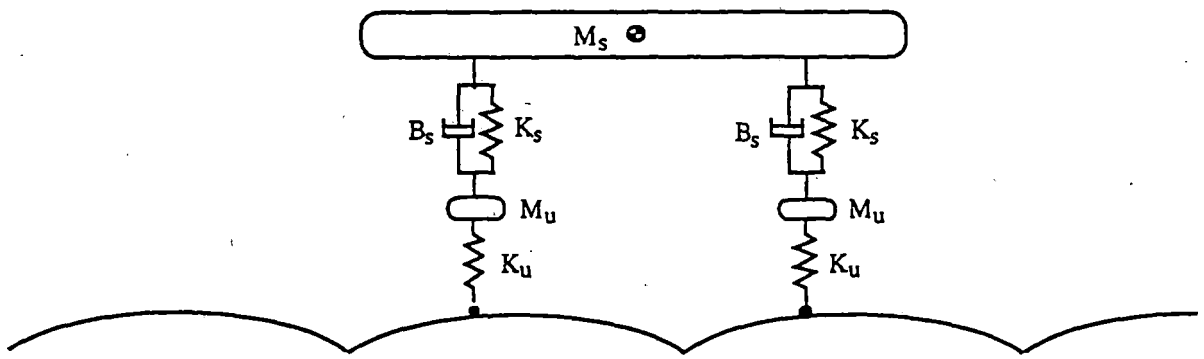

Model II

Table 4.7
Total RMS Performance of Two Suspension Vehicle Model To Camber
(Maximum Deflection = 0.01 m)

Model III

Total RMS of Sprung Mass Acceleration (g)				f_u = 1 Hz			f_u = 5 Hz		
ζ_s	ζ_u	ζ_a	f_s (Hz)	Front	Center	Rear	Front	Center	Rear
0.25	0.25	0	0.75	0.0128	0.0053	0.0116	0.0791	0.0242	0.0747
0.25	0.5	0	0.75	0.0197	0.0079	0.0179	0.0670	0.0226	0.0627
0.25	0.75	0	0.75	0.0255	0.0101	0.0234	0.0630	0.0217	0.0588
0.25	0.25	0	1	0.0177	0.0073	0.0154	0.1066	0.0330	0.0983
0.25	0.5	0	1	0.0268	0.0108	0.0237	0.0921	0.0309	0.0838
0.25	0.75	0	1	0.0347	0.0137	0.0308	0.0869	0.0296	0.0790

Total RMS of Gap Variation (m)				f_u = 1 Hz			f_u = 5 Hz		
ζ_s	ζ_u	ζ_a	f_s (Hz)	Front	Center	Rear	Front	Center	Rear
0.25	0.25	0	0.75	0.0032		0.0032	0.0015		0.0015
0.25	0.5	0	0.75	0.0028		0.0029	0.0010		0.0010
0.25	0.75	0	0.75	0.0025		0.0026	0.0008		0.0008
0.25	0.25	0	1	0.0031		0.0031	0.0014		0.0014
0.25	0.5	0	1	0.0027		0.0028	0.0010		0.0010
0.25	0.75	0	1	0.0024		0.0025	0.0008		0.0008

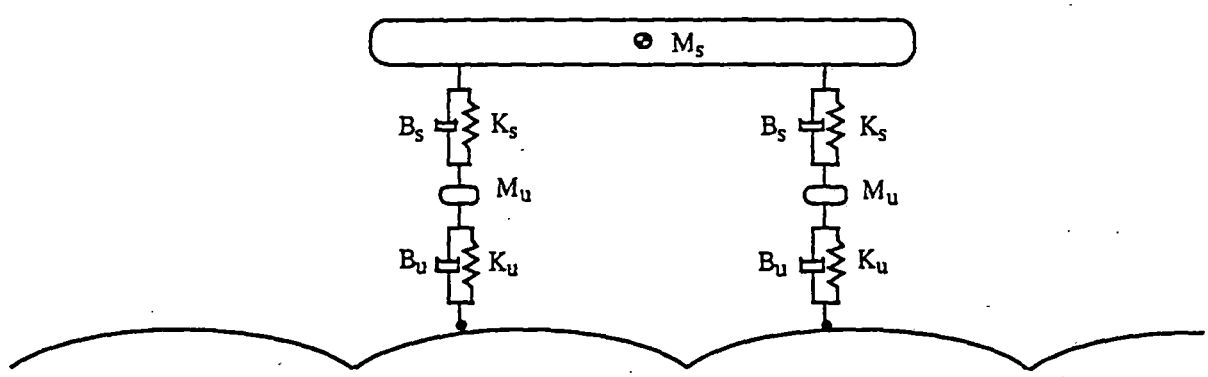

Model III

Table 4.7
Total RMS Performance of Two Suspension Vehicle Model To Camber
(Maximum Deflection = 0.01 m)

Model IV

Total RMS of Sprung Mass Acceleration (g)				f_u = 2.5 Hz			f_u = 5 Hz		
ζ_s	ζ_u	ζ_a	f_s (Hz)	Front	Center	Rear	Front	Center	Rear
0.25	0.25	0.25	0.75	0.0415	0.0168	0.0381	0.0583	0.0207	0.0541
0.25	0.25	0.5	0.75	0.0301	0.0120	0.0276	0.0472	0.0175	0.0434
0.25	0.25	0.75	0.75	0.0238	0.0093	0.0218	0.0394	0.0149	0.0361
0.25	0.25	0.25	1	0.0550	0.0219	0.0493	0.0806	0.0282	0.0726
0.25	0.25	0.5	1	0.0408	0.0160	0.0364	0.0657	0.0239	0.0586
0.25	0.25	0.75	1	0.0325	0.0126	0.0289	0.0551	0.0204	0.0489

Total RMS of Gap Variation (m)				f_u = 2.5 Hz			f_u = 5 Hz		
ζ_s	ζ_u	ζ_a	f_s (Hz)	Front	Center	Rear	Front	Center	Rear
0.25	0.25	0.25	0.75	0.0029		0.0029	0.0014		0.0014
0.25	0.25	0.5	0.75	0.0027		0.0027	0.0017		0.0017
0.25	0.25	0.75	0.75	0.0026		0.0026	0.0020		0.0020
0.25	0.25	0.25	1	0.0027		0.0028	0.0014		0.0014
0.25	0.25	0.5	1	0.0026		0.0027	0.0017		0.0017
0.25	0.25	0.75	1	0.0026		0.0026	0.0020		0.0020

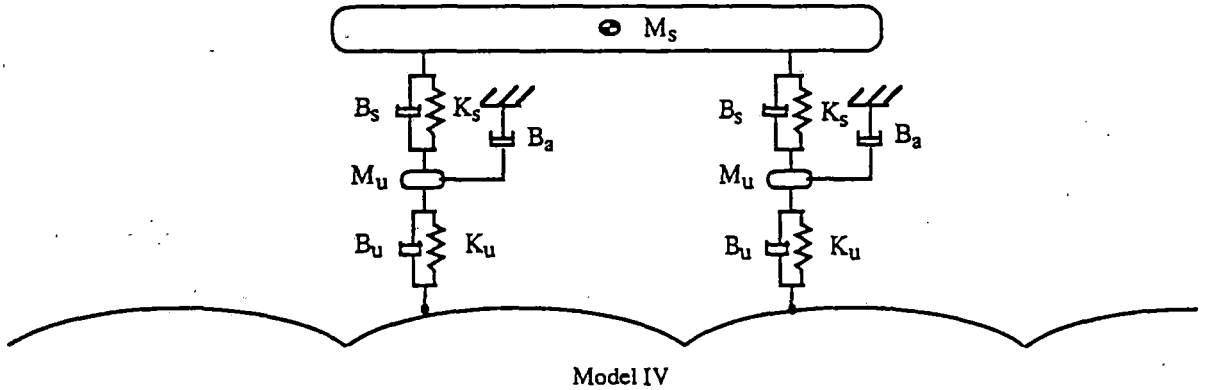

Model IV

Table 4.8
Total RMS Performance of Multi-Suspension Vehicle Model To Camber

Model I

Design						Total RMS of Sprung Mass Acceleration (g)					
	ζ_s	ζ_u	ζ_a	f_s	f_u	1st	2nd	3rd	4th	5th	6th
a	0	NA	0.125	1	NA	0.0149	0.0090	0.0030	0.0030	0.0090	0.0149
b	0.125	NA	0	1	NA	0.0254	0.0155	0.0059	0.0059	0.0154	0.0254
c	0	NA	0.125	1.5	NA	0.0362	0.0217	0.0073	0.0073	0.0217	0.0362
d	0.125	NA	0	1.5	NA	0.0487	0.0295	0.0108	0.0107	0.0294	0.0487

Design						Total RMS of Gap Variation (m)					
	ζ_s	ζ_u	ζ_a	f_s	f_u	1st	2nd	3rd	4th	5th	6th
a	0	NA	0.125	1	NA	0.0031	0.0031	0.0030	0.0030	0.0031	0.0030
b	0.125	NA	0	1	NA	0.0032	0.0031	0.0030	0.0030	0.0031	0.0029
c	0	NA	0.125	1.5	NA	0.0032	0.0032	0.0030	0.0030	0.0032	0.0031
d	0.125	NA	0	1.5	NA	0.0034	0.0032	0.0030	0.0031	0.0032	0.0029

Model II

Design						Total RMS of Sprung Mass Acceleration (g)					
	ζ_s	ζ_u	ζ_a	f_s	f_u	1st	2nd	3rd	4th	5th	6th
a	0.25	0	0	0.75	1	0.0054	0.0033	0.0011	0.0011	0.0032	0.0054
b	0.25	0	0	0.75	5	0.0769	0.0462	0.0156	0.0156	0.0462	0.0769
c	0.25	0	0	1	1	0.0076	0.0046	0.0015	0.0015	0.0046	0.0076
d	0.25	0	0	1	5	0.0847	0.0509	0.0171	0.0171	0.0508	0.0847

Design						Total RMS of Gap Variation (m)					
	ζ_s	ζ_u	ζ_a	f_s	f_u	1st	2nd	3rd	4th	5th	6th
a	0.25	0	0	0.75	1	0.0035	0.0035	0.0035	0.0035	0.0035	0.0035
b	0.25	0	0	0.75	5	0.0062	0.0064	0.0063	0.0063	0.0062	0.0064
c	0.25	0	0	1	1	0.0035	0.0035	0.0035	0.0035	0.0035	0.0035
d	0.25	0	0	1	5	0.0046	0.0048	0.0047	0.0047	0.0046	0.0048

Table 4.8
Total RMS Performance of Multi-Suspension Vehicle Model To Camber

Model III

Design	ζ_s	ζ_u	ζ_a	f_s	f_u	Total RMS of Sprung Mass Acceleration (g) 1st	2nd	3rd	4th	5th	6th
a	0.25	0.25	0	0.75	1	0.0079	0.0047	0.0016	0.0016	0.0047	0.0079
b	0.25	0.25	0	0.75	5	0.0380	0.0228	0.0077	0.0077	0.0228	0.0379
c	0.25	0.25	0	1	1	0.0109	0.0065	0.0022	0.0022	0.0065	0.0108
d	0.25	0.25	0	1	5	0.0518	0.0311	0.0105	0.0104	0.0310	0.0517

Design	ζ_s	ζ_u	ζ_a	f_s	f_u	Total RMS of Gap Variation (m) 1st	2nd	3rd	4th	5th	6th
a	0.25	0.25	0	0.75	1	0.0032	0.0032	0.0032	0.0032	0.0032	0.0032
b	0.25	0.25	0	0.75	5	0.0015	0.0015	0.0015	0.0015	0.0015	0.0015
c	0.25	0.25	0	1	1	0.0031	0.0031	0.0031	0.0031	0.0031	0.0032
d	0.25	0.25	0	1	5	0.0014	0.0014	0.0014	0.0014	0.0014	0.0014

Model IV

Design	ζ_s	ζ_u	ζ_a	f_s	f_u	Total RMS of Sprung Mass Acceleration (g) 1st	2nd	3rd	4th	5th	6th
a	0.25	0.25	0.25	0.75	2.5	0.0253	0.0152	0.0051	0.0051	0.0152	0.0253
b	0.25	0.25	0.25	0.75	5	0.0316	0.0190	0.0064	0.0064	0.0190	0.0316
c	0.25	0.25	0.25	1	2.5	0.0331	0.0199	0.0067	0.0066	0.0198	0.0331
d	0.25	0.25	0.25	1	5	0.0434	0.0261	0.0088	0.0087	0.0260	0.0433

Design	ζ_s	ζ_u	ζ_a	f_s	f_u	Total RMS of Gap Variation (m) 1st	2nd	3rd	4th	5th	6th
a	0.25	0.25	0.25	0.75	2.5	0.0028	0.0029	0.0029	0.0028	0.0029	0.0029
b	0.25	0.25	0.25	0.75	5	0.0014	0.0014	0.0014	0.0014	0.0014	0.0014
c	0.25	0.25	0.25	1	2.5	0.0027	0.0027	0.0027	0.0027	0.0027	0.0028
d	0.25	0.25	0.25	1	5	0.0014	0.0014	0.0014	0.0014	0.0014	0.0014

Table 4.9

Camber Disturbance Amplitude To Achieve a 0.04g RMS Acceleration

DESIGN	a		b		c		d	
	Camber (cm)	RMS Gap (cm)	Camber (cm)	RMS Gap (cm)	Camber (cm)	RMS Gap (cm)	Camber (cm)	RMS Gap (cm)
I	2.68	0.80	1.57	0.45	1.1	0.34	1.22	0.35
II	7.4	2.6	0.52	0.33	5.2	1.8	0.47	0.22
III	5.1	1.62	1.06	0.16	3.7	1.2	0.76	0.11
IV	1.6	0.46	1.26	0.17	1.21	0.34	0.93	0.13

guideways since two span systems have camber amplitude which are less than 50% of those occurring in simple spans with the same thermal gradient [23].

5. VEHICLE PERFORMANCE TRAVERSING A FLEXIBLE, ELEVATED GUIDEWAY

5.1 Guideway Performance Parameters

For elevated guideways, the guideway deflections, moments and stresses are important performance variables in addition to vehicle performance parameters. As a vehicle or vehicle train traverses a guideway structure, time varying forces are imparted to the guideway as a result of vehicle passage and the guideway responds dynamically. The response of the guideway for a fixed vehicle configuration and load is a function of vehicle speed or span crossing frequency. In particular the guideway response is a function of the ratio of the vehicle crossing frequency to the span natural frequency, which is designated as

$$V_C = (V/L_S)/f^* \tag{5.1}$$

V_C = crossing frequency ratio
V = vehicle velocity
L_S = span length
f^* = span first mode bending frequency

At values of crossing frequency ratio less than 0.2, a vehicle crosses the span in time period long compared to its natural period of oscillation and the span responds quasi-statically, while at crossing frequencies approaching 1.0 and higher, the vehicle crosses the span in a time period close to the span natural period and generates span dynamic motions which may exceed the quasi-static response by factors of greater than 1.5-2.0 depending on the vehicle and span configuration.

To provide a consistent basis for evaluation of the uniform cross section, single and double span guideways considered in this report, the span natural frequency identified in Eq. (5.1) is defined in terms of span parameters as:

$$f^* = 0.5\pi/L_S^2 \quad EI/\rho A \tag{5.2}$$

E = material elastic modulus
I = cross section inertia
ρ = material density
A = span cross section area

For the simple single and double span guideways, a measure of performance is the dynamic deflection occurring at midspan. Consistent with the definitions introduced above, the nondimensional midspan deflection is defined as:

$$Y = y/y^* \tag{5.3}$$

where y = midspan deflection
y^* = normalizing deflection

The normalizing deflection is defined as the midspan deflection which occurs for a simple span loaded at midspan by a single concentrated load of value W and is given as:

$$y^* = 2WL_S^3/\pi^4EI \tag{5.4}$$

where the concentrated load is selected equal to the vehicle weight W.

The span dynamic response may be illustrated for a limiting case loading condition, in which the vehicle loads imparted to the guideway are represented as a traveling constant amplitude "pressure" load with a value equivalent to a uniformly distributed load per unit length of W/L_S. This loading distribution is characteristic of maglev vehicles which have magnets uniformly distributed along the vehicle and for which a constant amplitude magnet force is generated as the vehicle traverses the span. The length of the pressure load with an amplitude of W/L_S crossing the span at velocity V is denoted L_p.

The results of computing the span dynamic response and determining the maximum value of the midspan deflection as a function vehicle crossing frequency for several values of the ratio of L_p to L_S are plotted for a single span in Figure 5.1 and for a double span in Figure 5.2. The data at small values of crossing frequency near 0.2 essentially yield a quasi-static response with the deflection for values of L_p/L_S of one or greater equal to 0.64 for the single span and 0.45 for the double span. These values of deflection reflect the differences in deflection generated by a distributed load in comparison to the deflection generated by a point load on a simple span. For values of L_p/L_S less than one as the ratio of L_p/L_S decreases, the maximum deflection decreases since the total load decreases. The quasi-static deflection of the double span of total length $2L_S$ is approximately 70% of the deflection of a single span for the same span properties reflecting the influence of continuity at the double span midpoint. The data in Figure 5.1 indicate for several speeds in the range of crossing frequencies of 0.2 to 0.8, that small levels of span

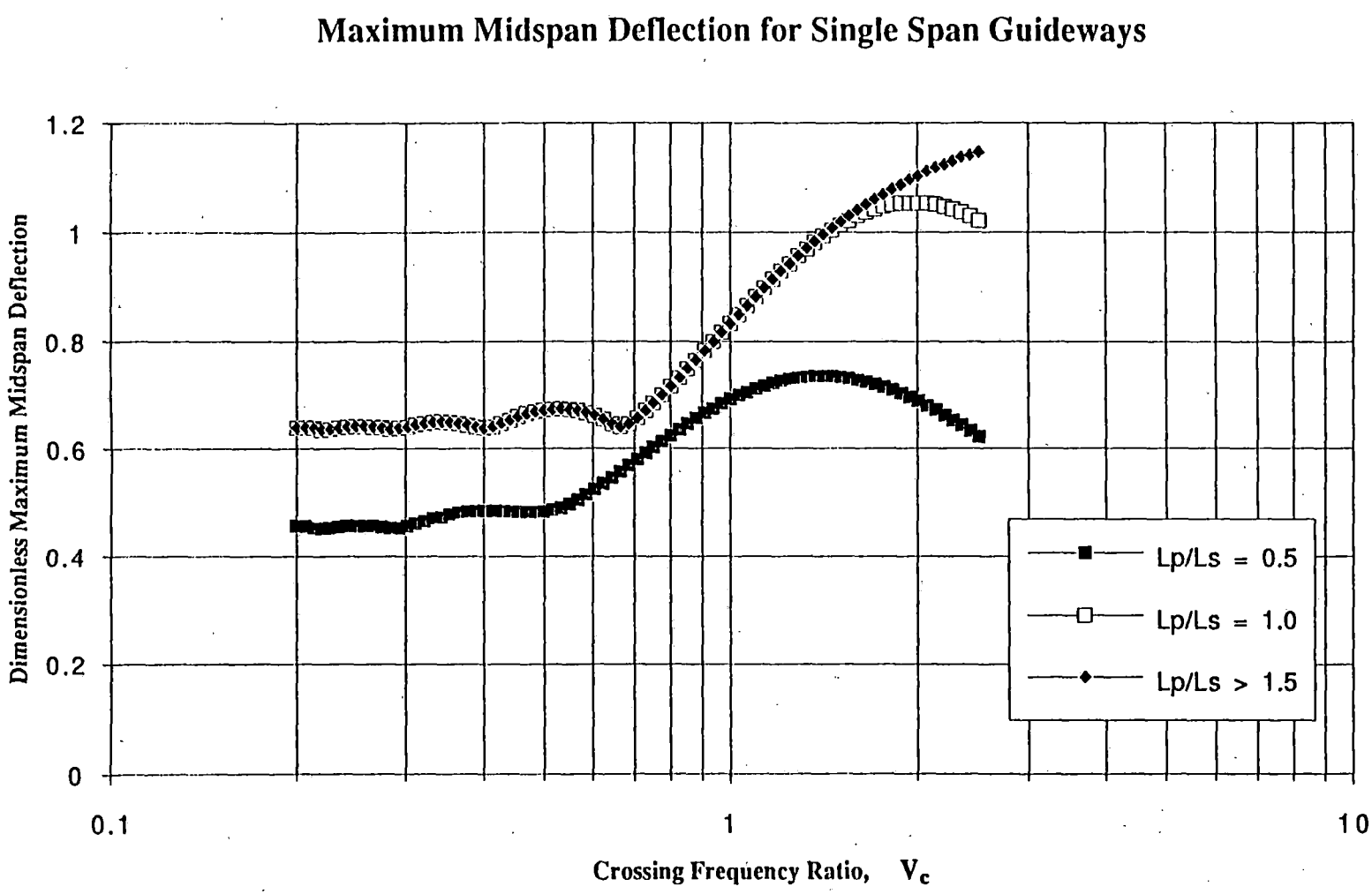

Figure 5.1 Single Space Response To Traveling Pressure Load

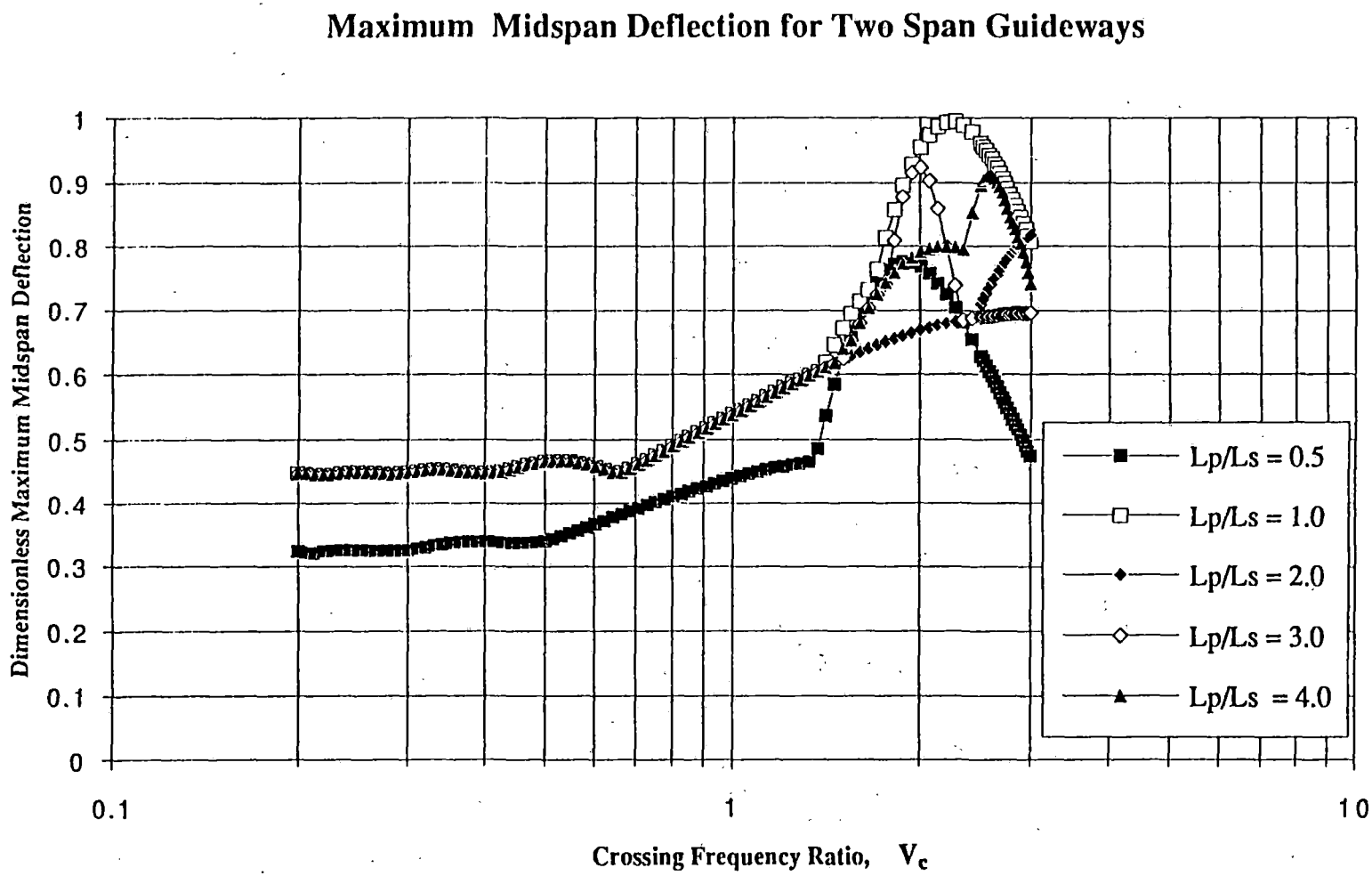

Figure 5.2 Double Span Response To Traveling Pressure Load

dynamic amplification occur at submultiples of the span resonant frequency. However, as speed increases significant dynamic amplification occurs for crossing frequencies of 0.8 or greater. A monotonic increase occurs in the range of crossing frequencies to 1.8 with a maximum normalized dynamic deflection for $L_p/L_s = 1.0$ of 1.15 compared with the low speed case 0.64, or a ratio of high speed to low speed deflection of 1.64. For other values of pressure length similar results occur for all values of L_p/L_s greater than one, illustrating the significant dynamic amplification which occurs at values of crossing frequency ratio exceeding 1.0. It is noted that for a 25 m length span a crossing frequency ratio of 1.0 occurs with a span natural frequency of 4 Hz, at a velocity of 100 m/s.

The two span data in Figure 5.2 illustrates similar dynamic amplification characteristics to the single span data. For all pressure distributions L_p/L_s greater than one, the dynamic amplification factors for $0.2 < Vc < 1.3$ are nearly identical, indicating that multicar trains which produce constant pressure loading do not generate substantially increased dynamic loads in comparison to single cars of length greater than or equal to one span.

5.2 Vehicle Response Traversing Flexible Guideways

As vehicles traverse elevated structures, coupled dynamic interactions may occur in which the vehicle dynamic forces excite the span and conversely the span provides a dynamic deflection to excite the vehicle. To illustrate the characteristics of the interaction of maglev vehicles with guideway systems, a vehicle with a model II suspension traversing an elevated guideway span is considered. The parameters for the vehicle/guideway system are summarized in Table 5.1.

Data are presented in plots of (1) the maximum midspan deflection occurring due to a vehicle passage normalized by y* as a function of the crossing velocity, (2) the peak values of acceleration occurring on the vehicle at front, center and rear positions normalized by the product of y* and the span frequency squared as a function of V_C and (3) the suspension magnetic gap variation normalized by y* as a function of V_C. The results of a set of simulations for a single vehicle with front and rear suspension boggies separated by 21.25 m traversing a single 25 m span are summarized in Figure 5.3, while data for the vehicle crossing a double span of 50 m total length are summarized in Figure 5.4.

The data for the single span show that at low speeds the midspan deflection ratio is 0.5, since for the finite length vehicle only half the vehicle weight, one suspension boggie can be at midspan at any instant. The midspan deflection ratio increases with increasing speed and as V_C approaches 0.9 reaches a value of 1.15 which is more than twice the low

Table 5.1 System Parameters for Configuration II

$$\frac{m_s}{m_s + m_u} = 0.25$$

$$\frac{2\pi f^*}{\sqrt{k_{si}/m_s}} = \frac{5}{\sqrt{\text{No of Suspensions}}}$$

$$\frac{2\pi f^*}{\sqrt{k_{ui}/m_{ui}}} = \frac{5}{7}$$

$$\xi_{si} = \frac{B_{si}}{\sqrt{k_{si}\, m_s}} = \frac{0.25}{\sqrt{\text{No of Suspensions}}}$$

$$\xi_{ui} = \frac{B_{ui}}{\sqrt{k_{ui}\, m_{ui}}} = 0$$

$$\frac{I_v}{m_s L_v^2} = 0.0576$$

$$\frac{L_v}{L_s} = 1$$

$$\left(\frac{L_d}{L_s}\right)_{\text{Two Suspensions}} = 0.85$$

$$\left(\frac{L_d}{L_s}\right)_{\text{Six Suspensions}} = 0.17$$

$$\xi_{bm} = \frac{b_m}{4\pi\rho a f_m} = 0.02$$

$$\left(\frac{L_p}{L_s}\right) = 0.15$$

$$\left(\frac{L_b}{L_s}\right) = 2$$

$$\frac{m_s + m_u}{\rho\, a\, L_s} = 0.5$$

$$V_c = \frac{V}{L_s f^*}$$

$$Y_m = \frac{y_m}{y^*} \quad \text{(Midspan Deflection)}$$

$$\ddot{Y}_s = \frac{\ddot{y}_s}{y^*\, f^{*2}} \quad \text{(Sprung Mass Acceleration)}$$

$$Y_g = \frac{y_g}{y^*} \quad \text{(Gap Variation)}$$

where

b_m = The damping coefficient for the mth mode beam vibration

f_m = The natural frequency for the m th mode beam vibration

ρ = The density of the guideway

a = The cross sectional area of the guideway

V = The vehicle traversing velocity

y_m = Maximum midspan deflection

$\ddot{y}_s$ = Maximum sprung mass acceleration

y_g = Maximum magnetic gap variation

$$m_u = \sum m_{ui}$$

$$f^* = \frac{\pi}{2L_s^2}\sqrt{\frac{EI}{\rho a}}$$

$$y^* = \frac{2(m_u+m_s)gL_s^3}{\pi^4 EI}$$

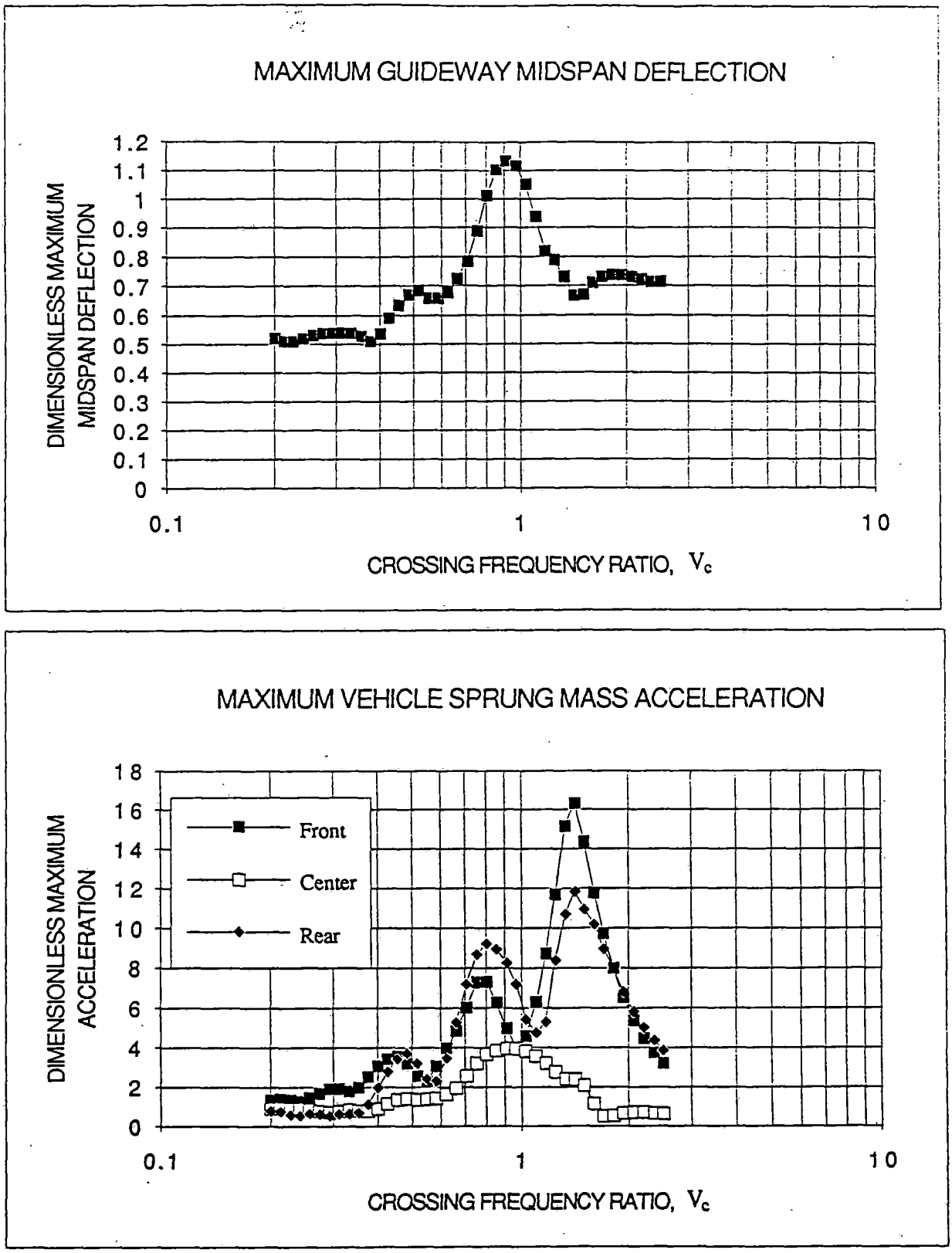

Figure 5.3 Response of Single Vehicle with Two Bogies Crossing A Single Span

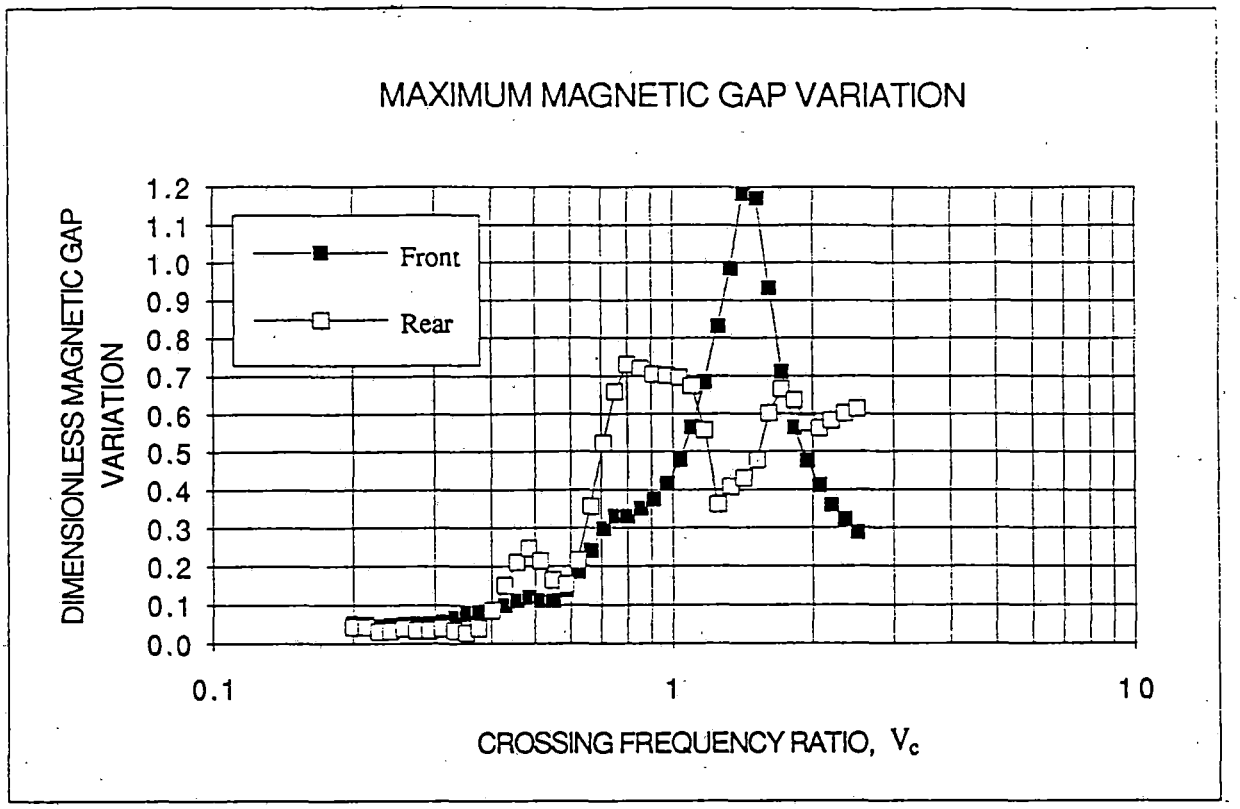

Figure 5.3 Response of Single Vehicle with Two Bogies Crossing A Single Span

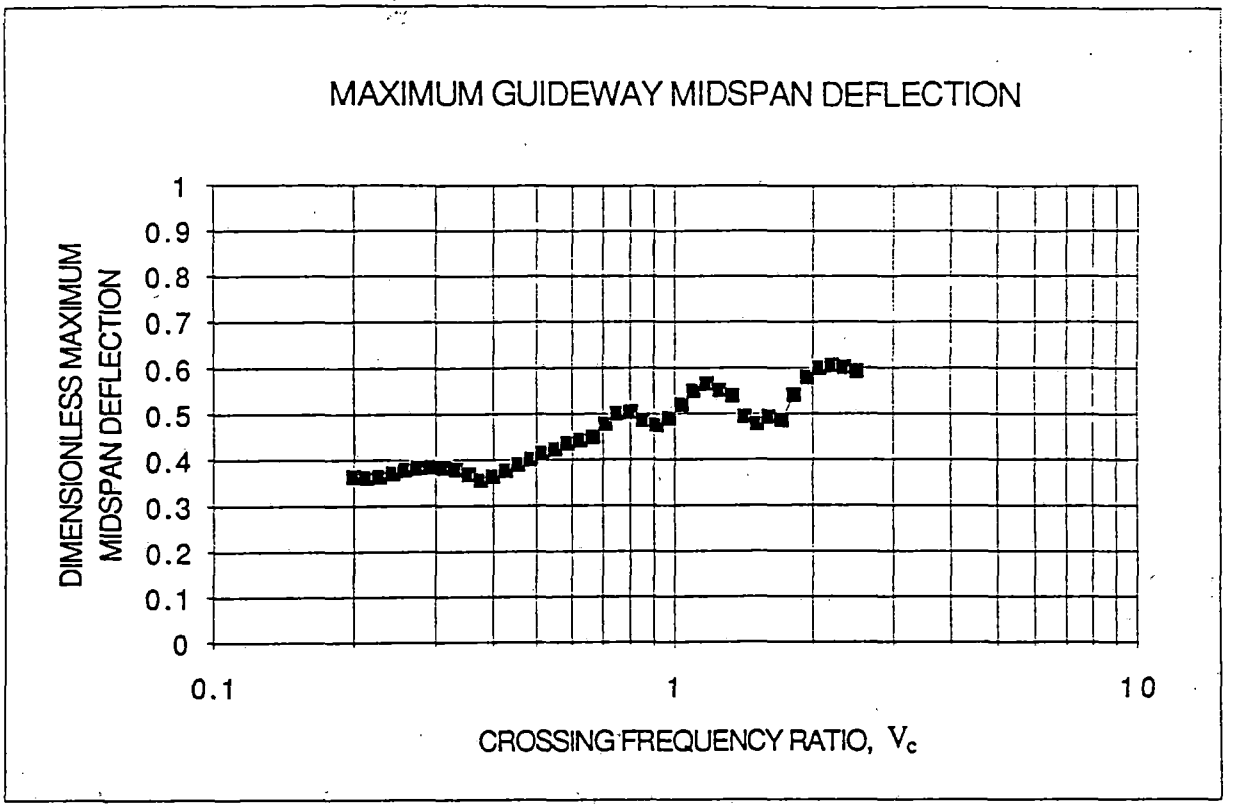

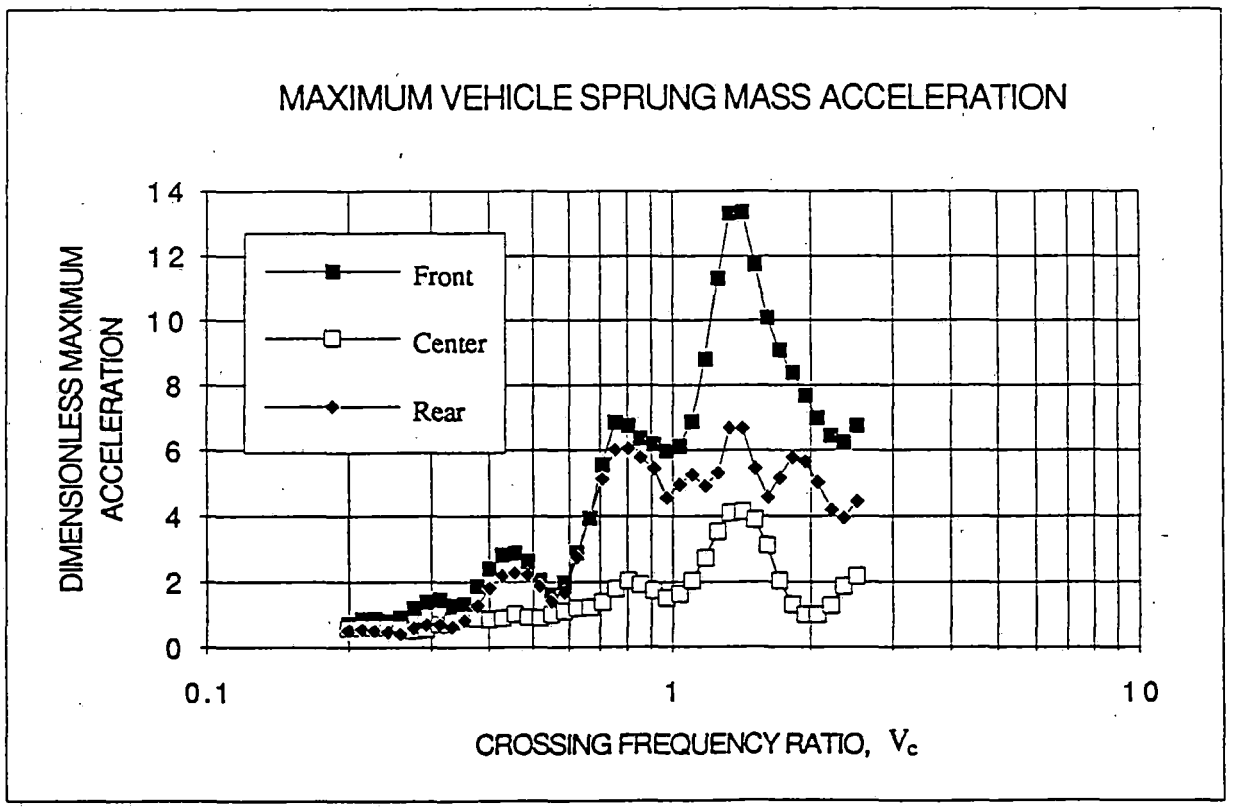

Figure 5.4 Response of a Single Vehicle with Two Bogies Crossing a Double Span

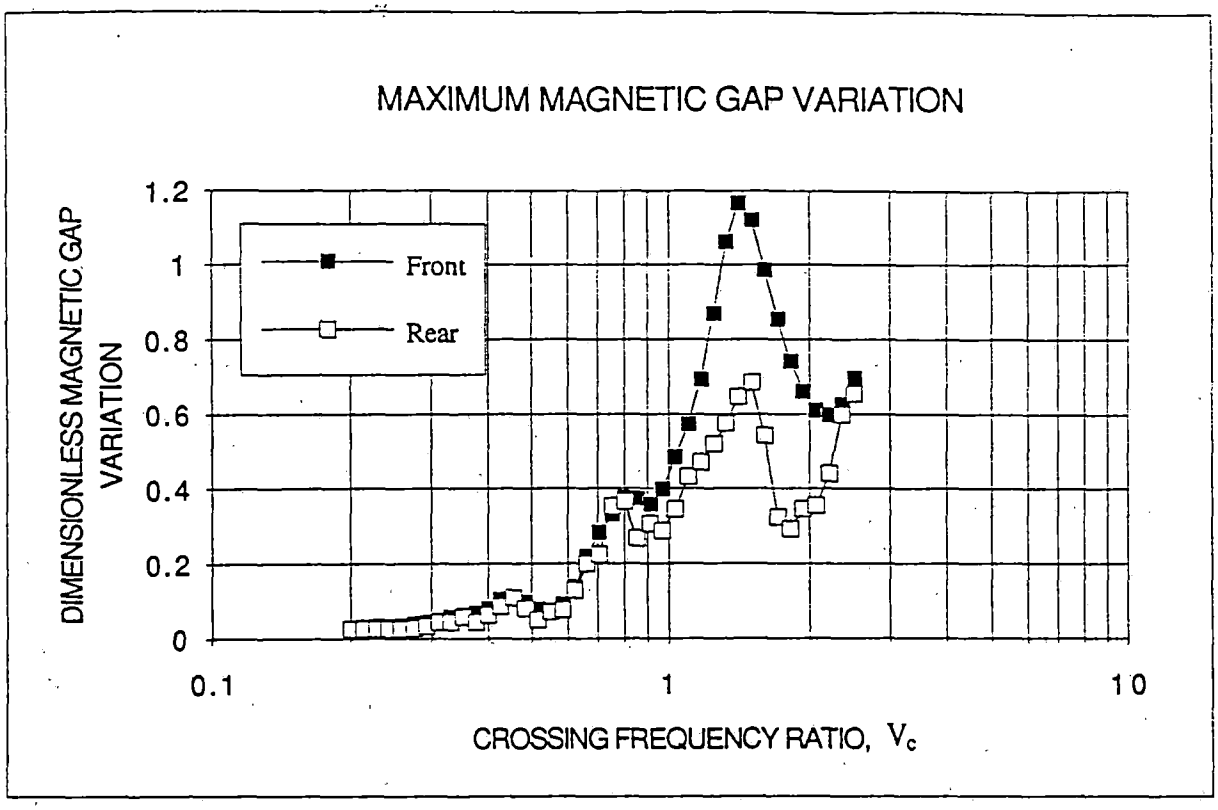

Figure 5.4 Response of a Single Vehicle with Two Bogies Crossing a Double Span

speed value of deflection. The nondimensional peak accelerations for the vehicle are largest at vehicle front and rear and reach peak values at speeds corresponding to values of V_C of 0.8-0.9 and then at values of V_C equal to 1.4 where the vehicle has substantial pitch motion as it traverses the elevated guideway system. The magnetic gap variation shows that at values of $V_C = 0.9$ and 1.3, the gap variations respectively approach values of 75% and 120% of the span normalizing deflection. For a nominal suspension with a 10 cm gap and guideway with a 1.0 cm normalizing deflection, the gap variation is 10% of the suspension gap. Comparing the data with that of Figure 5.1 for the constant pressure loads indicates the influence of vehicle/guideway interactions at the conditions occurring at V_C near 0.9 and then the significant vehicle pitch response near a V_C of 1.4.

Data summarized in Figure 5.4 for a double span guideway show that the normalized midspan deflections at low speeds are approximately 0.4 and that the maximum deflections occur at values of V_C equal to 0.8 and 1.1 and are respectively 0.5 and 0.58. These maximum deflections are less than 60% of those occurring in the single span guideway. The vehicle peak accelerations also occur at values of V_C near 0.8 and 1.1 and result primarily from vehicle pitch motion. The peak accelerations at $V_C = 0.8$ and $V_C = 1.1$ are respectively approximately 70% and 85% of those in the single span case. The maximum magnetic gap variations for values of V_C less than 1.0 are approximately 50% of the single span while for V_C greater than one the gap variations are 95% of the single span data.

Figure 5.5 presents data illustrating the influence of a three car train with each vehicle having two boggies on system response. The three car train increases the maximum span deflection by approximately 50% since for a vehicle with only front and rear boggies, the formation of a train places two boggies in close proximity with a total load equivalent to one full car body weight. Similarly the maximum acceleration for the train is approximately 50% higher than for the single vehicle and occurs at the front of the second car (and rear of the first car). The magnetic gap variations also increase by about 50%. These data show that with a two boggie suspension, the interactions of a train of vehicles with the guideway at operating speeds with V_C greater than 1.0 yield substantially increased span deflections, vehicle accelerations and gap variations in comparison to a single vehicle passage.

Figure 5.6 displays data for a single car with six suspensions distributed along the car. These data show that span deflection increases significantly by 50% from $V_C = 0.7$ to $V_C = 1.3$ and then decreases as Vc is increased until Vc = 1.5, at which pont as V_C increases the span deflections increase to almost double the values of $V_C = 1.3$. The data

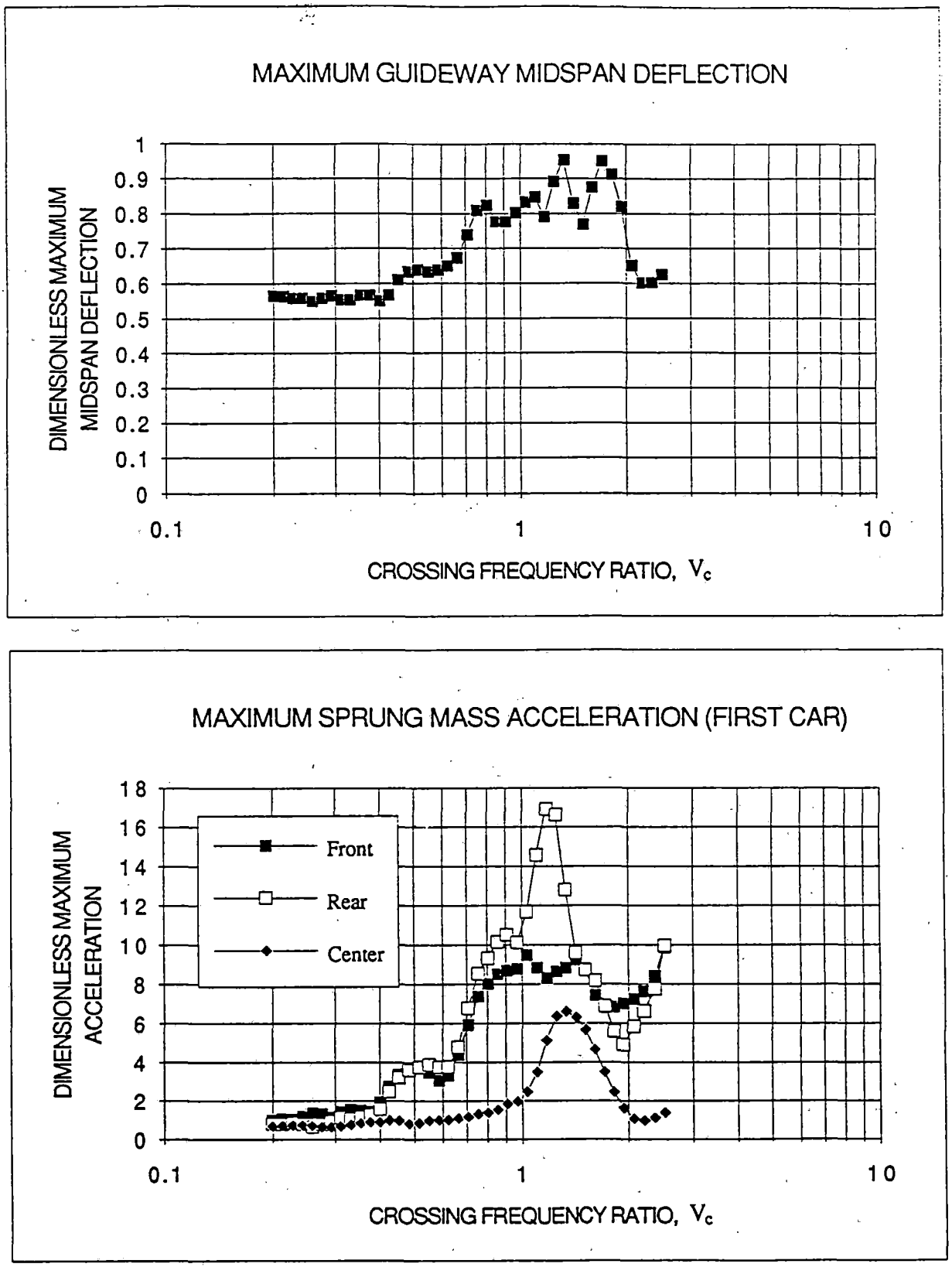

Figure 5.5 Response of Three Car Vehicle Train with Two Bogies Per Car Crossing a Double Span

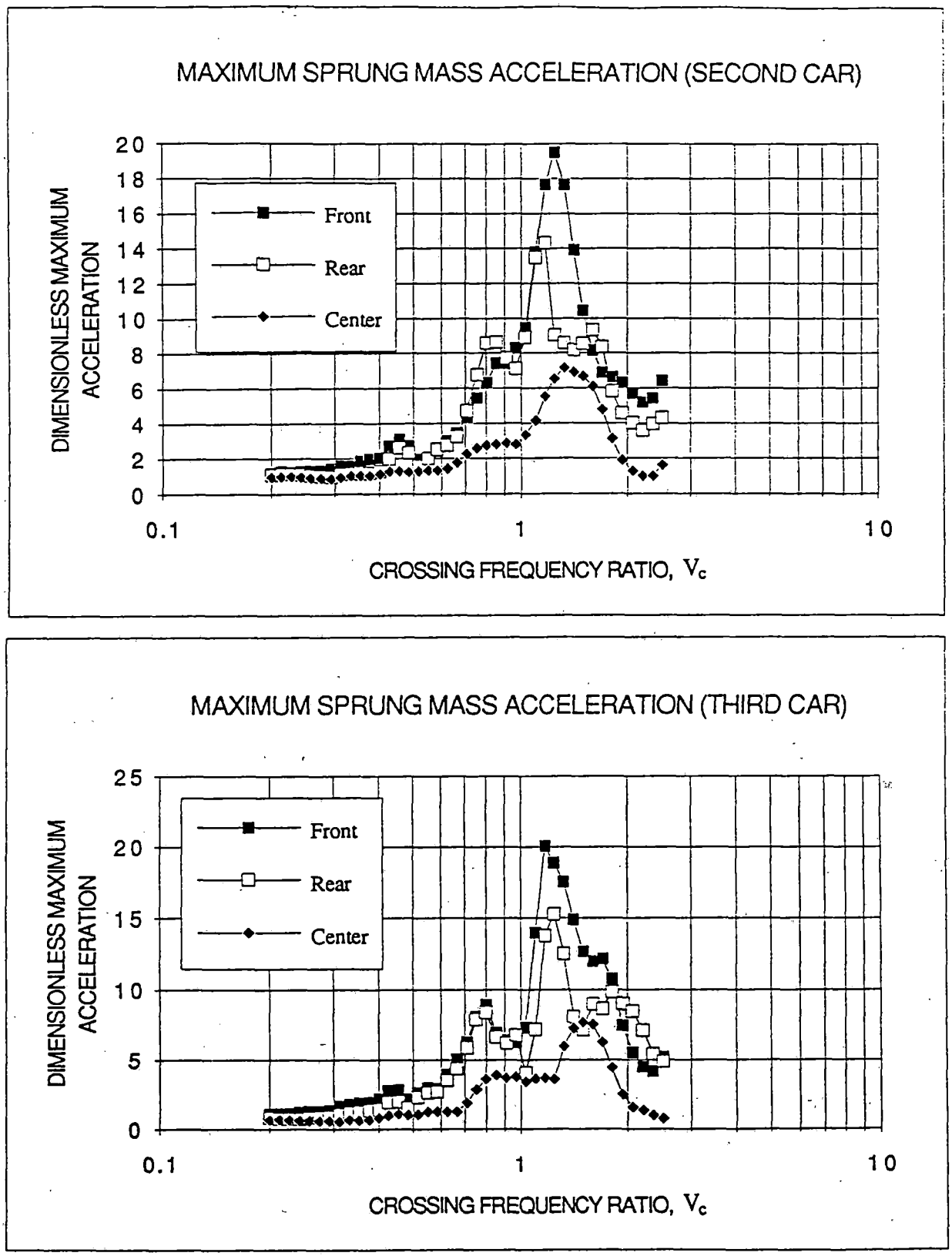

Figure 5.5 Response of Three Car Vehicle Train with Two Bogies Per Car Crossing a Double Span

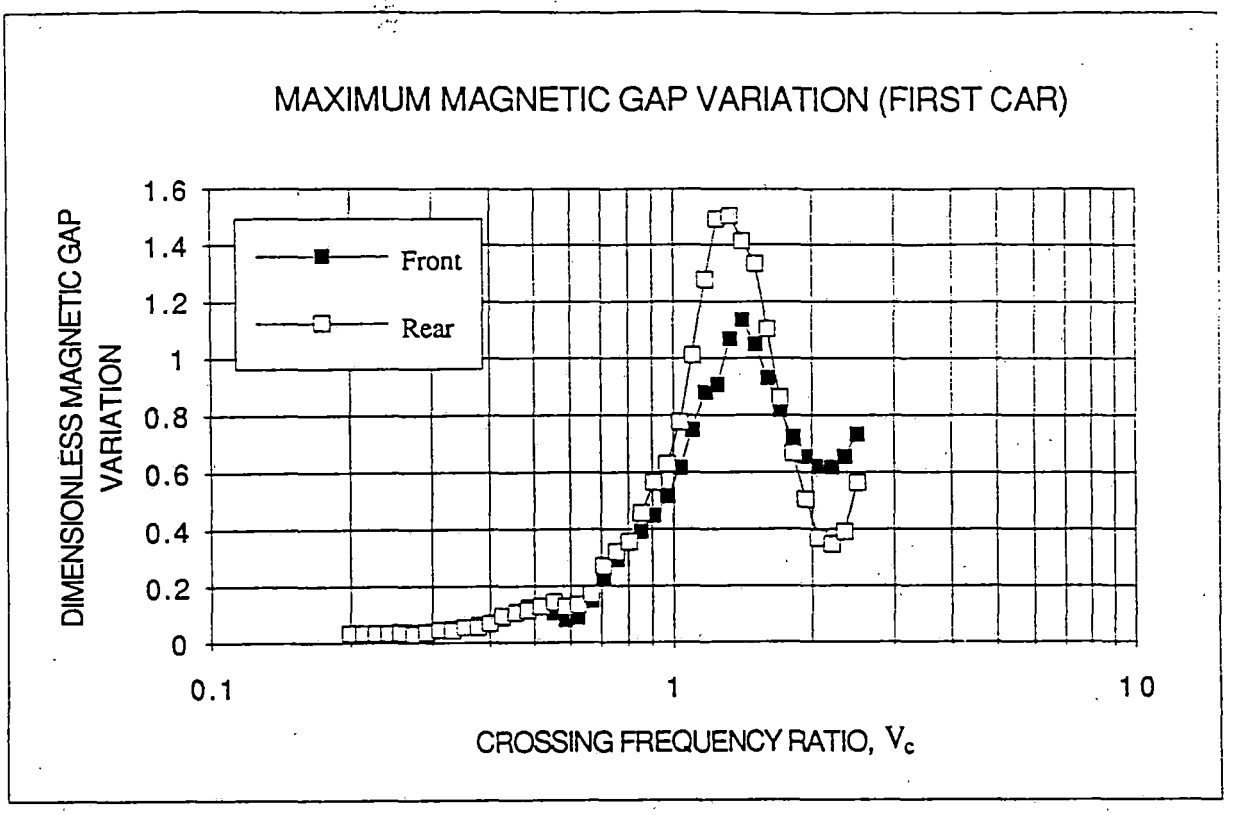

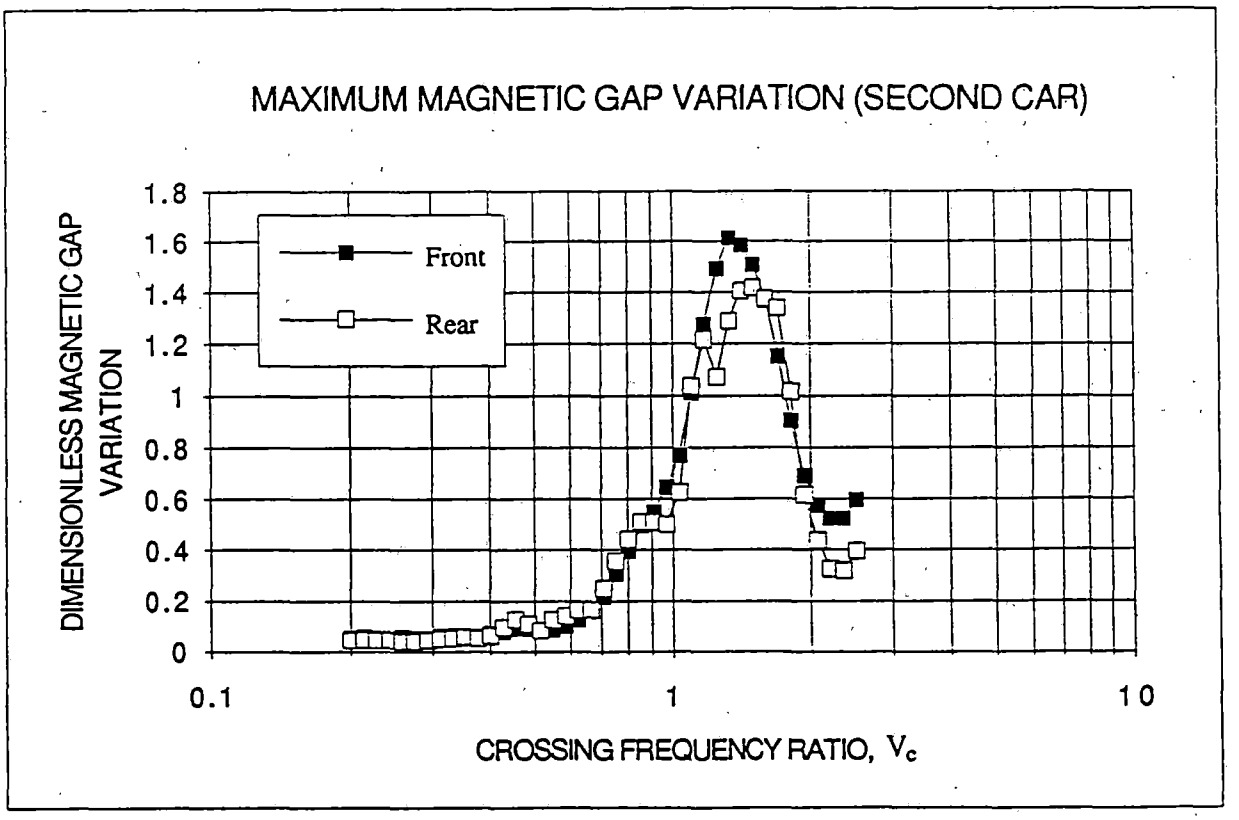

Figure 5.5 Response of Three Car Vehicle Train with Two Bogies Per Car Crossing a Double Span

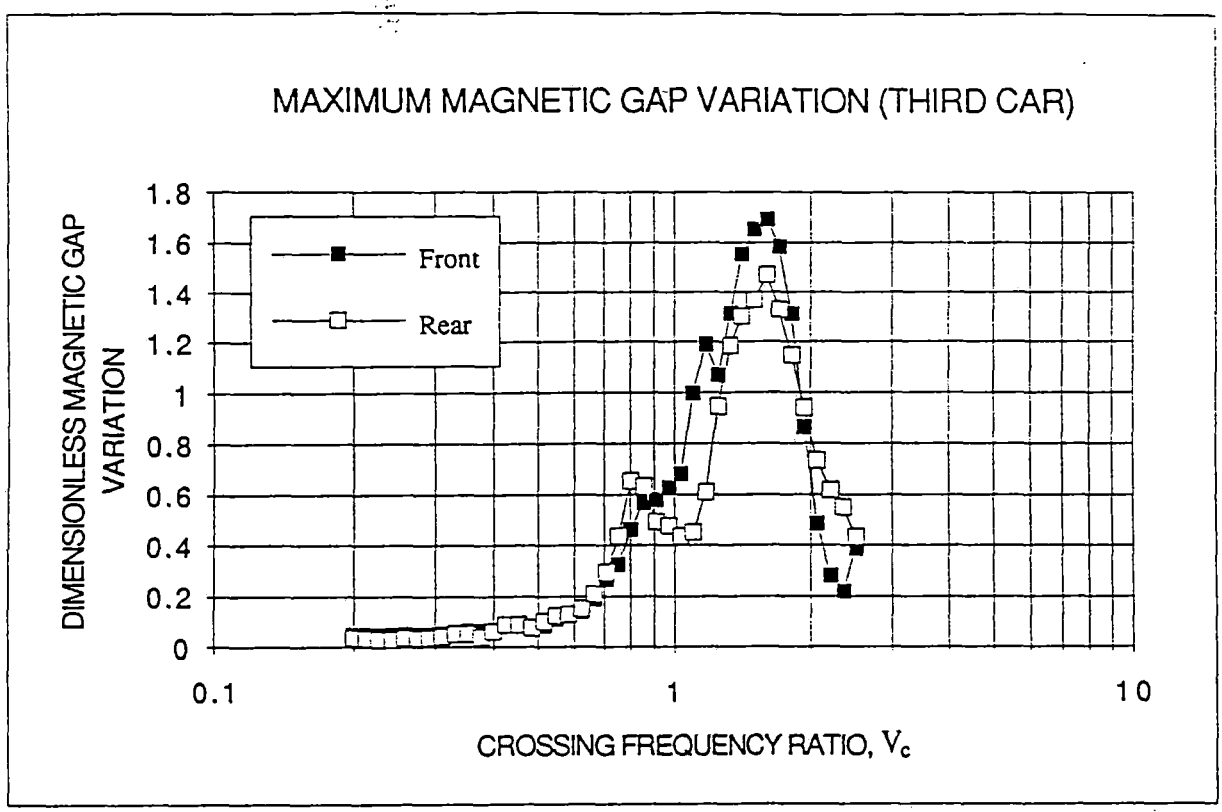

Figure 5.5 Response of Three Car Vehicle Train with Two Bogies Per Car Crossing a Double Span

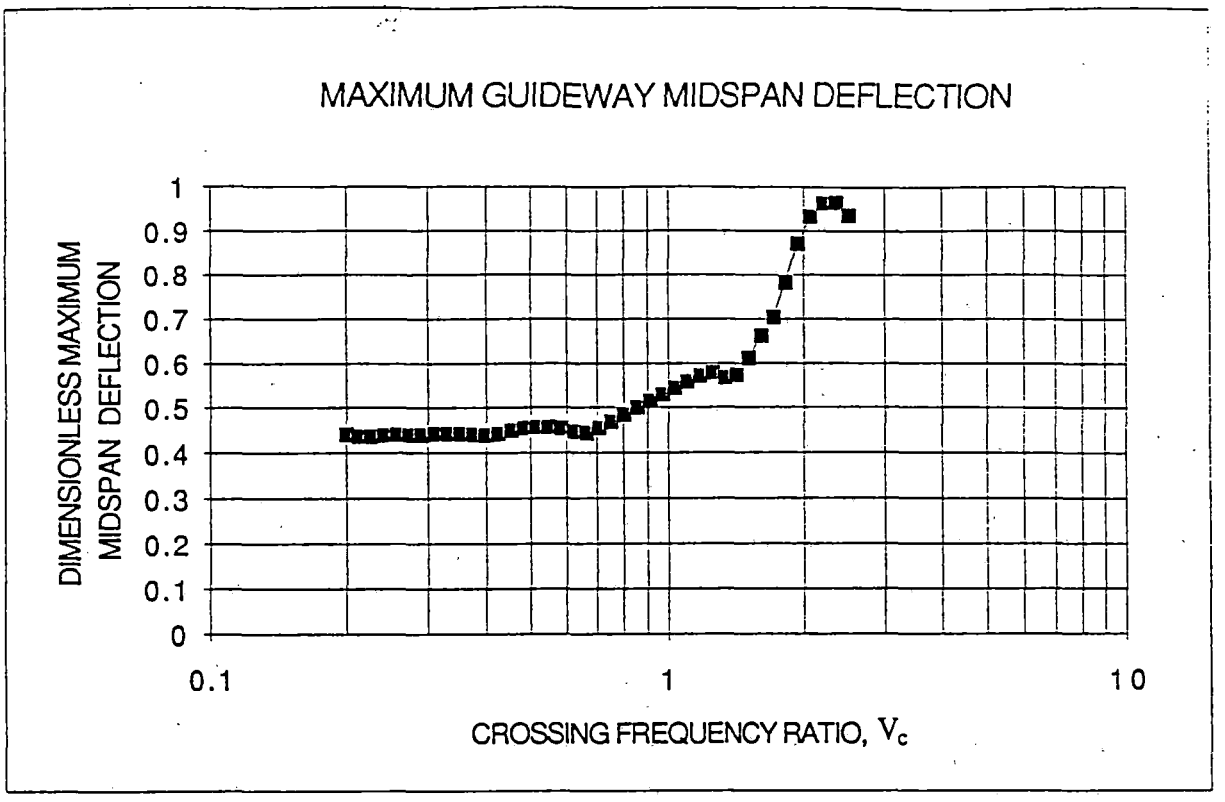

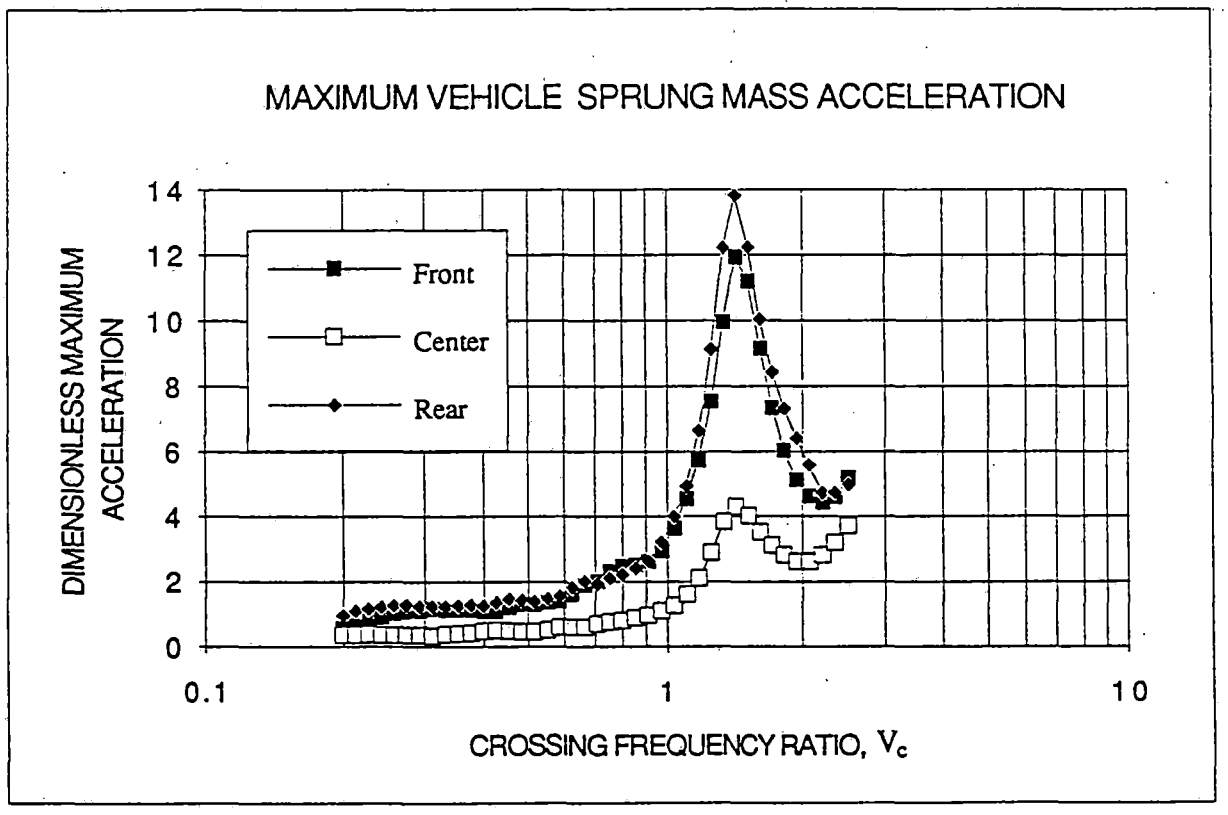

Figure 5.6 Response of a Single Car with Six Bogies Crossing a Double Span

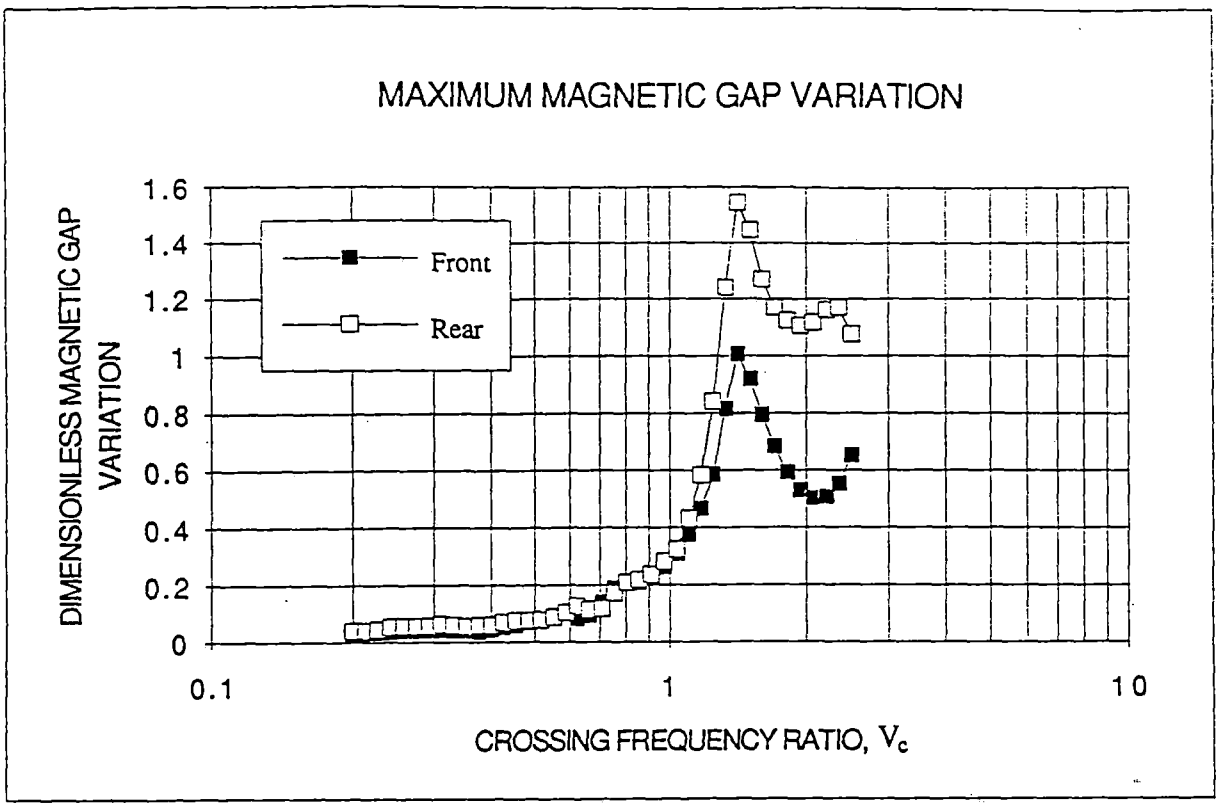

Figure 5.6 Response of a Single Car with Six Bogies Crossing a Double Span

show in comparison to data for the two boggie vehicle that for V_c less than 1.0, the maximum span deflections and vehicle accelerations are reduced and that multiple suspensions improve the ride quality.

Data in Figure 5.7 correspond to a three car train with vehicles having six suspensions each. These data indicate that peak span deflections, vehicle accelerations and magnetic gap variations occurring for Vc greater than 1.0 are reduced significantly in comparison to the three car train using two boggies per vehicle with peak acceleration levels limited to 50% of those for the train with two boggies per car. Thus, the use of distributed suspensions for multiple vehicle trains leads to significant decreases in dynamic interactions for operation above the crossing frequency ratio of 1.0.

5.3 Span Parametric Designs

To illustrate the influence of ride quality constraints on elevated span design a number of parametric studies have been conducted for single and double span designs for a vehicle with six model II suspensions distributed along the vehicles. The baseline parameters for these cases are summarized in Table 5.2. Several span designs are considered with various span cross section moments of inertia which are characterized in terms of their values of static deflection. The corresponding span natural frequencies are also tabulated as well the values of crossing frequency based on 125 m/s operation. As the guideway spans become more flexible, the static deflection increases, the natural frequency decreases and the corresponding crossing frequency ratio increases. As y* increases from 0.5 to 2.5 cm, the natural frequency decreases by more than a factor of two and the crossing frequency doubles and thus increased static deflection and dynamic amplification may occur.

The maximum midspan deflections and vehicle rms accelerations for a vehicle traversing the span system have been computed for the condition in which the vehicle has crossed a sufficient number of spans for initial condition transients to die out. Summary performance data are presented in Figure 5.8 for a single span design, based on single vehicle operation. The data show as more flexible spans are considered, the dynamic amplification factor increases. As design values of y* are increased from 0.5 cm to 2.5 cm, the dynamic amplification (y/y*) increases from 0.67 to almost 0.91. In a similar manner the vehicle accelerations increase with more flexible spans. As design values of y* are increased from 0.5 cm to 2.5 cm, the rms acceleration at the vehicle center, front and rear respectively increase from 0.007 g, 0.03 g and 0.031 g to 0.058 g, 0.19 g and 0.24 g. The acceleration levels at the vehicle front and rear are greater than those at the center by a factor of almost 3-4.

Table 5.2

Parameters For Illustrative Performance Study

(a) Vehicle Configuration

Vehicle Model	II	II	IV
Vehicle Weight (kg)	53,840		
f_s (Hz)	1.0		
f_u (Hz)	3.5	1.75	3.5
ζ_s	0.25	0.25	0.25
ζ_a	0	0	0.25
ζ_u	0	0	0.25

(b) Configuration For Single and Double Span Guideways With 25 m Span Length

Y^* (cm)	f^* (Hz)	V_c
0.5	9.4	0.53
1.0	6.7	0.74
1.5	5.4	0.93
2.5	4.2	1.19

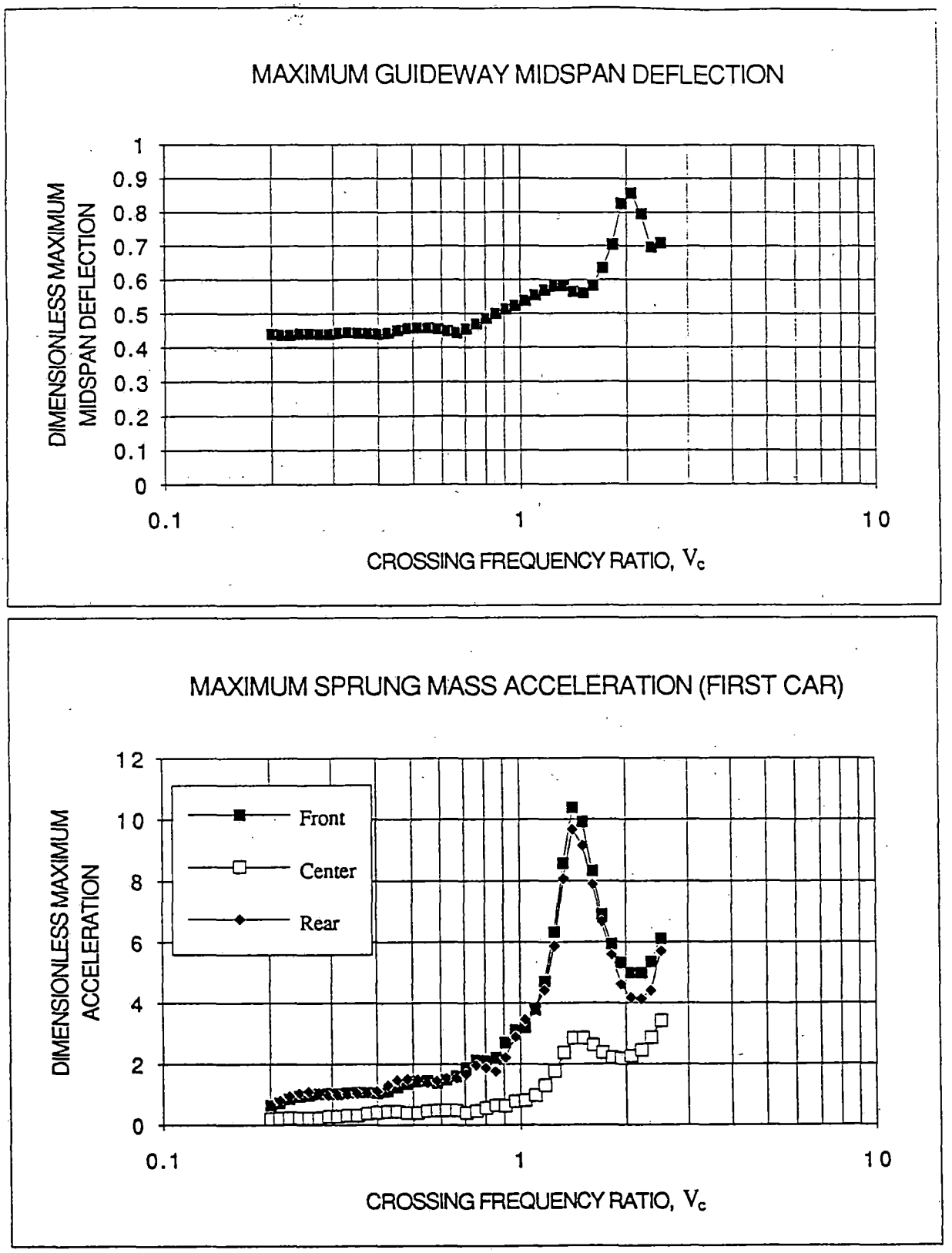

Figure 5.7 Response of a Three Car Train with Six Bogies Per Car Crossing a Double Span

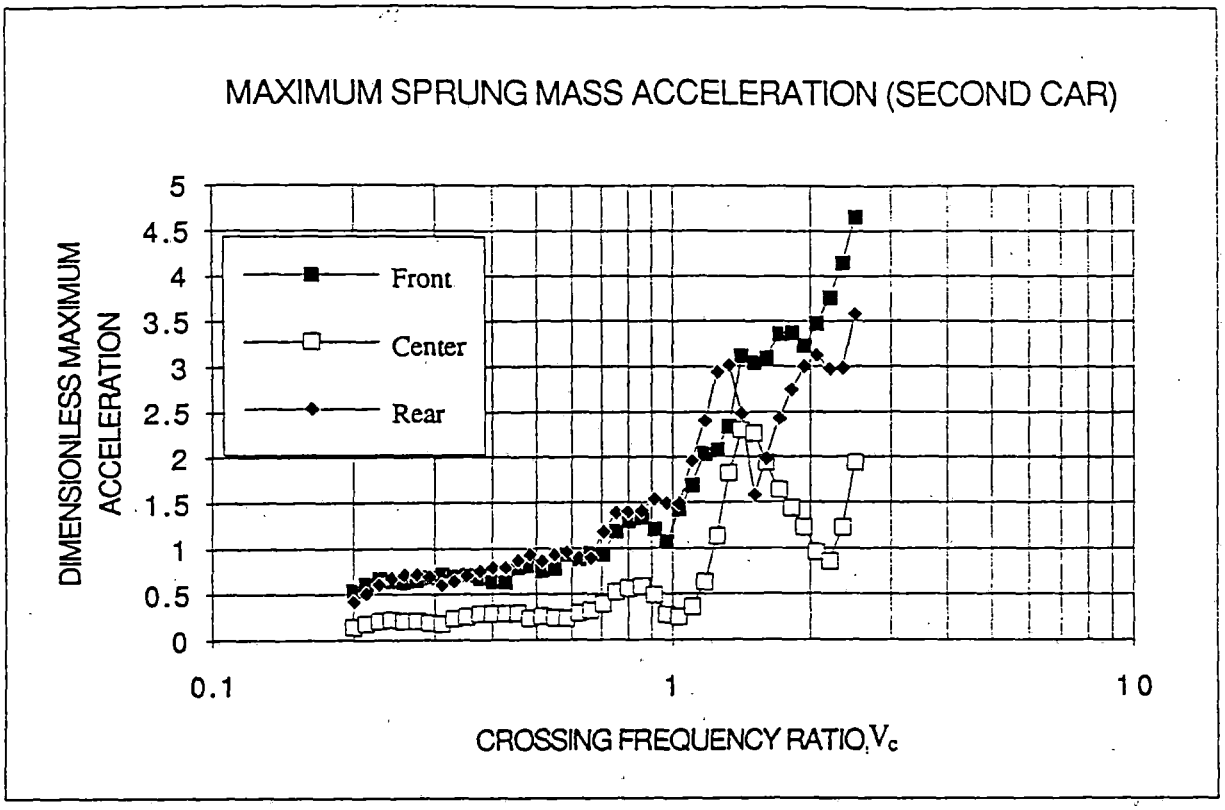

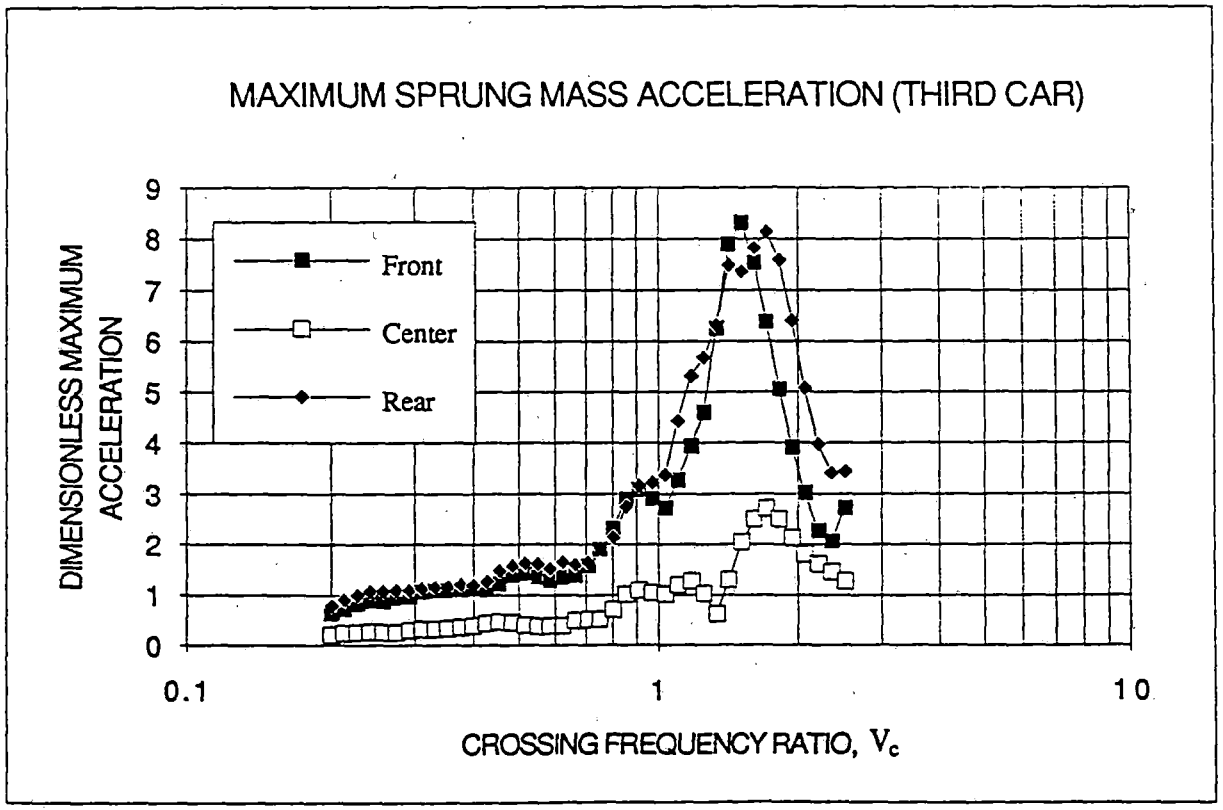

Figure 5.7 Response of a Three Car Train with Six Bogies Per Car Crossing a Double Span

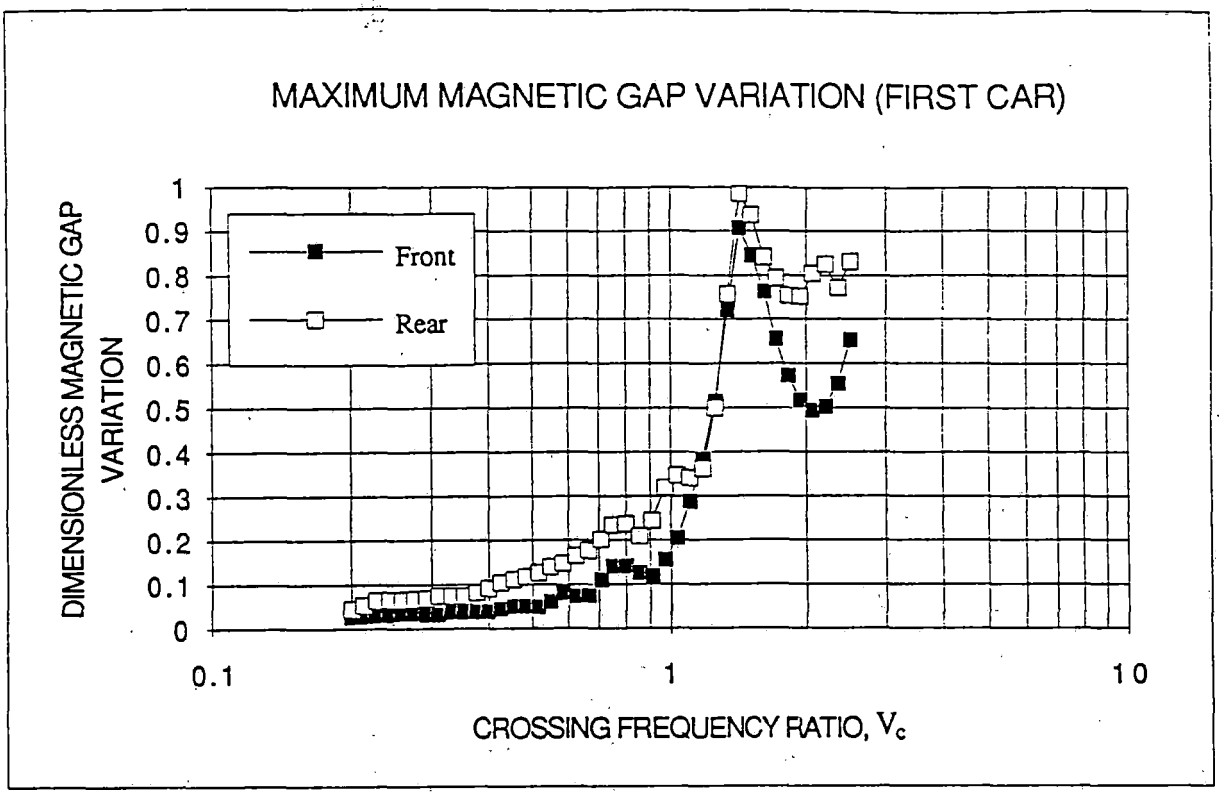

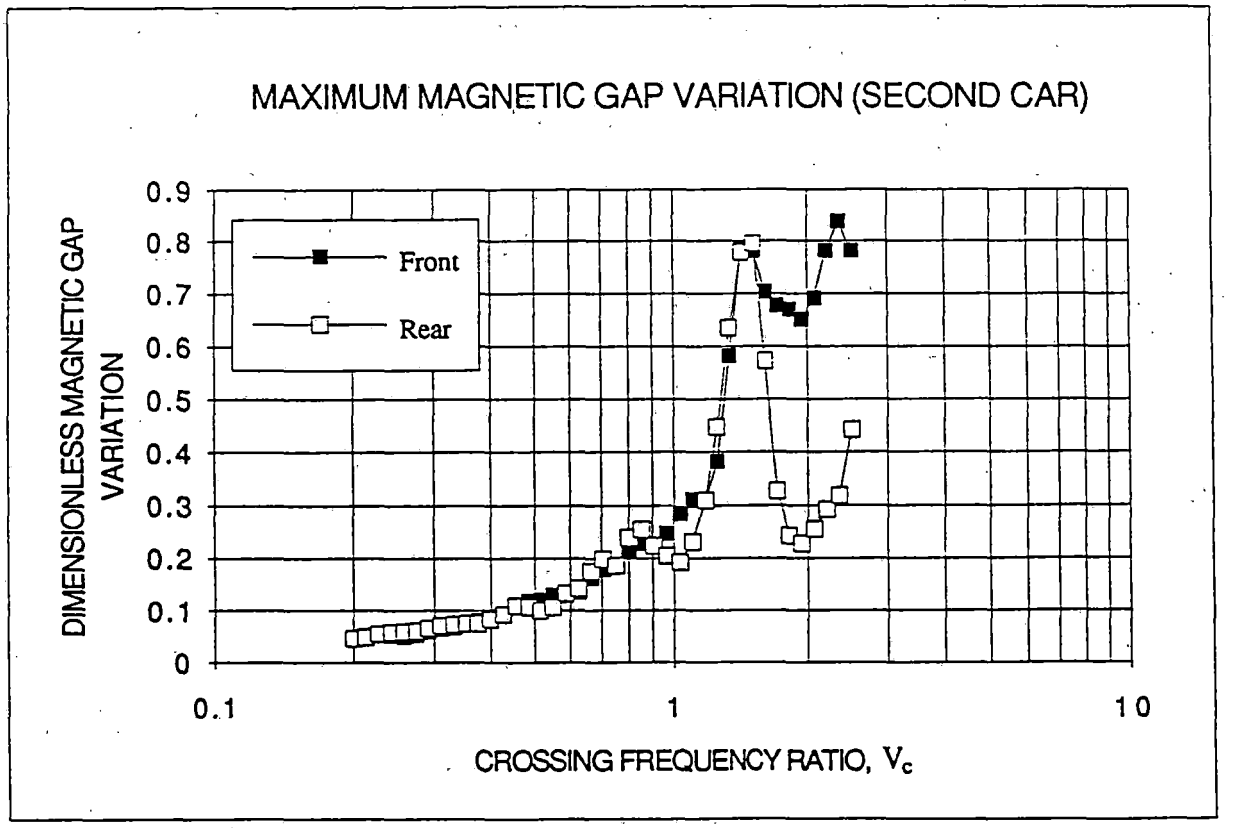

Figure 5.7 Response of a Three Car Train with Six Bogies Per Car Crossing a Double Span

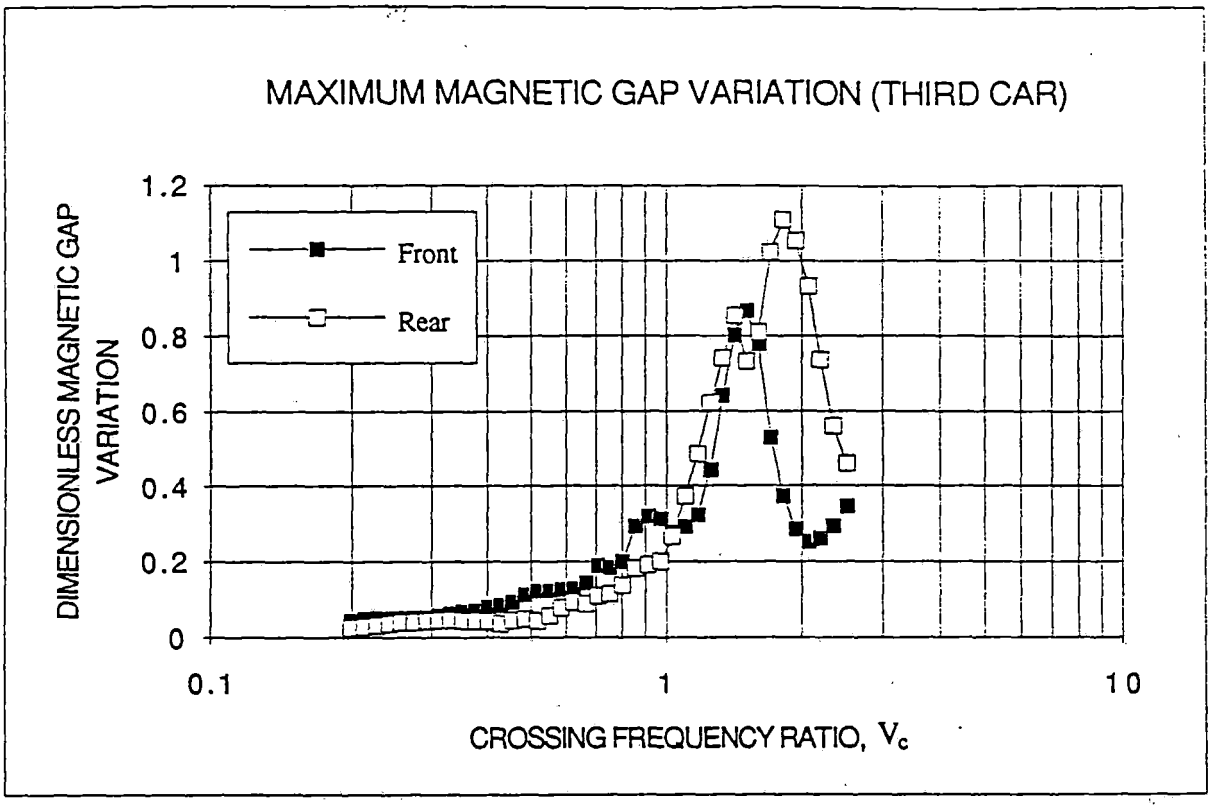

Figure 5.7 Response of a Three Car Train with Six Bogies Per Car Crossing a Double Span

Model II with f_u = 3.5 Hz and Six Bogies Per Car

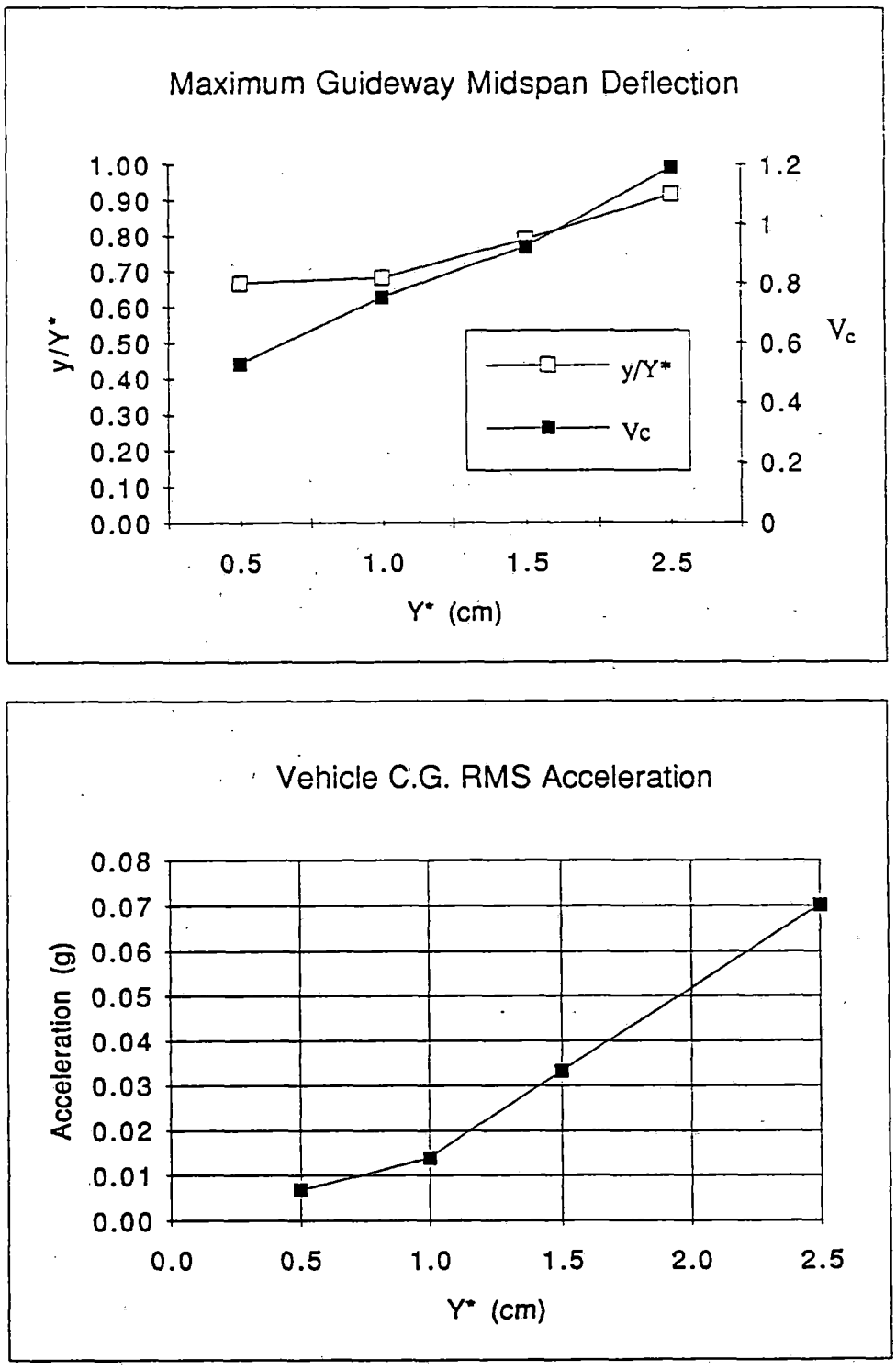

Figure 5.8 Response of a Single Vehicle Crossing Single Span Guideways

Model II with f_u = 3.5 Hz and Six Bogies Per Car

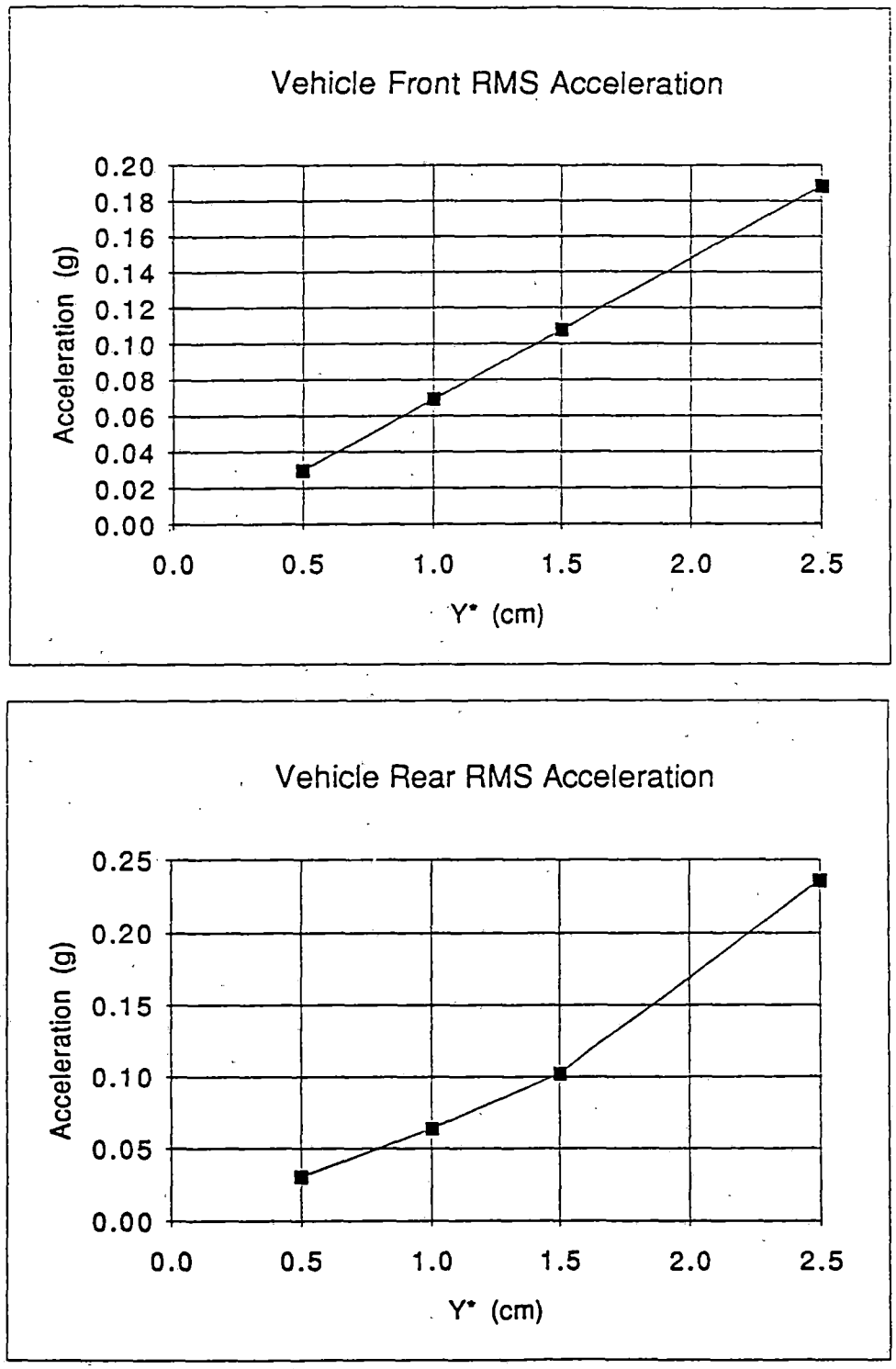

Figure 5.8 Response of a Single Vehicle Crossing Single Span Guideways

Model II with f_u = 3.5 Hz and Six Bogies Per Car

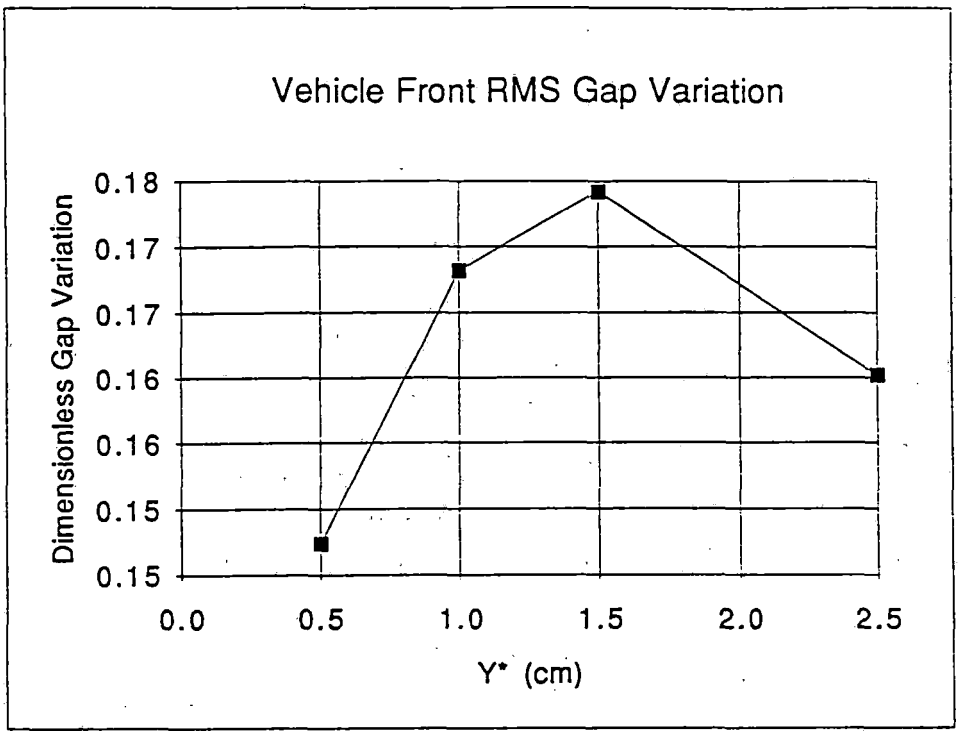

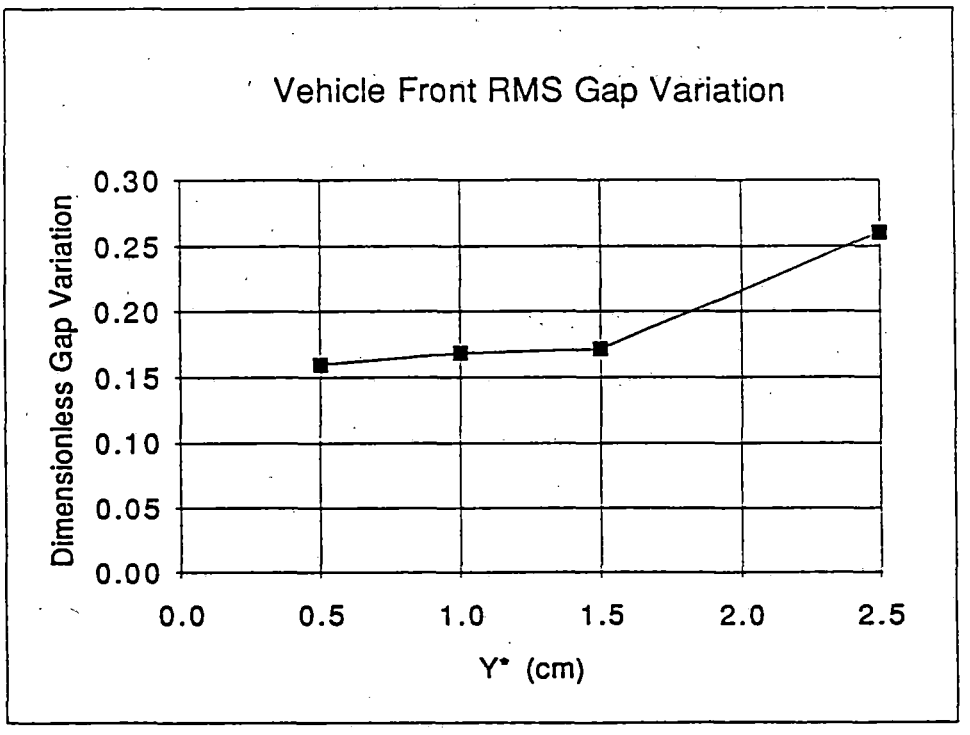

Figure 5.8 Response of a Single Vehicle Crossing Single Span Guideways

Data in Figure 5.9 which correspond to a three car train crossing single span guideways, illustrate similar trends to the single vehicle data. The span dynamic amplification factors as a function of speed are similar to the single car case. The accelerations in the three car train again are greater at the front and rear of each vehicle than at the center with the first and third cars in general experiencing higher accelerations than the middle car. The maximum accelerations occurring in the three car train are similar in value to those in the single vehicle case.

Data are presented in Figures 5.10 and 5.11 for single vehicles and three car trains traversing double span guideways. These data also indicate that as the design deflection is increased both span dynamic amplification factors and vehicle accelerations increase. Additionally, in all of these cases the vehicle front and rear accelerations are approximately 2-4 times the acceleration at the center of a vehicle.

Additional data for vehicles equipped with model II suspensions with a reduced primary suspension frequency of 1.75 Hz are summarized in Figures 5.12 and 5.13 respectively for single and double span guideway designs. These data show that reducing the primary suspension stiffness leads to a reduction in vehicle rms acceleration levels and to increased rms gap variations.

Data for vehicles employing model IV suspensions crossing single and double span guideways are summarized respectively in Figures 5.14 and 5.15. These data illustrate similar trends to the data for the model II suspension.

To illustrate the influence of ride quality constraints on span design the equivalent design values of y* required so that maximum specified levels of rms acceleration are satisfied at any point on the car in a three car train have been determined from the data in Figures 5.8-5.15 and summarized in Table 5.3. The values of y* are directly related to span stiffness.

The data show that the span design flexibility may be increased by almost a factor of two if the constraints on vehicle acceleration are increased from 0.04 g to 0.08 g, thus ride quality has a direct influence on the design stiffness which can be selected for the guideway. The data also show that the same level of acceleration can be obtained with a two span guideway which has reduced stiffness in comparison to a single span guideway with a stiffness reduction of 30 to 40% in the double span guideway yielding the same acceleration levels as the single span guideway.

Data in Table 5.3 correspond to suspension model II which is characteristic of an EDS suspension with no damping employed in the secondary suspension. Two different designs of the suspension have been considered. A design with f_u = 3.5 Hz which may correspond to a relatively stiff null flux type of suspension with a nominal operating gap of

Model II with f_u = 3.5 Hz and Six Bogies Per Car

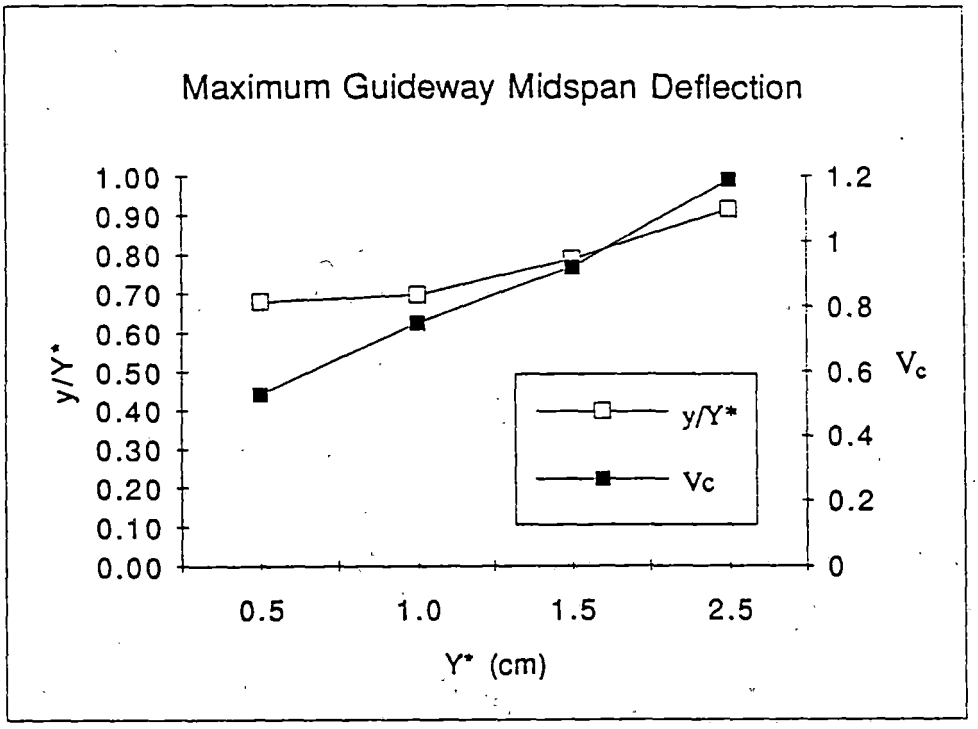

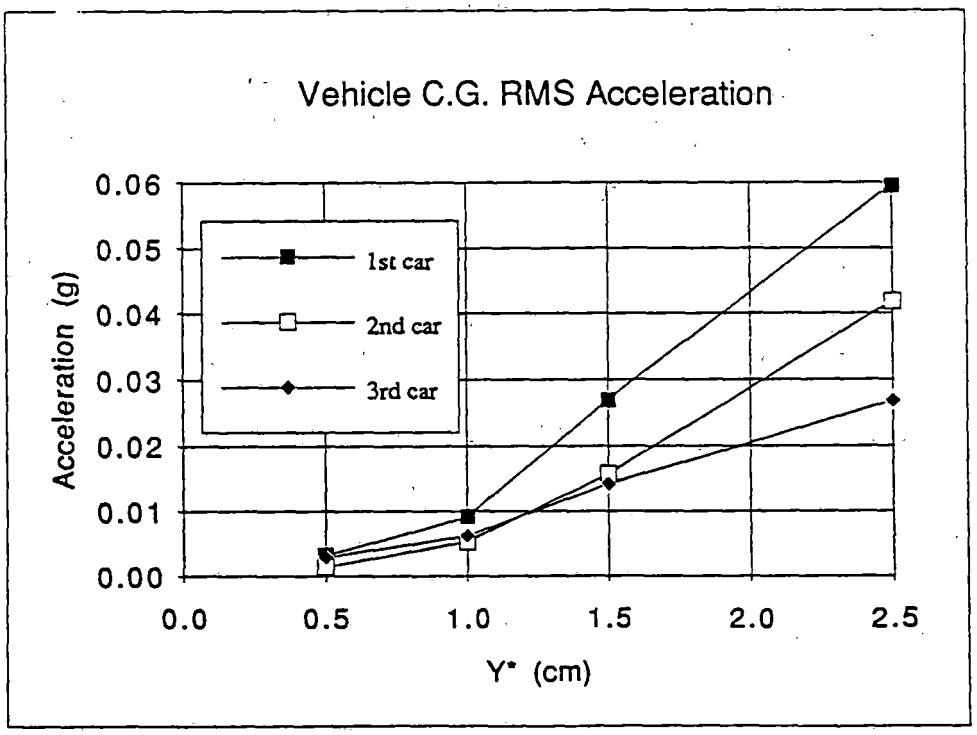

Figure 5.9 Response of a Three Car Train Crossing Single Span Guideways

Model II with f_u = 3.5 Hz and Six Bogies Per Car

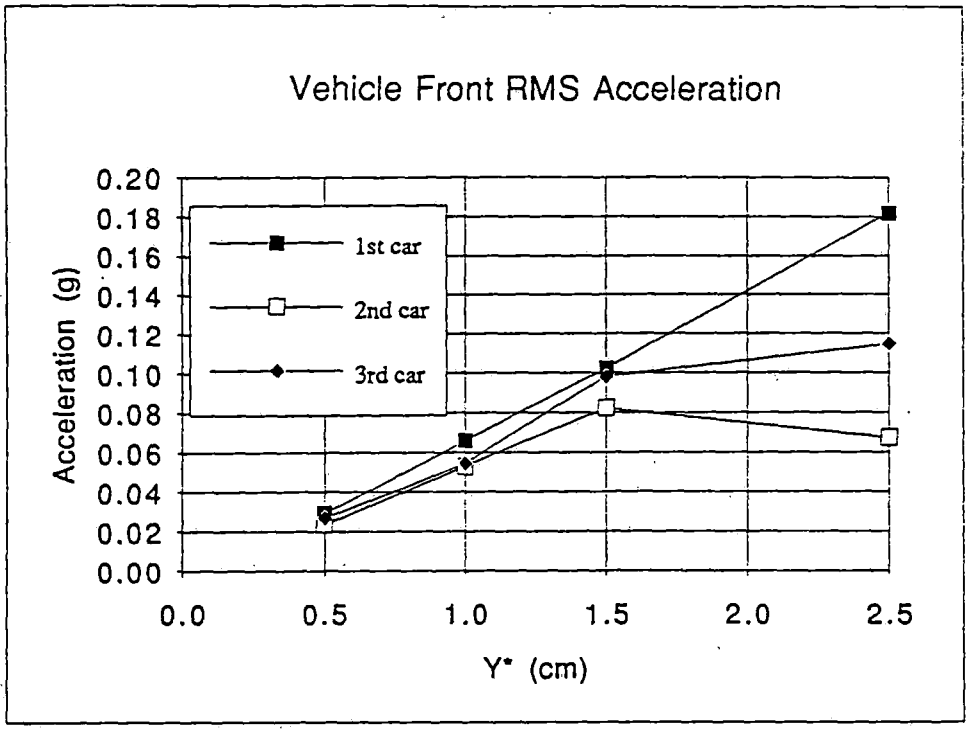

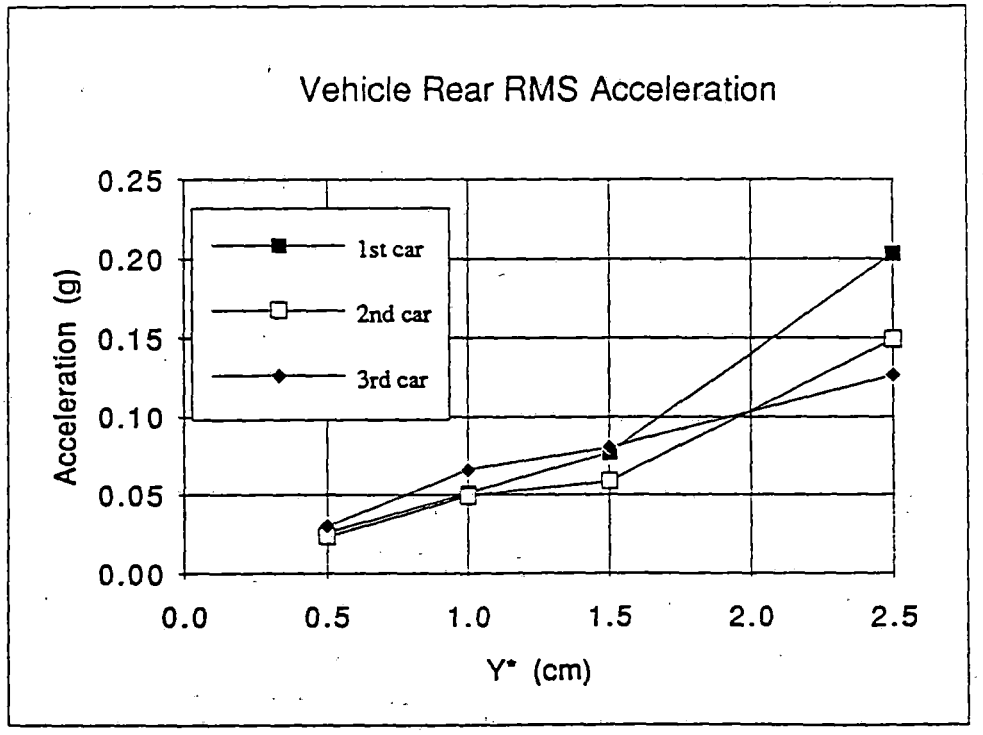

Figure 5.9 Response of a Three Car Train Crossing Single Span Guideways

Model II with f_u = 3.5 Hz and Six Bogies Per Car

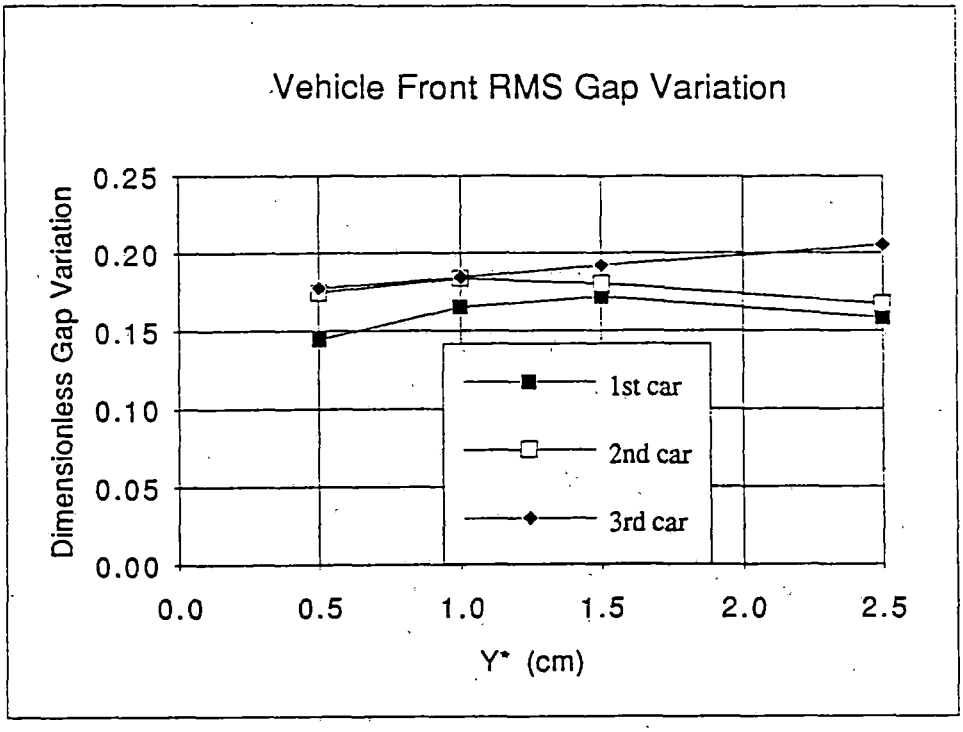

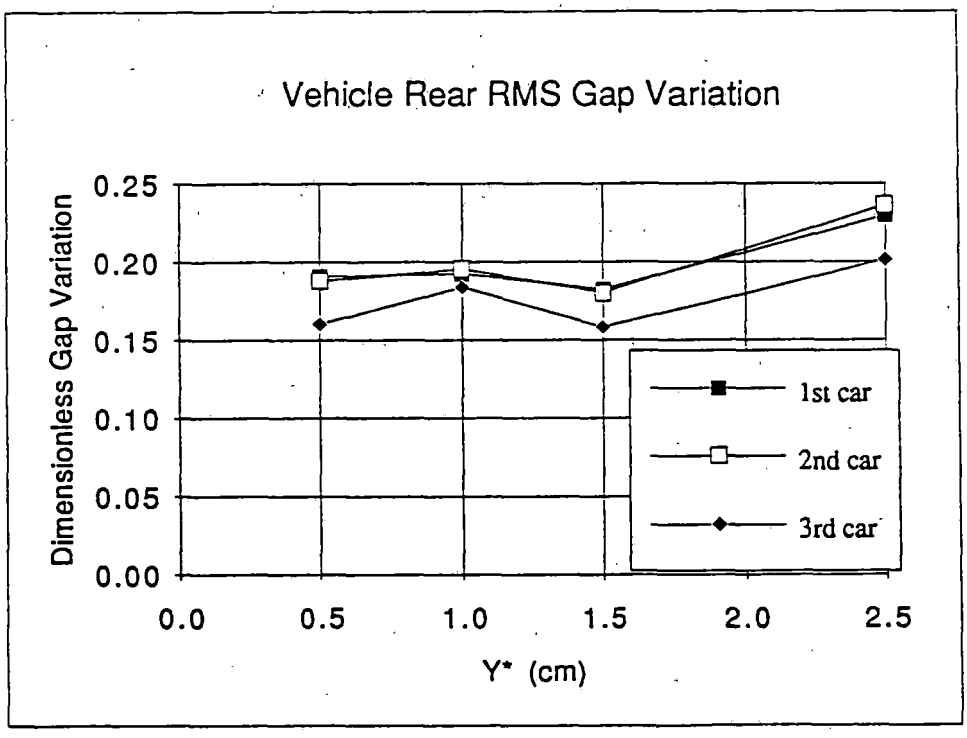

Figure 5.9 Response of a Three Car Train Crossing Single Span Guideways

Model II with $f_u = 3.5$ Hz and Six Bogies Per Car

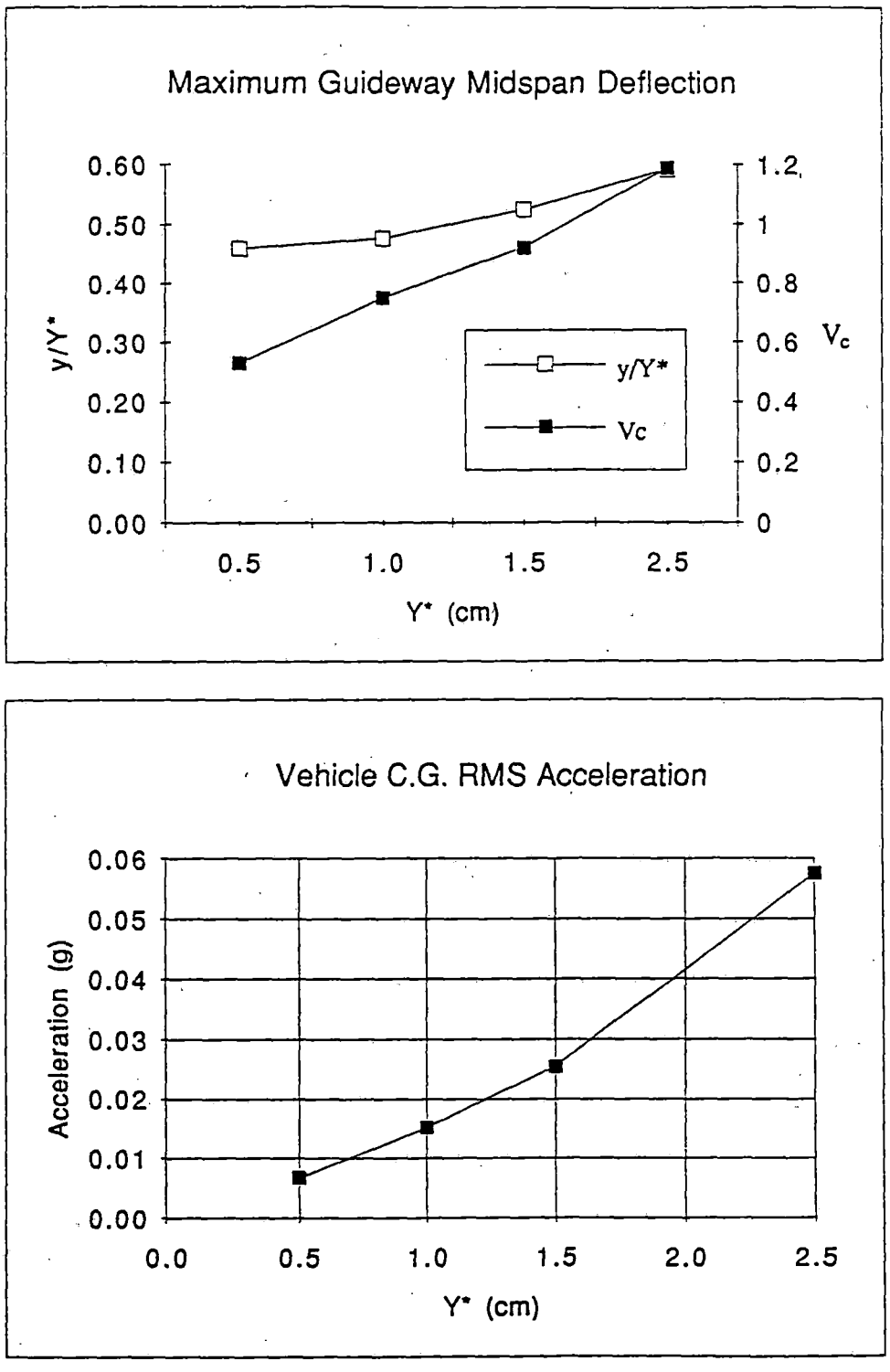

Figure 5.10 Response of a Single Vehicle Crossing Double Span Guideways

Model II with f_u = 3.5 Hz and Six Bogies Per Car

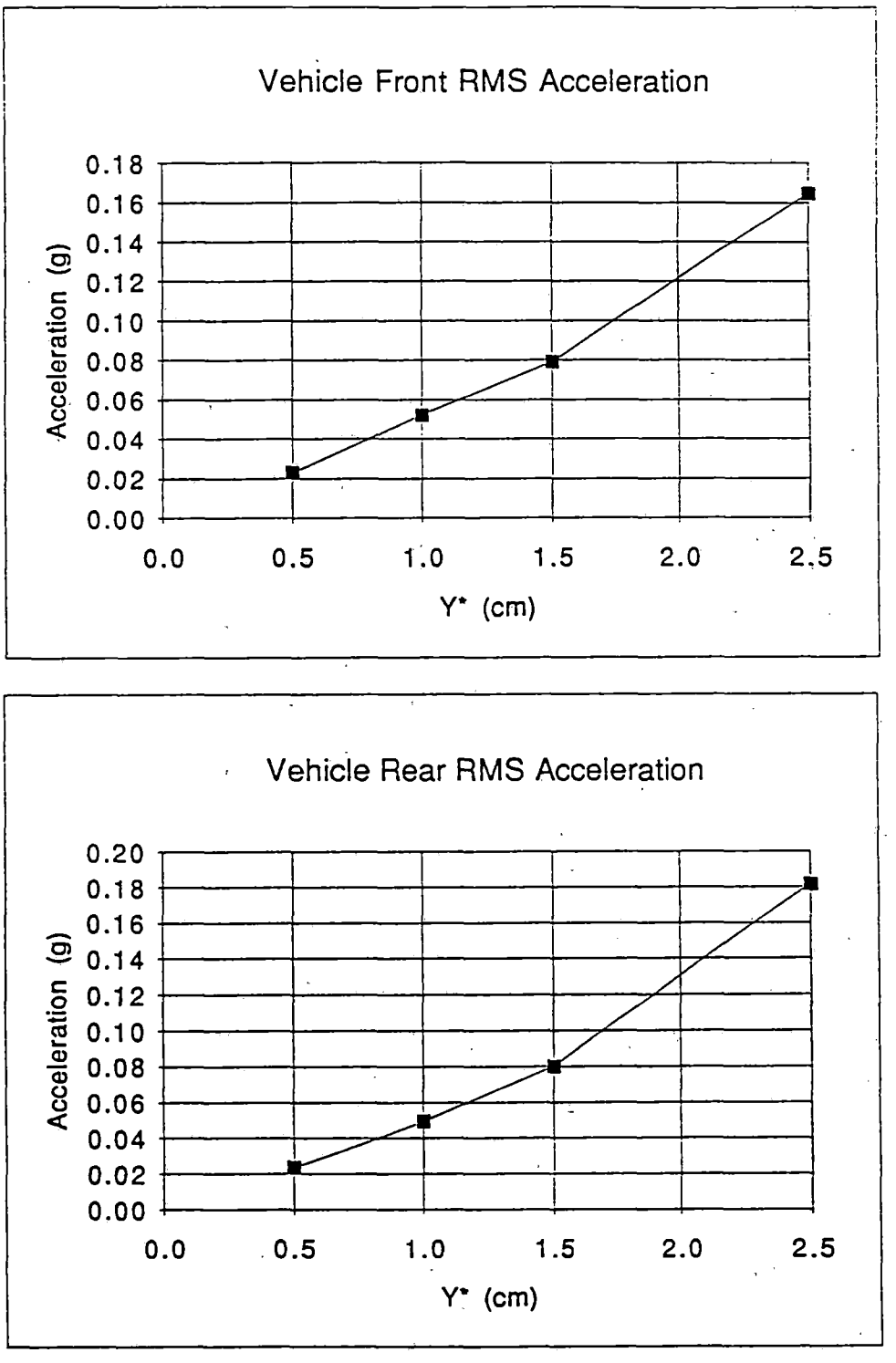

Figure 5.10 Response of a Single Vehicle Crossing Double Span Guideways

Model II with f_u = 3.5 Hz and Six Bogies Per Car

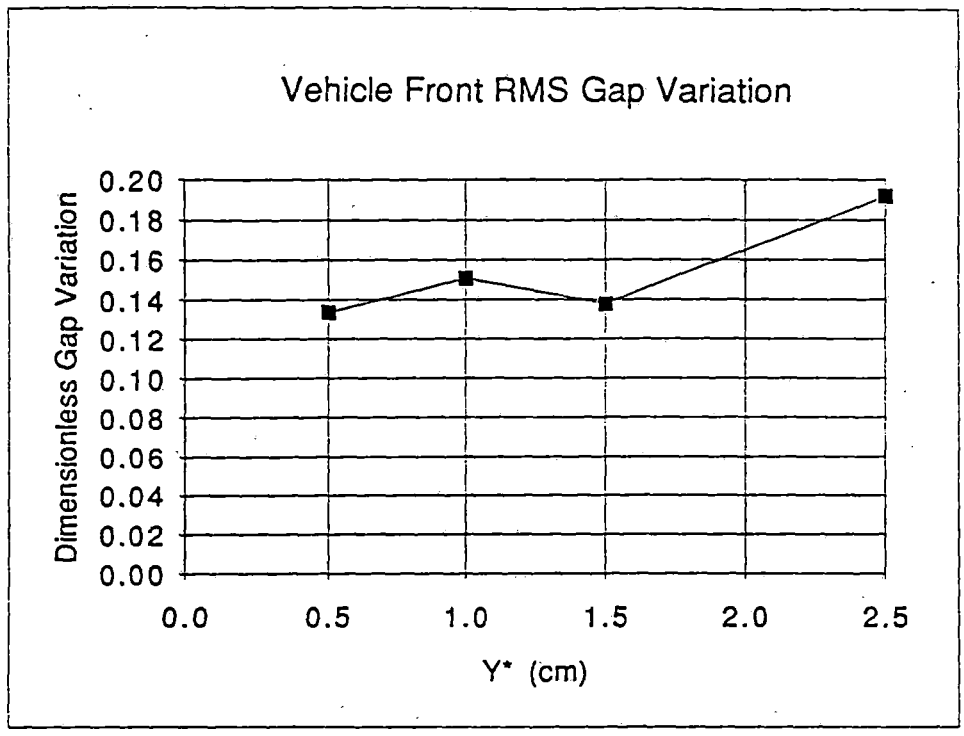

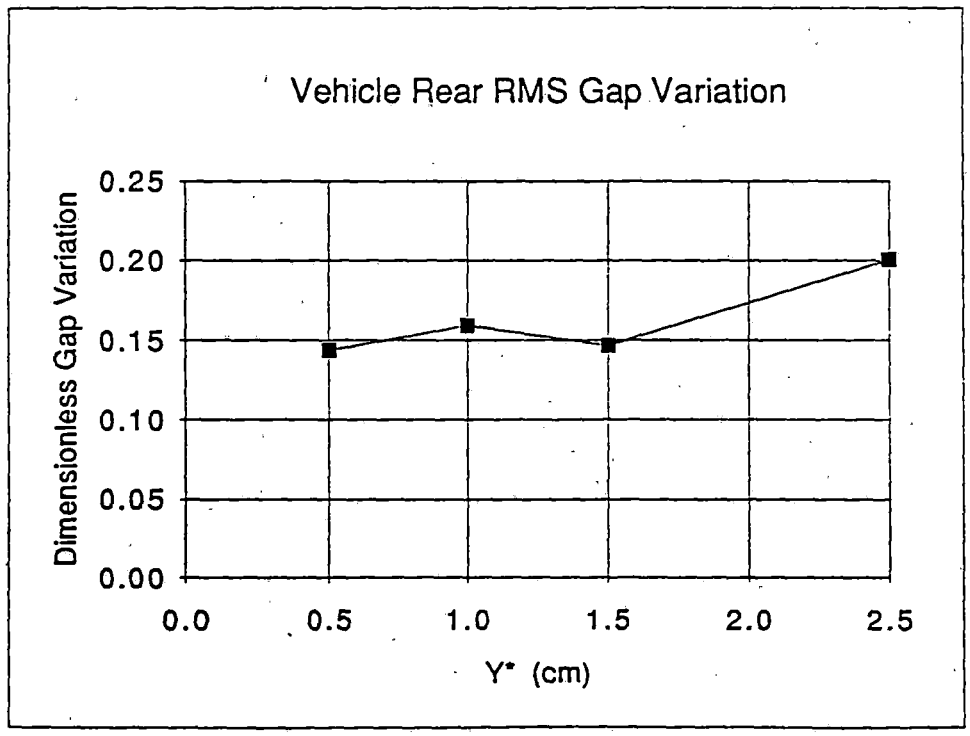

Figure 5.10 Response of a Single Vehicle Crossing Double Span Guideways

Model II with f_u = 3.5 Hz and Six Bogies Per Car

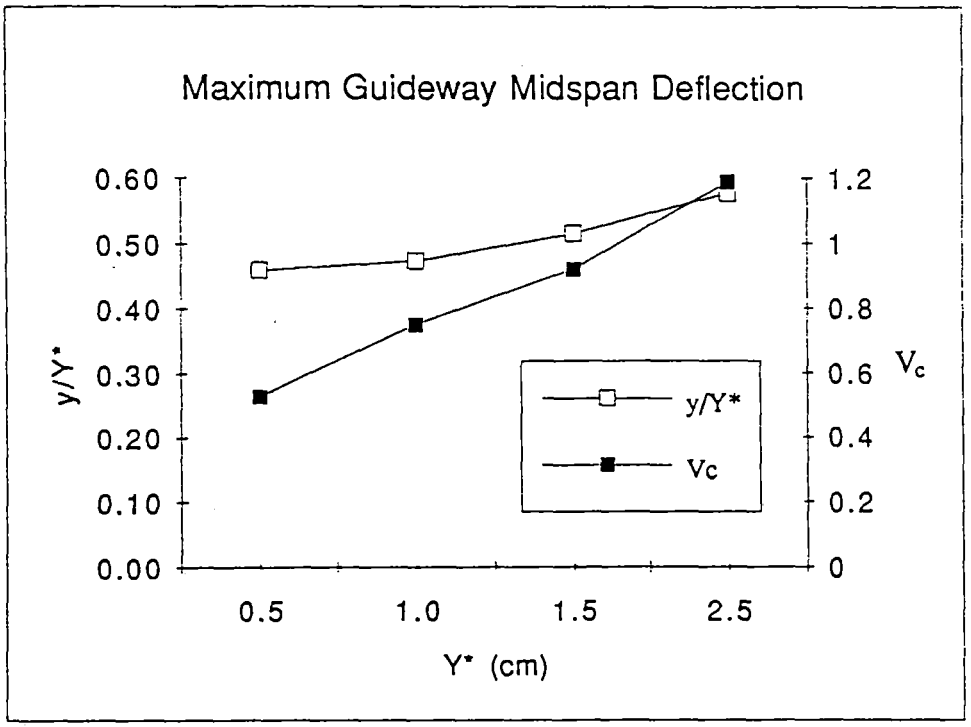

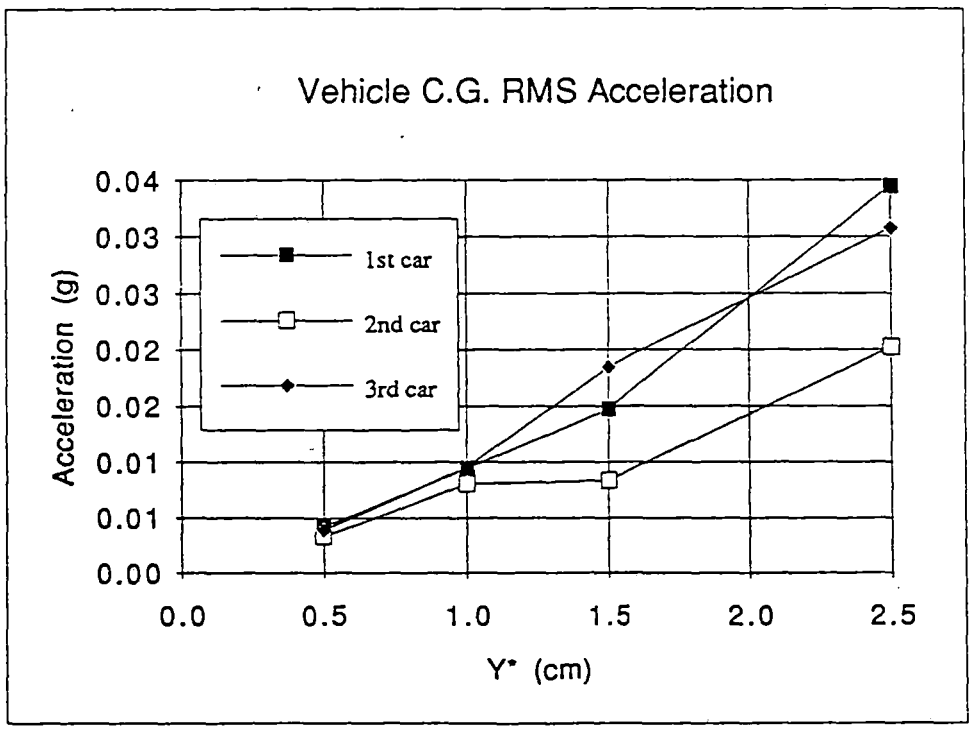

Figure 5.11 Response of a Three Car Train Crossing Double Span Guideways

Model II with f_u = 3.5 Hz and Six Bogies Per Car

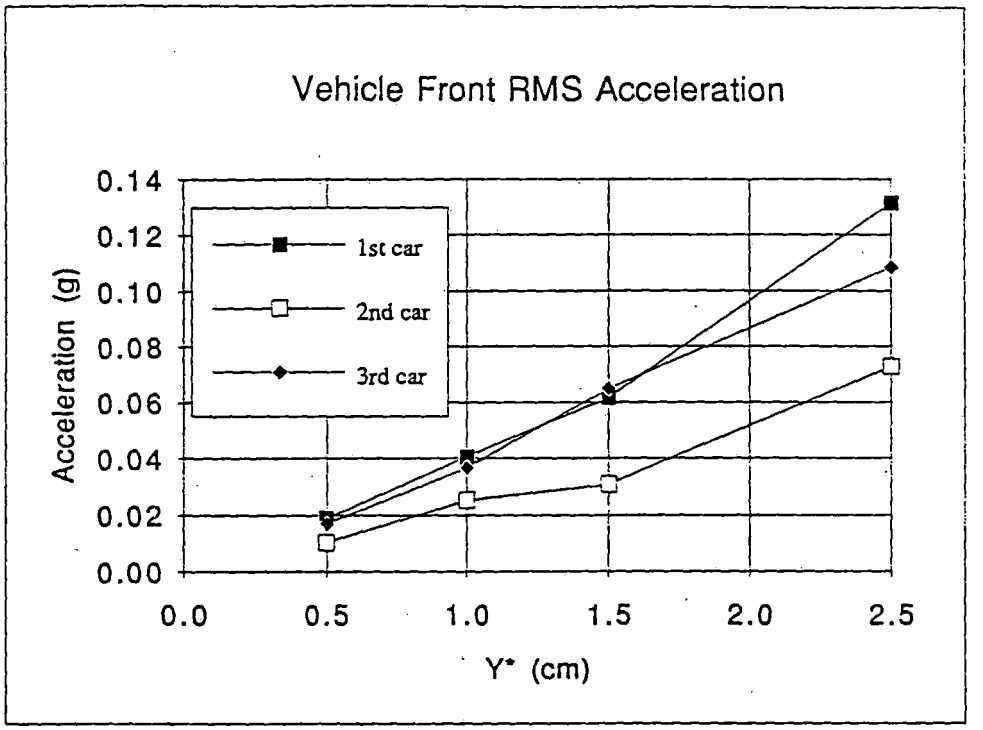

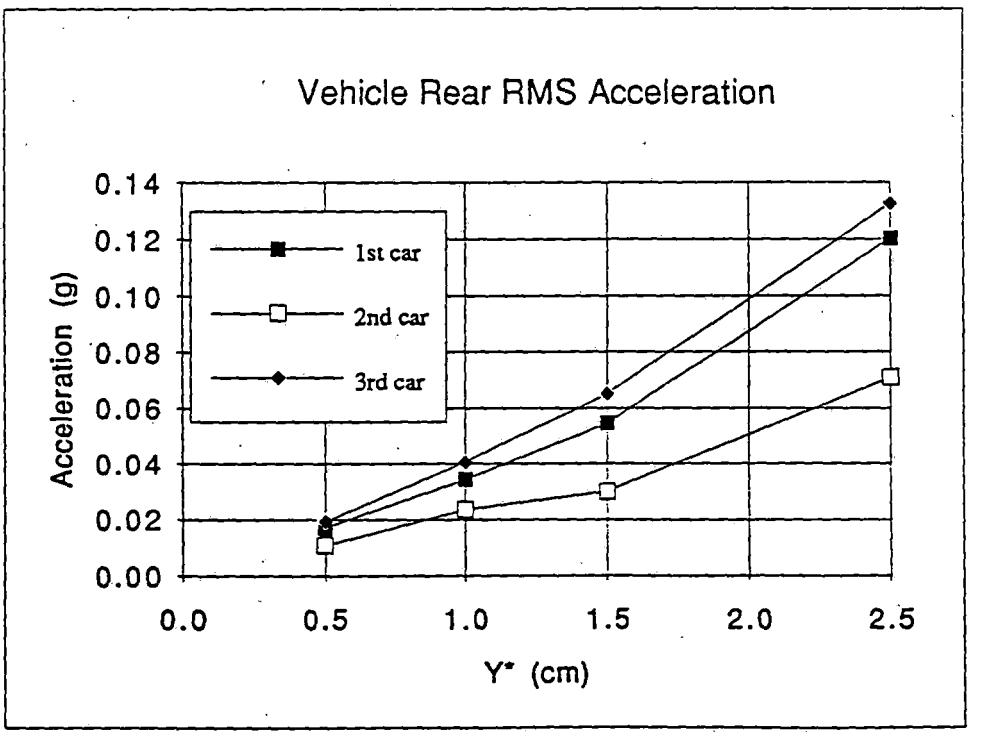

Figure 5.11 Response of a Three Car Train Crossing Double Span Guideways

Model II with $f_u = 3.5$ Hz and Six Bogies Per Car

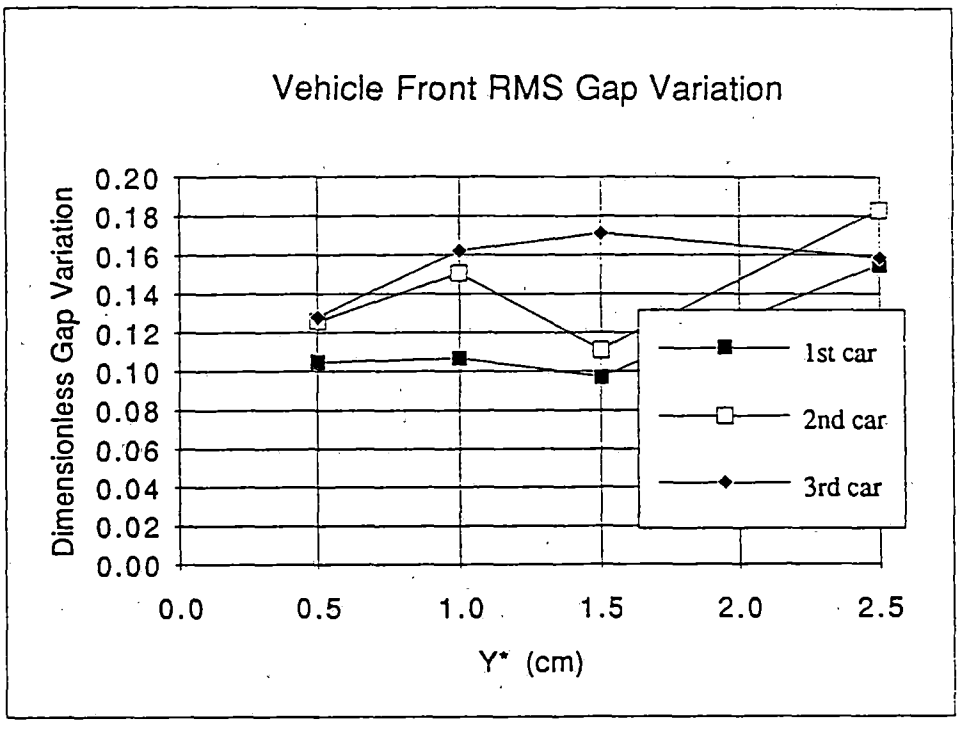

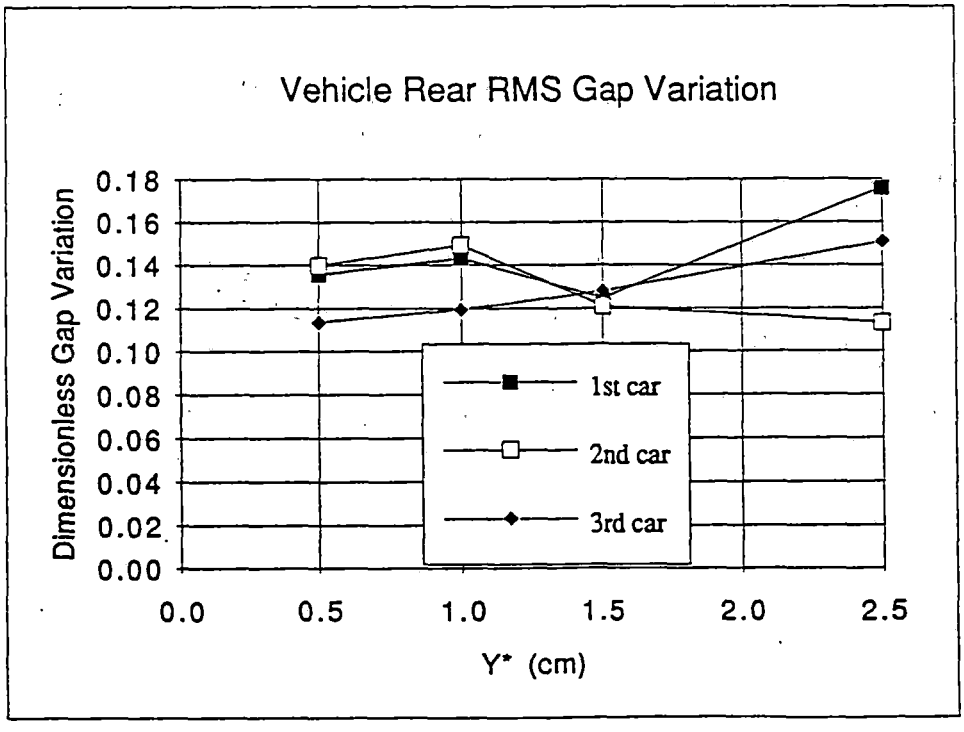

Figure 5.11 Response of a Three Car Train Crossing Double Span Guideways

Model II with f_u = 1.75 Hz and Six Bogies Per Car

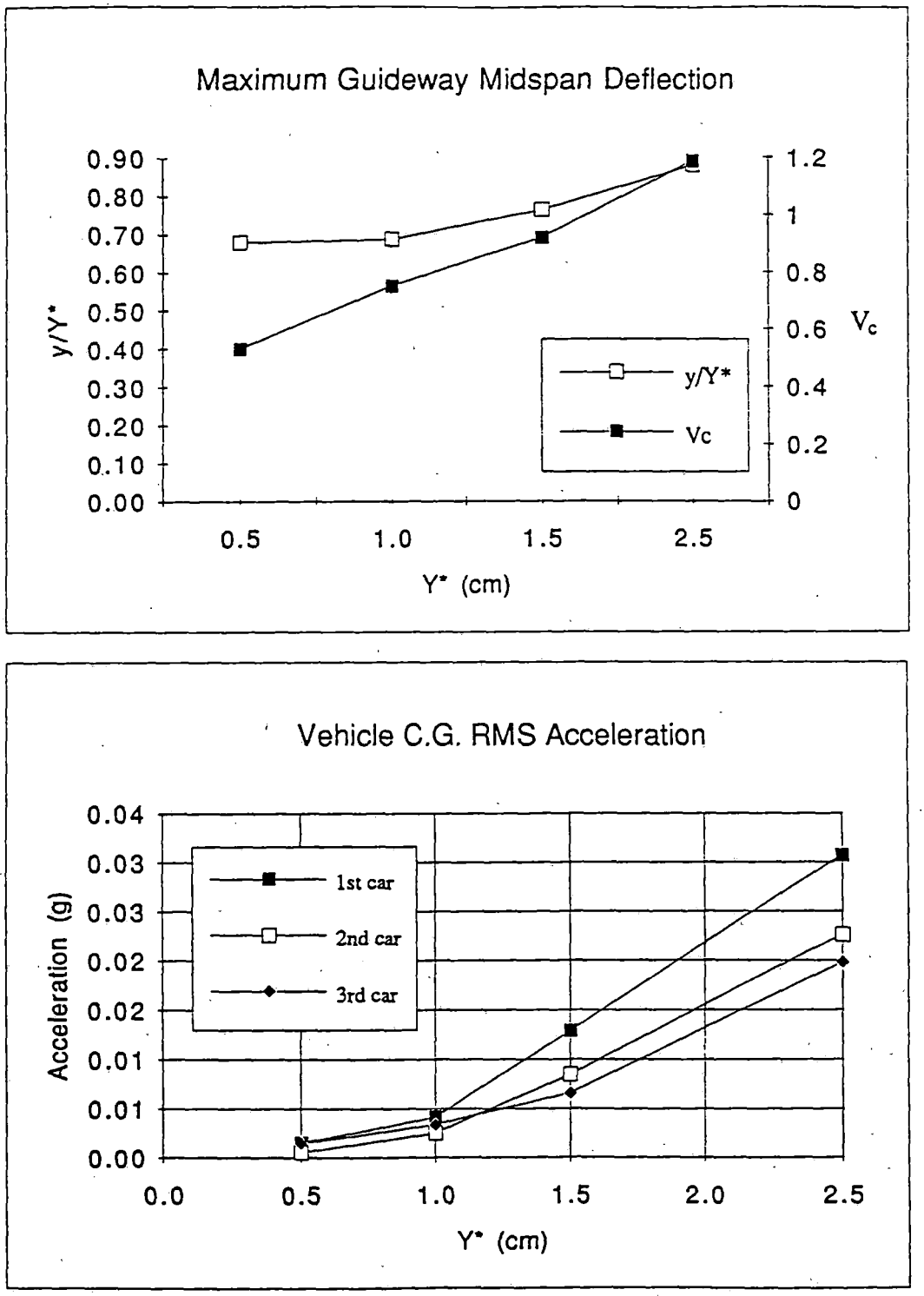

Figure 5.12 Response of a Three Car Train Crossing Single Span Guideways

Model II with f_u = 1.75 Hz and Six Bogies Per Car

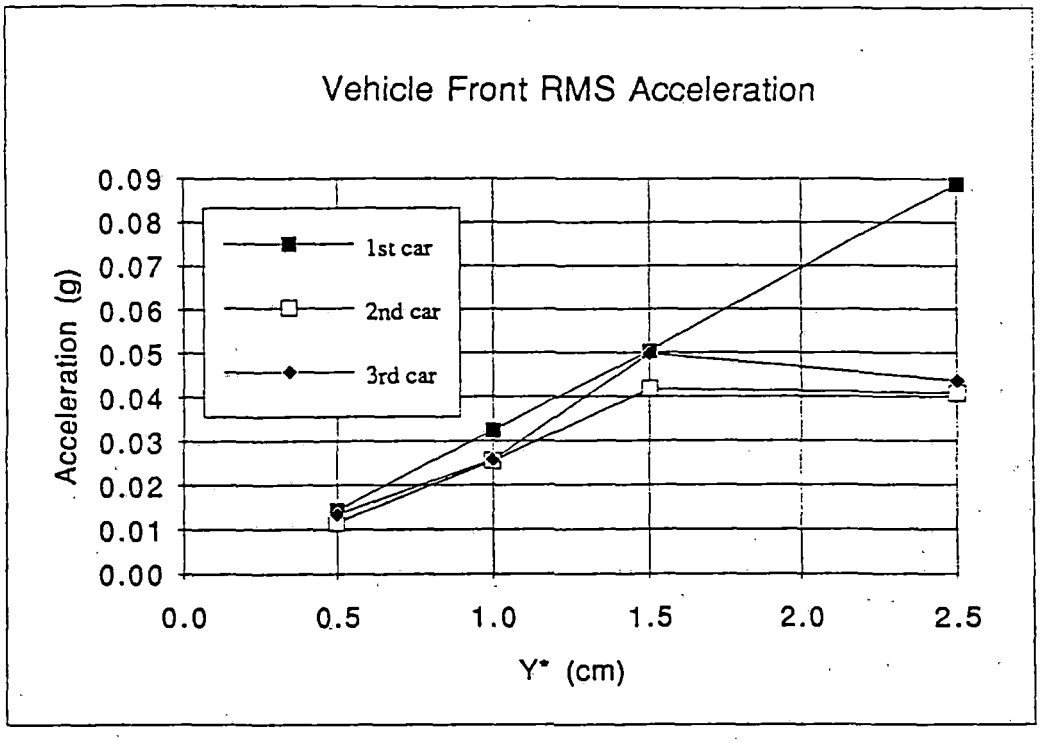

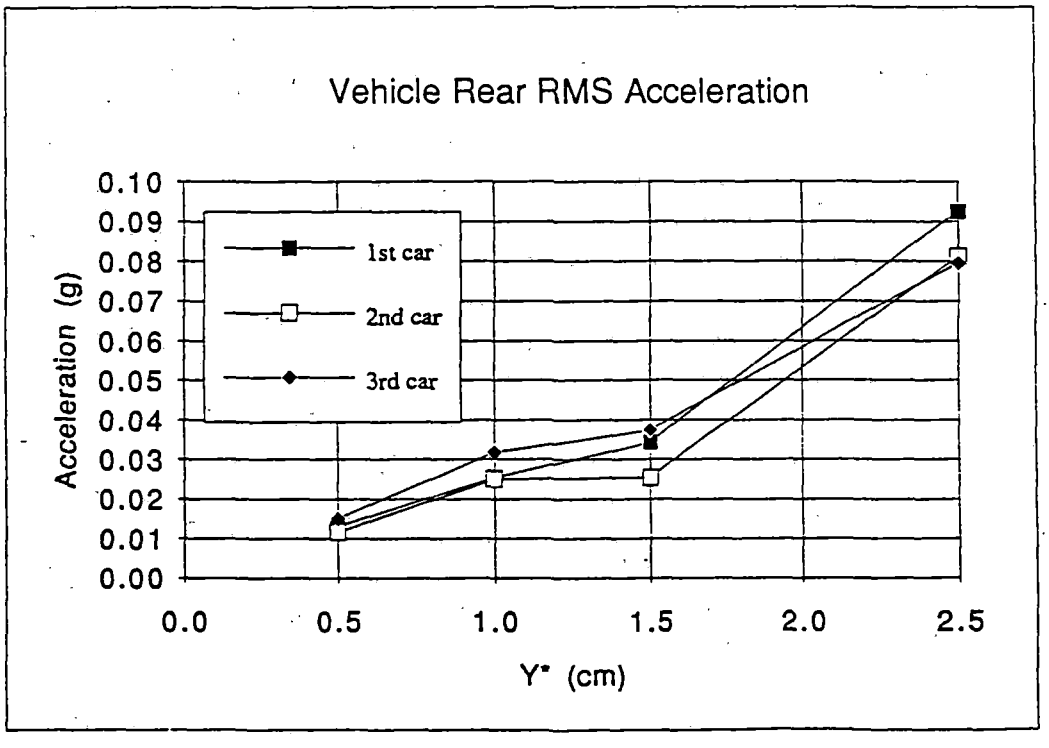

Figure 5.12 Response of a Three Car Train Crossing Single Span Guideways

Model II with f_u = 1.75 Hz and Six Bogies Per Car

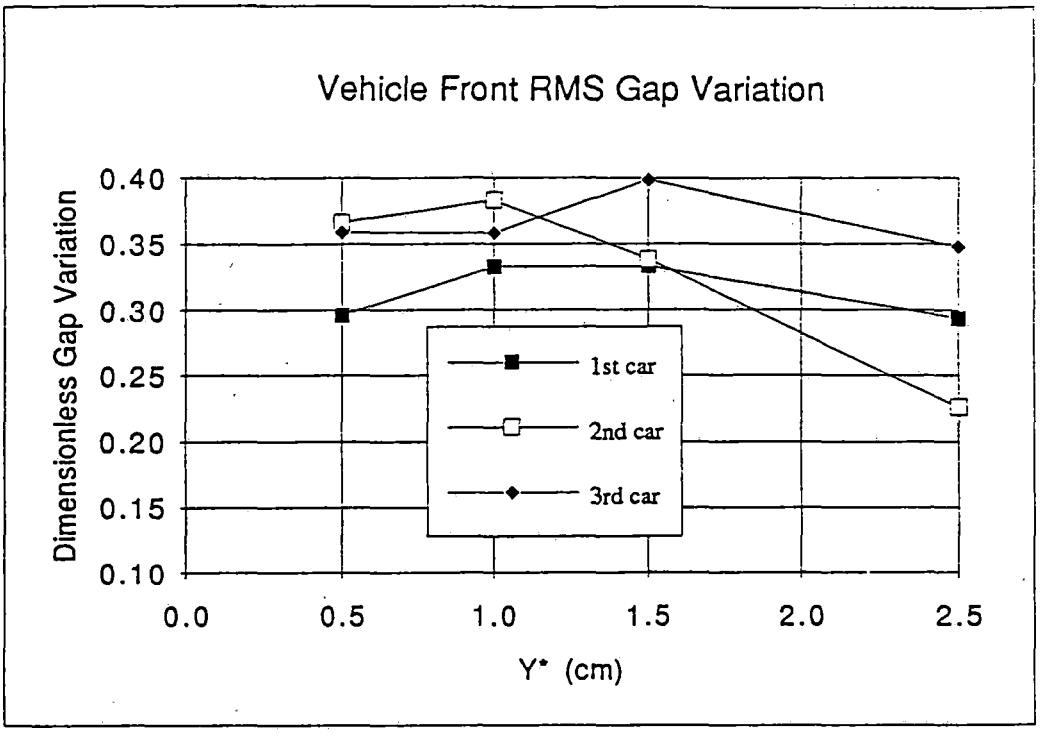

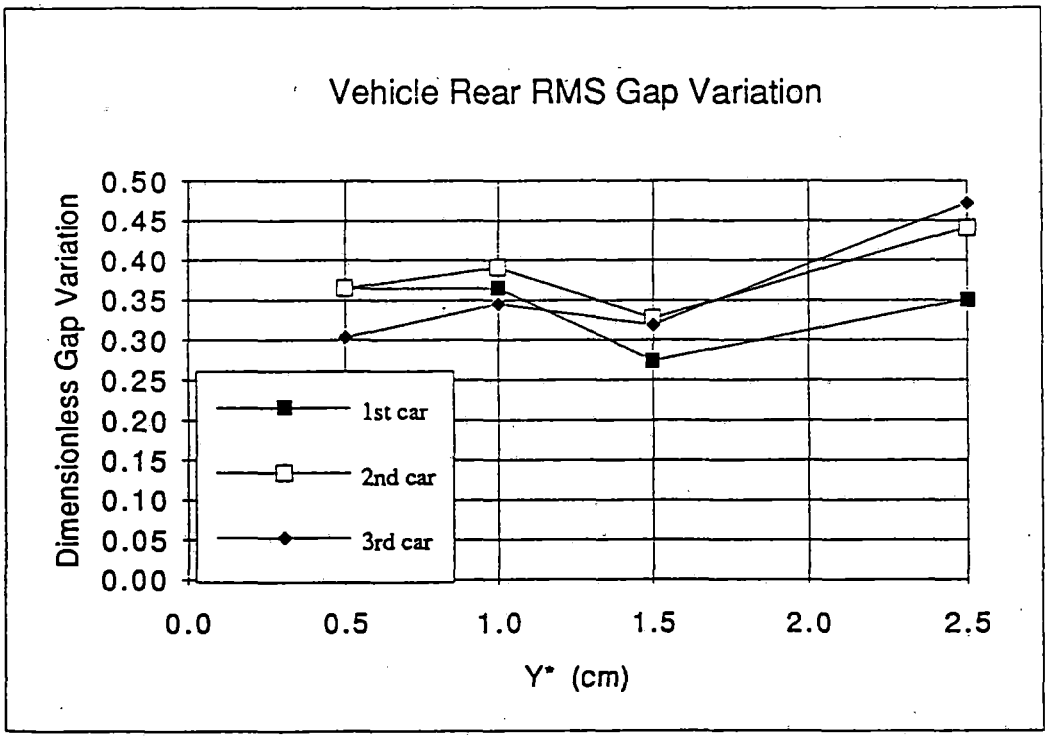

Figure 5.12 Response of a Three Car Train Crossing Single Span Guideways

Model II with f_u = 1.75 Hz and Six Bogies Per Car

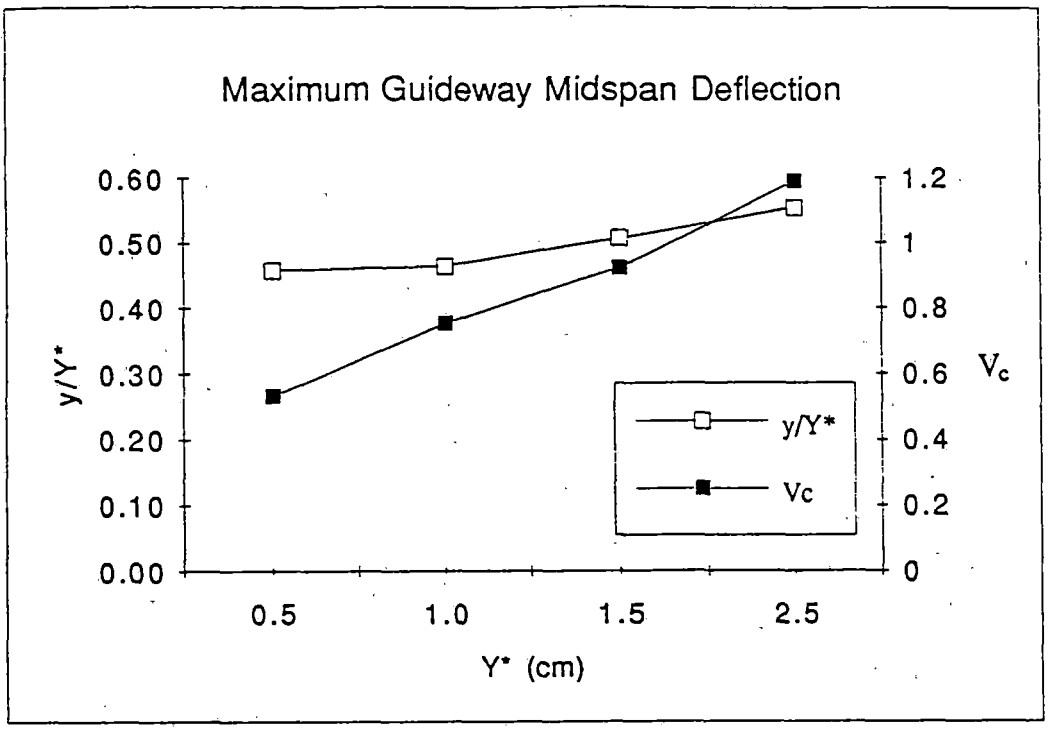

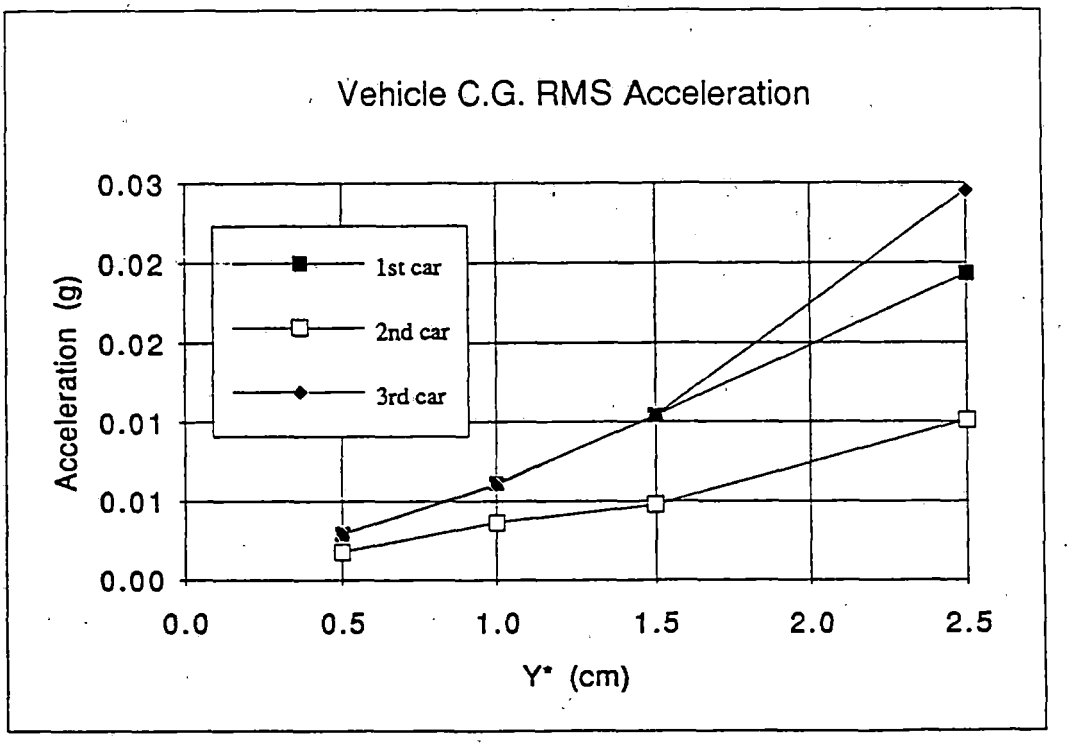

Figure 5.13 Response of a Three Car Train Crossing Double Span Guideways

Model II with f_u = 1.75 Hz and Six Bogies Per Car

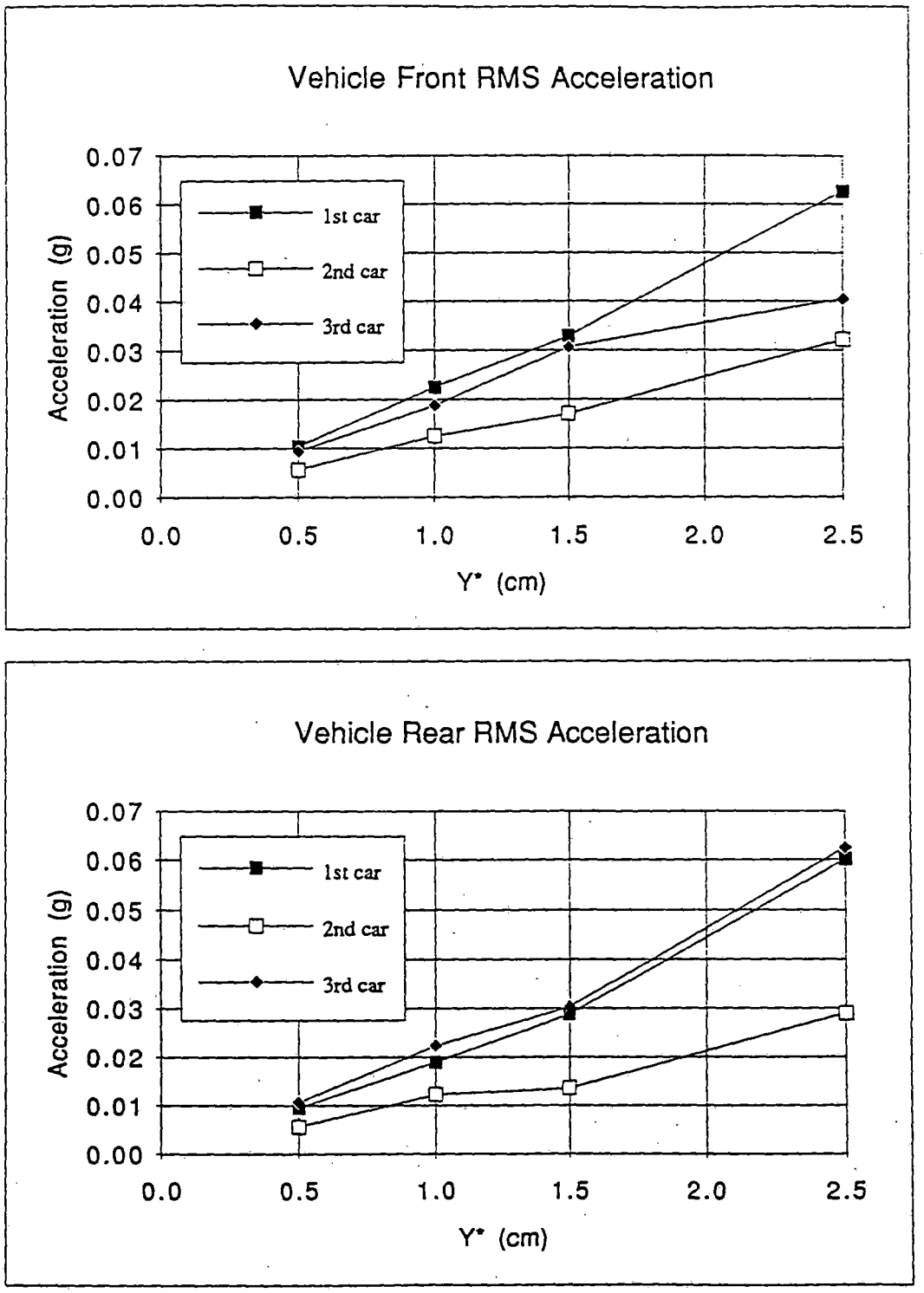

Figure 5.13 Response of a Three Car Train Crossing Double Span Guideways

Model II with f_u = 1.75 Hz and Six Bogies Per Car

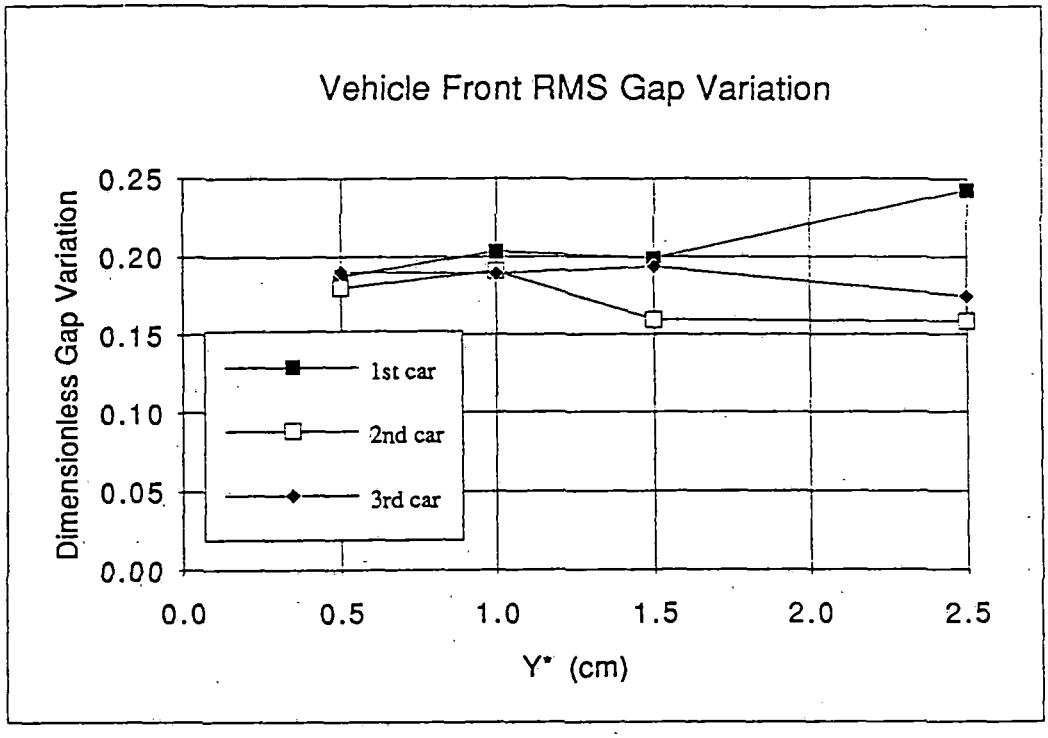

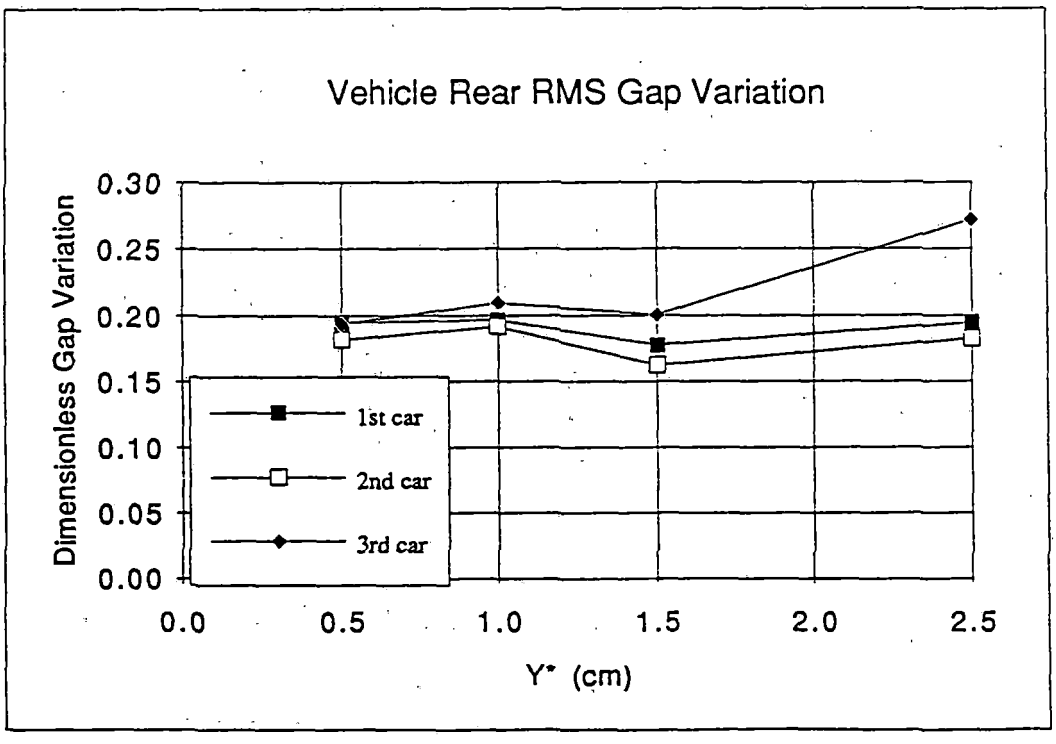

Figure 5.13 Response of a Three Car Train Crossing Double Span Guideways

Model IV with f_u = 3.5 Hz and Six Bogies Per Car

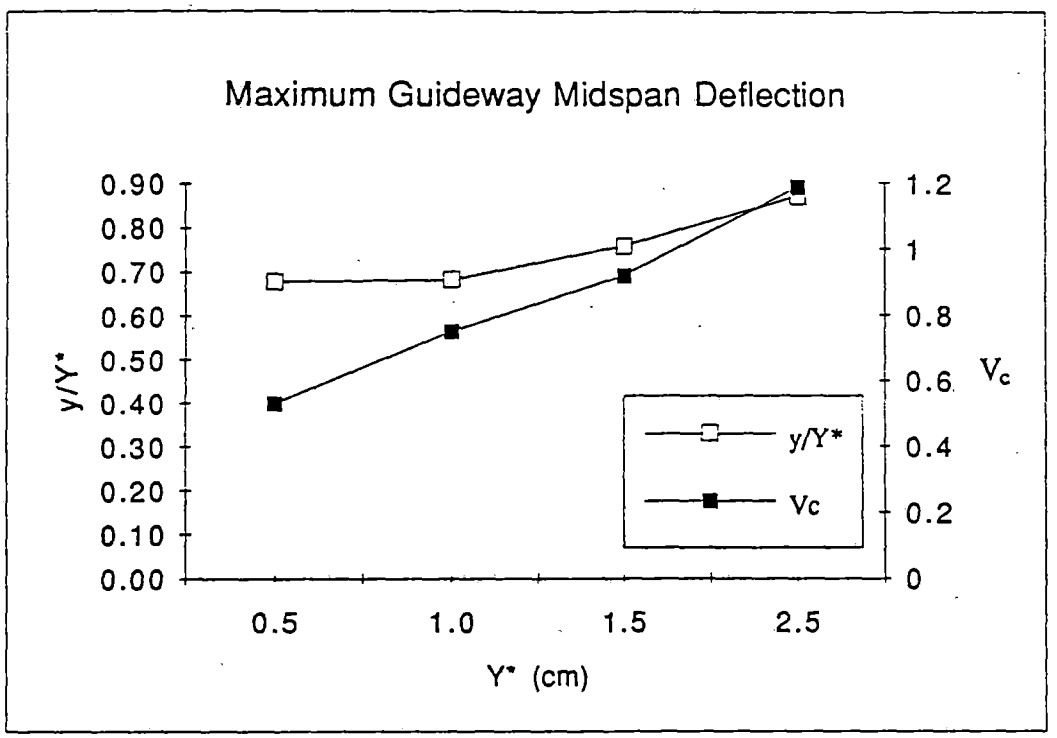

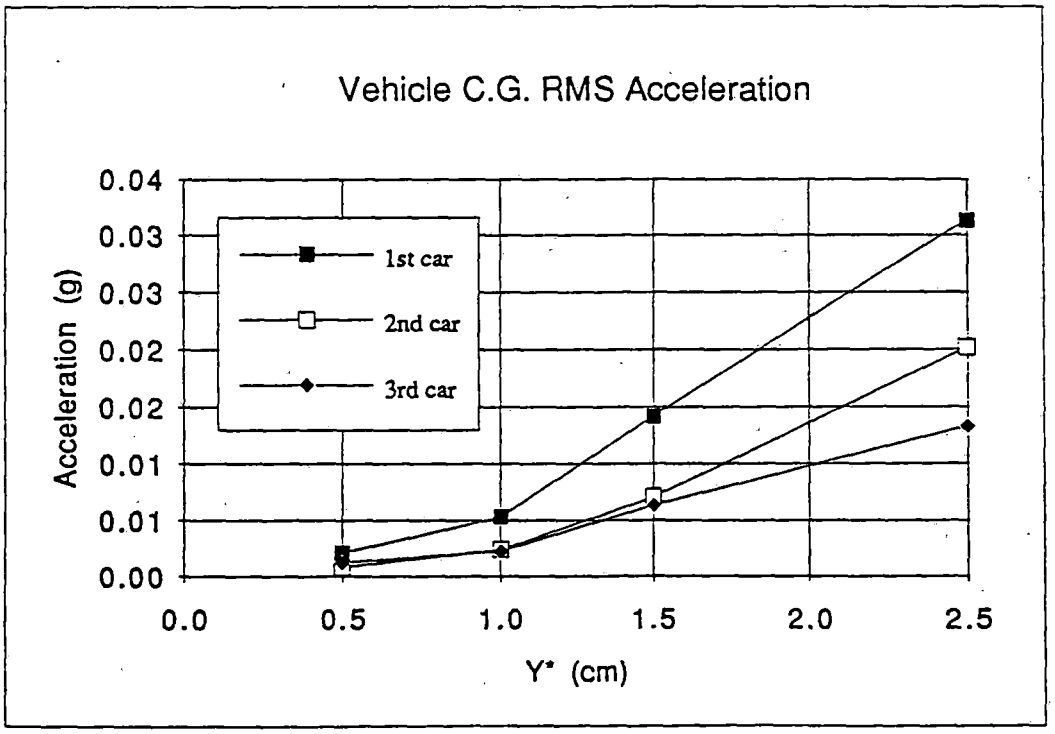

Figure 5.14 Response of a Three Car Train Crossing Single Span Guideways

Model IV with f_u = 3.5 Hz and Six Bogies Per Car

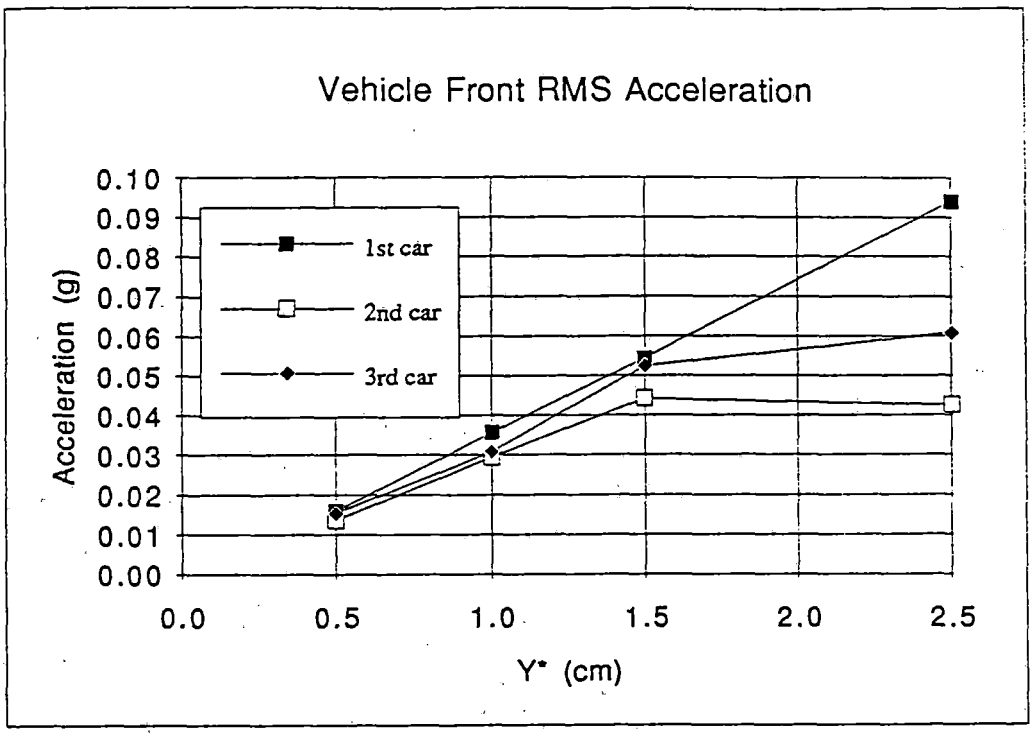

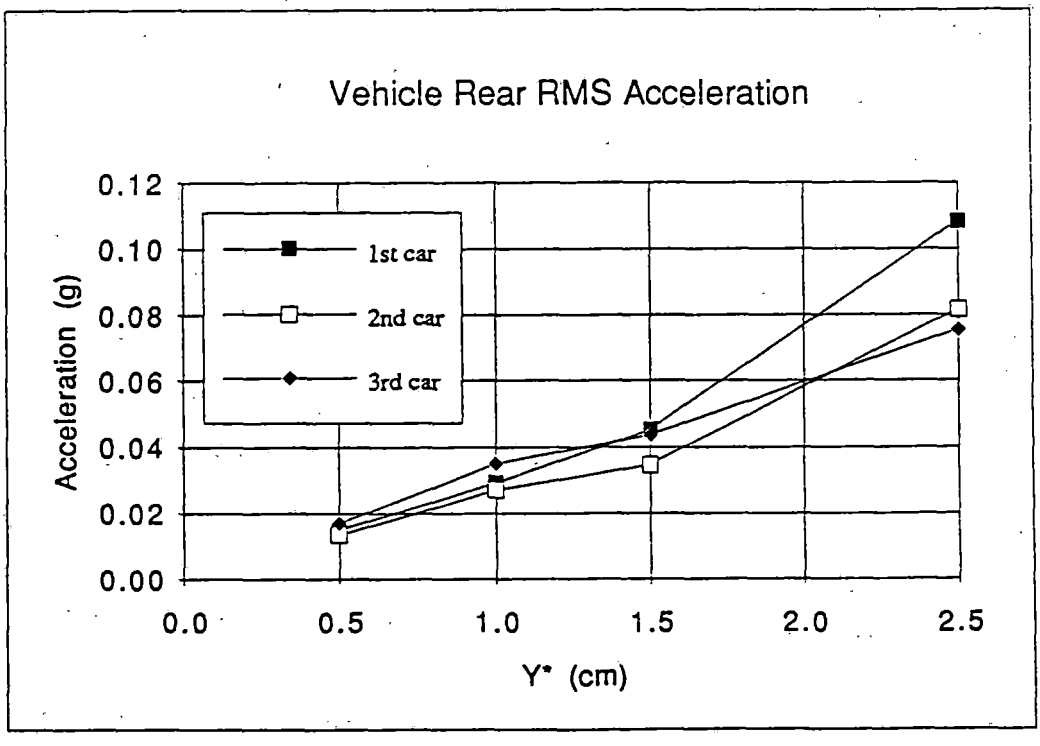

Figure 5.14 Response of a Three Car Train Crossing Single Span Guideways

Model IV with f_u = 3.5 Hz and Six Bogies Per Car

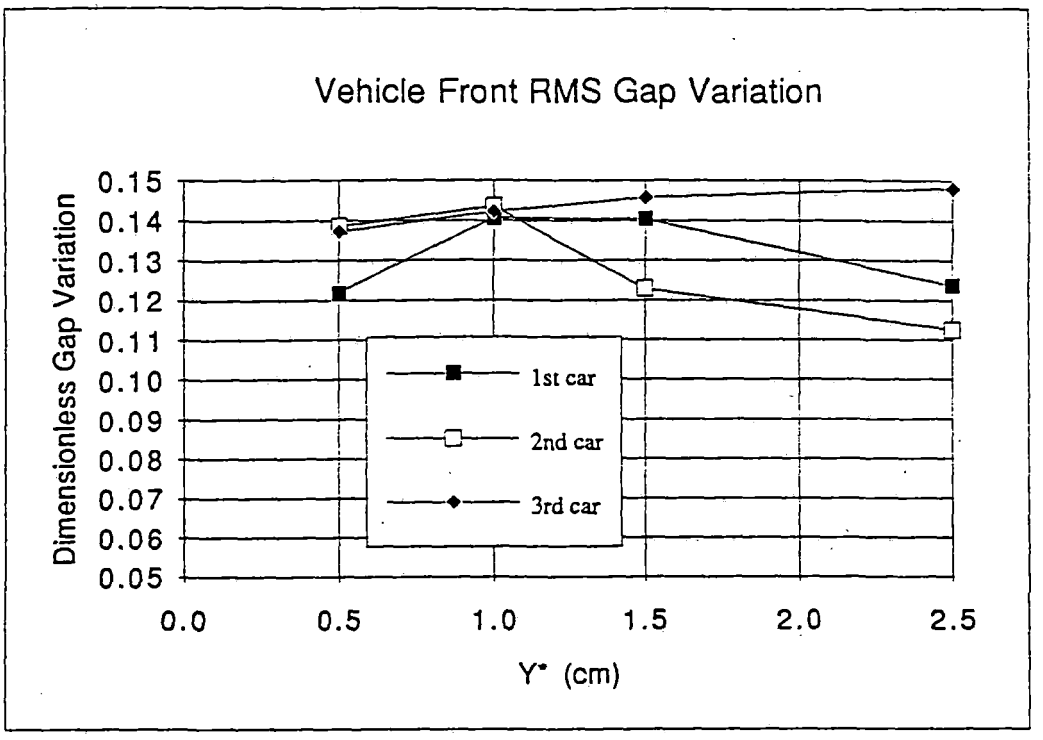

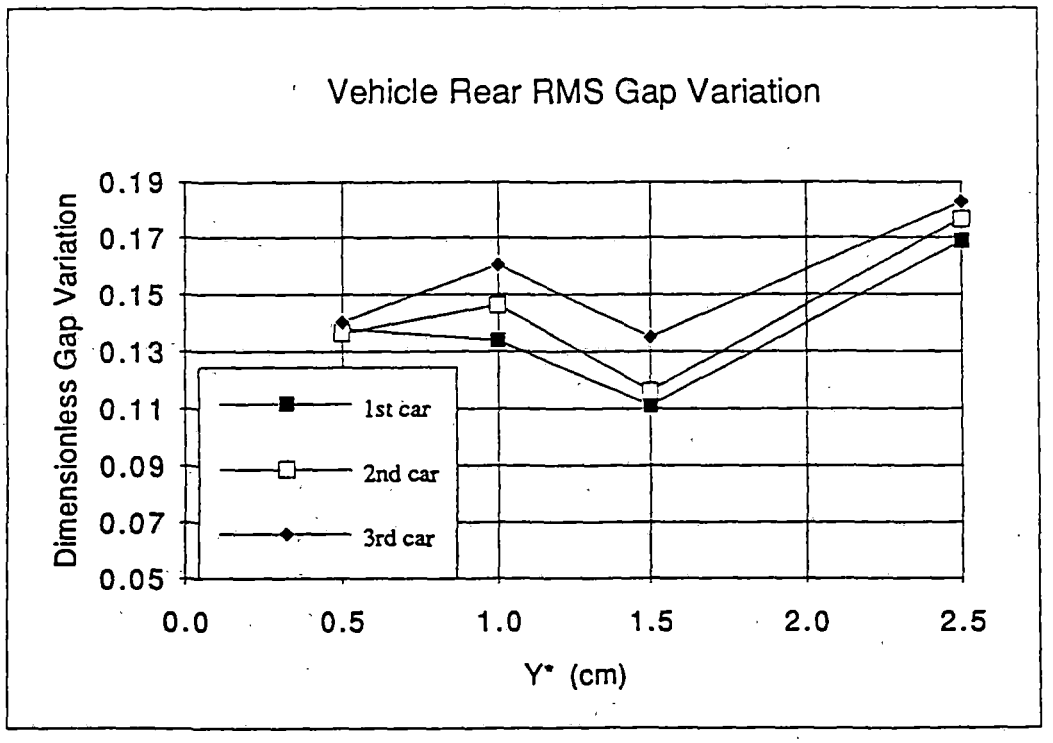

Figure 5.14 Response of a Three Car Train Crossing Single Span Guideways

Model IV with f_u = 3.5 Hz and Six Bogies Per Car

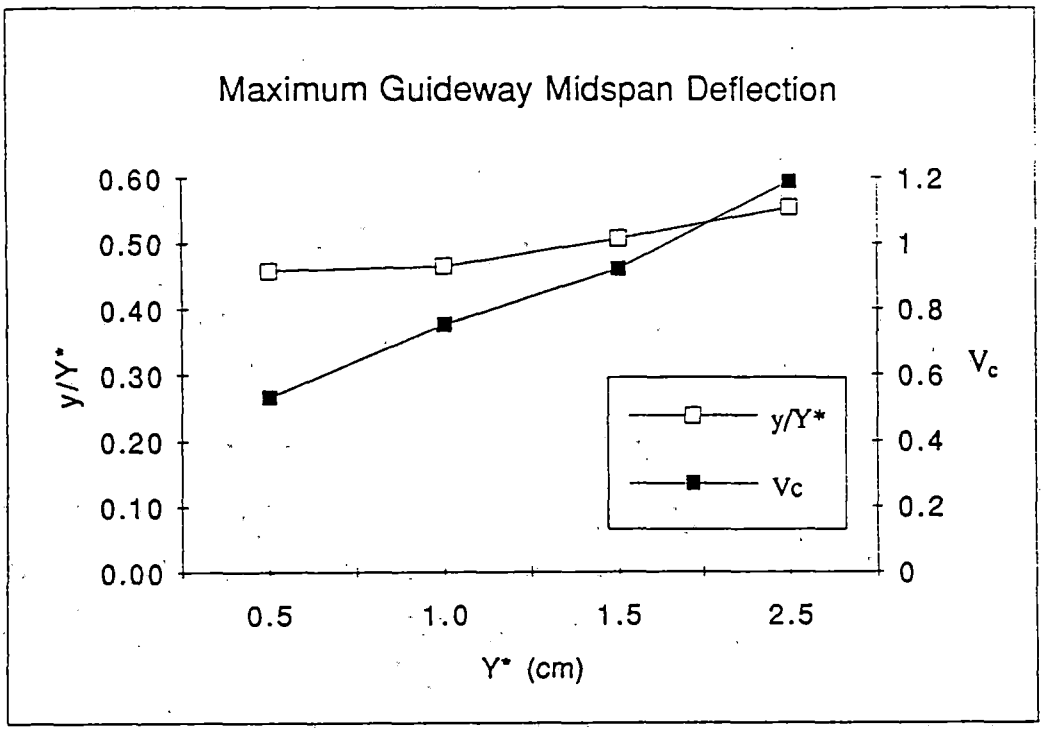

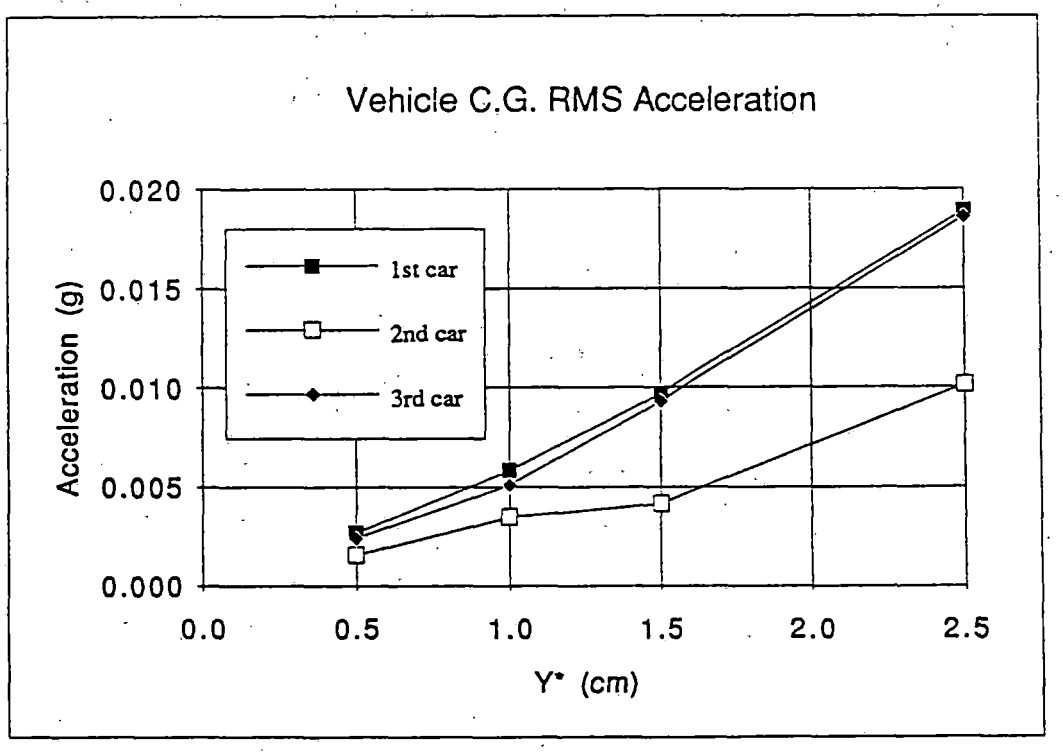

Figure 5.15 Response of a Three Car Train Crossing Double Span Guideways

Model IV with f_u = 3.5 Hz and Six Bogies Per Car

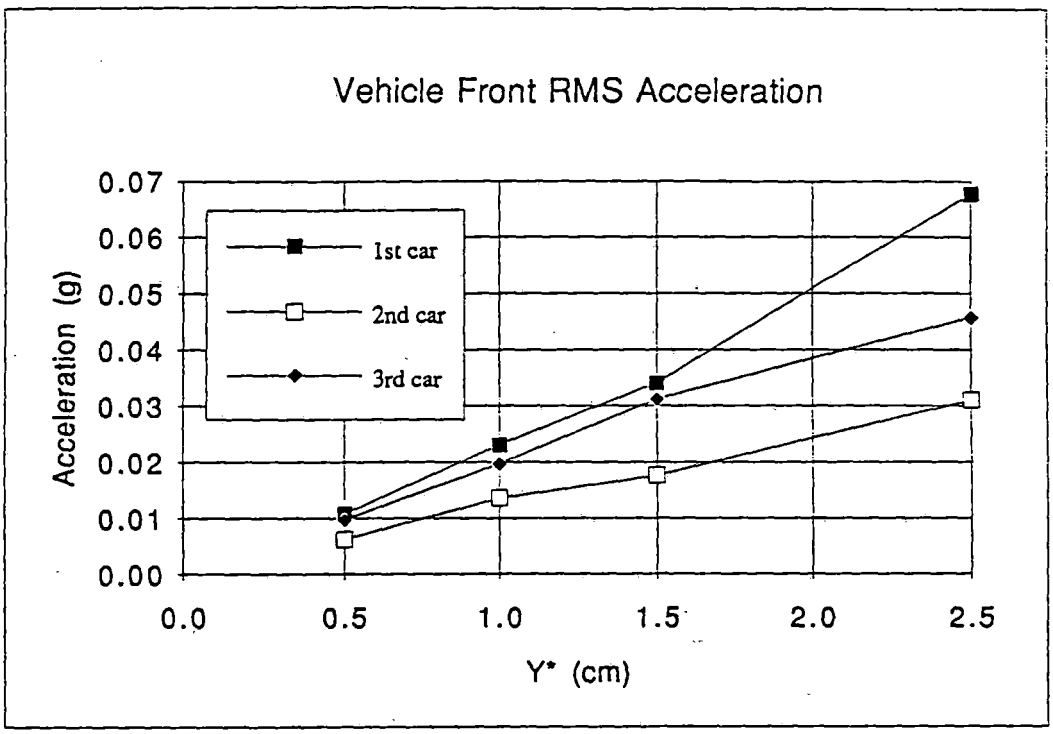

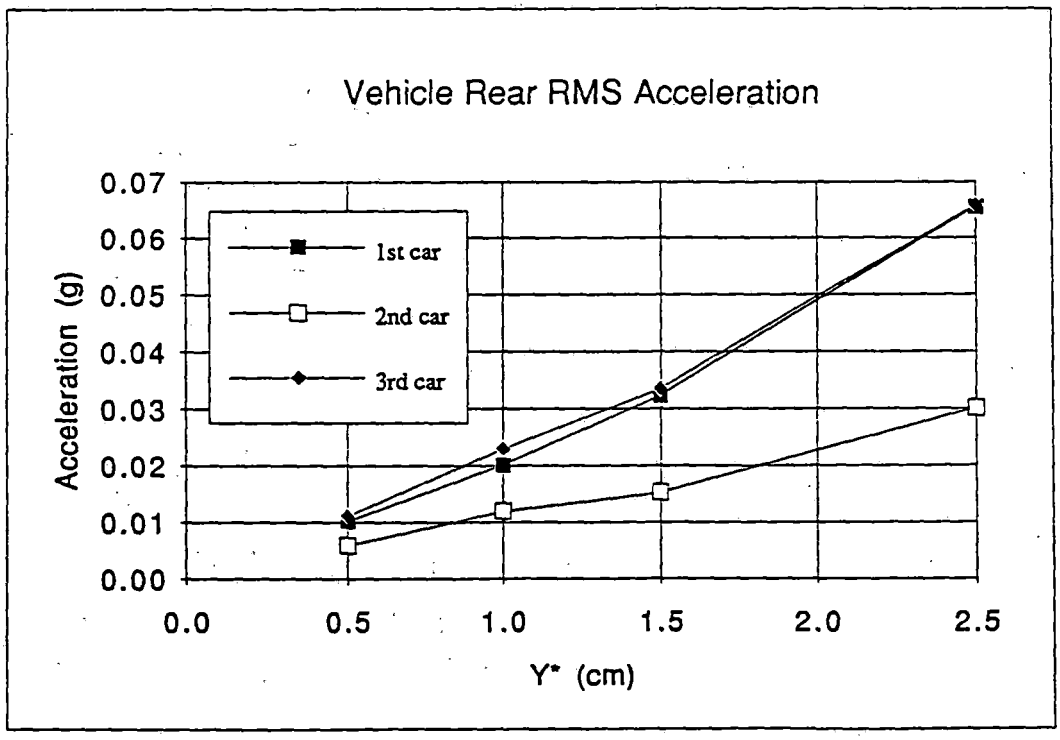

Figure 5.15 Response of a Three Car Train Crossing Double Span Guideways

Model IV with f_u = 3.5 Hz and Six Bogies Per Car

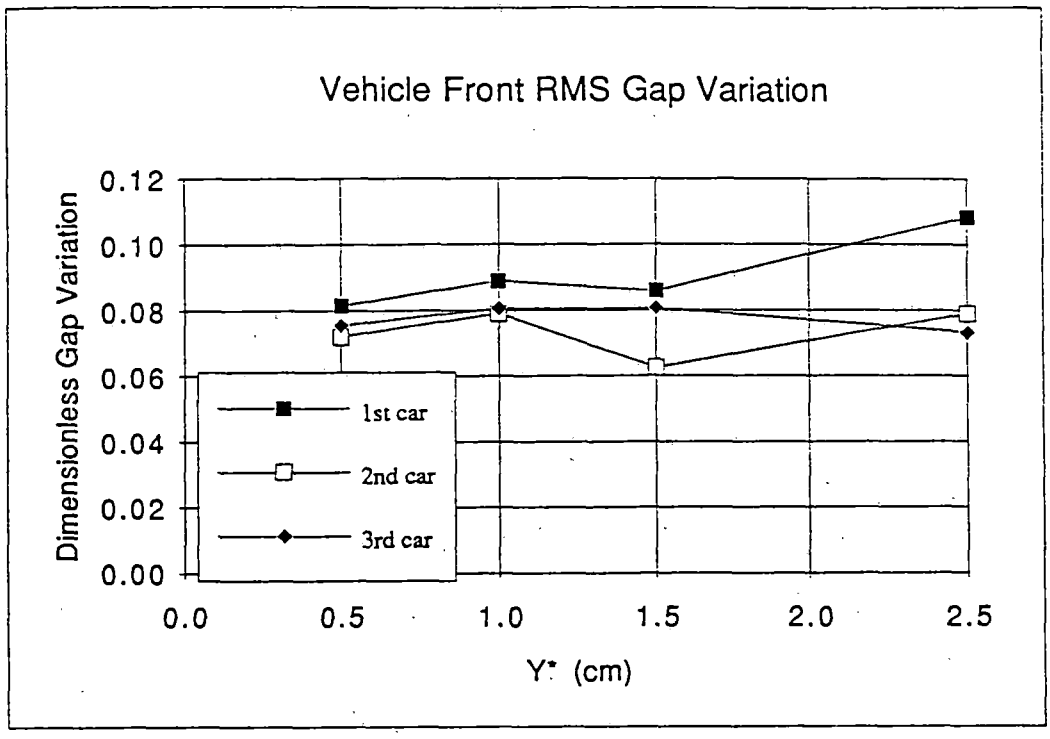

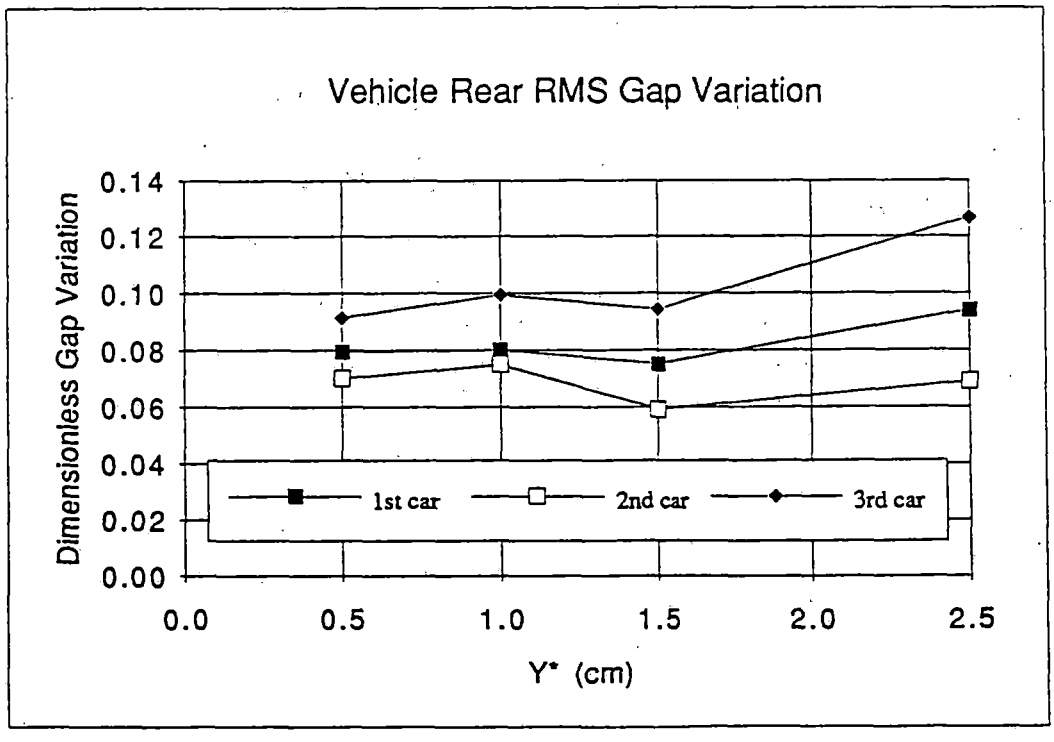

Figure 5.15 Response of a Three Car Train Crossing Double Span Guideways

Table 5.3

Values of Span Stiffness (y*) Required To Meet Specified

RMS Acceleration Levels For Three Car Trains

RMS Acceptance Level	0.04g		0.06g		0.08g	
	y* (cm)	Gap/y*	y* (cm)	Gap/y*	y* (cm)	Gap/y*
Model II f_u = 3.5 Hz						
Single Span	0.64	0.19	0.92	0.20	1.19	0.19
Double Span	0.98	0.16	1.4	0.17	1.72	0.17
Model II f_u = 1.75 Hz						
Single Span	1.22	0.38	1.76	0.39	2.27	0.44
Double Span	1.73	0.22	2.4	0.26	>2.5	-----
Model IV f_u = 3.5 Hz						
Single Span	1.11	0.16	1.65	0.15	2.06	0.16
Double Span	1.68	0.10	2.27	0.12	>2.5	-----

2 cm and a less stiff suspension design with fu = 1.75 Hz which may correspond to a coil interacting with a sheet guideway at a nominal gap of 8 cm. Additional data are presented for model IV which corresponds to an EMS suspension with a nominal gap of 0.8 cm. This suspension employs active control of the magnetic forces to generate damping forces on the magnetic module. The parameters of the three configurations have been selected to be generally representative of possible EDS and EMS suspensions; however, a great deal of design freedom exists in both EDS and EMS suspensions and other higher or lower stiffness--nominal operation gap configurations could be developed.

For the suspension parameters considered, the low stiffness-large gap EDS suspension requires nominally the same levels of guideway stiffness to meet a given level of rms acceleration as the EMS suspension, while the stiffer EDS suspension requires guideway stiffness which are 70-100% stiffer than the other two design cases to meet a given level of rms acceleration. For the 0.04 g rms acceleration requirement, using a double span guideway, the rms magnetic gap variation for the lower stiffness EDS suspension is 0.4 cm or about 5% of the nominal operating gap of 8 cm, while the rms magnetic gap variation for the EMS suspension is 0.17 cm which is 21% of the nominal 0.8 cm gap.

If the rms acceleration requirement were increased to 0.06 g, then the stiffness could be reduced to 70% of the value for 0.04 g rms accelerations. The gap variation for the lower stiffness EDS suspension is 0.6 cm which is 75% of the nominal 8 cm gap, while for the EMS suspension the gap is 0.28 cm or 34% of the nominal gap. If the acceleration constraints were relaxed further, the EMS suspension would be constrained by rms gap variations. The large gap-lower stiffness EDS suspension is not constrained by gap variations and further reductions in guideway stiffness could be made if acceleration constraints were relaxed further. However, for relatively tight rms acceleration constraints, of less than 0.06 g, the two suspensions considered require similar levels of guideway stiffness. For this same range of acceleration constraints, the stiffer EDS suspension requires spans which are approximately 70% stiffer than the low stiffness EDS design and has rms gap variations which are less than 15% of the nominal 2 cm gap.

The data described above have illustrated the relative influence of acceleration and magnetic gap constraints on guideway design for selected suspension configurations. These constraints are fundamental; however, their relative levels of importance can be significantly influenced by modifications to suspension design including the utilization of active secondary suspension and damping concepts which may be incorporated directly into the secondary suspension or through aerodynamic or magnetic forces impacted directly on the vehicle body.

6. SUMMARY AND RECOMMENDATIONS

6.1 Summary

Vehicle-guideway dynamic interaction models have been developed to determine the vertical plane interactions between magnetically levitated vehicles and guideways. The models represent the basic characteristics of magnetically levitated vehicles which relate directly to ride quality, as measured by accelerations occurring on the vehicle, and to the variations in the magnetic gaps occurring between the vehicle suspensions and the guideway which relate directly to overall performance and safety. The models formulated are linear and thus are appropriate for use in the early stages of system designs to identify important performance features related to suspension capabilities and guideway requirements. For specific designs, more detailed, nonlinear models are appropriate. In particular, the vehicle guideway interaction models developed represent characteristics of electromagnetic and electrodynamic suspension systems in terms of vehicle vertical plane pitch/heave motions. The models do not represent the lateral plane motions of vehicles or include aspects of vehicle propulsion or braking.

The vehicle models have been considered interacting with guideways which are characterized by random roughness, by a number of discreet guideway disturbances which are characteristic of elevated spans (step discontinuities due to span alignment, slope discontinuities due to pier misalignment and camber due to guideway thermal gradients) or by elevated, flexible guideway systems which experience dynamic motions due to vehicle passage.

Four specific vehicle configurations have been considered. Configurations I, II and III are representative of a number of the characteristics of EDS configurations with Configuration I representing a system in which magnets are mounted directly on the vehicle and only the magnetic suspensions interact with the guideway. In Configurations II and III magnetic suspension modules interact with the guideway with the module connected to the vehicle through a secondary suspension containing passive stiffness (II) and passive stiffness and damper elements (III). The Configuration IV suspension represents a number of the features of an electromagnetic system and employs parameters which represent an equivalent active EMS suspension interacting with the guideway and a passive secondary suspension connecting the magnetic module to the vehicle body. The four suspension configurations have been studied utilizing one-dimensional vehicle models, as well as finite length vehicle models which employ from two to six suspension modules. Current proposals for the development of magnetically levitated vehicle systems include proposals

which have two suspension modules beneath the vehicle and proposals which include a multiple number of suspension modules supporting vehicles.

To illustrate the capabilities of the basic suspension configurations, vehicles have been studied traversing guideways characterized by random roughness which have equivalent values of rms roughness to those of welded steel rail. The rms vehicle accelerations generated in the vehicle body and the rms magnetic gap variations occurring obetween magnetic suspension modules and the guideway have been determined for vehicles traveling 125 m/s. The results of the studies have indicated that one-dimensional vehicle models generally produce vehicle accelerations which are comparable to those occurring near the center of two-dimensional vehicle models, and that the two-dimensional vehicles have maximum accelerations at the front and rear vehicle positions. For the suspensions considered, the front and rear accelerations may in some cases exceed the center accelerations by factors of 1.5-3.0. The multiple suspension models which distribute the suspensions along the vehicle body have reduced accelerations along the vehicle body in comparison to vehicles employing only front and rear suspensions.

For all of the suspension configurations considered, suspension design parameters were identified which yield 0.04 g rms carbody accelerations with magnetic gap variations which are within 30% of a nominal gap of 5 cm for EDS configurations and 0.8 cm for EMS configurations. These suspension configurations included:

(1) Configuration I in which all magnetic modules are directly mounted on the vehicle and damping is achieved either through active aerodynamic or magnetic means

(2) Configuration II in which a magnetic module or modules representing 25% of the vehicle total mass are connected to the vehicle with a suspension employing passive stiffness and damping elements and with magnetic module forces which yield no damping

(3) Configuration III which is identical to Configuration II but employs additional active or passive elements which are added to achieve damping depending on the relative velocity between the magnetic module and the guideway

(4) Configuration IV which employs additional active damping which is a function of the magnetic module absolute velocity

All four of these configurations were shown to be capable of meeting 0.04 g rms car body acceleration levels with magnetic gap variations which are within 30% of nominal gaps. Thus, with respect to suspension performance on guideways with roughness similar to that of welded steel rail, it has been shown that it is possible for a variety of magnetic

suspension configurations to meet reasonable acceleration levels (0.04 g) in terms of rms accelerations and reasonable magnetic gap variations (30% of nominal gap). Detailed analysis has also shown that these suspensions will also meet ride quality specifications based on the one hour ISO criteria.

These studies generally have indicated for the configurations and vehicle parameters considered that secondary suspension natural frequencies in the range of 1 Hz to 0.75 Hz are required to meet a 0.04 g rms acceleration limit at the operating speed of 125 m/s on guideways with roughness levels similar to welded steel rail.

The responses of finite length vehicles operating at 125 m/s to three types of discrete perturbations which are characteristic of elevated span systems have been determined for nominal 25 meter span guideways. In these studies vehicles were run over a sufficient number of discrete perturbations to reach a steady-state condition in which rms acceleration levels and rms magnetic gap variations could be determined for each of the basic suspension configurations. For each of the four suspension configurations the levels of step disturbance amplitude were determined which would allow the vehicles to meet a 0.04 g rms acceleration while traversing periodic step discontinuities. For all four configurations it was found that step disturbance amplitudes in the range of 1 cm could be tolerated by selected suspension designs with secondary suspension natural frequencies on the order of 0.75 Hz for each of the four configurations while achieving rms gap variations which are less than 35% of the nominal gap. It is noted that discontinuities in the range of 1 cm would result in magnet/guideway contact for suspensions with nominal gaps of 1.0 cm or less.

Response of vehicles to periodic changes in pier misalignment which are representative of slope changes in spans, have shown that suspension design parameters exist which can provide 0.04 g rms acceleration levels of each of the EDS configurations, and which can accommodate pier vertical height misalignments on the order of 1.6 cm for 25 m span systems while achieving maximum magnetic gap variations in the range of 0.6-0.8 cm. In a similar manner, Configuration IV designs can accommodate approximately 1.6 cm pier misalignments with rms gap variations ranging from approximately 0.1-0.2 cm.

The vehicle rms accelerations and magnetic gap variations have been determined for vehicles crossing spans with periodic camber disturbances which are characteristic of the types of disturbances generated due to thermal gradients in spans. For each of the basic suspension configurations the levels of camber disturbance which can be tolerated while achieving a 0.04 g rms acceleration level have been determined. For the parameters representing suspension Configurations I, II and III camber disturbances on the order of

1.0 cm or greater can be tolerated while meeting the ride quality specifications. For Configuration IV designs, amplitudes on the order of 1.0 cm could also be accommodated; however, the rms gap variation constraints would preclude the accommodation of camber significantly greater than 1.0 cm if rms gap variations of less than 30% of the nominal gap were required. Thus, with respect to camber, constraints on gap variation as well as acceleration can provide upper bounds to permissible camber amplitudes. The limitations on camber have led to a proposal to employ two-span, continuous guideways rather than single span guideways in some maglev systems since two-span systems have typical camber amplitudes which are less than 50% of those occurring in simple spans with the same thermal gradient.

An extensive series of studies have been performed to determine the factors which influence flexible elevated guideway span designs when traversed by magnetically levitated vehicles. A set of design case studies have been conducted for two EDS suspension configurations which employ magnetic modules coupled to a vehicle with a passive secondary suspension and which employ no magnetic damping nor aerodynamic damping (one configuration has a high magnetic suspension stiffness while the other has a lower stiffness), and for a typical EMS configuration design which employs a magnetic module coupled to the vehicle with a passive secondary suspension and which employs active gap control. These configurations have been studied to determine the influence of ride quality constraints and magnetic gap variation constraints on the level of flexibility which can be accommodated in flexible span systems. The studies have shown for three vehicle trains traversing elevated span systems at 125 m/s that significant dynamic amplification of span deflections can occur and that these need to be considered directly in the evaluation of both vehicle ride quality and span deflection. For the EDS systems considered, it was found that the specification of vehicle ride quality in effect provides a direct constraint on span flexibility. If vehicle ride quality rms acceleration constraints were changed from 0.04 g to 0.08 g for the vehicle body, a span which had a stiffness which was half that of a span designed for 0.04 g rms acceleration could be accommodated. Similarly it was found that if a two span, continuous system were employed rather than a single span, the span stiffness could be reduced by approximately 40% in comparison to a single span design. The study also indicated for the range of parameters considered that a reduction of the stiffness of the magnetic suspension module results in the ability to accommodate a more flexible span system while providing the same level of ride quality. In particular the reduction of the magnetic suspension module natural frequency by a factor of two allows an approximate decrease in span stiffness by a factor of two.

The data presented in the study show that comparable span flexibility is required for both the EMS suspensions and the EDS suspensions for the range of suspension parameters selected. The parameters were selected to be generally representative of possible EDS and EMS suspensions; however, a great deal of design freedom exists for both types of suspensions and other higher or lower stiffness-nominal gap configuration suspensions could be developed which could have superior performance to those considered.

For the suspension parameters considered, the low stiffness-large gap EDS suspension requires nominally the same levels of guideway stiffness to meet a given level of rms acceleration as the EMS suspension, while the stiffer EDS suspension requires guideway spans which are 70-100% stiffer than the other two design cases to meet a given level of rms acceleration. As acceleration constraints are relaxed, the EMS suspension eventually reaches a limit at which the magnetic gap variations provide the primary constraints to further reductions in guideway stiffness. The EDS suspension configurations considered have gap variations which are a sufficiently small fraction of the total gap that as acceleration constraints are relaxed they can accommodate greater levels of guideway flexibility. Thus, the data illustrate that for systems in which relatively tight ride quality constraints are employed, for the configuration parameters considered, both the EMS and EDS configurations have similar guideway stiffness requirements. For systems in which rms acceleration levels are relaxed, the EDS suspensions can accommodate more flexible guideway designs before magnetic gap variations represent limiting constraints.

6.2 Recommendations

This study has shown that elevated guideway designs and construction tolerances for both EDS and EMS suspension configurations have constraints which result from the specification of ride quality criteria. The configurations studied have been represented by idealized linear models which include all the important effects of magnetic suspension systems interacting with guideways. It is recommended that more detailed suspension models which may include active control features incorporated directly into the suspensions and into vehicle bodies be developed and evaluated. Since the suspension and guideway designs considered in this report have been limited by ride quality, the employment of active control, particularly on the vehicle body, could possibly relieve the suspension constraints and thus allow both increased construction tolerances and increased guideway flexibility. The investigation of these implications are important with respect to the overall installation and maintenance costs of guideway structures for magnetically levitated systems.

This study has been restricted to an investigation of the vertical plane interactions between vehicles and guideways. In magnetic suspension systems the lateral plane interactions and coupled vertical plane interactions have been shown to be important for a number of vehicle/guideway configurations. Thus, the efforts of this study should be extended to assess lateral plane interactions and the possible coupling which can occur between vertical and lateral plane interactions in magnetically levitated vehicle systems.

Finally it is noted that while the study has been able to identify the limits placed upon selected construction tolerances as well as the stiffness of guideway spans, additional cost data in a more detailed evaluation of guideway systems is required to determine the sensitivity of guideway costs to both construction and guideway stiffness requirements.

7. REFERENCES

1. Proise, M., "Establishing the Best Magnetically Levitated High-Speed Transportation System for the United States," SAE Paper 901476, 1990.

2. Takeda, H., "Development of Superconducting Maglev in Japan: Present State and Future Perspective," SAE Paper 901478, 1990.

3. Heinrich, K. and Kretzschmar, R. eds., "Transrapid Maglev System," Hestra-Verlag, Dramstadt, 1989.

4. Wyczalek, F.A., "HSST Magnetic Levitation Trains: Past, Present and Future," Magnetic Levitation Technology and Transportation Strategies, SAE, SP-834, 1990.

5. Coffee, H.T., Chilton, F. and Hoppie, L.O., "Magnetic Levitation of High-Speed Ground Vehicles," Proceedings of Applied Superconductivity Conference, 1972.

6. Danby, G. and Powell, J., "Integrated Systems for Magnetic Suspension and Propulsion of Vehicles," Proceedings of Applied Superconductivity Conference, 1972.

7. Carmichael, G.E. and Dorn, N.P., "National Maglev Initiative-Annual Report," U.S. Department of Transportation, November, 1991.

8. Wormley, D.N., et al., "Elevated Guideway Cost-Ride Quality Studies for Group Rapid Transit System," Report DOT-TSC-OST-77-54, 1977.

9. Sussman, D. and Wormley, D., "Measurement and Evaluation of Ride Quality in Advanced Ground Transportation Systems," Transportation Research Record 894, Washington, DC, 1982.

10. Jacobson, I., et al., "Comparison of Passenger Comfort Models in Buses, Trains and Airplanes," Transportation Resarch Record 646, 1977.

11. Pepler, R.D., et al., "Development of Techniques and Data for Evaluating Ride Quality," Report DOT-TSC-77-1, 1978.

12. Anon., "Guide for the Evaluation of Human Exposure to Wholebody Vibration," ISO Standard 2631, International Organization for Standarization, 1978.

13. Dover, R.M. and Hathaway, W.T., "Safety of High Speed Magnetic Levitation Transportation Systems," Report DOT/FRA/ORD-90-09, 1990.

14. Sinha, P.K., Electromagnetic Suspension Dynamics and Control, Pergamon Press Ltd., London, 1987.

15. Barrows, T., "Aerodynamic Forces on Maglev Vehicles," Second Symposium for the National Maglev Initiative, Argonne National Laboratory, April, 1992.

16. Young, J.W. and Wormley, D.N., "Optimization of Linear Vehicle Suspensions Subjected to Simultaneous Guideway and External Force Disturbance," ASME Journal of Dynamic Systems, Measurement and Control, June, 1973.

17. Karnopp, D and Trikha, A., "A Comparative Study of Optimization Techniques for Shock and Vibration Isolation," Journal of Engineering Industry, Trans. ASME, Vol. 91, 1969.

18. Aitkenhead, W., "Magneplane International System Concept Definition," Second Symposium for the National Maglev Initiative, Argonne National Laboratory, April, 1992.

19. Samavedam, G., "Foster-Miller Maglev System Concept Definition," Second Symposium for the National Maglev Initiative, Argonne National Laboratory, April, 1992.

20. Perkowski, J., "Maglev System Concept Definition Presentation," Second Symposium for the National Maglev Initiative, Argonne National Laboratory, April, 1992.

21. Wong, J.Y., Theory of Ground Vehicles, Wiley-Interscience, N.Y., 1978.

22. Kortum, W. and Wormley, D., "Dynamic Interactions Between Traveling Vehicles and Guideway Systems," Journal of Vehicle System Dynamics, Vol. 10, 1981.

23. Samavedan, G. and Purple, A., "Thermal Effects and Mitigation Methods for Continuous Sheet Guideways," U.S. Department of Transportation, January 1992.

24. Rao, S.S., Mechanical Vibration, Addison-Wesley Publishing Company, 1986.

25. Wormley, D.N., et al., "Multispan Elevated Guideway Design for Passenger Transport Vehicles," U.S. Department of Transportation Technical Report DOT-TSC-FRA-75-4, 1975.

Appendix A

Vehicle Models and the Computation of Vehicle Performance

Two models are developed to represent magnetically levitated vehicles. The models have four suspension configurations. Table A1 defines the symbols used in the models.

Table A1. Symbol Definitions

Symbol	Definition
m_u	Unsprung mass
m_s	Sprung mass
$\frac{m_u}{m_s + m_u}$	Ratio of unsprung to total mass
L_i	Distance from the c.g. of the sprung mass to the i-th suspension.
I_y	Pitch moment of inertia
$\ddot{Z}_s$	Sprung mass acceleration
$\ddot{Z}_u$	Unsprung mass acceleration
Z_{gi}	Guideway displacement at the i-th suspension
θ	Pitch angle
S	Magnetic gap variation
s	Laplace operator
n	Number of suspension
$S_g(\omega)$	Spectral density function of the surface profile $= \frac{Av}{\omega^2}$ Where A = constant v = vehicle velocity
ω_s	Angular natural frequency of secondary suspension $= \sqrt{\frac{K_s}{m_s}}$
ω_{si}	Angular natural frequency of the i-th secondary suspension $= \sqrt{\frac{K_{si}}{m_{si}}}$
ω_u	Angular natural frequency of primary suspension $= \sqrt{\frac{K_u}{m_u}}$
ω_{ui}	Angular natural frequency of the i-th primary suspension $= \sqrt{\frac{K_{ui}}{m_{ui}}}$

ζ_s	Damping ratio of secondary suspension $= \frac{B_s}{2\sqrt{K_s m_s}}$
ζ_{si}	Damping ratio of the i-th secondary suspension $= \frac{B_{si}}{2\sqrt{K_{si} m_{si}}}$
ζ_u	Damping ratio implemented by magnetic field $= \frac{B_u}{2\sqrt{K_u m_u}}$
ζ_{ui}	Damping ratio implemented by magnetic field from the i-th suspension $= \frac{B_{ui}}{2\sqrt{K_{ui} m_{ui}}}$
ζ_a	Absolute damping ratio of primary suspension $= \frac{B_a}{2\sqrt{K_u m_u}}$
ζ_a	Absolute damping ratio of primary suspension for cases without secondary suspension $= \frac{B_a}{2\sqrt{K_s m_s}}$
ζ_{ai}	Absolute damping ratio of the i-th primary suspension $= \frac{B_{ai}}{2\sqrt{K_{ui} m_{ui}}}$
ζ_{ai}	Absolute damping ratio of the i-th primary suspension for cases without secondary suspension $= \frac{B_{ai}}{2\sqrt{K_{si} m_s}}$

A1. One Dimensional Model

One dimensional vehicle models with and without secondary suspension are developed. Figure A1 is a schematic of the models with various suspension configurations. The transfer functions to compute the magnetic gap variation and sprung and unsprung mass accelerations of models without secondary suspension are:

$$\frac{S}{Z_g} = \frac{NUM1}{DEN} \qquad (A.1.1)$$

$$\frac{\ddot{Z}_s}{Z_g} = \frac{NUM2}{DEN} \qquad (A.1.2)$$

where s is the Laplace operator and

$$NUM1 = -s^2 - 2\zeta_a \omega_s s \qquad (A.1.3)$$

$$NUM2 = s^2 \left(2\zeta_s \omega_s s + \omega_s^2 \right) \qquad (A.1.4)$$

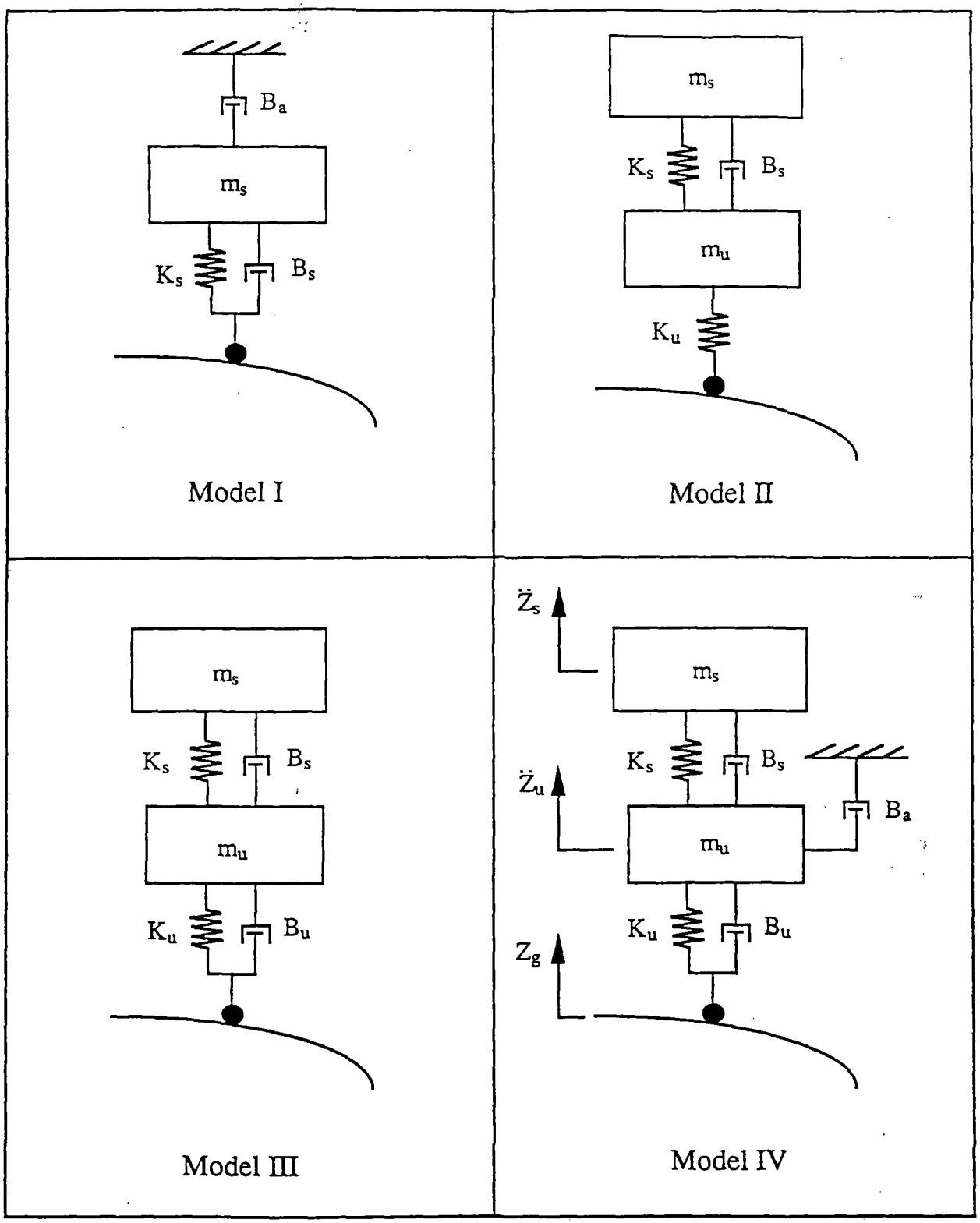

Figure A1. One Dimensional Vehicle Model With Four Suspension Configurations

$$DEN = s^2 + 2\left\{\left(\zeta_s + \zeta_a\right)\omega_s\right\}s + \omega_s^2 \qquad (A.1.5)$$

The transfer functions to compute the magnetic gap variation and sprung and unsprung mass accelerations for the models with secondary suspension are

$$\frac{S}{Z_g} = \frac{NUM1}{DEN} \qquad (A.1.6)$$

$$\frac{\ddot{Z}_s}{Z_g} = \frac{NUM2}{DEN} \qquad (A.1.7)$$

$$\frac{\ddot{Z}_u}{Z_g} = \frac{NUM3}{DEN} \qquad (A.1.8)$$

respectively where

$$NUM1 = -s^4 - \left[(1 + \frac{m_s}{m_u})2\zeta_s\omega_s + 2\zeta_a\omega_u\right]s^3 - \left[4\zeta_s\omega_s\zeta_a\omega_u + (1 + \frac{m_s}{m_u})\omega_s^2\right]s^2$$

$$- (2\zeta_a\omega_u\omega_s^2)s \qquad (A.1.9)$$

$$NUM2 = (4\zeta_s\omega_s\zeta_u\omega_u)s^4 + (2\zeta_s\omega_s\omega_u^2 + 2\zeta_u\omega_u\omega_s^2)s^3 + (\omega_s^2\omega_u^2)s^2 \qquad (A.1.10)$$

$$NUM3 = (2\zeta_u\omega_u)s^5 + (\omega_u^2 + 4\zeta_s\omega_s\zeta_u\omega_u)s^4 + (2\zeta_u\omega_u\omega_s^2 + 2\zeta_s\omega_s\omega_u^2)s^3$$

$$+ (\omega_s^2\omega_u^2)s^2 \qquad (A.1.11)$$

$$DEN = s^4 + \left[(1 + \frac{m_s}{m_u})2\zeta_s\omega_s + 2\zeta_a\omega_u + 2\zeta_u\omega_u\right]s^3 +$$

$$\left[(1 + \frac{m_s}{m_u})\omega_s^2 + 4\zeta_s\omega_s\zeta_a\omega_u + 4\zeta_s\omega_s\zeta_u\omega_u + \omega_u^2\right]s^2$$

$$+ (2\zeta_a\omega_u\omega_s^2 + 2\zeta_u\omega_u\omega_s^2)s + (\omega_s^2\omega_u^2) \qquad (A.1.12)$$

This model represents model IV in Figure A1. It can be reduced to model III by setting ζ_a to zero. It can be further reduced to model II if ζ_u set to zero.

A2. Finite Length Model

The schematic of the finite length vehicle with and without secondary suspensions is shown in Figure A2. The state equations for the model with multiple primary suspensions are:

$$\frac{dZ_s}{dt} = \dot{Z}_s \tag{A.2.1}$$

$$\frac{d\dot{Z}_s}{dt} = -\left(\sum_{i=1}^{n} \omega_{si}^2\right) Z_s - \left\{2\sum_{i=1}^{n} \left(\zeta_{si} + \zeta_{ai}\right) \omega_{si}\right\} \dot{Z}_s - \left(\sum_{i=1}^{n} \omega_{si}^2 L_i\right) \theta$$

$$- \left\{2\sum_{i=1}^{n} \left(\zeta_{si} + \zeta_{ai}\right) \omega_{si} L_i\right\} \dot{\theta} + \sum_{i=1}^{n} \omega_{si}^2 Z_{gi} + 2\sum_{i=1}^{n} \zeta_{si}\, \omega_{si}\, \dot{Z}_{gi} \tag{A.2.2}$$

$$\frac{d\theta}{dt} = \dot{\theta} \tag{A.2.3}$$

$$\frac{d\dot{\theta}}{dt} = \frac{m_s}{I_v}\left[\left(\sum_{i=1}^{n} \omega_{si}^2 L_i\right) Z_s - \left\{2\sum_{i=1}^{n} \left(\zeta_{si} + \zeta_{ai}\right) \omega_{si} L_i\right\} \dot{Z}_s - \left(\sum_{i=1}^{n} \omega_{si}^2 L_i^2\right) \theta\right.$$

$$\left. - \left\{2\sum_{i=1}^{n} \left(\zeta_{si} + \zeta_{ai}\right) \omega_{si} L_i^2\right\} \dot{\theta} + \sum_{i=1}^{n} \omega_{si}^2 L_i Z_{gi} + 2\sum_{i=1}^{n} \zeta_{si}\, \omega_{si}\, L_i\, \dot{Z}_{gi}\right] \tag{A.2.4}$$

And the state equations for the finite length model with multiple secondary suspensions are:

$$\frac{dZ_s}{dt} = \dot{Z}_s \tag{A.2.5}$$

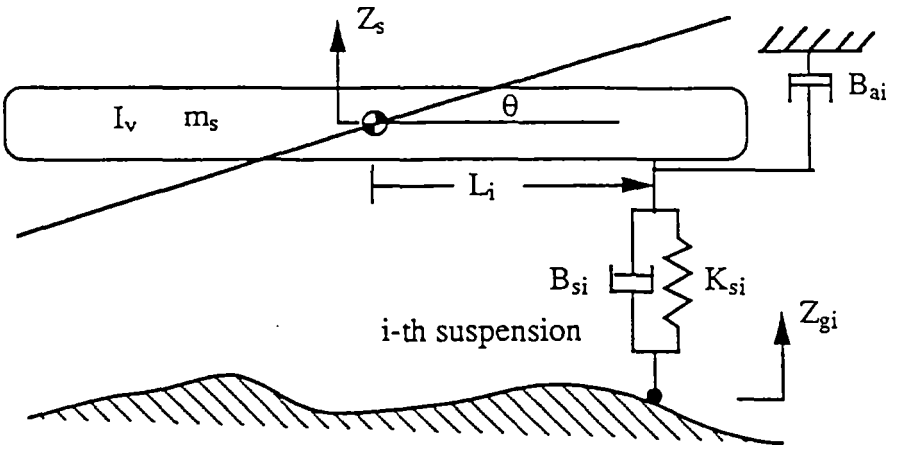

(a) model without secondary suspension

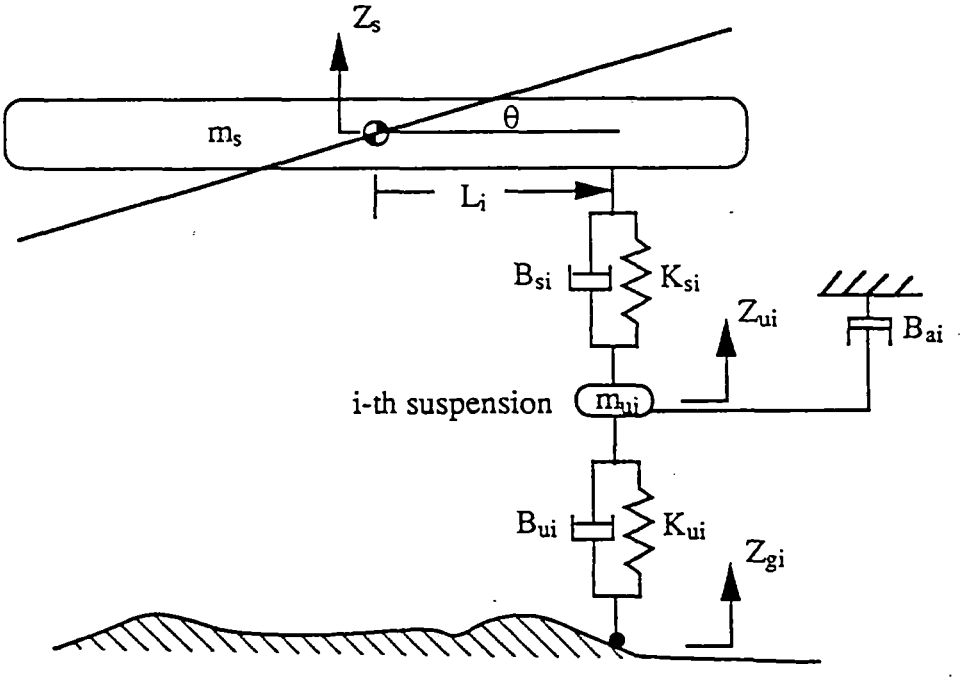

(b) model with secondary suspensions

Figure A2. Finite Length Multi-Suspension Models With And Without Secondary Suspension

$$\frac{d\dot{Z}_s}{dt} = -\left(\sum_{i=1}^{n} \omega_{si}^2\right)Z_s - \left(2\sum_{i=1}^{n} \zeta_{si}\omega_{si}\right)\dot{Z}_s - \left(\sum_{i=1}^{n} \omega_{si}^2 L_i\right)\theta - \left(2\sum_{i=1}^{n} \zeta_{si}\omega_{si}L_i\right)\dot{\theta}$$

$$+ \sum_{i=1}^{n} \omega_{si}^2 S_i + 2\sum_{i=1}^{n} \zeta_{si}\omega_{si}\dot{S}_i + \sum_{i=1}^{n} \omega_{si}^2 Z_{gi} + 2\sum_{i=1}^{n} \zeta_{si}\omega_{si}\dot{Z}_{gi} \qquad \text{(A.2.6)}$$

$$\frac{d\theta}{dt} = \dot{\theta} \qquad \text{(A.2.7)}$$

$$\frac{d\dot{\theta}}{dt} = \frac{m_s}{I_v}\left[-\left(\sum_{i=1}^{n} \omega_{si}^2 L_i\right)Z_s - \left(2\sum_{i=1}^{n} \zeta_{si}\omega_{si}L_i\right)\dot{Z}_s - \left(\sum_{i=1}^{n} \omega_{si}^2 L_i^2\right)\theta - \left(2\sum_{i=1}^{n} \zeta_{si}\omega_{si}L_i^2\right)\dot{\theta}\right.$$

$$\left. + \sum_{i=1}^{n} \omega_{si}^2 L_i S_i + 2\sum_{i=1}^{n} \zeta_{si}\omega_{si}L_i\dot{S}_i + \sum_{i=1}^{n} \omega_{si}^2 L_i Z_{gi} + 2\sum_{i=1}^{n} \zeta_{si}\omega_{si}L_i\dot{Z}_{gi}\right] \qquad \text{(A.2.8)}$$

$$\frac{dS_i}{dt} = \dot{S}_i \qquad \text{(A.2.9)}$$

$$\frac{d\dot{S}_i}{dt} = \frac{m_s}{m_u}n\omega_{si}^2 Z_s + 2n\frac{m_s}{m_u}\zeta_{si}\omega_{si}\dot{Z}_s + \frac{m_s}{m_u}n\omega_{si}^2 L_i\theta + 2n\frac{m_s}{m_u}\zeta_{si}\omega_{si}L_i\dot{\theta}$$

$$- \left(\frac{m_s}{m_u}n\omega_{si}^2 + \omega_{ui}^2\right)S_i - \left(2n\frac{m_s}{m_u}\zeta_{si}\omega_{si} + 2\zeta_{ai}\omega_{ui} + 2\zeta_{ui}\omega_{ui}\right)\dot{S}_i$$

$$- \frac{m_s}{m_u}n\omega_{si}^2 Z_{gi} - \left(2n\frac{m_s}{m_u}\zeta_{si}\omega_{si} + 2\zeta_{ai}\omega_{ui}\right)\dot{Z}_{gi} - \ddot{Z}_{gi} \qquad \text{(A.2.10)}$$

The above model represents model IV of the finite length vehicle model. It can be reduced to model III by setting ζ_{ai} to zero. It can be further reduced to model II by setting ζ_{ui} to zero.

A3. Ride Quality

Ride quality is a subjective evaluation of many factors. However, many studies have correlated accelerations with ride comfort. In this study, the "reduced comfort" criterion from the International Organization for Standardization (ISO) for a one-hour exposure time is adopted as an index of the ride quality requirement for a vehicle traversing an irregular guideway.

To compute the ISO based accelerations, the power spectral density of the sprung mass acceleration for a vehicle traveling along a randomly irregular guideway is first calculated as follows:

$$S_{\ddot{y}_s} = |H(\omega)|^2 \, S_g(\omega) \qquad \text{(A.3.1)}$$

where $S_{\ddot{y}}$ is the power spectral density of the sprung mass acceleration; $|H(\omega)|$ is the transfer function of vehicle sprung mass acceleration subjected to a guideway input; and S_g is the guideway irregularity spectral density function in terms of temporal frequency. For a vehicle traveling at the velocity V (m/sec), the transformation of temporal frequency to spatial frequency is

$$\omega \text{ (Hz)} = \Omega \text{ (cycle/m)} \times V \text{ (m/sec)} \qquad \text{(A.3.2)}$$

Therefore, the guideway irregularity spectral density function in terms of temporal frequency, $S_g(\omega)$, can be related to that in terms of spatial frequency, $S_g(\Omega)$, as

$$S_g(\omega) = S_g(\Omega=\frac{\omega}{V}) \frac{d\Omega}{d\omega} = \frac{S_g(\Omega=\frac{\omega}{V})}{V} \qquad \text{(A.3.3)}$$

The spectral density function for guideway roughness, $S_g(\Omega)$, generally can be expressed as

$$S_g(\Omega) = \frac{A}{\Omega^n} \qquad \text{(A.3.4)}$$

where A and n are experimentally determined parameters. For the simulations conducted in the report, the guideway is assumed to have similar roughness to welded steel rail. For this

type of guideway, A is equal to 6.1×10^{-8} m and n is equal to 2*. After substituting (A.3.4) into (A.3.3), the guideway irregularity spectral density function in terms of temporal frequency for welded steel rail can be written as:

$$S_g(\omega) = \frac{AV}{\omega^2} \qquad \text{(A.3.5)}$$

The corresponding spectral density of sprung mass acceleration in (A.3.1) is

$$S_{\ddot{y}_s} = |H(\omega)|^2 \frac{AV}{\omega^2} \qquad \text{(A.3.6)}$$

The result in (A.3.6) can be used directly to calculate the root mean square (rms) value of sprung mass acceleration by integrating the power spectral density function. To compare with ISO criterion, the rms acceleration is integrated in one-third octave bands as:

$$(\ddot{y}_s)_{\text{rms (one-third octave band)}} = \left\{ \int_{\omega_l}^{\omega_u} S_{\ddot{y}_s}(\omega)\, d\omega \right\}^{1/2} \qquad \text{(A.3.7)}$$

with the upper and lower bounds:

$$\omega_u = \omega_c \exp(\frac{1}{6}\ell n2)$$
$$\omega_l = \omega_c \exp(-\frac{1}{6}\ell n2)$$

where ω_c is the center frequency of the corresponding band.

The total rms can also be computed from the spectral density function by integrating the function from zero to infinity. In this report, however, the integration is computed from 0.1 Hz to 80 Hz, since in the very high and very low frequency ranges the spectral density function does not contribute much to the integration if the total rms exists, and in actual applications the high frequency guideway inputs are mostly filtered and the input function given in (A.3.5) might overestimate the guideway roughness in the low frequency range.

---

* In obtaining the values of A and n, $S_g(\Omega)$ is defined as

$$S_g(\omega) = \frac{1}{2\pi}\int_0^{\infty} R_f(\tau)e^{-j\omega\tau}\, d\tau$$

[Ω] : cycle/m

$$(\ddot{y}_s)_{\text{total rms}} = \int_{0.1}^{80} S_{\ddot{y}_s}(\omega)\, d\omega \qquad \text{(A.3.8)}$$

The total rms values of unsprung mass acceleration and gap variation can also be obtained by following the same procedures.

Appendix B

The partial differential equation of motion for a Bernoulli-Euler beam resting upon multiple supports and excited by an arbitrary forcing function may be derived as [24]:

$$EI\frac{\partial^4 y}{\partial X^4} + \rho a\frac{\partial^2 y}{\partial t^2} + b\frac{\partial y}{\partial t} = f(X,t) \qquad (B.1)$$

where:

EI = beam bending rigidity
ρa = beam mass per unit length
b = beam damping per unit length
$f(X,t)$ = time and spatially varying force per unit length
y = guideway transverse displacement
X = spatial horizontal coordinate
t = time

The guideway model (B.1) can be put in a non-dimensional form as:

$$\frac{\partial^4 y}{\partial x^4} + \left(\frac{\pi L_b}{L_s}\right)^4 \frac{\partial^2 y}{\partial \tau^2} + \frac{bL_b^4}{EI}(2\pi f^*)\frac{\partial y}{\partial \tau} = \frac{L_b^4}{EI} f(x,\tau) \qquad (B.2)$$

where:

$x = X/L_b$
L_b = beam length
L_s = span length
$\tau = 2\pi f^* t$
$f^* = \frac{\pi}{2L_s^2}\sqrt{\frac{EI}{\rho a}}$
= the first mode natural frequency of a single simply supported beam of length L_s

Using the modal analysis technique [24], the transverse motion $y(x,\tau)$ of the beam may be written as an infinite sum of the products of time varying modal coefficients $\alpha_m(\tau)$ and modal shape functions $\phi_m(x)$ as:

$$y(x,\tau) = y^* \sum_{m=1}^{\infty} \alpha_m(\tau)\,\phi_m(x) \qquad (B.3)$$

where:

$$y^* = \frac{2WL_s^3}{\pi^4 EI}$$

= the first mode deflection of a single simply supported beam of length L due to a single concentrated force equal to the weight of the vehicle W loaded at midspan

The modal shape functions $\phi_m(x)$ and modal coefficients $\alpha_m(\tau)$ must satisfy the following equations:

$$\frac{d^4\phi_m(x)}{dx^4} - \omega_m^2 \left(\frac{\pi L_b}{L_s}\right)^4 \phi_m(x) = 0 \tag{B.4}$$

$$\frac{d^2\alpha_m(\tau)}{d\tau^2} + 2\xi_m\omega_m \frac{d\alpha_m(\tau)}{d\tau} + \omega_m^2 \alpha_m(\tau) = \frac{L_s}{2W} \int_0^1 f(x,\tau)\, \phi_m(x)\, dx \tag{B.5}$$

where ξ_m is the damping ratio corresponding to the m-th modal shape.
The modal shape functions $\phi_m(x)$ are normalized such that:

$$\int_0^1 \phi_m^2(x)\, dx = 1 \tag{B.6}$$

The modal shape functions and the eigenvalues for a beam with single span or multiple spans that satisfy (B.4) and (B.6) can be found in [25].

The forcing term on the right hand side of (B.5) is represented in a general form. If the force acting over the beam due to vehicle crossing is considered as constant pressure distributed along finite pad length, the term $f(x,\tau)$ then can be written as:

$$f(x,\tau) = \frac{1}{L_p} \sum_{i=1}^{q} \left\{ \frac{(m_u + m_s)\, g}{N} + K_{ui}\, \Delta z_i(\tau) + B_{ui}\, \Delta \dot{z}_i(\tau) \right\} \tag{B.7}$$

where

L_p = suspension pad length
$(m_u + m_s)\, g$ = total weight of vehicle
N = total number of suspensions
q = number of suspensions which is currently acting on the beam
K_{ui} = spring constant of the i-th suspension
B_{ui} = dashpot constant of the i-th suspension
Δz_i = displacement of the i-th suspension

Substituting (B.7) into the right hand side of (B.5), the differential equation determining the modal coefficient $\alpha_m(\tau)$ for time varying pressure load distributing along finite pad length is given as:

$$\frac{d^2\alpha_m(\tau)}{d\tau^2} + 2\xi_m\omega_m\frac{d\alpha_m(\tau)}{d\tau} + \omega_m^2\alpha_m(\tau) = \frac{L_s}{2L_p}\sum_{k=1}^{q}\left\{\left(\frac{1}{N} + \frac{\omega_{uk}^2\,\Delta z_k + 2\xi_{uk}\omega_{uk}\,\Delta\dot{z}_k}{N\,(r+1)\,g}\right)\int_{Xk_i}^{Xk_f}\phi_m(x)\,dx\right\} \tag{B.8}$$

where

$$\omega_{uk} = \sqrt{\frac{K_{uk}}{m_{uk}}}$$

$$\xi_{uk} = \frac{B_{uk}}{2m_{uk}\omega_{uk}}$$

$$r = \frac{m_s}{m_u}$$

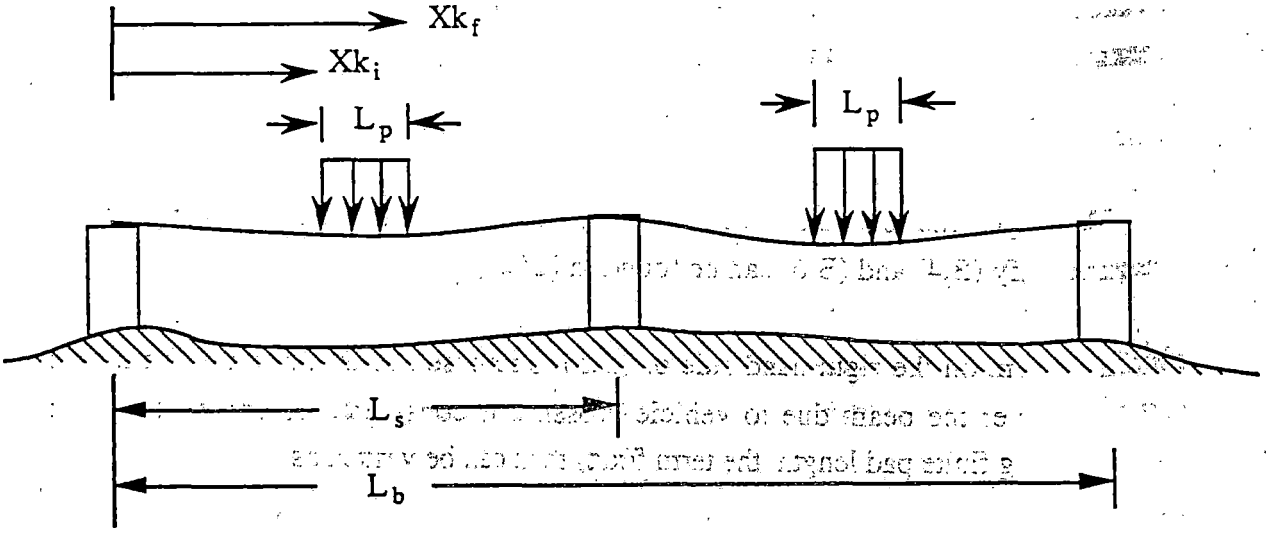

Figure B.1 Guideway Geometry

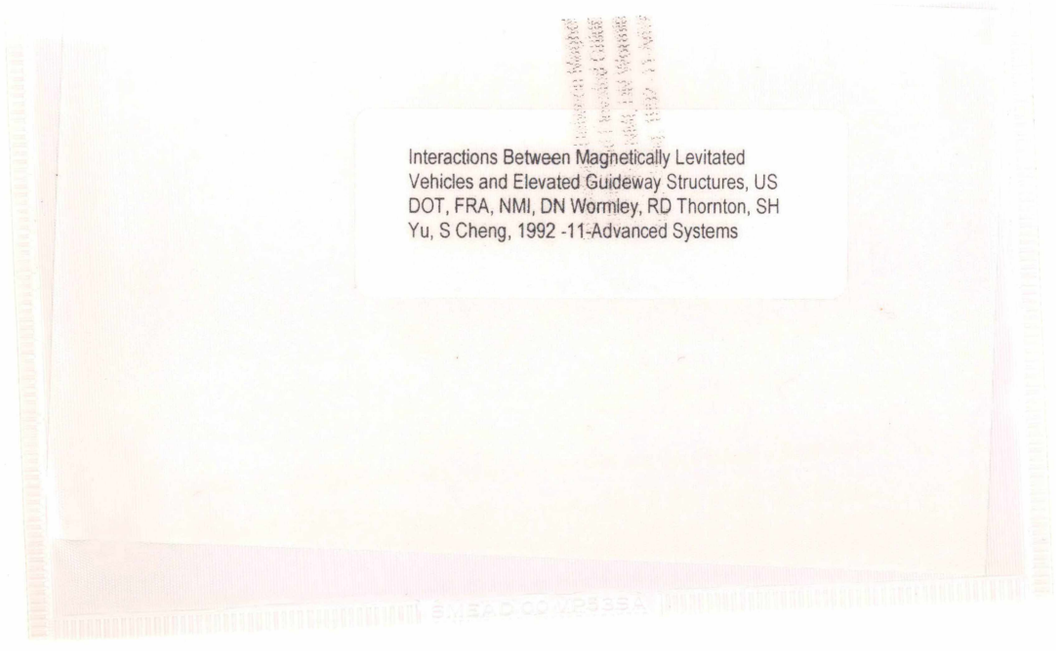

Interactions Between Magnetically Levitated Vehicles and Elevated Guideway Structures, US DOT, FRA, NMI, DN Wormley, RD Thornton, SH Yu, S Cheng, 1992 -11-Advanced Systems